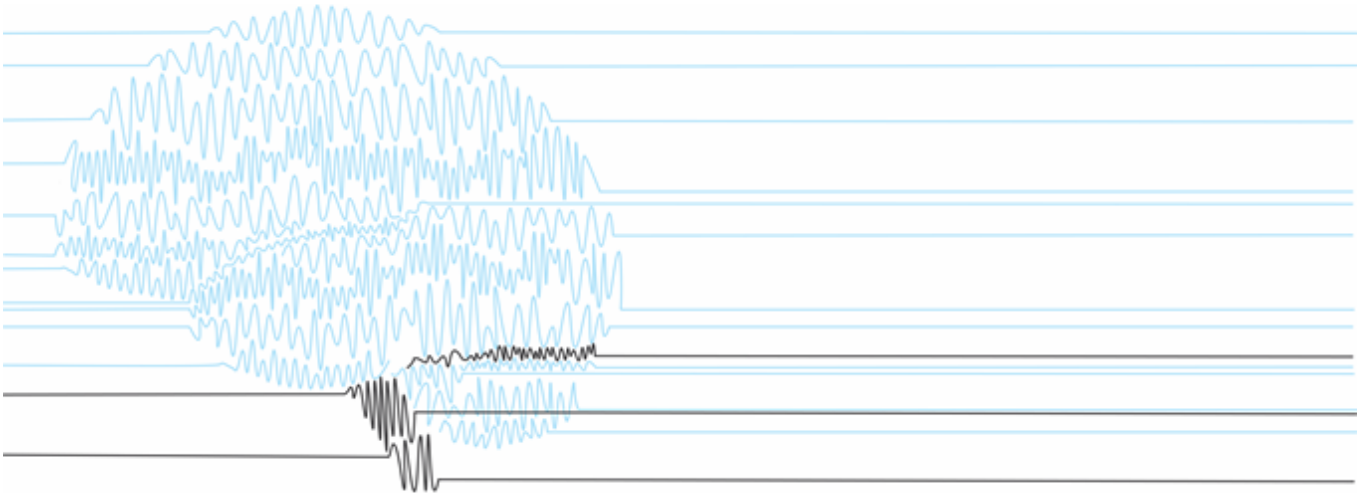

Neurophysiology of non-motor complications in Parkinson's disease: role of the locus coeruleus

eman ta zabal zazu

Universidad del País Vasco

Euskal Herriko Unibertsitatea

Elena Paredes Rodríguez

Leioa, 2020

eman ta zabal zazu

Universidad del País Vasco

Euskal Herriko Unibertsitatea

Neurophysiology of non-motor complications in Parkinson's disease: role of the locus coeruleus

Doctoral thesis presented by Elena Paredes Rodríguez

Leioa, 2020

This work has been supported by the MINECO´s fund SAF2016-77758-R (AEI/FEDER, UE) and the Government of the Basque Country T747-13. Elena Paredes Rodríguez has held a predoctoral fellowship for the Training of Research Personnel (Formación de Personal Investigador) for the period 2016-2020.

Conflict of interest

The authors declare no conflicts of interest.

Agradecimientos

Me gustaría empezar dando las gracias a las directoras de mi tesis, Cristina Miguélez y Luisa Ugedo, las personas que han hecho posible llegar a la meta que nos propusimos hace cuatro años. Gracias Cristina por confiar en mí en un primer momento y contar conmigo en estos años, por toda tu ayuda, tus consejos, infinita dedicación y, sobre todo, por haber estado siempre ahí cuando he necesitado contar contigo. Gracias Luisa, por haberme aconsejado y ayudado siempre que me ha hecho falta, así como por tu esfuerzo y trabajo durante todos estos años haciendo que sigamos adelante. Gracias a las dos por vuestra confianza y por haberme hecho crecer personal y profesionalmente, he aprendido mucho de ambas, tanto para esta etapa como para las que vendrán.

Al resto del grupo gracias por todo el apoyo y los ánimos. Teresa, gracias por estar siempre con una sonrisa, aconsejarme cuando lo he necesitado y por ser la organizadora de las sesiones cafeteras. A Jose Ángel, por los buenos momentos escapando de salas de combate, y por último a Lise por traer aire fresco al laboratorio. Por supuesto gracias a las personas que han estado junto a mi desde el comienzo. A Sergio por ser mi compi de despacho por excelencia y, en consecuencia, por toda la ayuda, empatía y el infinito apoyo durante estos años, y por los tantos momentos de risa cuando la concentración estaba en zona baja. A Mario, por su apoyo en muchos cafés, por transmitir tranquilidad cuando es necesario y por todos sus consejos científicos e informáticos tan valiosos. A la artista Lorena, por la alegría que me ha aportado, todo el apoyo, las risas y, sobre todo, por los suministros de azúcar en esta última etapa.

Igualmente quiero dar las gracias a los grupos de investigación con los que he tenido la oportunidad de colaborar en este tiempo. Por un lado, gracias a la profesora

Esther Berrocoso de la Universidad de Cádiz por haberme dado la oportunidad de pasar dos meses en su laboratorio y haber podido aprender tanto de ello. Gracias Meri por tu ayuda, paciencia y consejos, me alegro mucho de haber estado colaborando contigo durante esta estancia. Gracias Carmen y Sonia por hacerme disfrutar y conocer la vida gaditana fuera del laboratorio. En definitiva, quiero agradecer a todo el grupo por vuestra acogida, buen humor y funcionar como un equipo. Por otro lado, thank you so much Professor Tony Pickering for giving me the opportunity to do my research stay in your lab, where I learned many new things. I am truly grateful for your time, dedication and for making possible my unforgettable experience in Bristol. Thanks to all the lab members, it was great to learn so much from you. And of course, thanks to the spectacular group of friends I met at Hodgkin house during my stay, you made me feel at home.

Además, tengo que agradecer a aquellos que no forman parte del grupo, pero sin duda forman parte de este camino. Darle las gracias al rey de las oscilaciones, Asier, por todos tus consejos, pero sobre todo por estar dispuesto a ayudar en todo momento de manera desinteresada. Nerea gracias por echarme un cable siempre que lo he necesitado y haberme aconsejado tanto en mis inicios. Gracias también al resto de becarios del departamento por las comidas, cenas o poteos compartidos, y en especial gracias a aquellas que han estado al otro lado de Patch a horas intempestivas y al tránsfugo de micro, Unai. Gracias también a Tere, por animarnos y conocernos tan bien, acertando con un vistazo si somos afortunados o no en nuestra búsqueda de neuronas.

Porque lo que lleva a seguir andando este recorrido no es sólo aquello que ocurre en el laboratorio sino también todo lo que lo rodea. Gracias a mis amigas, ya sabéis quienes sois, porque haya crecido con vosotras u os haya encontrado a lo largo de los años me hacéis reír, disfrutar y darme cuenta de dónde se encuentra lo

verdaderamente importante. También, aunque quede mal escribirlo, gracias a los Hamijos, porque no me imagino la universidad sin alguno de vosotros, gracias por tantísimos momentos de risa y seguir estando ahí. En especial te agradezco Sara, todo el apoyo y consejos que me has dado durante estos años, pero especialmente en esta etapa, gracias por hacer que mantenga la perspectiva.

Especialmente quiero dar las gracias a mi familia, desde mis padres, hermanos, mi abuela… a los sobris más pequeñitos. Infinitas gracias por apoyarme siempre y haberme hecho ser quien soy, sin vosotros no hubiese podido conseguirlo. Jon Ander, gracias por haber estado a mi lado todo este tiempo, tu apoyo incondicional y entender los claros y los oscuros de este camino. Gracias de corazón por hacer que todo sea mejor y más fácil contigo.

A todos, gracias por formar parte de esta tesis

INDEX

ABBREVIATION LIST

6-OHDA	6-hydroxydopamine
ACSF	Artificial cerebrospinal fluid
ANOVA	Analysis of the variance
AUC	Area under the curve
CL *	Contralateral
COX	Cytochrome-c-oxidase
DA	Dopamine
ECoG	Electrocorticogram
eEPSC	Evoked excitatory postsynaptic currents
eIPSC	Evoked inhibitory postsynaptic currents
(p)ERK	(phosphorylated) Extracellular signal-regulated kinases 1 and 2
i.p.	Intraperitoneal
i.v.	Intravascular
IL *	Ipsilateral
IRK	Inwardly-rectifying potassium
KPBS	Potassium-PBS
LC	locus coeruleus
L-DOPA	3,4-Dihydroxy-L-phenylalanine methyl ester
LFP	Local field potential
MFB	Medial forebrain bundle
PFC	Prefrontal cortex
mPFC	Medial prefrontal cortex
MPTP	1-methyl 4-phenyl 1,2,3,6-tetrahydropyridine
NA	Noradrenaline

PC *	Paw compression
PD	Parkinson's disease
PFC	Prefrontal cortex
PGi	paragigantocellularis
RM	Repeated measures
S.E.M.	Standard error of the mean
sEPSC	Spontaneous excitatory postsynaptic currents
sIPSC	Spontaneous inhibitory postsynaptic currents
SNc	Substantia nigra pars compacta
TH	Tyrosine hydroxylase
WB	Western Blot

***** Only in tables and figures

1. INTRODUCTION

1. INTRODUCTION

1.1. Parkinson's disease

Parkinson's disease (PD) is a neurodegenerative disorder characterized by the degeneration of dopaminergic neurons in the substantia nigra pars compacta (SNc), striatal dopamine (DA) depletion and presence of Lewy aggregates containing alpha-synuclein. Clinically, PD major manifestation is the motor impairment, but non-motor symptoms are also present and severely affect the quality of life of the patients.

1.1.1. Epidemiology and etiology

In 1817, James Parkinson published "An essay on the shaking palsy" where first described this unclassified syndrome until then. Later in the 19th century, Jean Martin Charcot and William Rutherford Sanders proposed to name the disorder as "maladie de Parkinson" or Parkinson's disease in acknowledgment for his adequate definition (Goedert and Compston, 2018). Two centuries later, PD has become the second most common neurodegenerative disorder, affecting approximately 0.3 % of the world's population, 1% of the individuals older than 60 years old (the mean age of onset) and increasing until 3% in those older than 80 years old (de Lau and Breteler, 2006; Poewe et al., 2017).

The etiology of PD is still poorly understood in idiopathic cases, which represent the 90% of the total patients. The remaining 10% is associated to a genetic mutation cause (genes involved: α-synuclein, parkin, DJ-1, PINK1 and LRRK2 among others), especially in those cases with an onset age younger than 50 (de Lau and Breteler, 2006; Wirdefeldt et al., 2011). The principal risk factors implicated in

the development of the disease are the increasing age and family history, although exposure to traumatic brain injury or various toxins, like MPTP (1-methyl 4-phenyl 1,2,3,6-tetrahydropyridine) or pesticides (rotenone or paraquat), are also proposed (Langston et al., 1983; Betarbet et al., 2000; Thiruchelvam et al., 2000; Poewe et al., 2017).

1.1.2. Symptomatology

It is now accepted that PD is characterized not only by its motor symptoms, but also by non-motor features.

A) Motor symptoms

The cardinal features of PD are mainly the motor symptoms, which are frequently unilateral or at least asymmetrical. Following the Movement Disorder Society clinical diagnostic criteria for PD, parkinsonism is defined as bradykinesia (slowness in spontaneous and voluntary movement), in combination with either resting tremor (rhythmic tremor that disappears during voluntary movement), rigidity (muscle stiffness), or both. Other motor symptoms such as walking problems or postural instability are commonly present (Postuma et al., 2015).

B) Non-motor symptoms

Most of the patients suffer non-motor dysfunctions, which can occur as early non-motor manifestations of PD or appear in the late stages of the disease. The presymptomatic or prodromal phase is often characterized by olfactory dysfunction, autonomic dysregulation, pain, sleep and mood disorders while the symptomatic phase is accompanied by somatomotor symptoms and impaired cognitive functioning (Poewe et al., 2017) (**Figure 1.1**).

The most frequent non-motor symptoms are neuropsychiatric disorders (depression and anxiety) (Schrag and Taddei, 2017; Ryan et al., 2019), mild cognitive impairment and dementia (Svenningsson et al., 2012; Aarsland et al., 2017), autonomic dysfunction (orthostatic hypotension, urogenital dysfunction and constipation) (Martinez-Martin et al., 2015; Leclair-Visonneau et al., 2018), pain presented as nociceptive (musculoskeletal and visceral) and neuropathic (radicular and central) types (Wasner and Deuschl, 2012), sleep disorders (excessive sleepiness or sleep attacks) (Stacy, 2002; Gjerstad et al., 2006), impaired visual function (Murueta-Goyena et al., 2019), hyposmia, apathy, fatigue and psychosis (visual hallucinations and delusions) (Bohnen et al., 2008; Schapira et al., 2017).

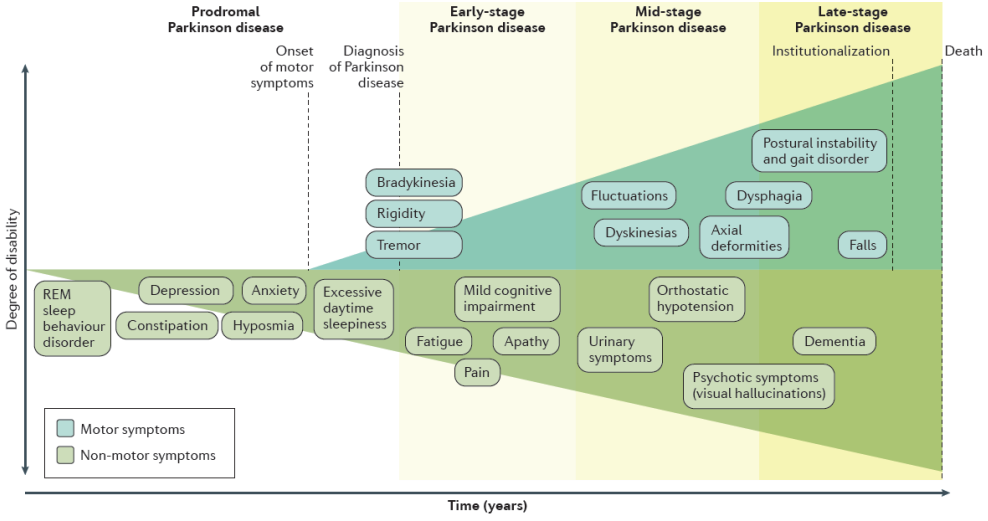

Figure 1.1. Motor and non-motor symptoms in Parkinson's disease. The non-motor features in PD involve numerous functions of the central and autonomic system. Some symptoms appear in the prodromal phase, preceding the motor dysfunction and some other non-motor symptoms are more prominent in the course of the disease. Image taken from Poewe et al. (2017).

1.1.3. Neuropathology

PD is characterized by the neurodegeneration of dopaminergic and other cell types in the brain. Several studies have demonstrated the involvement of neuronal inclusions of α-synuclein and mitochondrial dysfunction contributing to cellular oxidative stress, degeneration and death.

A) Neurodegeneration of the nigrostriatal pathway

Pathogenesis of PD has been focused on the degeneration of dopaminergic neurons in the SNc, which affects lateral nigral projections to the putamen and the function of the basal ganglia network (Kish et al., 1988). The basal ganglia are a collection of subcortical structures involved in the cortico-basal ganglia-thalamo-cortical loop (Maurice et al., 1999), which are essential for motor control, but also participate in learning, cognition and memory functions (Nambu et al., 2002; Packard and Knowlton, 2002; Graybiel, 2005; Kravitz et al., 2010). Motor symptoms are evident when about 80% of striatal DA and 50-60% of nigral neurons are lost (Fearnley and Lees, 1991; Wirdefeldt et al., 2011).

Parkinsonism is often associated with changes in cortico-basal ganglia-thalamo network. Indeed, nigrostriatal DA loss has opposing effects on the direct (striatum-SN pars reticulate and globus pallidus internal) and indirect (striatum-globus pallidus externus-subthalamic nucleus-SN pars reticulate and globus pallidus internal) pathways. When DA loss occurs, direct pathway activity (dopaminergic D1-receptor dependent) is reduced while indirect pathway activity (dopaminergic D2-receptor dependent) increases, resulting in a strong increase in the firing rate of GABAergic basal ganglia output neurons (substantia nigra pars reticulate and internal globus pallidus). Then, hyperactivity of output structures inhibits

thalamocortical and brainstem areas, eliciting the parkinsonian state (Alexander et al., 1986; DeLong, 1990; Kravitz et al., 2010) (**Figure 1.2**).

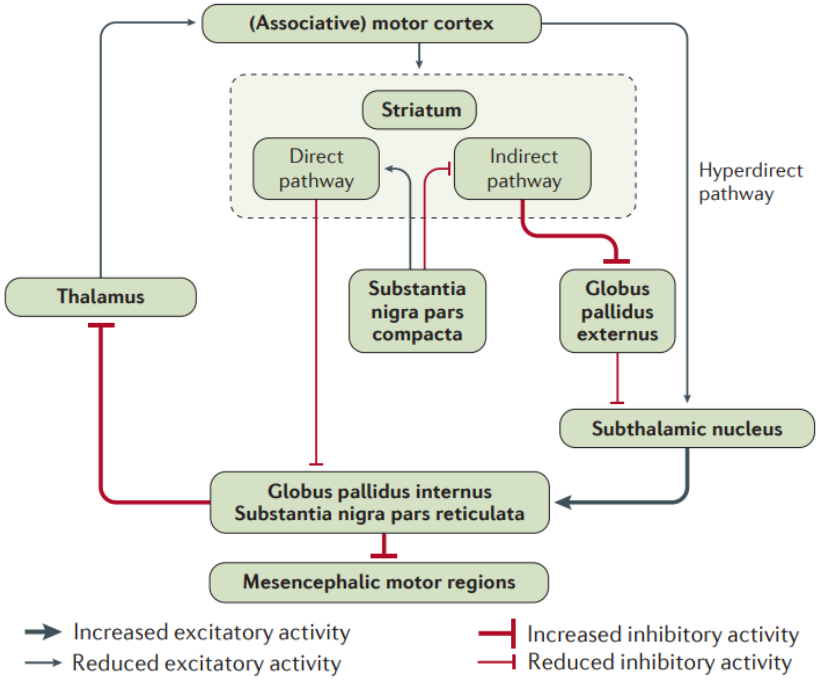

Figure 1.2. Simplified basal ganglia circuitry changes in Parkinson's disease. The principal components of this circuitry are the striatum (caudate and putamen), the external segment of the globus pallidus, the internal segment of the globus pallidus (entopeduncular nucleus, in rat), the substantia nigra pars compacta and reticulate and the subthalamic nucleus; all these structures are involved in the cortico-basal ganglia-thalamo-cortical loop. Taken from Poewe et al. (2017).

During parkinsonism, the basal ganglia undergo an adaptation to DA loss causing changes in neural oscillation (presence of rhythmic fluctuations at specifics frequency bands) and synchronization (whether oscillations in two brain nuclei show a consistent phase relationship at specifics frequency bands). In particular, there is excessive synchronization between some of the basal ganglia nuclei, which also show enhanced oscillatory activity in several frequency bands. These alterations

are clinically relevant, since treatments capable of supressing them improve the motor performance of the patient at the same time (Brown et al., 2001; Kühn et al., 2006, 2008).

B) Neurodegeneration causes

Oxidative stress and mitochondrial dysfunction

One possible cause of the neurodegeneration during PD is the oxidative stress. Since Schapira in 1990 first documented it in idiopathic PD patients (Schapira et al., 1990), large number of studies consider that mitochondrial dysfunction plays a pivotal role in the disease causing cellular damage and eventual cell death (reviewed in Winklhofer and Haass, 2010). In fact, mitochondrial impairment is linked to excessive reactive oxygen species, altered enzymes from the electron transport chain, impaired bioenergetics (decreased ATP production) and oxidative stress (generation of free radicals), leading to cellular dysfunction (Schapira, 2008; Blesa et al., 2015).

Mitochondrial dysfunction in PD has been usually related to deficiencies in the complex I (NADH dehydrogenase), which is an enzyme of the respiratory chain. A recent meta-analysis of results published regarding the mitochondrial complex I activity in PD patients has shown a strong reduction in the SN and peripheral muscle (Holper et al., 2019). Deficiency in blood platelets of untreated patients, in leukocytes and in the prefrontal cortex has been reported as well (Yoshino et al., 1992; Haas et al., 1995; Müftüoglu et al., 2004; Parker et al., 2008). However, complex I is not the only one affected in PD patients. Activity of complex IV (cytochrome-c-oxidase, COX) is also reduced in the frontal cortex (meta-analysis Holper et al., 2019) and in leukocytes (Müftüoglu et al., 2004) when compared to the controls. Complex II activity is slightly lower in platelets and lymphocytes in

PD (Yoshino et al., 1992). Complex III activity was also reduced in platelets of PD compared with controls (Haas et al., 1995). Other evidence for mitochondrial dysfunction in PD is related to genetic forms of the disease, since the mutation of specific genes coding for proteins like parkin or PINK1, leads to mitochondrial dysfunction (Müftüoglu et al., 2004; Valente et al., 2004).

Inclusions of α-synuclein

The cell loss in the SNc is accompanied by the widespread presence of insoluble α-synuclein protein fibrils, which conform aggregates that form the Lewy bodies. These aggregates may be responsible for the onset and progression of the disease, but they do not appear all over the brain at the same time. Indeed, recent publications have suggested that the α-synuclein pathology begins in the gut and travels up to the brain, via the vagal nerve. Once in the brain, it may spread following the six stages defined by Braak and colleagues (Ulusoy et al., 2013; Kim et al., 2019).

According to Braak's theory (Braak et al., 2003, 2004), the first α-synuclein aggregates in the central nervous system appear in the anterior olfactory structures and the dorsal motor nucleus of the vagus nerve, following by lower raphe system and the locus coeruleus (LC) in stage 2 (**Figure 1.3A**). It is not until stage 3 that the SNc is affected together with the amygdala, tegmental pedunculopontine nucleus, and the higher raphe nuclei, among others. During stage 4, α-synuclein spreads to the hippocampal formation and specific cortical areas (**Figure 1.3B**) and finally, in the last two stages (5 and 6), almost the whole cortex is damaged (**Figure 1.3C**). The pathological process underlying PD would consist of a prodromal period followed by a symptomatic one when the disease is usually diagnosed. The presymptomatic or prodromal phase occurs during stages 1-3 and the symptomatic phase during stages 4-6 (Chaudhuri and Schapira, 2009; Braak and Del Tredici, 2016).

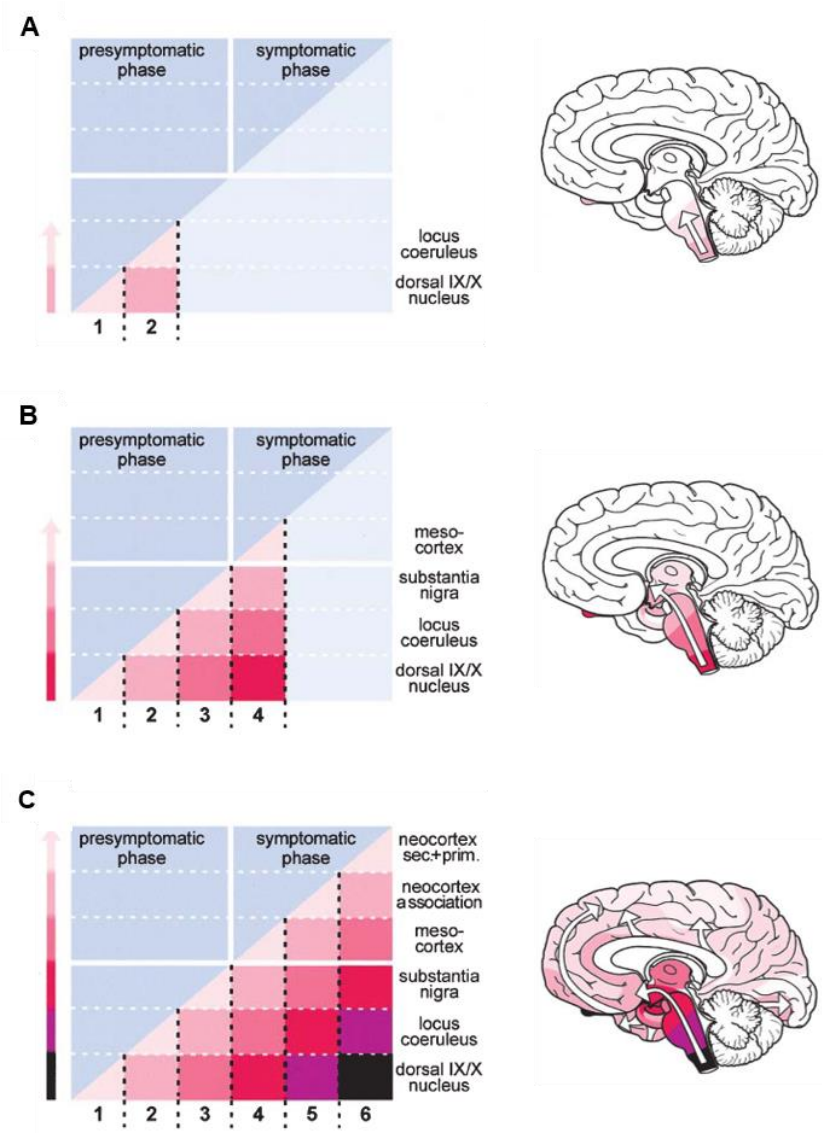

Figure 1.3. Schematic progression of Parkinson's disease according to Braak's theory. A) During stage 1 the olfactory bulb, anterior olfactory nucleus, and dorsal motor nucleus of the vagus nerve are affected. In stage 2, the lesion ascends to the LC, gigantocellular reticular nucleus, and caudal raphe nuclei. B) The central subnucleus of the amygdala, the cholinergic nuclei of the basal forebrain, and the pars compacta of the substantia nigra are reached in stage 3. The cerebral cortex becomes involved at stage 4. C) In stages 5 and 6, the lesions reaches the cerebral cortex. Image taken and modified from Braak et al. (2003).

According to this theory, damage to other areas precedes the degeneration of SNc neurons, affecting glutamatergic, noradrenergic, serotonergic, histaminergic and cholinergic cells (Del Tredici et al., 2002; Braak et al., 2003). In particular, LC noradrenergic cells share some intrinsic cellular factors with SNc neurons that are thought to increase the vulnerability to neurodegeneration in PD. Both contain neuromelanin, enzymatic metabolism and autoxidation of catecholamines yield products leading to oxidative stress, exhibit autonomous peacemaking activity involving cytosolic calcium oscillations and an extensive axonal arborization with multiple synaptic and paracrine neurotransmitters release sites (reviewed in Martin-Bastida et al., 2017; Oertel et al., 2019; Vila, 2019).

This heterogeneous and progressive neurodegeneration may explain the diverse symptomatology of PD, which includes motor and non-motor alterations (Chaudhuri and Schapira, 2009). Indeed, PD is more likely to be a multisystem disorder rather than a pure motor disease.

1.1.4. Treatment

As mentioned above, the pathophysiological process in PD involves many areas and multiple neurotransmitter pathways, beyond the nigrostriatal dopaminergic system. Therefore, PD treatment requires includes not only dopaminergic medication, but also drugs acting on others neurotransmitter systems.

A) Motor symptoms treatment

Dopaminergic therapy

3,4-Dihydroxy-L-phenylalanine methyl ester (L-DOPA or levodopa) is considered the most efficient anti-parkinsonian drug since its introduction in the

late 60s (Cotzias et al., 1967). DA is administered as its immediate precursor L-DOPA, which is a small neutral molecule and is transported across the blood-brain barrier by a large amino acid transporter. To avoid peripheral decarboxylation, L-DOPA is commonly administered in combination with a decarboxylase inhibitor (carbidopa or benserazide) that increases its central biodisponibility. Once in the brain, L-DOPA is converted into DA (Fahn, 2008).

Although the standard oral L-DOPA therapy is well established in the clinic and provides general satisfactory symptomatic relief, it has major limitations. L-DOPA does not control some motor complications like freezing or "off" periods (times when L-DOPA is not working optimally) and its long-term use is associated with the development of dyskinesia (uncontrolled, involuntary movements) and motor fluctuations (Olanow et al., 2009; Hirao et al., 2015). In order to avoid motor fluctuations, pharmacological research is focused on new administration ways to allow continuous infusion of the drug (Olanow et al., 2014).

Catechol-O-methyltransferase inhibitor (entacapone or tolcapone) is often combined with L-DOPA in order to prolong its effect (Connolly and Lang, 2014). Monoamine oxidase type B inhibitors (rasagiline, selegiline or safinamide) reduce DA metabolism and are usually administered in combination with L-DOPA or dopaminergic agonists (Kalia and Lang, 2015; Dietrichs and Odin, 2017).

Alternative treatments to L-DOPA therapy are also used. In this sense, dopaminergic agonists (pramipexole, ropinirole, rotigotine or apomorphine) are often prescribed alone or in combination with other dopaminergic drugs (Connolly and Lang, 2014).

Other treatments

Some non-dopaminergic drugs are also prescribed for ameliorating the motor symptoms. Adenosine A2A receptors antagonist (istradefylline) has been approved in August 2019by the U.S. Food and Drug Administration (FDA) in combination to L-DOPA/carbidopa to treat "off" periods (Research, 2019). Amantadine is often used to treat motor symptoms in early PD, and in 2017 an extended release formulation was also approved for treating dyskinesia in the United States (Drug Approval Package: Gocovri (amantadine extended-release); Kalia and Lang, 2015). Anticholinergic drugs (trihexyphenidyl or benztropine) can be used alone or in combination with other drugs, especially in patients with tremor although its efficacy shows high interindividual variability (Connolly and Lang, 2014).

Surgery is directed at treating L-DOPA motor complications that are severe enough to justify the surgical risk (Munhoz et al., 2016). Bilateral deep brain stimulation of the subthalamic nucleus is now an established evidence-based therapy for motor fluctuations and dyskinesia in patients with advanced PD, although the globus pallidus internus may be an alternative surgical target (Poewe et al., 2017). At present, clinical trials are testing ultrasound surgery, a permanent and irreversible procedure which seems to improve the motor performance in PD patients with asymmetric parkinsonism through unilateral subthalamotomy (Martínez-Fernández et al., 2018).

B) Non-motor symptoms treatment

It is important to determine if the non-motor symptoms in PD are independent or not from the motor symptoms, in order to manage them properly. Unlike the majority of motor features of PD, non-motor symptoms have often limited treatment options, which are not specific for parkinsonian patients (Martinez-Martin et al., 2011; Engels et al., 2019).

Dopaminergic therapy

Although not for all symptoms, some studies have described that non-motor complications intensity is inversely related to the efficacy of L-DOPA/dopaminergic agonists in motor performance, as for pain (Nebe and Ebersbach, 2009) and sleep disorders (Rektorova et al., 2008; Trenkwalder et al., 2011).

Dopaminergic therapy, mainly dopaminergic agonists that bind D3 receptors, as rotigotine and pramiprexol, improves depression in some patients with PD (Willner, 1997; Sauerbier et al., 2017; Schrag and Taddei, 2017; Ryan et al., 2019). Other dopaminergic agonist, ropinirole, also caused significant improvement of depressive and anxiety symptoms, in addition to controlling motor and sleep symptoms (Rektorova et al., 2008).

Clinical management of sleep disorders is complex because most of the antiparkinsonian drugs can alter sleep architecture and induce sleepiness as a side effect (Schapira et al., 2017). However, the dopaminergic agonists, ropirinole and rotigotine, improved motor symptoms and sleep scores (Rektorova et al., 2008; Trenkwalder et al., 2011).

Musculoskeletal pain is the most common form of pain related to PD and usually responds to dopaminergic medication (Wasner and Deuschl, 2012). Pain can be significantly alleviated by adjustments of L-DOPA treatment (Nebe and

Ebersbach, 2009) and transdermal administration of rotigotine, which improves the perception of the affective dimension of PD-associated pain (Rascol et al., 2016; Timmermann et al., 2017). In both cases, the improvement was attributed to benefits in the motor function.

Although apathy following subthalamic stimulation responded to ropinirole administration (Czernecki et al., 2008), the evidence regarding the effect of dopaminergic medication in this non-motor complication is still scarce.

Other treatments

Depressive symptoms are often treated with those antidepressants used in major depression as, selective serotonin reuptake inhibitors, selective noradrenaline (NA) reuptake inhibitors, tricyclic antidepressants, serotonin and NA reuptake inhibitors, and monoamine oxidase inhibitors (Schrag and Taddei, 2017; Ryan et al., 2019). There are no general agreement regarding the effect of deep brain stimulation surgery of the subthalamic nucleus or globus pallidus internus in depressive and anxiety symptoms (Couto et al., 2014; Pusswald et al., 2019).

Eszopiclone and melatonin are considered acceptable for the treatment of insomnia, and melatonin and clonazepam are the two main pharmacotherapies for REM behaviour disorder (Albers et al., 2017; Videnovic, 2018).

Severe pain is improved with prolonged-release formulation of opioids (oxycodone–naloxone) (Trenkwalder et al., 2015) while painful dystonia may be relieved with botulinum injections (Bruno et al., 2016, 2018). The selective serotonin and norepinephrine reuptake inhibitor, duloxetine, reported pain relief in PD patients as well (Djaldetti et al., 2007).

As for neuropsychiatric symptoms, evidence supports the use of cholinesterase inhibitors, rivastigmine, to treat mild to moderate dementia in PD

(Aarsland et al., 2017). In addition, a controlled trial of rivastigmine showed marked improvement in apathy in PD patients without dementia (Devos et al., 2014). Psychosis, including visual hallucinations and delusions, are usually treated with serotonergic-based antipsychotics (pimvaserin) (Schapira et al., 2017; Weintraub and Mamikonyan, 2019).

Regarding autonomic dysfunction, in patients with orthostatic hypotension fludrocortisone and noradrenergic drugs (α_1-adrenoceptor agonists, NA transporter inhibitors or droxidopa (approved in the United States)) are often used. Constipation is usually managed by fibre supplements or laxatives. Urinary dysfunction is treated with anticholinergic agents (oxybutynin or tolterodine), β3-adrenergic agonists (mirabegron) and botulinum toxin injections (Palma and Kaufmann, 2018).

1.2. The locus coeruleus

The LC is the main source of NA in the brain (Dahlstroem and Fuxe, 1964). Despite being one of the smallest nuclei in the brain, thanks to its strategic location, the LC is a crucial nucleus whose broad noradrenergic projection network explains its implication in many physiological functions and pathological conditions.

1.2.1. Neuroanatomy

A) Localization and composition

The LC is a bilateral nucleus, densely composed by noradrenergic neurons. It is located in the upper dorsolateral pontine tegmentum and is considered the principal noradrenergic nucleus in the central nervous system in humans (**Figure 1.4**) (Amaral and Sinnamon, 1977) and rodents (Dahlstroem and Fuxe, 1964) (**Figure 1.5**).

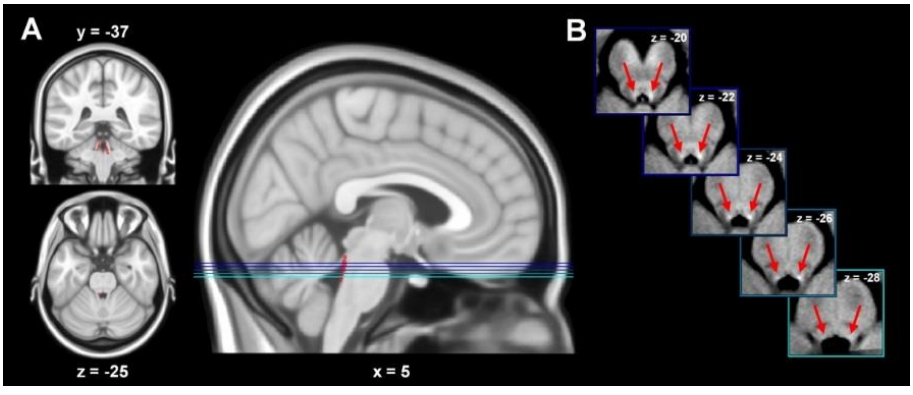

Figure 1.4. Bilateral location of the *locus coeruleus* in a human brain. (A) Spatial extent of the LC (shown in red). (B) Axial slices corresponding to the highlighted lines in the sagittal image. Taken from Murphy et al. (2014).

Figure 1.5. Representation of the bilateral location of the *locus coeruleus* in the rat brain. Coronal slice showing the ventrolateral location to the fourth ventricle (4V). Taken and modified from Paxinos and Watson, 2007.

Noradrenergic neurons are the biggest cell population within the LC and at least two types of cells have been observed, large multipolar and smaller fusiform cells (Swanson, 1976). However, GABAergic interneurons also inhabit the LC making synapses and efficiently inhibiting the noradrenergic neurons (Aston-Jones et al., 2004; Jin et al., 2016; Breton-Provencher and Sur, 2019).

B) Neurochemical content

Within the nucleus, in addition to NA, other neurotransmitters are present such as galanin (Holets et al., 1988), neuropeptide Y (Holets et al., 1988), glutamate (Kaehler et al., 1999b; Timmerman et al., 1999; Somogyi and Llewellyn-Smith, 2001), serotonin (Kaehler et al., 1999a), GABA (Nitz and Siegel, 1997; Kaehler et al., 1999b; Somogyi and Llewellyn-Smith, 2001; Aston-Jones et al., 2004), DA (Versteeg et al., 1976; Kaehler et al., 1999b) or glycine (Somogyi and Llewellyn-Smith, 2001).

Receptor expression is also very heterogeneous. Anatomical and functional studies have revealed the presence of adrenergic (α_1 and α_2) (Young and Kuhar,

1980; Chamba et al., 1991; Alba-Delgado et al., 2012a), acetylcholine (nicotinic) (Egan and North, 1986; Léna et al., 1999), cannabinoid (CB_1) (Scavone et al., 2010), corticotropin releasing factor (CRF_1) (Reyes et al., 2007), dopaminergic (D_1, D_2, $D_{2/3}$) (Yokoyama et al., 1994; Shelkar et al., 2017; Stark et al., 2018), GABAergic ($GABA_A$ and $GABA_B$) (Sinkkonen et al., 2000; Wang et al., 2015), glutamatergic (mGlu, AMPA and NMDA) (Van Bockstaele and Colago, 1996; Dubé and Marshall, 1997; Chandler et al., 2014; Kimura et al., 2015), opioid (μ-opioid and κ-opioid) (Mansour et al., 1994; Van Bockstaele et al., 1996; Reyes et al., 2009; Medrano et al., 2017), orexin ($orexin_1$, $orexin_2$) (Marcus et al., 2001) and serotonergic ($5\text{-}HT_{2A}$, $5\text{-}HT_{2C}$,$5\text{-}HT_3$) (Parker et al., 1996; Ortega et al., 2012; de Freitas et al., 2016) receptors.

C) Efferent and afferent projections

Despite being a tiny nucleus, the LC sends an enormous projecting network, which influences the activity of nuclei all over the brain (**Figure 1.6A**). It sends descending projections to the spinal cord (Westlund et al., 1983; Howorth et al., 2009a; Hirschberg et al., 2017) and densely innervates ascending areas of the CNS as the amygdala (McCall et al., 2017; Llorca-Torralba et al., 2019), cerebellum (Schwarz et al., 2015), dorsal raphe (Kim et al., 2004), hippocampus (Kempadoo et al., 2016; Takeuchi et al., 2016), olfactory bulb (Shipley et al., 1985), paraventricular thalamic nucleus (Beas et al., 2018), superior colliculus (Li et al., 2018a) and cortex, including prefrontal, orbitofrontal, anterior cingulate and primary motor cortices (Chandler et al., 2014; Hirschberg et al., 2017). An individual LC neuron may project to a single or, on the contrary, to various projection areas (Chandler et al., 2019); however, it is not clear if LC afferents differ depending on the projection target. The SNc and the ventral tegmental area also receive modest noradrenergic innervation from the LC (Baldo et al., 2003; Mejías-Aponte et al., 2009). Those areas with intense

dopaminergic innervation as the striatum show sparse noradrenergic innervation (Mason and Fibiger, 1979; Berridge et al., 1997; Delfs et al., 1998; Fitoussi et al., 2013; Zerbi et al., 2019).

The LC can influence dopaminergic transmission distally. Devoto and collaborators have extensively characterized that LC-tyrosine hydroxylase (TH) positive fibres can co-release not only NA but also DA in the cortex, including prefrontal, parietal and occipital cortices involving α_2 adrenoceptor-mediated mechanisms (Devoto et al., 2001, 2003, 2004, 2005a, 2005b). More recently, other authors have also supported that LC activation promotes DA release in the thalamus and hippocampus, contributing to stress and cognitive functions (Smith and Greene, 2012; Kempadoo et al., 2016; Yamasaki and Takeuchi, 2017; Beas et al., 2018).

As for the afferences (**Figure 1.6B**), the LC also receives a large variety of inputs including those from the cerebellum (Breton-Provencher and Sur, 2019), central amygdala (Breton-Provencher and Sur, 2019), dorsal raphe (Kim et al., 2004; Lu et al., 2012), hypothalamus (Marcus et al., 2001; Breton-Provencher and Sur, 2019), paragigantocellularis (PGi) (Aston-Jones et al., 1986; Breton-Provencher and Sur, 2019), periaqueductal gray (Breton-Provencher and Sur, 2019), prepositus hypoglossi (Aston-Jones et al., 1986; Breton-Provencher and Sur, 2019), superior colliculus (Breton-Provencher and Sur, 2019), prefrontal cortex (Lu et al., 2012; Torres-Sanchez et al., 2018; Breton-Provencher and Sur, 2019), SNc (Breton-Provencher and Sur, 2019) and ventral tegmental area (Deutch et al., 1986).

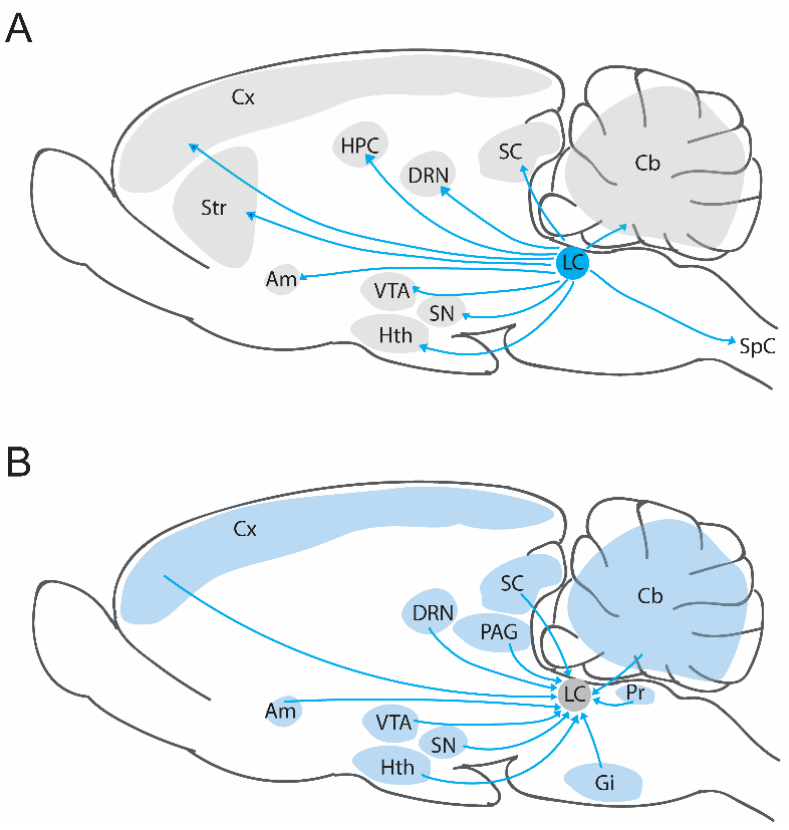

Figure 1.6. Main afferent and efferent projections in the *locus coeruleus* in the rodents' brain. A) The locus coeruleus (LC) sends projections to the amygdala (Am), cerebellum (Cb), cortex (Cx), dorsal raphe nucleus (DRN), hippocampus (HPC), hypothalamus (Hth), striatum (Str), spinal cord (SpC), substantia nigra (SN), superior colliculus (SC) and ventral tegmental area (VTA). B) The LC receives afferents from the amygdala (Am), cerebellum (Cb), cortex (Cx), dorsal raphe nucleus (DRN), gigantocellular nucleus (Gi), hypothalamus (Hth), periaqueductal gray (PAG), prepositus nucleus (Pr), substantia nigra (SN), superior colliculus (SC) and ventral tegmental area (VTA).

1.2.2. Physiology of the locus coeruleus

A) Electrophysiology properties

The LC neurons display two different modes of activity, tonic and phasic discharge (**Figure 1.7**).

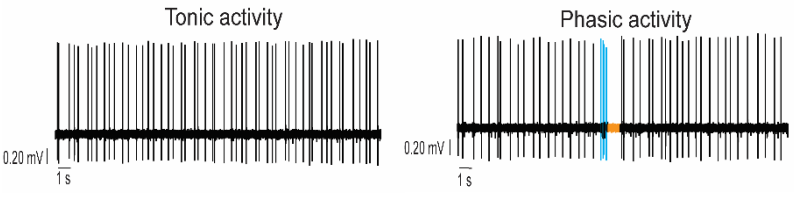

Figure 1.7. Locus coeruleus modes of activity. LC neurons are characterized by discharging in tonic and phasic mode.

Tonic activity of LC neurons is characterized by exhibiting autonomous peacemaking activity, where a combination of Na^+, K^+ and Ca^{2+} currents regulates the spontaneous activity of the cell (Williams et al., 1984, 1988, 1991; Osmanović et al., 1990; Forsythe et al., 1992; Alreja and Aghajanian, 1993; Osmanović and Shefner, 1993; de Oliveira et al., 2010; Sanchez-Padilla et al., 2014; Matschke et al., 2015, 2018). The activation of different receptors also regulates LC tonic activity. The α_2-adrenoceptors, which are associated with the $G_{i/o}$ heterotrimeric G-protein, are the main controllers. The activation of these receptors by NA leads to a progressive reduction in the firing activity, through local feed-back inhibition, and this effect is blocked by pre-treatment with α_2-adrenoceptors antagonists (Cedarbaum and Aghajanian, 1976; Egan et al., 1983; Freedman and Aghajanian, 1984; Elam et al., 1986; Ruiz-Ortega and Ugedo, 1997). Moreover, GABA exerts tonic inhibition acting onto $GABA_B$ receptors in developing rats (Wang et al., 2015).

In addition to the tonic activity, LC neurons are able to discharge in a phasic mode or burst. An increase in the number of burst discharges has been seen to augment the release of NA in the medial prefrontal cortex (mPFC), a target of LC projections (Florin-Lechner et al., 1996). This mode of function has been associated to responses to sensorial stimuli or to the task processing, that will evoke a burst discharge of LC neurons (Grant and Weiss, 2001; West et al., 2009, 2010). This phasic mode is consistently associated with a low tonic discharge and high levels of task activity performance. On the contrary, higher levels of tonic activity with low phasic response to task events has been related to poor performance on tasks that require focused attention and corresponds to apparent increases in distractibility (Aston-Jones and Cohen, 2005).

Regarding the oscillatory activity, investigations performed in slices containing the LC have provided evidence of a tendency across the nucleus to discharge following a synchronous pattern, it is believed that electrical coupling between dendrites outside the cell body region promote this synchrony (Christie et al., 1989; Ishimatsu and Williams, 1996). However, the synchronous pattern within the LC disappears with age in adult rats (Christie et al., 1989). In this line, a recent study in anaesthetized rats, using a high-channel density recordings to gather a dense data package from the LC population, shows that only a small proportion of unit pairs have synchronized spontaneous discharge. Moreover, this little synchronized activity was found to be present only in subsets of LC neurons which tend to project to similar forebrain targets (Totah et al., 2018).

B) Cell diversity

The availability of new technologies, as optogenetics and chemogenetics, that allow efficient activation/inhibition of specific anatomical projections or cellular subtypes, unravelled that the LC is a more heterogeneous nucleus than previously proposed. Indeed, there is emerging evidence suggesting that the LC does not necessarily act functionally as a uniform cluster of neurons, but more as specialized subsets. Various publications demonstrate that subpopulations of LC neurons send different projections to the mPFC, orbitofrontal cortex, motor cortex, spinal cord or basolateral amygdala (Chandler et al., 2014; Li et al., 2016; Hirschberg et al., 2017; Llorca-Torralba et al., 2019).

Along with the segregate connections, LC neurons that innervate the PFC (mPFC or orbitofrontal cortex) differ biochemically and electrophysiologically from the neurons projecting to the motor cortex. For instance, the majority of the LC neurons project to the PFC and contains higher levels of mRNA transcripts coding for markers of excitability and release (AMPA receptor subunit GluR1, NMDA receptor subunit NR1, VMAT2 and voltage-gated sodium channel subunit β3), display increased spontaneous firing rate, as well as enhanced size and frequency of glutamate-mediated excitatory postsynaptic currents (Chandler et al., 2014). Electrophysiological specialization of spinally projecting LC neurons was also reported, since the action potential duration was shorter and the afterhyperpolarization was smaller in comparison to the rest of LC neurons (Li et al., 2016). In a recent publication (Totah et al., 2018) two types of LC units were identified according to their spike waveform width, which show different firing frequency and spatial distribution. Despite overall sparse population synchrony, neurons with a brief synchronous activity (over submilliseconds) were more likely

to project to the same forebrain region. These recent findings suggest an important cellular diversity and distinct functional roles of LC neurons.

Apart from the cell diversity, the LC also accounts sex differences at molecular and functional levels, suggesting that this dimorphism may influence behavioural differences for certain diseases, as anxiety. A recent study showed elevated expression of the prostaglandin EP3 receptor in the LC from female mice, whose agonism produced a stronger inhibitory effect on LC firing and LC-driven anxiety behaviour (Mulvey et al., 2018). In addition, significant reduction in the μ-opioid receptor-mediated inhibition and μ-opioid receptor expression has been reported in the LC from females rats, what has been related to less impulsive behaviour and higher perseverative responses in comparison to male rats (Guajardo et al., 2017).

1.2.3. Implication of the locus coeruleus in physiological and pathological conditions

As consequence of its widespread axonal projections, the LC has a critical role in a diverse range of functions as the nociceptive transmission, anxiety, sleep/wake states and cognition.

One of the most studied physiological function of the LC is its participation in the nociceptive transmission. Sensory stimulation triggers the transmission of the information from the spinal cord to supra-spinal levels as the PGi, which innervates the LC, and from there the signal is send to the thalamus and cortical structures (Andrezik et al., 1981; Aston-Jones et al., 1986; Ennis et al., 1992; Llorca-Torralba et al., 2016; Neves et al., 2018; Vazey et al., 2018; Breton-Provencher and Sur, 2019). On one hand, the LC is implicated in the descending pain modulatory pathway

through its projections to the spinal cord. The NA released at spinal levels suppresses the transmission of the sensory information via α_2-adrenoreceptors, promoting analgesia in control and pain model animals (Hentall et al., 2003; Hirschberg et al., 2017). On the other hand, optoactivation of the LC evoked antinociceptive or pronociceptive effects, suggesting the existence of different subpopulations in the LC with bidirectional influence in pain perception and aversion/anxiety (Hickey et al., 2014). Cellular segregation has helped to further characterize the LC diversity. Selective activation of cells with ascending projections to the mPFC or to the basolateral amygdala promotes emotional aversive aspects of pain in a model of neuropathic pain (Hirschberg et al., 2017; Llorca-Torralba et al., 2019).

The LC noradrenergic system also plays a major role in the apparition of negative emotions such as anxiety, stress, defensive and aversive behaviour, driven by the activation of different efferent projections. Activation of the LC-mPFC and LC-basolateral amygdala pathways mentioned above is aversive and anxiogenic in control animals (Hirschberg et al., 2017; McCall et al., 2017; Llorca-Torralba et al., 2019). At the same time, stimulation of inputs originated in the central amygdala to the LC increases tonic LC activity and induces anxiety-like and aversive behaviours, through the endogenous corticotropin releasing hormone (McCall et al., 2015). Interestingly, corticotropin-releasing factor antagonist administration during stress decreased tonic LC discharge, which was opioid-mediated (Curtis et al., 2012). Moreover, activation of LC projections to the superior colliculus mediates stress-induced accelerated defensive responses to looming, in an adrenergic receptor dependent manner (Li et al., 2018a). Regarding the implication of the LC in depression, depressive-like behaviour is observed following loss of LC noradrenergic neurons (Szot et al., 2016).

The LC noradrenergic neurons have been long related to the modulation between sleep/waking states proving a causal relationship between LC noradrenergic neuron firing, sleep-to-wake transitions and maintenance of wakefulness (Aston-Jones and Bloom, 1981a; Carter et al., 2010). More recently, it has been revealed that GABAergic neurons in the LC reduce noradrenergic neuron mediated arousal (Breton-Provencher and Sur, 2019). In addition, LC noradrenergic neuron activation accelerates behavioural emergence from deep isoflurane anaesthesia, through β and α_1-adrenorecceptors (Vazey and Aston-Jones, 2014).

Noradrenergic fibres originated in the LC have been identified in brain areas related to memory/cognition such as the dorsal hippocampus and PFC. It has long been believed that dopaminergic signalling in the dorsal hippocampus comes mainly from the ventral tegmental area (Lisman and Grace, 2005). However, recent publications have reported that LC-TH^+ fibres densely innervate the dorsal hippocampus, co-realising both neurotransmitters, NA and DA and subsequently promoting spatial learning and memory via the dopaminergic D1/D5 receptor (Kempadoo et al., 2016). Other authors reported that LC activation successfully enhances memory retention, presumably mimicking the response to environmental novelty (Takeuchi et al., 2016). The LC also regulates cognitive functions through its projection to the PFC. Indeed, lesion of these noradrenergic afferents impairs attentional set-shifting, a measure of attention and cognitive flexibility (Newman et al., 2008), and stimulation of LC terminals in the PFC improves it (Cope et al., 2019).

Interestingly, many of the pathological situations triggered by the dysfunction of the LC are present in PD, stressing the role of this nucleus in the development of the non-motor complications of the disease.

1.3. The noradrenergic system in Parkinson's disease

In the last decades, researchers have shown increasing interest in further understanding the pathophysiological basis of the non-motor symptoms present in PD, with special focus on the noradrenergic system.

1.3.1. Noradrenergic dysfunction in Parkinson's disease

A) Anatomical and functional studies

There is substantial evidence showing degeneration of the noradrenergic system in patients with PD. Numerous anatomical *post mortem* studies in brains of patients with PD have documented a moderate to severe cell loss (around 30-90%) and Lewy body pathology in the LC, equal in magnitude throughout the rostral-caudal parts of the nucleus (Gaspar and Gray, 1984; Chan-Palay and Asan, 1989; German et al., 1992; Bertrand et al., 1997; Zarow et al., 2003; McMillan et al., 2011). Specifically, neuromelanin-containing medium-size LC neurons present somatic and dendritic alterations, whereas smaller non-noradrenergic LC cells do not show severe pathological changes (Patt and Gerhard, 1993). Consistent with LC neuron loss, patients with PD show decreased noradrenergic innervation of LC target structures, including prefrontal and motor cortex, striatum, thalamus, hypothalamus, and cerebellum (Kish et al., 1984; Shannak et al., 1994; Pavese et al., 2011; Pifl et al., 2012; Sommerauer et al., 2018b). The atrophy of TH-containing axons is not restricted to the central nervous system, since a prominent loss of noradrenergic innervations of the peripheral autonomic system has been demonstrated, including the left cardiac ventricle (Hakusui et al., 1994; Takatsu et al., 2000; Slaets et al., 2015). Recent neuromelanin-sensitive magnetic resonance studies found progressive loss of the LC signal in both, idiopathic or genetic PD

patients and late- or early-stage patients; even distinguishing a lower signal in those PD patients with depressive symptoms (Sasaki et al., 2006; Ohtsuka et al., 2013; Castellanos et al., 2015; Schwarz et al., 2017; Wang et al., 2018). ^{18}F-dopa positron emission tomography imaging, as an index of monoaminergic nerve terminal function, have also demonstrated reduced uptake in the LC, indicating progressive loss of noradrenergic terminal function in parkinsonian patients (Pavese et al., 2011) (**Figure 1.8**). LC in vivo imaging has the potential to provide new pathophysiological insights, as it is likely to change with disease progression, and stratify patients according to noradrenergic dysfunction (Betts et al., 2019). In fact, it was recently shown that in vivo magnetic resonance imaging of brain cell water delineates the LC not only in human, but also in mice (Watanabe et al., 2019), and that pupil diameter covaries with blood-oxygen-level-dependent functional magnetic resonance in human LC (Murphy et al., 2014).

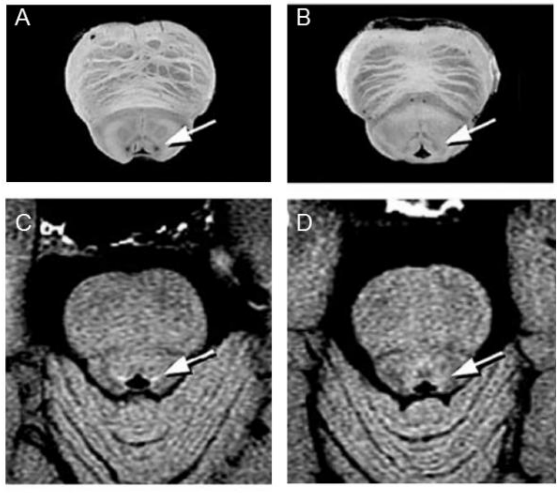

Figure 1.8. Findings in the locus coeruleus of Parkinson's disease patients. (A) Macroscopic image from the brain of a cadaver without PD showing presence of neuromelanin in the LC (arrow). (B) Macroscopic image from the brain of a patient with pathologically proven PD with reduced neuromelanin pigment in the LC (arrow). (C) Neuromelanin magnetic resonance of a healthy control, hyperintensity found at the LC (arrow). (D) Neuromelanin magnetic resonance of a patient with PD, the hyperintensity areas indicating the LC (arrow) do not emerge. Taken and modified from Sasaki et al. (2006).

Anatomical studies using the unilaterally 6-OHDA lesioned rat model show that the number of LC neurons is not affected by the DA loss (Miguelez et al., 2011b; Oliveira et al., 2017; Ostock et al., 2018), but MPTP-treated monkeys exhibit LC cell loss (Pifl et al., 1991). Few electrophysiological studies using anaesthetized 6-OHDA lesioned animals have also revealed that experimental DA degeneration influences LC neuron basal activity. In this regard, results are contradictory reporting increased or decreased activity, and altered response to antidepressant agents in parkinsonian rodents (Wang et al., 2009; Miguelez et al., 2011a, 2011b).

B) Neurochemical studies

Although plasma NA levels are elevated in de novo patients with PD (Ahlskog et al., 1996), neurochemical studies have reported lower levels of the neuronal NA metabolite, dihydroxyphenylglycol, in the cerebrospinal fluid (Goldstein et al., 2012), as well as marked reduction of DA-beta-hydroxylase activity, an enzyme responsible for hydroxylation of DA to NA, in parkinsonian patients (Hurst et al., 1985; O'Connor et al., 1994). Regarding changes in adrenergic receptors in PD, an in vitro autoradiographic study showed upregulation of α_1- and β_1- adrenoreceptors and reduced density of α_2-adrenoreceptors in the PFC of post mortem parkinsonian patients (Cash et al., 1984).

Animal studies performed in the unilateral 6-OHDA model have reported that NA levels in different projection areas are variably decreased. In the PFC of the lesioned hemisphere, some authors found unchanged (Delaville et al., 2012a, 2012b) or reduced NA concentrations (Shin et al., 2014; Ostock et al., 2018). Similarly, other areas with sparse noradrenergic innervation, as the striatum, show unchanged (Shin et al., 2014; Ostock et al., 2018) or lower NA levels (Ostock et al., 2015) but increased noradrenergic transporter sites (Chotibut et al., 2012). Bilateral models of 6-OHDA

show, however, more robust NA deficits in the cortex and striatum (Vieira et al., 2019). Another widely used model of PD, the MPTP-treated monkeys, exhibits clear noradrenergic damage, such as lower NA concentrations in several brain regions and reduced noradrenergic innervation of the SNc and the subthalamic nucleus (Pifl et al., 1991; Masilamoni et al., 2017). Some publications have also reported low NA striatal, cortical and olfactory bulb tissue content in MPTP-treated mice (Dluzen, 1992; Luchtman et al., 2009; Nayyar et al., 2009; Ando et al., 2018). Evidence regarding the integrity of the noradrenergic system in transgenic mice models of PD is more scarce but also stresses noradrenergic impairment in some, but not all, parkinsonian genotypes, as parkin- or LRRK-null mice, Pink1-/-rats or mice expressing A53T human α-synuclein (Giasson et al., 2002; Von Coelln et al., 2004; Sotiriou et al., 2010; Grant et al., 2015; Giaime et al., 2017; Cullen et al., 2018).

1.3.2. Implications of the noradrenergic dysfunction in Parkinson's disease

The degeneration of the noradrenergic system in the CNS and periphery occurring in PD is associated with a broad spectrum of non-motor symptoms that encompass autonomic, behavioural and cognitive parameters. In accordance with the predicted Braak's stages, the different clinical features due to noradrenergic dysfunction can be observed along the progression of the disease (Halliday et al., 2011) and, often appear before the onset of motor symptoms. Detecting noradrenergic impairment could be used as a diagnostic biomarker for early detection of the neurodegeneration (Betts et al., 2019). The following non-motor complications appear in the course of the disease and can be associated, at least in part, with malfunctioning of LC neurons.

Sympathetic autonomic dysfunction

Patients with symptomatic orthostatic hypotension exhibit decreased LC neuromelanin signal on magnetic resonance studies (Sommerauer et al., 2018a) and low plasma levels of NA, which is associated with supersensitivity of vascular adrenergic receptors and an up-regulation of platelet α_2-adrenoceptors (Senard et al., 1990). The clearest clinical laboratory correlate of dysautonomia in PD is the loss of myocardial noradrenergic innervation, detected by cardiac sympathetic neuroimaging (Jain and Goldstein, 2012). Urinary and sexual dysfunctions are late features of PD related to degeneration of brain regions that innervate the bladder, among them the LC (Micieli et al., 2003; Park and Stacy, 2009).

Sleep disturbances

Sleep impairments, which are often premotor manifestations may underlie LC dysfunction, since this nucleus contributes to the control of arousal and sleep-wake cycle (Carter et al., 2010). In fact, post mortem examinations of patients with REM sleep behaviour disorder without motor symptoms revealed neuronal loss and Lewy bodies in the LC (Uchiyama et al., 1995). Recently, neuromelanin-sensitive magnetic resonance have linked LC neuromelanin levels with amount of REM sleep without atonia in patients with PD (Sommerauer et al., 2018a).

Sensory features: pain

Despite the link between the noradrenergic system and the nociception, this relationship has been hardly explored in patients with PD. Treatment with duloxetine, a selective serotonin and norepinephrine reuptake inhibitor, relieved pain symptoms with a suspected central origin in 65% of the patients. Improvements in subjective measures included better quality of life and general pain scores, but no effect on heat-pain threshold have been reported (Djaldetti et al., 2007).

Neuropsychiatric disorders

There is strong evidence supporting the correlation between noradrenergic function and depression in patients with PD. In fact, in PD patients with depression neuroimaging and neuropathological studies have demonstrated a reduction of [^{11}C]RTI-32 (catecholaminergic binding ligand) binding in the LC and projecting regions of the limbic system areas (cingulate cortex, thalamus, ventral striatum or amygdala), as well as gliosis and cell loss at the LC level (Remy et al., 2005; Frisina et al., 2009). Mostly, selective serotonin reuptake inhibitors and tricyclic antidepressants have demonstrated significant, but not total, clinical improvement (Schrag and Taddei, 2017; Ryan et al., 2019). In fact, a negative correlation was found between the level of DA and NA transporter availability in the LC and the severity of anxiety in patients with PD and depression (Remy et al., 2005).

The loss of LC neurons and decreased noradrenergic connections to forebrain areas are associated with cognitive dysfunction in PD (Cash et al., 1987; Rommelfanger and Weinshenker, 2007; Vazey and Aston-Jones, 2012; Sommerauer et al., 2018a). Flexibility in cognitive processing is an essential function of PFC and loss of prefrontal noradrenergic input has been proposed to contribute to prodromal cognitive deficit (Vazey and Aston-Jones, 2012). Although dementia in PD is related to a substantial reduction in cortical cholinergic markers, PD patients with dementia show more severe loss of noradrenergic input from the LC to cortical areas, in comparison with the cases without dementia (Chan-Palay and Asan, 1989). Furthermore, the presence of dementia in patients with PD was associated with significantly lower LC neuronal counts (Zweig et al., 1993). Other studies have also related dementia severity to LC dysfunction, since the signal obtained through neuroimaging of the LC was significantly decreasing over these three conditions:

control, patients with PD and patients with PD and mild cognitive impairment (Li et al., 2019).

Animal studies

At the behavioural level, regardless discrepancies found through the scientific publications, parkinsonian animals tend to mimic the human symptomatology showing motor and also non-motor impairment (Titova et al., 2017). An array of studies report that rodents lesioned with 6-OHDA or MPTP show anxious and depressive behaviour, pain, cognitive and sleep disturbances (Monaca et al., 2004; Pérez et al., 2009; Berghauzen-Maciejewska et al., 2014; Vo et al., 2014; Kamińska et al., 2017; Charles et al., 2018; Campos et al., 2019; Domenici et al., 2019), more notably in bilateral models of the disease (Ferro et al., 2005; Tadaiesky et al., 2008; Santiago et al., 2010; Bonito-Oliva et al., 2014; Vieira et al., 2019). Although the participation of other nuclei cannot be ruled out, the role of the LC in the mentioned symptoms is widely accepted as previously mentioned.

1.3.3. Neuroprotective effect of noradrenaline on dopaminergic degeneration

Preclinical studies combining noradrenergic and dopaminergic dual lesions have suggested a neuroprotective effect of NA in the process of neurodegeneration of the dopaminergic neurons. Data from MPTP lesions in mice and marmosets stress that LC damage leads to a loss of dopaminergic neurons in the SNc, followed by more pronounced motor deficits (Mavridis et al., 1991; Marien et al., 1993; Bing et al., 1994; Fornai et al., 1995, 1997; Yao et al., 2015; Li et al., 2018b). Conversely, the damage produced by MPTP is reduced when the synthesis of NA is boosted (Kilbourn et al., 1998; Archer, 2016) or the NA transporter is knocked out

(Rommelfanger et al., 2004). A recent publication using mutant mice characterized by the progressive degeneration of DA neurons demonstrated that chronic pharmacological NA transporter blockade ameliorates such degeneration and the subsequent motor impairment (Kreiner et al., 2019). Peripheral administration of the NA transporter blocker atomoxetine also reduced dopaminergic damage in a lipopolysaccharide inflammatory rat model of PD (Yssel et al., 2018). Direct NA damage by the administration of the neurotoxin N-(2-chloroethyl)-N-ethyl-2-bromobenzylamine also produces motor deficits and dopaminergic cell loss in control rats (Af Bjerkén et al., 2019). The mechanism underlying this neuroprotective effect is still unknown, although some publications suggest that NA deficit accelerates DA neurodegeneration by promoting microglial inflammation in the SNc (Yao et al., 2015; Af Bjerkén et al., 2019). Some studies performed in 6-OHDA lesioned rodents also suggest that noradrenergic lesions in parkinsonian rats augment DA neuron vulnerability (Ostock et al., 2014) leading to lower DA levels (Srinivasan and Schmidt, 2003) and worsening of motor performance (Srinivasan and Schmidt, 2003, 2004; Wang et al., 2010; Shin et al., 2014; Ostock et al., 2018). However, other studies using the same 6-OHDA model did not reproduce the latter findings (Delaville et al., 2012a; Guimarães et al., 2013; Ostock et al., 2014; Shin et al., 2014).

Although wide evidence supports the neuroprotective role of the noradrenergic system in parkinsonian animal models, the clinical relevance of this findings are still unknown.

2. HYPOTHESIS AND OBJECTIVES

2. HYPOTHESIS AND OBJECTIVES

PD is a neurodegenerative disorder, which was defined initially by its motor symptoms. However, nowadays it is widely accepted that it is more likely to be a complex disorder rather than a pure motor disease. One of the first area undergoing degeneration in PD is the LC. This nucleus provides extensive innervation throughout the brain, mPFC among others, and plays a fundamental neuromodulatory role participating in stress responses, emotional memory and control of motor, sensory and autonomic functions. Considering these findings, we hypothesized that dopaminergic lesion induces modifications in the LC that could be responsible for the appearance of non-motor PD symptoms.

The **global aim** of this study was to investigate the impact of the DA depletion in the function of LC neurons and the subsequent behavioural consequences.

To this end, the **specific objectives** of the present study were:

I. **To investigate in vivo the electrophysiological changes induced by the DA depletion in LC neuron activity.**

For this purpose, we measured tonic and phasic electrical activity of LC neurons in sham and 6-OHDA lesioned rats. We also analysed its modulation by the α_2-adrenergic agonist, UK 14,304, and L-DOPA.

II. **To characterise the oscillatory activity and synchronization in the LC and between the LC and the mPFC after DA depletion.**

For this purpose, we analysed simultaneous recordings of the LFP and ECoG activity in sham and 6-OHDA lesioned rats. We also investigated the effect of L-DOPA administration in absence or presence of the dopaminergic lesion.

III. **To evaluate ex vivo the impact of DA depletion in neuron activity and excitatory and inhibitory synaptic transmission in the LC.**

For this purpose, we performed whole-cell patch-clamp recordings of LC neuron intrinsic properties, and analysed glutamatergic and GABAergic synaptic transmissions in LC neurons from sham and 6-OHDA rats.

IV. **To investigate the histochemical changes in the LC and modifications regarding the nociceptive and anxious behaviour in parkinsonian rats**

For this purpose, we measured the TH and extracellular signal-regulated kinases 1 and 2 (ERK1/2) expression using the western blot (WB) technique and COX activity in the LC from sham and 6-OHDA rats. In addition, we carried out a battery of nociceptive and anxious behavioural tests in the same experimental groups

3. EXPERIMENTAL PROCEDURES

3. EXPERIMENTAL PROCEDURES

3.1. Animals

139 male Sprague–Dawley rats (SGiker facilities from the University of the Basque Country or Janvier Labs) of 7 weeks of age (±190 g) at the beginning of the experiments were used. They were housed in groups of three-five in standard laboratory conditions (22 ± 1 °C, 55 ± 5% of relative humidity, and a 12:12 h light/dark cycle) with ad libitum access to food and water. Every effort was made to minimize animal suffering and to use the minimum number of animals per group and experiment. Experimental procedures comply with the ARRIVE guidelines and were performed in accordance with the EU Directive 2010/63/EU and Spanish (RD 53/2013) regulations for the care and use of laboratory animals. All protocols were reviewed and approved by the Local Committee for Animal Experimentation at the University of the Basque Country (Leioa, Spain; CEEA/M20-2015-024) and the University of Cadiz (27-04-2016-0872, P001/16).

3.2. Drugs

The drugs used in this study are shown in **Table 3.1**.

All drugs were prepared on the day of the experiment. Benserazide, chloral hydrate, desipramine, L-DOPA, RX 821002, UK14,304 and Dolethal were prepared in physiological saline (0.9% NaCl) and 6-OHDA in milli-Q water containing 0.02% ascorbic acid. For ex vivo recordings drug stocks were prepared in milli-Q water (D-AP5, gabazine, QX 314 chloride and strychnine) or in DMSO (CGP55845, DNQX and picrotoxin) and diluted in artificial cerebrospinal fluid right before application.

Table 3.1. Drugs and antibodies used in the study.

Drug	Activity	Purchased from
6-OHDA hydrochloride (6-Hydroxydopamine)	Catecholaminergic neurotoxin	Sigma-Aldrich
Benserazide hydrochloride	Peripheral DOPA-decarboxylase inhibitor	Sigma-Aldrich
CGP55845	$GABA_B$ receptor antagonist	Tocris
Chloral hydrate	Anaesthetic	Sigma-Aldrich
D-AP5	NMDA antagonist	Tocris
Desipramine hydrochloride	NA reuptake inhibitor	Sigma-Aldrich
DNQX	Non-NMDA receptor antagonist	Sigma-Aldrich
Dolethal (Pentobarbital Sodium)	Anaesthetic	Vetoquinol
Gabazine	$GABA_A$ receptor antagonist	Sigma-Aldrich
Isoflurane	Anaesthetic	Esteve
L-DOPA	Precursor of dopamine	Sigma-Aldrich
Picrotoxin	$GABA_A$ receptor antagonist	Abcam
QX 314 chloride	Na^+ channel blocker	Tocris
RX 821002 hydrochloride	α_2-adrenoceptor antagonist	Sigma-Aldrich
Strychnine hydrochloride	Glycine receptor antagonist	Sigma-Aldrich
UK14,304 tartrate	α_2-adrenoceptor agonist	Tocris

Antibody	Activity	Purchased from
Rabbit anti-TH	Primary antibody	Merk-Millipore or Pierce
Biotinylated goat anti-rabbit IgG	Secondary antibody	Vector Laboratories
Goat Anti-rabbit IgG	Secondary antibody	LI-COR
Mouse anti-ERKt	Primary antibody	Cell signaling
Goat anti-mouse IgG	Secondary antibody	LI-COR
Rabbit anti-pERK	Primary antibody	Neuromics
Goat Anti-rabbit IgG	Secondary antibody	LI-COR

3.3 Experimental design

The design and timeline of the experiments are shown in **Figure 3.1.** At the beginning of all the studies, rats received 6-OHDA or vehicle injections into the right medial forebrain bundle (MFB); the groups are referred to as sham or 6-OHDA rats. Prior to the electrophysiological or behavioural experiments, the dopaminergic lesion was screened using the cylinder test. Only those animals showing a use of the contralateral forelimb compatible with severe dopaminergic loss (see section 3.6.1) further followed the experimental protocol. At the end of the experiments, TH immunostaining confirmed *post mortem* the severe dopaminergic depletion.

Study I

In vivo single-unit extracellular recordings of LC cells were obtained two (sham n=8 and 6-OHDA n=9) and four (sham n=11 and 6-OHDA n=13) weeks after the stereotaxic injection of 6-OHDA or corresponding vehicle. In order to study LC tonic and phasic neuron activity, baseline recordings and sensory-evoked responses triggered by a paw compression were acquired in anaesthetized rats. For studying the effect of DA replacement, L-DOPA (24 mg/kg plus benserazide 12 mg/kg, i.p.) was administered and LC cell recordings were obtained from 30 to 90 min after. An additional set of animals (8 sham and 9 6-OHDA animals) received cumulative increasing doses of the α_2-adrenoceptor agonist, UK 14,304.

Study II

In vivo local field potential (LFP) from the LC and electrocorticograms (ECoG) from the mPFC were recorded four weeks after the lesion in anaesthetized rats (sham n=9 and 6-OHDA n=11). LFP and ECoG were simultaneously recorded in absence or presence of L-DOPA (24 mg/kg plus benserazide 12 mg/kg, i.p.), as

described above. In addition, the impact of a paw compression in the LFP and ECoG was analysed.

Study III

Ex vivo, patch clamp electrophysiological recordings were performed four weeks after the lesion in brain slices from 23 sham and 27 6-OHDA animals. LC basal intrinsic properties, as well as spontaneous and evoked glutamatergic and GABAergic synaptic transmission were evaluated.

Study IV

TH expression and ERK1/2 activation were studied by WB procedures (6 animals per group). In a parallel group of animals (sham n=6; 6-OHDA n=6), COX activity was also analysed. Nociceptive and anxiety testing was performed in sham (n = 8) and 6-OHDA lesioned rats (n = 11). Nociceptive behaviour was evaluated one week before and during four weeks (once per week) after the surgery. Anxiety behaviour was evaluated five weeks after the lesion.

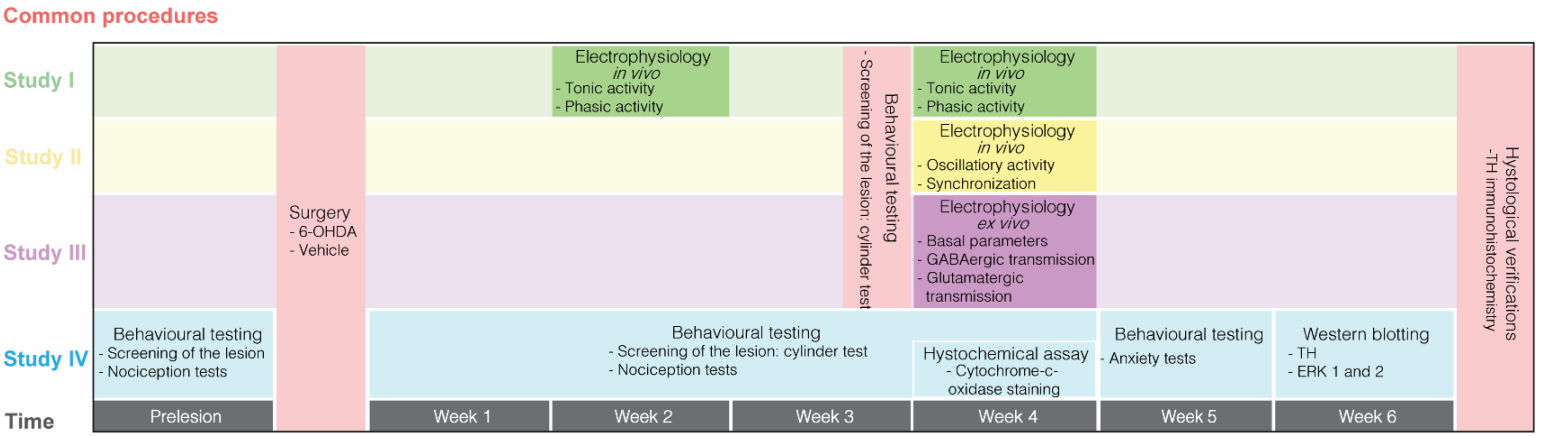

Figure 3.1. Schematic representation of the experimental design in the four studies. At the beginning, all animals received a vehicle or 6-OHDA injection into the right medial forebrain bundle. **Study I:** *in vivo* single-unit extracellular recordings were obtained two and four weeks after the surgery. At those time points, tonic and sensory-evoked phasic activity of the LC cells was evaluated. **Study II**: oscillatory and synchronization activity from the LC LFP and the mPFC ECoG were recorded four weeks after the lesion. **Study III:** four weeks after the lesion, whole cell patch clamp recordings from LC cells were performed in brain slices. **Study IV**: behavioural tests were evaluated one week before the lesion and during five weeks after; COX activity was evaluated during the fourth week and TH and ERK1 and 2 activation was obtained in the sixth week. Histological verifications of the severity of dopaminergic lesion was done by TH immunostaining at the end of each set of experiments.

3.4. Dopaminergic lesion with 6-OHDA

The most extensively used animal model of PD is the 6-OHDA lesioned rat model (Ungerstedt, 1968). The toxin is injected in the MFB, where enters in the dopaminergic fibres of the neurons through the DA transporter. Retrogradely 6-OHDA is transported to the dopaminergic cell bodies of the SNc where it causes the neuronal death.

Animals were unilaterally lesioned with 6-OHDA following the protocol described in (Miguelez et al., 2011b) with some modifications and represented in **Figure 3.2**. Animals were anesthetized with isoflurane (4% for induction and 1.5-2% for maintenance) and placed in the stereotaxic frame (David Kopf® Instruments, Tujunga, California, EEUU, model 957). For preventing damage in the noradrenergic system, desipramine (25 mg/kg, i.p.) was administered thirty minutes before the injection of 6-OHDA. The scalp was incised, the skull exposed and a hole (0.5-1 mm diameter) drilled over the right MFB. 6-OHDA (3.5 µg/µl) was injected using a Hamilton syringe in the following coordinates (relative to bregma and the dural surface): AP=-4.0 mm, ML=-0.8 mm, DV=-8.0 mm, (tooth bar=+3.4; 2 µl deposit); and AP=-4.4, ML=-1.2, DV=-7.8 (tooth bar=-2.4; 2.5 µl deposit). The toxin was infused at a rate of 1 µl per min by a syringe infusion pump (KDS Scientific, Massachusetts, USA). The needle was left in the site of injection for additional 2-4 mins to allow the toxin to diffuse into the structure, before its slow retraction. Sham animals received exactly the same procedures, but using vehicle (0.02% ascorbic acid in MiliQ water) instead of 6-OHDA. The severity of the dopaminergic loss was first screened with the cylinder test and verified post mortem with TH immunohistochemical assays.

The 6-OHDA solutions were prepared daily for each session and changed every 2-3 h. The solution was kept in the dark and on ice during surgery to avoid oxidation, which is indicated by a colour change (clear to brown-pink colour).

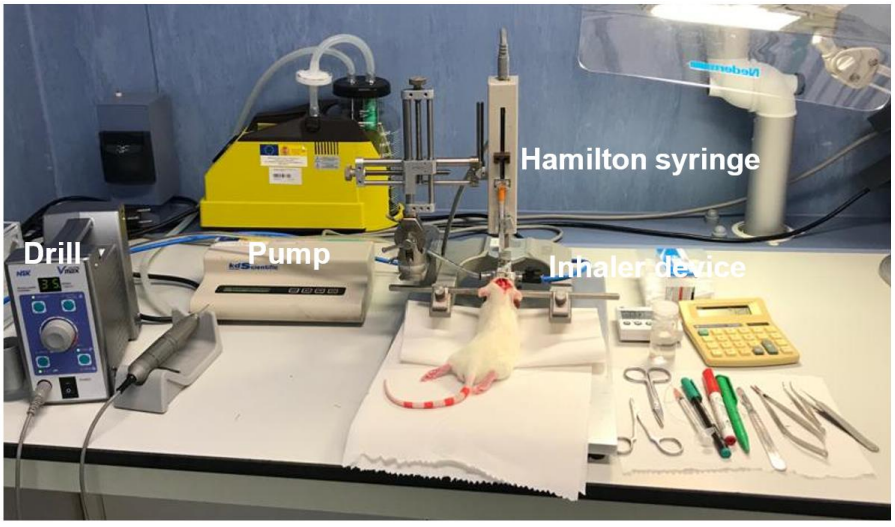

Figure 3.2. 6-OHDA lesion procedure. Animals were mounted on a stereotaxic frame and maintained under isoflurane anaesthesia. A hole was drilled on the skull and 6-OHDA was injected by means of a Hamilton syringe connected to a pump.

3.5. Electrophysiology procedures

3.5.1. In vivo single-unit extracellular recordings of *locus coeruleus* neurons in anesthetized rats

A) Animal preparation

Animals were anaesthetized intraperitoneally with chloral hydrate. For induction of the anaesthesia, 420 mg/kg was used, followed by continuous administration of the anaesthetic at a rate of 115.5 mg/kg/h, using a peristaltic pump to keep a steady level of anaesthesia. For intravenous drug administration, a catheter

was inserted in the jugular vein. After, the animal was placed in the stereotaxic frame (David Kopf® Instruments, Tujunga, California, EEUU, model 957) and the body temperature was maintained at 37 °C for the entire experiment by means of a heating pad connected to a rectal probe (RTC-1 Thermo Controller, Cibertec).

The head was oriented at 15º to the horizontal plane (nose down) and a burhole was drilled and using a hydraulic microdrive (David Kopf® Instruments, Tujunga, California, EEUU, model 640) the electrode was stereotaxically lowered in coordinates of the LC (relative to lambda): AP: -3.7 mm, ML: -1.1 mm, DV: -5.5 to -6.5 mm (Paxinos and Watson, 1997).

For those experiments when ECoG activity of the mPFC was recorded, a 1-mm-diameter steel screw was placed above the right mPFC and juxtaposed to the dura (coordinates relative to bregma: AP: +2.6 mm and ML: -0.6 mm) (Paxinos and Watson, 1997). All recordings were performed in the hemisphere lesioned with 6-OHDA (**Figure 3.3**).

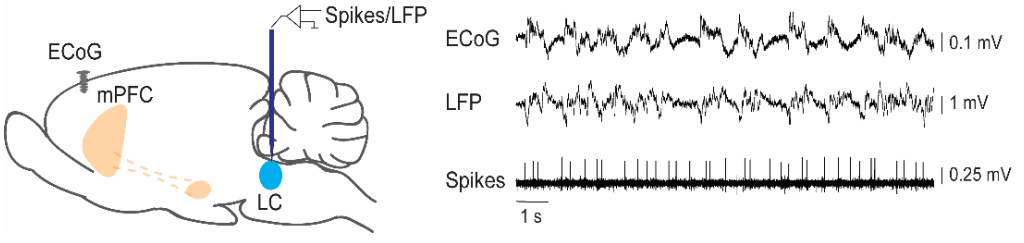

Figure 3.3. Representation of the in vivo electrophysiological studies. Scheme showing the glass electrode in the LC and the mPFC ECoG recording locations. On the right, representative recording tracks of the ECoG, LC-LFP and spikes are shown.

B) Recording electrode preparation

For the recording electrode preparation, Omegadot single glass micropipettes (TW150F-4, World Precision Instruments, UK) were pulled using an automatic vertical electrode stretcher (Narishige Scientific Intrument Lab, model PE-2). After, the tip of the electrode was broken to a tip diameter of 1-2.5 μm (approximately 5–7 MΩ) and filled with a 2% solution of Pontamine Sky Blue in 0.5% sodium acetate.

C) In vivo electrophysiological recordings

Single-unit extracellular recording

LC neuron single-unit extracellular signal from the electrode was first pre-amplified (10X) and later amplified (100X) in a high-input impedance amplifier (Cibertec S.A., model amplifier 88) where the signal was also bandpass filtered (1000 Hz), and then monitored on an oscilloscope (Tektronix® 5111A) and audio monitor (Cibertec S.A., model AN-10). Next, the signal was bandpass filtered at 30-3000 Hz in a second amplifier (Cibertec S.A. model 63AC) and neuron action potentials (spikes) were digitized using computer software (CED micro 1401 interface and Spike2 software, Cambridge Electronic Design, UK). LC neurons were identified by standard criteria (Cedarbaum and Aghajanian, 1976) which included: spontaneous activity displaying a regular rhythm, firing rate between 0.5 and 5 Hz and characteristic spikes with a long-lasting positive–negative waveform (**Figure 3.4**). The basal firing rate was recorded for 3-5 min or until stable baseline was obtained. Procedure is represented in **Figure 3.5**.

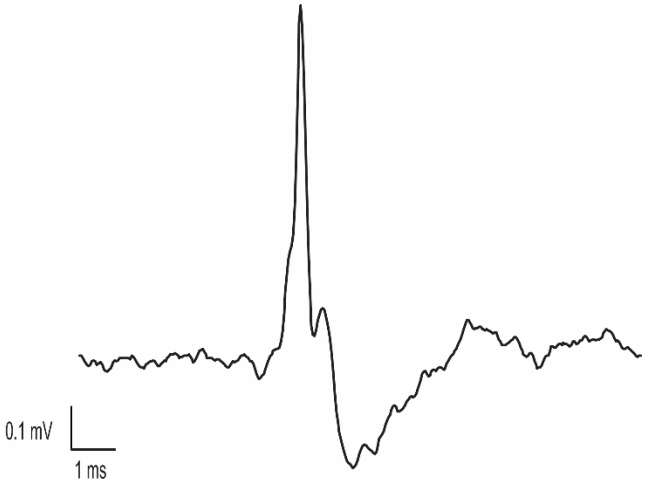

Figure 3.4. Example of a single spike from a locus coeruleus neuron recorded in vivo. Signal was taken from Spike2 recordings. The abscise and ordinate axes represent duration (ms) and amplitude (mV) of the action potential, respectively.

Local field potential

The LFP of the LC was recorded through the same glass electrode used for single-unit extracellular recordings, both signals were recorded at the same time. This signal was amplified (10X) and bandpass filtered (0.1-100 Hz) in a second amplifier (Cibertec S.A., model amplifier 63AC) (**Figure 3.5**). The discriminated LFP activity (sampled at 2500 Hz) was digitized, stored and analysed using computer software (CED micro 1401 interface and Spike2 software, Cambridge Electronic Design, UK).

Electrocorticogram activity

Simultaneous to the recording of the LC LFP, ECoG activity of the mPFC was recorded. The signal was pre-amplified (10X), amplified (200X) and bandpass filtered (0.1-1000 Hz) in an amplifier (Cibertec S.A., model amplifier 63AC) (**Figure 3.5**).

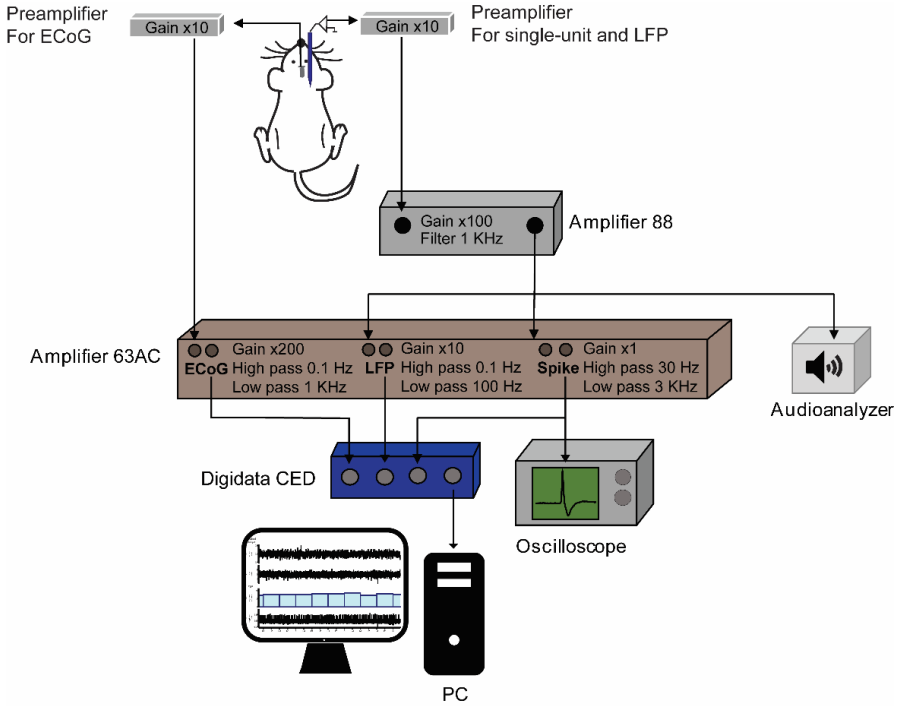

Figure 3.5. Schematic illustration of extracellular electrophysiological procedure *in vivo.* Briefly, the extracellular signal recorded was passed through high input impedance amplifiers, displayed in an oscilloscope, and monitored with an audioanalyser. The signals were analysed by means of the PC-based software Spike2.

Phasic activity

Phasic LC activation, triggered by a sensory stimulus, was recorded after stable basal spontaneous firing. Paw compression was applied manually for 1 s to the contralateral hind paw of the animal, using a surgical forceps as described in (Borges et al., 2017a). This sensory-evoked response is well characterized by a burst discharge followed by a suppression period. For each neuron recorded, sensory-evoked response was applied 5 times at the most with a 100-second interval; similar compression was applied to the ipsilateral paw. To prevent paw damage, no more than 4 neurons were studied per animal. Lastly, the changes in the potential evoked by the compression of the contralateral paw of the animal (event related potentials) were assessed by recording the LFP and the ECoG signals (Ehlers and Somes, 2002).

D) Drug administration

To evaluate the effect of DA replacement, L-DOPA (24 mg/kg plus benserazide 12 mg/kg, i.p.) was acutely administered and LC single unit, LFP and ECoG recordings were obtained from 30 to 90 min after drug administration (Aristieta et al., 2016).

To study the effect of the 6-OHDA lesion on the sensitivity of the α_2-adrenoceptors in the LC, increasing doses of the α_2-adrenoceptor agonist UK 14,304 (2.5-40μg/kg, i.v.) were tested. After complete inhibition of LC neuron activity, the α_2-adrenoceptor antagonist, RX 821002 (100μg/kg, i.v.) was administered to recover cell firing. The changes in firing rate evoked by UK 14,304 were expressed as the reduction relative to the basal firing rate. Sensory-evoked response was measured 40 s after each dose administration. Only one cell was studied in each animal after drug administration.

E) Data analysis

In vivo electrophysiological data was analysed off-line by Spike2 software (Cambridge Electronic Design, UK).

Tonic activity

The following parameters were analysed during a period of 40 s, after, or 90 s before drug administration:

- **Firing rate (Hz)**: Defined as the number of neuronal discharges per second. The data was represented in a bar histogram that showed the mean firing rate each 10 s.

- **Coefficient of variation (%)**: This parameter is related to the interval between consecutive discharges (inter-spike interval) and gives an idea of the regularity of the firing. The representation of the inter-spike interval histogram followed by the analysis ran by Spike 2 (script meaninx.s2s) led to the numerical value. Data was represented in percentage, as the division between the standard deviation and the mean value. The recording period analysed was the same as that one used for the analysis of the firing rate.
- **Burst spikes**: Some LC neurons showed burst firing activity (first interspike interval ≤ 80 ms; termination interspike interval ≤ 160ms). In those neurons the number of burst, percentage of spikes in burst, spikes per burst, burst interspike and burst length were analysed. The analysis of the burst firing was performed using the Spike 2 software (script w_burst.s2s) in the same period as the previous parameters.
- **Dose-effect curve:** Dose-concentration-effect curves were analysed for the best non-linear fit to a logistic three-parameter equation (Parker et al., 1996):

$$E = (E_{max}\,[A]^n)/(ED_{50}^n + [A]^n)$$

$[A]$ is the i.v. dose of the used drug
E is the effect on the firing rate induced by A
E_{max} is the maximal percentage change at "infinite" dose (100 %)
ED_{50} is the effective dose for eliciting 50 % of E_{max}
n is the slope factor of the dose-response curve.

- **Oscillatory activity and synchronization**: LFP and ECoG signals (sampled at 2500 Hz) were smoothed to 1 ms. Cells were classified as oscillatory pattern when the spike waveform autocorrelogram contained a second oscillation peak that was at least twice the magnitude of the random fluctuation and non-oscillatory when only one or no peak appeared.
- **Power spectrum and coherence.** The power spectrum of smoothed ECoGs and LFPs and coherence analyses between LFPs and ECoGs were analysed

using the fast Fourier transform (8192 block size). The mean coherence was calculated from 90-s epochs of data. Statistical significance of the coherence was determined by the equation: $1 - (1 - \alpha)\ 1 / (L - 1)$, where α is 0.95 and L is the number of windows used. The area under the curve (AUC) of coherence and power spectrum curves was calculated in the delta (δ: 0–5 Hz), theta (ϑ: 5–8 Hz), alpha (α: 8–12 Hz) and beta (β: 12–30 Hz) frequency range.

Phasic activity

The parameters of the sensory evoked-response, triggered by the paw compression, which are shown in **Figure 3.6**, were assessed:

- **Evoked firing rate (Hz)**: frequency between the first and last spike of the evoked response.
- **Suppression period (s)**: time after each evoked response in which there was no neuronal activity, until a spontaneous spike was discharged.
- **Percentage of change in the firing rate according to the baseline firing rate (%)**: the tonic activity was measured over an interval of 40 s, starting 10 s after each paw compression. Changes in the postcompression discharge were expressed as the percentage of change in the firing rate according to the baseline for each neuron.
- **Phasic:tonic ratio**: it was calculated as the ratio between evoked frequency and spontaneous activity, also known as signal-to-noise ratio (George et al., 2013).
- **Event related potential (mV)**: the potential is shown 0.5 s before and 2 s after the paw compression. The amplitudes of the peak to trough values at or around zero time were compared.

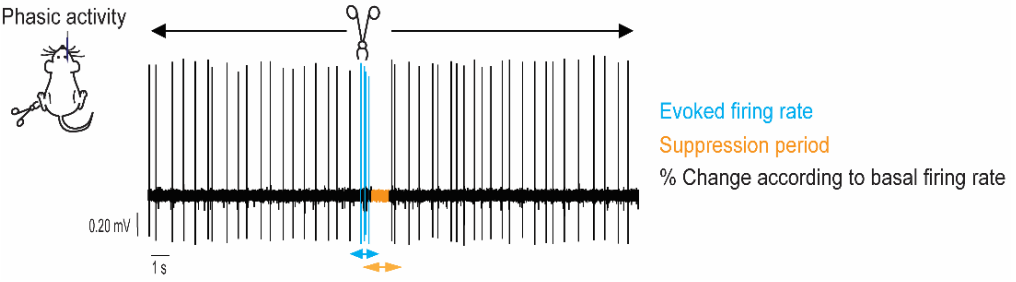

Figure 3.6. Phasic activity triggered by sensory stimulus recorded in locus coeruleus neurons. Parameters studied during the phasic response: evoked firing rate, duration of the suppression period and percentage of change in the firing rate according to the baseline.

3.5.2. Ex vivo patch-clamp recordings of *locus coeruleus* neuron activity in brain slices

A) Brain slice preparation

Rats were anesthetized with chloral hydrate (420 mg/kg, i.p) and perfused transcardially with ice-cold modified artificial cerebrospinal fluid (ACSF), saturated with 95% O2 and 5% CO2, and containing (in mM): 230 sucrose, 26 NaHCO3, 2.5 KCl, 1.25 NaH2PO4, 0.5 CaCl2, 10 MgSO4 and 10 glucose. Immediately, rats were decapitated and the brain was quickly removed. Coronal sections (220 μm) containing the LC were cut using a vibratome (Microm HM 650V) in cold modified ACSF. After cutting, LC slices were incubated to recover for at least 40 min before recording in warmed (35ºC) ACSF containing (in mM): 126 NaCl, 26 NaHCO3, 2.5 KCl, 1.25 NaH2PO4, 2 CaCl2, 2 MgSO4, 10 glucose, 1 sodium pyruvate and 4.9 L-glutathione reduced (equilibrated with 95% O2–5% CO2, pH 7.3–7.4, osmolarity 280-290mOsm/L).

B) Whole-cell patch clamp recordings

Slices were transferred into the recording chamber (**Figure 3.7A**) and perfused continuously with oxygenated ACSF heated to 32-34°C (TC-324B Single Channel Automatic Heater Controller, Warner Instruments). LC neurons were identified, using an upright microscope with infrared optics (Eclipse E600FN, Nikon) and a 60X water-immersion objective (60X/1.00 W, Nikon) (**Figure 3.7B**).

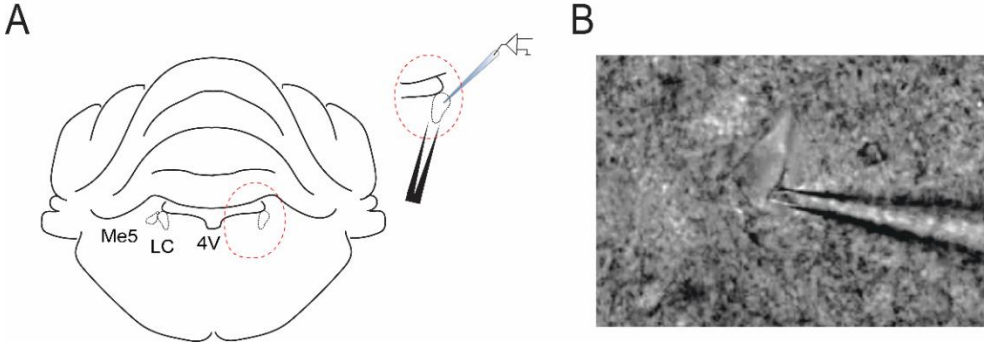

Figure 3.7. Representation of the experimental ex vivo study. (A) Schematic coronal section of a rat brain, illustrating the glass pipette and the stimulating electrode placed in the LC. (B) Image of a LC neuron with a recording patch pipette.

Pipettes were prepared from borosilicate glass capillaries (GC150F-10, Harvard Apparatus) with a micropipette puller (PC-10, Narishige) (impedance, 3–6MΩ). Recordings were obtained using an Axopatch 200B amplifier and Digidata 1322A digitizer (Molecular Devices, Sunnyvale, CA, USA) controlled by Clampex 10.3, the image was visualized in a TV monitor. In whole cell voltage-clamp recordings, cells were hold at –60 mV and series resistance was monitored by a step of –5 mV, discarding the data if it exceeded 25 MΩ or when the series resistance changed ± 20%. Signals were low-pass filtered at 2 kHz and sampled at 10 kHz for voltage clamp mode, and at 5 kHz and sampled at 20 kHz for current clamp mode (**Figure 3.8**).

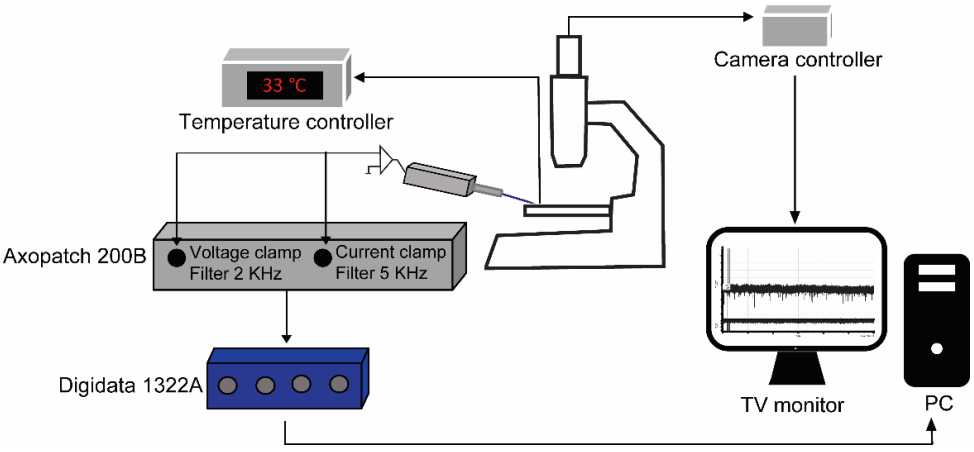

Figure 3.8. Schematic illustration of patch clamp electrophysiological recordings. Briefly, data from the recordings were acquired using an Axopatch 200B amplifier, digitized with a digidata and stored on-line using the pClamp 10 software. To visualize the cells, the image from the microscope was enhanced with a camera to a camera controller and displayed on a TV monitor.

Basal electrophysiological parameters

Intrinsic properties were recorded in whole cell voltage clamp and current clamp mode. For that purpose, borosilicate glass pipettes were filled with an internal solution containing (in mM): 130 K-Gluconate, 10 4-(2-hydroxyethyl)piperazine-1-ethanesulfonic acid (HEPES), 5 NaCl, 1 MgCl2, 1 ethylene glycol-bis(2-aminoethylether)-N,N,N',N'-tetraacetic acid (EGTA), 2 adenosine 5'-triphosphate magnesium salt (Mg-ATP), 0.5 guanosine 5'-triphosphate sodium salt hydrate (Na-GTP), and 10 phosphocreatine disodium salt hydrate (pH: 7.4, 280 mOsm). Junction potential between the pipette internal solution and the ACSF was 15 mV and was not corrected. First, voltage clamp recordings were performed and intrinsic properties of the neurons were analysed using Clampex software: membrane capacitance, membrane resistance, series resistance and time constant. After that, presence of resting inwardly-rectifying potassium (IRK) conductance was recorded by stepping the membrane potential from -50 to -120 mV in -10 mV increments,

100ms/step. Secondly, recordings from LC neurons were made in current clamp mode without current injection (I=0) in order to analyse action potential properties. Last, current pulses were injected, from 0 to 300 pA or -300 to 0 pA (50 pA steps), to evaluate the current-spike frequency and current-voltage curves, respectively.

GABAergic synaptic transmission

To record spontaneous inhibitory postsynaptic currents (sIPSC) and evoked inhibitory postsynaptic currents (eIPSC), NMDA, AMPA, $GABA_B$ and glycine receptor antagonists were added to the ACFS (50 μM APV, 20 μM DNQX, 1 μM CGP55845 and 1 μM strychnine, respectively). The internal solution contained (in mM): 135 CsCl, 3.6 NaCl, 1 MgCl2.6H2O, 10 HEPES, 2 QX-314, 0.1 Na4EGTA, 0.4 Na3GTP and 2 Mg1.5ATP (pH 7.3–7.4, 280-290mOsm/L). Junction potential between the pipette internal solution and the ACSF was 4 mV and was not corrected. sIPSC were recorded at least for 6 minutes. eIPSC were recorded applying five electric pulse trains (600 μA on average, Iso-Flex stimulus isolator A.M.P.I) at 5, 10 and 20 Hz using a bipolar tungsten electrode (TST33A05KT, World Precision Instruments) situated just under the LC. At the end of some experiments, gabazine (10 μM) was added to completely abolish all sIPSC and verify that the recorded signal was exclusively $GABA_A$ mediated transmission (**Figure 3.9A**).

Glutamatergic synaptic transmission

To record spontaneous excitatory postsynaptic currents (sEPSC) and evoked excitatory postsynaptic currents (eEPSC), $GABA_A$ receptor antagonist was added to the ACFS (50 μM picrotoxin). The glass pipettes were filled with an internal solution containing (in mM): 70 $CsSO_4$, 20 CsCl, 20 NaCl, 15 $MgCl_2$, 5 HEPES, 2 QX-314, 1 EGTA, 2 Mg ATP, and 0.5 Na-GTP (pH 7.3–7.4, 280-290mOsm/L). Junction

potential between the pipette internal solution and the ACSF was 15 mV and was not corrected. sEPSC were recorded at least for 6 minutes. eEPSC were evoked by passing five pulse trains (600 μA on average) at 10 Hz using a bipolar tungsten electrode situated just under the LC, as in the eEPSC. At the end of some experiments, DNQX (20 μM) was added to completely abolish sEPSC in order to check the glutamatergic transmission (**Figure 3.9B**).

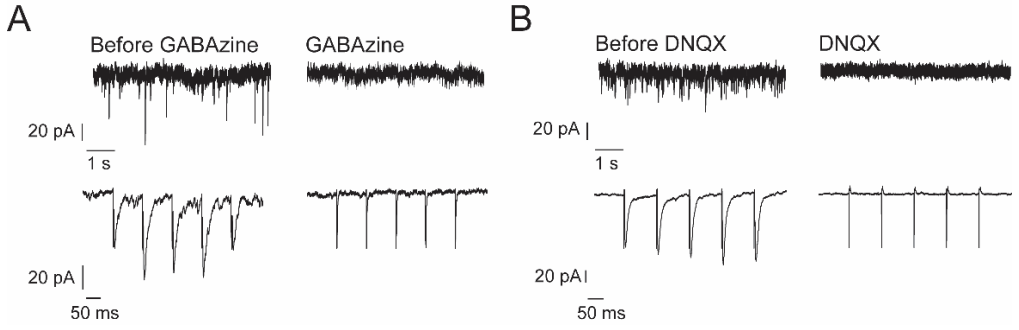

Figure 3.9. Representative spontaneous current traces. (A) Representative current traces of $GABA_A$ mediated sIPSC before and after GABAzine (10 μM) administration. (B) Representative current traces of glutamate-mediated sEPSC before and after DNQX (20 μM) administration.

C) Data analysis

Analyses were carried out off-line using Clampfit application of pClamp 10.3 software.

Basal electrophysiological parameters

- **Electrophysiological intrinsic properties**: membrane capacitance (pF), membrane resistance (MΩ), series resistance (MΩ) and time constant (ms) were measured 1 minute after gaining access to the cell in voltage clamp configuration (**Figure 3.10A**). The software automatically provides these parameters when a pulse of 5 mV is injected.

- **IRK current-voltage curve**: Using voltage clamp configuration, a current-voltage relationship was obtained when the membrane potential was hyperpolarized. Currents were analysed at each voltage injection step during a period of 80 ms.
- **Spontaneous firing frequency (Hz)**: Event frequency is defined as the number of neuronal discharges per second. It was recorded for 200 s, resting potential and threshold were analysed from the same period.
- **Spontaneous action potentials parameters:** peak amplitude (mV), duration (ms) and afterhyperpolarization amplitude (mV) were calculated by averaging at least 4 minutes of recording (**Figure 3.10B**).

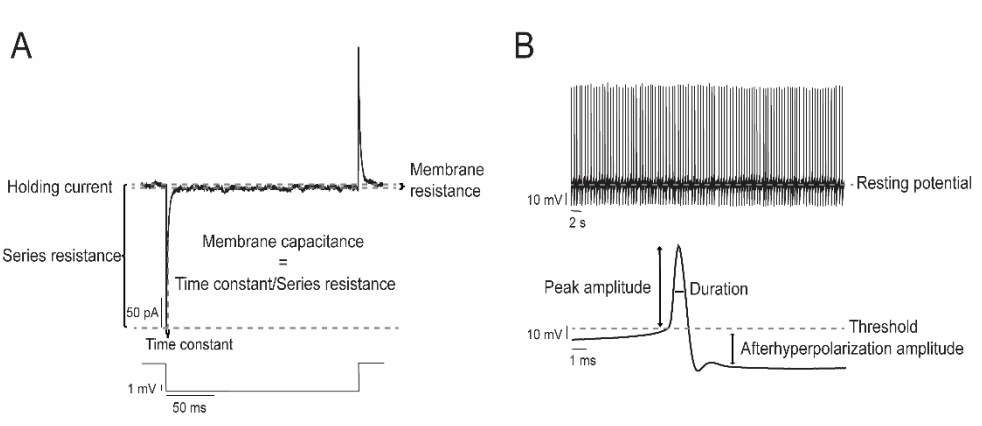

Figure 3.10. Patch clamp whole-cell recordings. (A) Representative trace of the current induced by a -5 mV step and intrinsic membrane properties. (B) Representative trace of spontaneous action potentials and parameters analysed.

- **Current-spike frequency:** current-spike frequency relationship was obtained when the cell was depolarized over several steps in current clamp mode. Currents were analysed at each current injection step during a period of 500 ms. Time after each depolarization in which there was no neuronal activity, until a spontaneous spike was discharge was also analysed an named as suppression period.

- **Current-voltage curves**: current-voltage relationship was obtained when the cell was hyperpolarized over several steps in current clamp configuration. Currents were analysed at each current injection step during a period of 500 ms.

GABAergic and glutamatergic postsynaptic currents

- **sIPSC and sEPSC parameters**: The peak of each spontaneous synaptic current was detected using a semiautomated sliding template detection procedure. The template was generated by averaging multiple spontaneous currents (different templates for sIPSC and sEPSC), the selection was fitted to 3 threshold of the template and each detected event was visually inspected and discarded if necessary. sIPSC and sEPSC were calculated by averaging at least 4 minutes of recording and the following kinetic parameters were calculated: event frequency (Hz), peak amplitude (pA), half-width (ms), 10-90% rise time (ms) and 90-10% decay time (ms) (**Figure 3.11**).

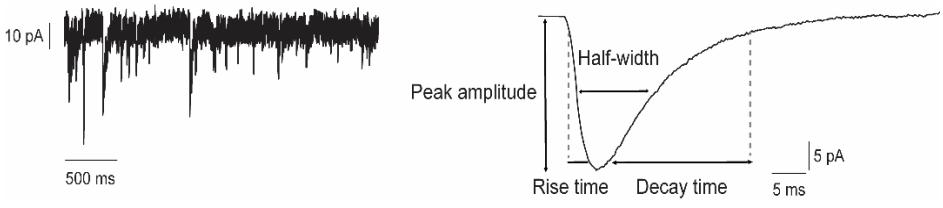

Figure 3.11. Whole cell voltage clamp recordings. Representative trace of spontaneous action potentials and parameters analysed.

- **eIPSC and eEPSC parameters**: The amplitude of eIPSC and eEPSC was calculated by averaging at least ten sweeps. Changes in the probability of GABA and glutamate release were evaluated measuring the PSC_n/PSC_1 ratio, where the amplitude of a consecutive PSC (PSC_n) was divided by the amplitude of the first PSC (PSC_1). Parameters defining GABAergic and glutamatergic short-term plasticity

3.6. Behaviour tests

All tests were conducted between 9:00 and 14:00 h and under dim lighting. Rats were transferred to a noise free testing room at least 30 minutes before the tests for environmental habituation. Before each trial, the apparatus was wiped with ethanol 33% to remove odour traces (**Figure 3.12**).

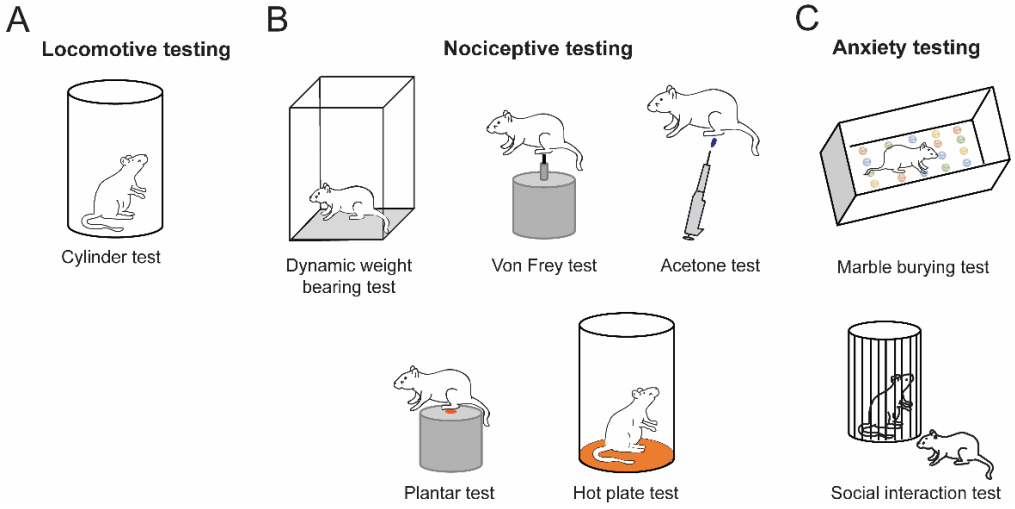

Figure 3.12. Schematic representation of the behavioural tests performed. (A) Locomotive behaviour was evaluated with the cylinder test in order to screen the severity of the 6-OHDA lesion. (B) Spontaneous (dynamic weight bearing test), mechanical (von Frey test) and thermal (plantar test and hot plate) nociception was assessed. (C) Anxiety-like behaviour was evaluated with the marble burying and social interaction tests.

3.6.1. Locomotive behaviour

Forelimb asymmetry was measured with the cylinder test. It is a sensitive and simple test extensively used for screening dopaminergic denervation in rodents hemilaterally lesioned with 6-OHDA. The use of each forelimb during vertical exploration is directly related to the striatal dopaminergic levels (Tillerson *et al.*, 2001).

In order to maximize exploration behaviours, animals were not acclimatized to the cylinder before the initial testing period (**Figure 3.12A**). Rats were placed individually in transparent glass cylinders (Ø 20 cm) with two mirrors positioned at a 90-degree angle behind the cylinder to allow visualization from all directions. The animals were videotaped and scored later. A measure of limb use asymmetry was obtained by counting the number of weight-bearing touches during 5 minutes.

Significant impairment in the lesioned group was defined by comparison with the sham animals. Less than 40% of contralateral paw usage was established as the cut-off value for significant impairment, this value corresponds to the mean minus 2 standard deviations of the performance measured in intact animals (Lundblad et al., 2005).

3.6.2. Nociceptive behaviour

The effect of the 6-OHDA lesion on nociception behaviour was evaluated one week before and for four weeks after the surgery (**Figure 3.12B**). No animal showed signs of damage in the paws once either study was completed.

Dynamic weight bearing

Spontaneous nociceptive behaviour was measured using the dynamic weight bearing test allowing the rat to move freely within the apparatus (Tétreault et al., 2011). The device (Bioseb, Boulogne, France) consisted of a Plexiglas enclosure (22 × 22× 30 cm) with a floor sensor composed of 44 × 44 captors (10.89 mm2 per captor) and a camera appointed to the place of the enclosure. Animals were not acclimatized to the enclosure before the initial testing period in order to maximize exploration behaviour. The rat was allowed to move freely within the apparatus for 5 min. Raw

data were synchronized with the image of the camera and processed by the device software. After the test, an observer validated the areas established, according to the video and the pressure map at the same time. Finally, we obtained the weight of the body distributed on each paw and spontaneous nociception was considered when there was a reduction in the dynamic weight bearing. Percentage of weight with respect to the total weight was represented.

Von Frey test

Sensitivity to non-nociceptive mechanical stimuli was tested using the electronic von Frey hair (Dynamic Plantar Aesthesiometer, Ugo Basile, Italy) (Berrocoso et al., 2011). Animals were placed individually in Plexiglass cages (18.5 x 21 x 13.5 cm) with a mesh floor and habituated for 30 minutes before starting the test. A single filament was applied perpendicular to the hind paw and the force increased (from 0 to 50 g, 20 s maximum) until paw withdrawal. Three measures of each paw were obtained with a separation of 5 minutes. The mean was calculated and established as nociceptive threshold. Mechanical sensitivity was indicated by a reduction in the force that provokes paw withdrawal (Llorca-Torralba et al., 2018).

Hot plate test

This test evaluates the sensitivity to nociceptive stimulus evoked by heat (Woolfe and Macdonald, 1944). Rats were placed into a glass cylinder standing on a hot metal plate maintained at 53 ± 0.5 °C. The time from when the rat was placed until the first hind paw withdrawal/licking was recorded in seconds and a cut-off time was set at 25 s. The time taken to elicit a nociceptive-like behaviour was interpreted as an index of nociceptive threshold and thermal sensitivity was indicated by a reduction in this time. One measurement was performed per day.

Plantar test

To assess sensitivity to nociceptive thermal stimuli the plantar test was used, also known as Hargreave's Method (Plantar Test Instrument, Ugo Basile, Italy) (Hargreaves et al., 1988). Rats were placed individually in small cages with a glass floor and were habituated for 30 minutes before starting the test. A constant intensity of radiant heat (50 A) was generated on the plantar surface of the hind paw until paw withdrawal occured (30-s cut-off). Three measures of each paw were obtained with a separation of 5 minutes. The mean of the three measurements was calculated and established as nociceptive threshold index and thermal sensitivity was indicated by a reduction in the force that provokes paw withdrawal

Acetone test

The acetone evaporation test is a technique used to measure the sensitivity to a non-nociceptive cold thermal stimulus and is considered an indicator of cold allodynia (Choi et al., 1994). A drop of acetone (100 μl) was placed gently on the plantar surface with a pipette. The acetone was applied four times in each hind paw with an interval of 5 min between each application. The responses were recorded according to the scale described previously (Flatters and Bennett, 2004): 0, no response; 1, quick withdrawal of the paw; 2, repeated flicking of the paw; 3, repeated flicking of the paw with persistent licking directed at the ventral side of the paw. The cumulative scores were obtained by summing the four scores for each rat and paw together, being the minimum score 0 (no response to any of the four trials) and the maximum possible 12 (repeated flicking and licking of paws on each of the four trials). Mean punctuation was obtained and divided by 4 and an increase in the response was indicative of cold allodynia.

3.6.3. Anxiety behaviour

The effect of the 6-OHDA lesion on anxiety-like behaviour was evaluated in the sixth week after the surgery (**Figure 3.12C**).

Marble burying test

The marble-burying test has been characterized as a model of anxiety and impulsive behaviour (Njung'e and Handley, 1991). This test is based on the observation that rats spontaneously use bedding material to bury unpleasant sources of discomfort. Rats were placed in Plexiglas cages (45cm x 45 cm x 35 cm) with 3 cm of woodchips on bottom and 20 marbles were spaced in grid-like manner (4x5). Following the 10-minute test period, subjects were carefully removed to minimize disturbance to the bedding. The number of marbles buried was registered, considering buried when at least 75% of the marble was covered with bedding.

Social interaction test

The social interaction test can be used as a measure of anxiety in animals (File and Hyde, 1978). A digital camera was mounted above the social apparatus to track the locomotion of the animal. The activity of the animal was recorded for 15 minutes. Two unfamiliar rats were placed in the arena (40cm x 24 cm x 18 cm); one was the test animal, allowed to move freely, and the other one was a control (Wistar rat), restricted to the cell. The duration of contact was measured and sniffing or approaching to the cell were scored. Data were presented in percentage, as the contact time obtained by the total time.

3.7. Histochemical and quantification procedures

After the behaviour and in vivo electrophysiology experiments, animals were anaesthetised deeply and transcardially perfused with 4% ice-cold buffered paraformaldehyde prepared in 0.1M phosphate buffer. Brains were removed and transferred to 4% ice-cold buffered paraformaldehyde in 0.1M phosphate buffer. In the case of the ex vivo study after decapitation, the remaining brain containing the striatum was transferred to the paraformaldehyde solution. 24 h after, brains were moved to a 25% sucrose and azide 0.1% solution until they sank. Coronal sections of 40 μm were cut using a freezing microtome.

3.7.1. Tyrosine hydroxylase immunostaining

Slices containing the striatum and SNc were processed for TH immunostaining to qualitatively confirm the decreased of dopaminergic fibres expected after induction of the 6-OHDA lesion. Brain sections were rinsed 3 times in potassium-PBS (KPBS), after the endogenous peroxidases were inactivated (3% H2O2 and 10% methanol in KPBS for 30 min). The sections were pre-incubated for 1 h in 5% normal goat serum and 1% Triton X-100 in KPBS. Subsequently, they were incubated overnight with the primary antibody (rabbit anti-TH diluted at 1:1000 in 5% normal goat serum and 0.5% Triton X-100). Afterwards, the sections were incubated with the secondary antibody for 2 h (biotinylated goat anti-rabbit IgG diluted at 1:200 in 2.5% normal goat serum and 0.5% Triton X-100). Sections were processed with an avidin–biotin–peroxidase complex (ABC kit) for 1 h, and the reaction was visualized with 3,3′-diaminobenzidine and 0.03% H_2O_2. Finally, the brain sections were rinsed in KPBS and mounted onto gelatine-coated slides, dehydrated, cleared in xylene and cover slipped with DPX mounting medium (**Figure 3.13**).

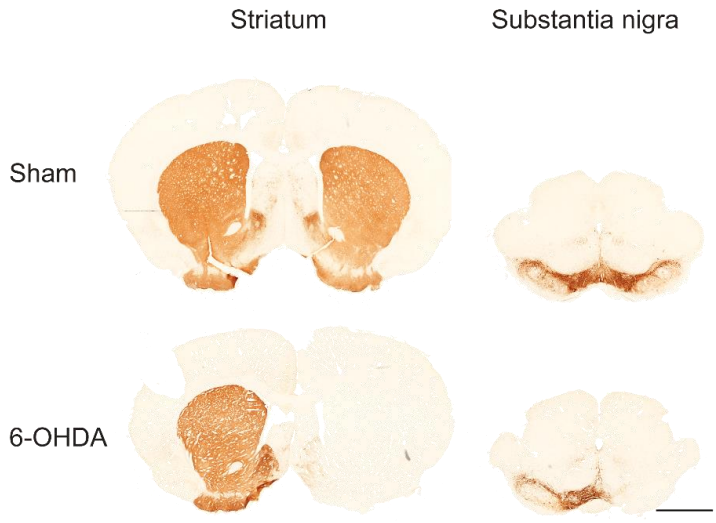

Figure 3.13. Representative photomicrographs of TH-immunostained striatum and substantia nigra. Sham (upper panels) and 6-OHDA (bottom panels) animals (scale bar 2 mm).

The TH immunoreactive dopaminergic fibres containing in the striatum were captured using a resolution digital scan (Epson) and analysed with ImageJ win-64 Fiji. Eight sections separated by 220 μm were used. The striatum was defined and optical density was expressed as the percentage of that in the ipsilateral side respect to the contralateral non-lesioned side after background subtraction. Only animals with more than 90% reduction in TH-fibre density in the striatum on the side ipsilateral to the lesion were included in the study.

3.7.2. Cytochrome-c-oxidase staining

In an extra set of animals, COX staining was performed as described in (Armentero et al., 2006; Blandini et al., 2007) with slight modifications. Twenty-four h after the perfusion, brains were moved to a 25% sucrose solution until they sank and coronal sections of 40 μm were cut using a freezing microtome. The day

after, sections containing the LC were placed in incubation medium with 0.05M PBS (pH 7.4), 1% sucrose, 0.05% nickel sulphate (II), 2.5μM imidazole, 0.025% 3,3′-diaminobenzidine, 0.015% COX, and finally 0.01% catalase was added to start the enzymatic reaction. COX staining was performed in darkness for 5 h at 37ºC. After, the sections were rinsed twice with PBS 0.05M and mounted on gelatine-coated slides. Then, sections were dehydrated in ascending series of alcohols, cleared in xylene and cover slipped with DPX mounting medium.

Digital images were obtained with an automated digital slide scanner (3DHistech, Pannoramic MIDI II). The mean IOD was determined by the selection of the nuclei of interest and subtracting the background for each section. Measurements were performed on three or four sections separated by 80 μM throughout the LC and was calculated the mean per animal. Results were expressed as the increase of optical intensity (Δ IOD %) of the ipsilateral lesioned hemisphere with respect to the intact or contralateral non-lesioned hemisphere.

3.8. Western blot

Animals were deeply anesthetised (Dolethal 60mg/kg, i.p.) and killed by decapitation and the LC was removed bilaterally. Equal amounts of protein from tissue homogenates were separated by SDS-PAGE (sodium dodecyl sulphate-polyacrylamide gel electrophoresis) and transferred to polyvinylidene difluoride membranes (PVDF). The membranes were probed overnight at 4 °C with primary antibodies against TH (rabbit anti-TH diluted at 1:1000), ERKt (mouse anti-ERKt diluted at 1:2000) and pERK (rabbit anti-pERK diluted at 1:2500). The primary antibodies were detected using the corresponding secondary antibody (goat anti-rabbit diluted at 1:10000, goat anti-mouse diluted at 1:10000, goat anti-rabbit diluted at 1:10000). The protein signals were detected using a LI-COR Odyssey® two-

channel quantitative fluorescence imaging system (Bonsai Advanced Technologies, Spain). Digital images of WB were analysed by densitometry using the ImageJ win-64 Fiji free access software (National Institutes of Health, USA), and the protein levels were normalized to the level of β-actin.

3.9. Statistical analysis of data

Experimental data were analysed using the computer programme GraphPad Prism (v. 5.01, GraphPad Software, Inc). The level of statistical significance was set at $p < 0.05$. Data are presented as the group mean ± standard error of the mean (S.E.M.).

- Electrophysiological studies: in vivo tonic, phasic and oscillatory activity; ex vivo intrinsic properties, action potential parameters, sIPSC and sEPSC were analysed using unpaired Student's t-test. The effect of L-DOPA administration in *in vivo* tonic, phasic and oscillatory activity; effect of UK 14,304; *ex vivo* IRK conductance, current-spike frequency and current-voltage relationships, eIPSC and eEPSC were analysed by 2-way analysis of variance ANOVA followed by post hoc comparisons using the Bonferroni post hoc test. The burst incidence, incidence of response and oscillatory pattern were analysed using Fisher's exact test. Relationships between the duration of the suppression period and basal firing rate or the evoked firing rate were analysed using Pearson correlation.
- Behavioural studies: anxiety testing were analysed using unpaired Student's t-test. Body weight of the rats and locomotive and nociceptive behaviour were analysed by repeated measures (RM) 2-way analysis of variance ANOVA followed by post hoc comparisons using the Bonferroni post hoc test.

- Histochemical studies: TH and COX optical density were analysed using paired Student's t-test. Western blot experiments were analysed by 2-way analysis of variance ANOVA followed by post hoc comparisons using the Bonferroni post hoc test.

4. RESULTS

4. RESULTS

4.1. STUDY I: Dopamine depletion alters tonic and phasic locus coeruleus neuron activity

In order to investigate the effect of dopaminergic denervation on the noradrenergic function, tonic electrophysiological properties of LC neurons were investigated two and four weeks after the dopaminergic loss. In addition, we investigated the phasic activation of LC neurons upon mechanical stimulation, since the LC is implicated in the modulation of sensory inputs (reviewed in Llorca-Torralba et al., 2016) and patients with PD suffer non-motor symptoms linked to this process (Djaldetti et al., 2004; Schestatsky et al., 2007; Tinazzi et al., 2008; Okada et al., 2016; Priebe et al., 2016). Finally, we studied the impact of DA replacement on LC neuron activity by acutely administering L-DOPA. Detailed statistical results belonging to this study are shown in **Annex I**.

4.1.1. Dopaminergic loss does not affect locus coeruleus neuron activity two weeks after the lesion

Two weeks after the vehicle or 6-OHDA injection, a total of 97 noradrenergic neurons were recorded in the LC: 55 neurons from the sham group (n = 8 animals) and 42 neurons from the 6-OHDA group (n = 9 animals). All cells recorded displayed the characteristic firing patterns of noradrenergic neurons, long-lasting positive–negative waveform (Cedarbaum and Aghajanian, 1976) and were localized within the LC. Basic electrophysiological parameters related to tonic activity as firing frequency, firing pattern and burst firing activity were similar between the 6-OHDA lesioned and sham groups (**Table 4.1**).

Table 4.1. Basal electrophysiological properties of locus coeruleus neurons two weeks after the surgery in sham and 6-OHDA animals.

	Sham (n=55)	6-OHDA (n=42)
Basal firing rate (Hz)	2.03 ± 0.14	2.05 ± 0.15
Coefficient of variation	35.2 ± 1.56	38.18 ± 2.11
Incidence of burst firing (%)	40 (22/55)	45 (19/42)
Spikes in burst (%)	5.40 ± 1.02	6.68 ± 2.28
Spikes/burst	2.05 ± 0.05	2.11 ± 0.07
Mean burst interspike (ms)	67.78 ± 2.05	69.2 ± 1.68
Mean burst length (ms)	73.77 ± 3.97	77.01 ± 4.45

Data are expressed as the mean ± S.E.M. of *n* cells from a total of 8 sham and 9 6-OHDA animals.

For methodological issues, phasic LC activity was recorded in a smaller subgroup of neurons. First, we analysed the incidence of the sensory-evoked response triggered by the paw compression, which was similar in 6-OHDA lesioned and sham rats. LC neurons from both groups responded in a similar way when the contralateral or ipsilateral paw were compressed, sham 86 % vs 6-OHDA 70 % and sham 70 % vs 6-OHDA 55 % respectively ($p > 0.05$, Fisher's exact test; **Figure 4.1**).

Next, we analysed the parameters of the phasic LC responses from those neurons that responded to the paw compression. The application of a single contralateral compression evoked a similar response in the two studied groups. DA depletion did not affect the post-stimulus frequency, subsequent suppression period or percentage of change in the firing frequency 10 s after paw compression according to the basal firing rate ($p > 0.05$, unpaired Student's t-test; **Figure 4.2A**). In the same way, when the compression was applied to the ipsilateral paw to the lesion, no modifications were observed between the groups for any of the studied parameters ($p > 0.05$, unpaired Student's t-test; **Figure 4.2B**).

Finally, we assessed if the phasic activity was influenced by the repetition of the paw compression. To do so, in some neurons, five sequential compressions were performed. Phasic LC responses parameters were identical along the repetitions for both, contralateral or ipsilateral paws, as previous reported in control and rats model of inflammatory pain (Borges et al., 2017a) ($p > 0.05$, 2-way ANOVA test for paw compression factor; **Figure 4.3A and B**).

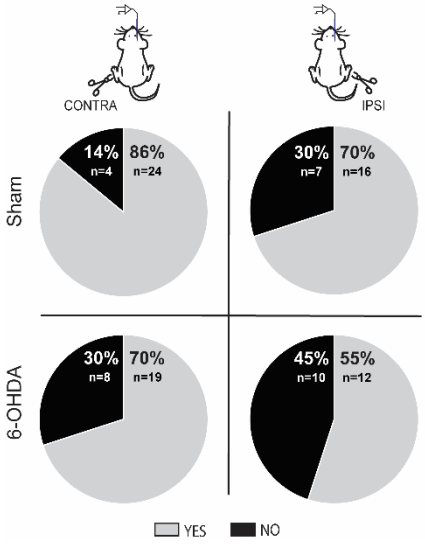

Figure 4.1. Incidence of sensory-evoked locus coeruleus phasic response two weeks after the surgery in sham and 6-OHDA animals. Graphs represent the percentage of neurons that showed (gray) or not (black) a sensory-evoked response. No significant difference was observed between groups. Data are expressed as *n* cells from a total of 8 sham and 9 6-OHDA animals.

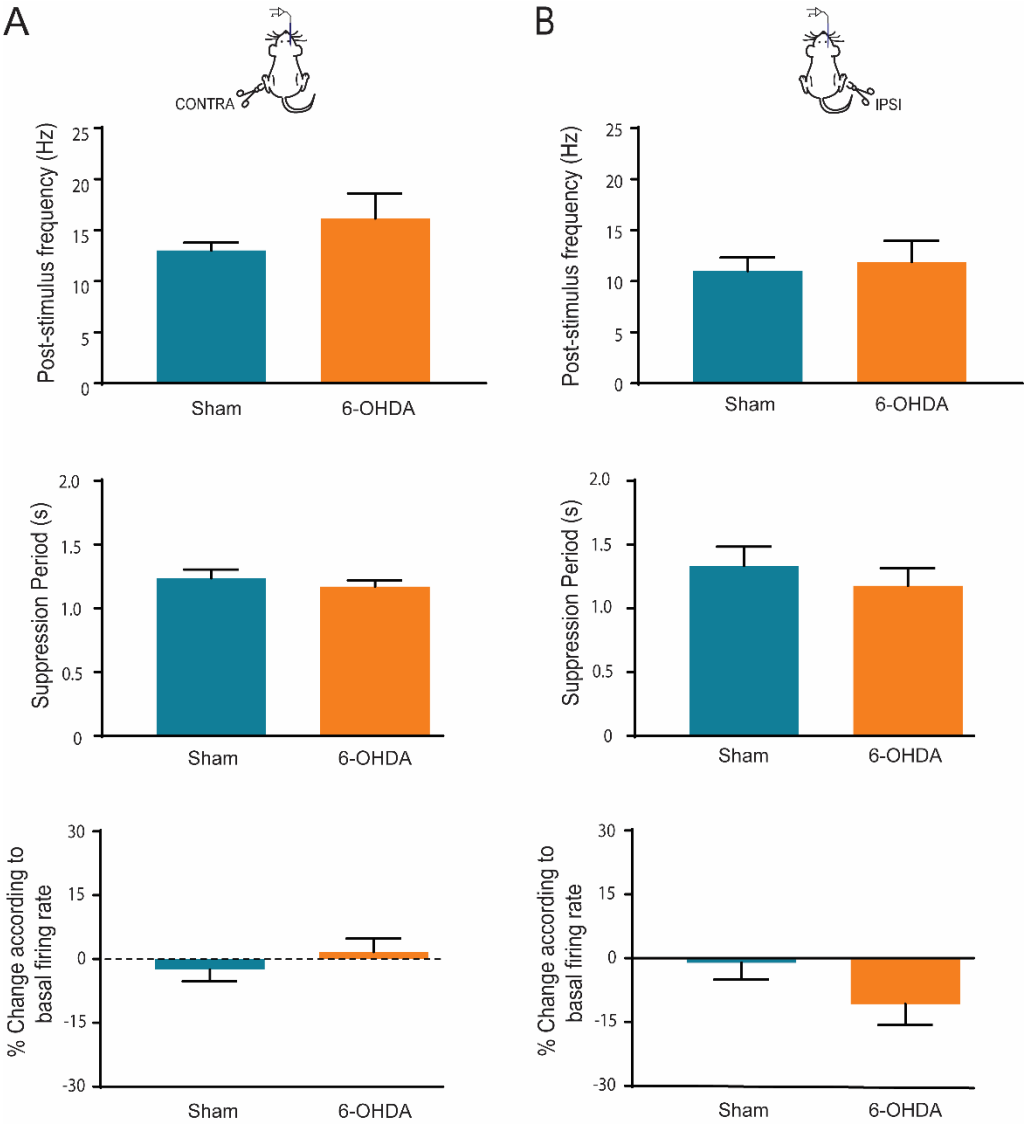

Figure 4.2. Sensory-evoked locus coeruleus phasic response to single paw compressions two weeks after the surgery in sham and 6-OHDA animals. (A) Graphs representing the effect of a single contralateral paw compression on the phasic response of LC neurons (n=24 cells from sham animals; n=19 cells from 6-OHDA animals). (B) Graphs representing the effect of a single ipsilateral paw compression on the phasic response from LC neurons (n=16 cells from sham animals; n=12 cells from 6-OHDA animals). Data are shown as the mean ± S.E.M. of *n* cells from a total of 8 sham and 9 6-OHDA animals.

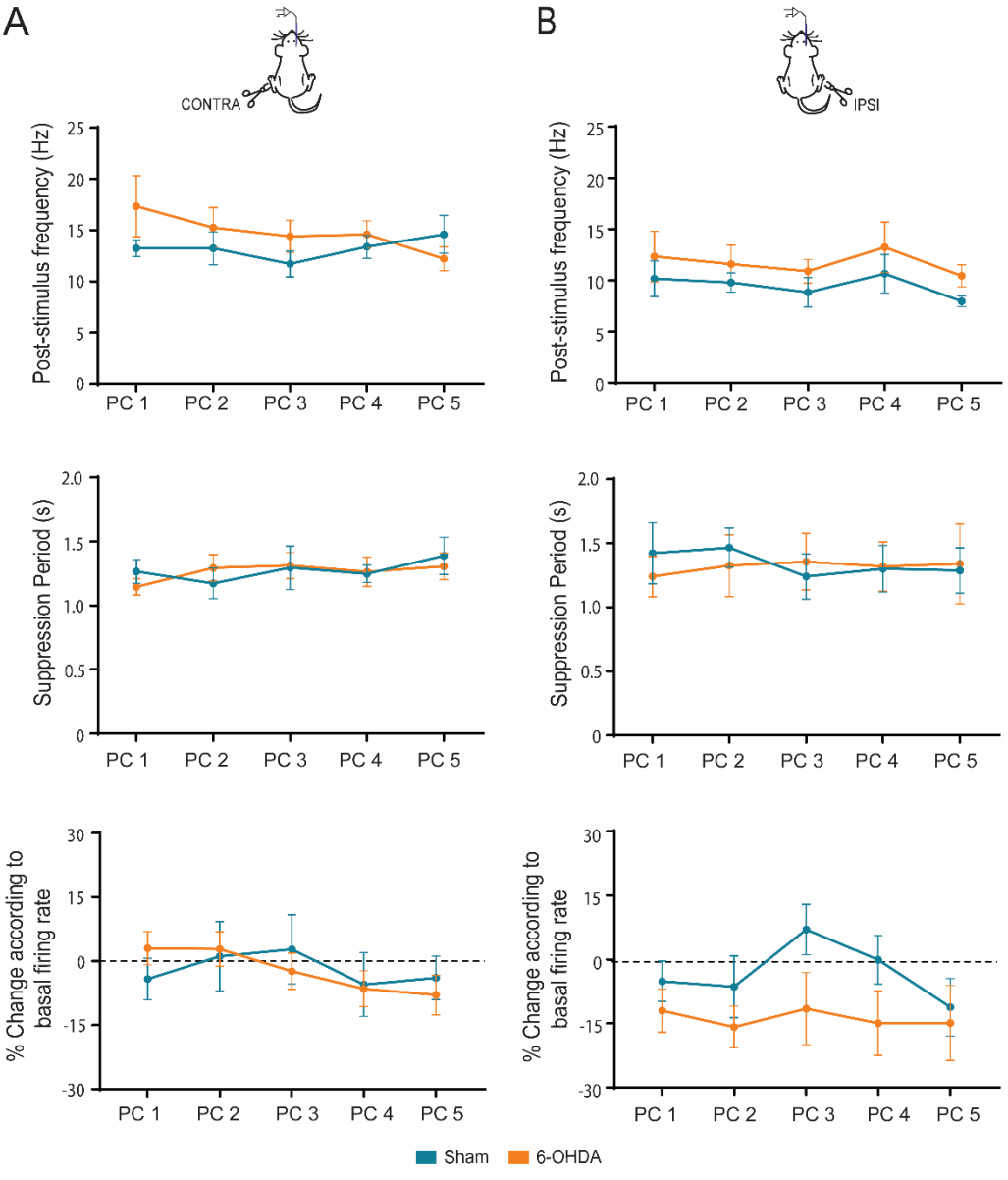

Figure 4.3. Sensory-evoked locus coeruleus phasic response to sequential contralateral paw compressions two weeks after the surgery in sham and 6-OHDA animals. (A) Graphs representing the effect of 5 sequential contralateral paw compressions on the LC phasic response (n=12 cells from sham animals; n=21 cells from 6-OHDA animals). (B) Graphs representing the effect of 5 sequential ipsilateral paw compressions on the LC phasic response (n=12 cells from sham animals; n=12 cells from 6-OHDA animals). Data are shown as the mean ± S.E.M. of *n* cells from a total of 8 sham and 9 6-OHDA animals.

4.1.2. Dopamine replacement restores locus coeruleus tonic and phasic activity four weeks after the dopaminergic lesion

Four weeks after the vehicle or 6-OHDA injection, a total of 126 noradrenergic neurons were recorded in the LC: 75 neurons from the sham group (n = 11 animals) and 51 neurons from the 6-OHDA group (n = 13 animals). After analysing tonic and phasic responses in basal conditions, L-DOPA was administered (24 mg/kg plus benserazide 12 mg/kg, i.p.), and recordings were obtained between 30 and 90 min following the injection.

Basal spontaneous LC neuron activity significantly decreased four weeks after the 6-OHDA lesion ($p < 0.05$, Bonferroni's post hoc test). Interestingly L-DOPA acute administration (24 mg/kg plus benserazide 12 mg/kg, i.p.) recovered the basal values confirming that this modification was produced by the DA loss. LC neuron firing pattern and burst activity were not modified in the 6-OHDA lesioned group or after the L-DOPA administration ($p > 0.05$, 2-way ANOVA test; **Table 4.2**).

Table 4.2. Basal electrophysiological properties of locus coeruleus neurons four weeks after the surgery in sham and 6-OHDA animals, in absence or presence of L-DOPA.

	Sham (n=75)	6-OHDA (n=51)	Sham L-DOPA (n=31)	6-OHDA L-DOPA (n=35)
Basal firing rate (Hz)	**2.33 ± 0.12**	**1.87 ± 0.10 ***	2.24 ± 0.21	2.06 ± 0.17
Coefficient of variation	38.78 ± 1.43	37.13 ± 1.81	41.78 ± 2.71	40.23 ± 2.47
Incidence of burst firing (%)	39 (29/75)	37 (19/51)	61 (19/31)	49 (17/35)
Spikes in burst (%)	7.22 ± 1.24	5.35 ± 1.69	6.77 ± 2.27	6.6 ± 1.61
Spikes/burst	2.03 ± 0.03	2 ± 0	2.16 ± 0.12	2 ± 0
Burst interspike (ms)	67.55 ± 2.09	68 ± 1.56	70.21 ± 1.21	70.29 ± 1.64
Burst length (ms)	75.44 ± 3.62	68.23 ± 1.55	84.53 ± 7.88	77.35 ± 3.82

Data are expressed as the mean ± S.E.M. of *n* cells from a total of 8-11 sham and 9-13 6-OHDA animals. *$p < 0.05$, Bonferroni's post hoc test.

Then, we analysed the sensory-evoked responses in absence or presence of L-DOPA and for methodological issues this was recorded in a smaller subgroup of neurons. The dopaminergic loss did not modify the incidence of responses of LC neurons when the contralateral (sham 87 % and 6-OHDA 77 %) or ipsilateral (sham 52 % and 6-OHDA 39 %) paw were compressed ($p > 0.05$, Fisher's exact test; **Figure 4.4A**). However, L-DOPA administration significantly reduced the incidence of response in both, sham and 6-OHDA animals to the contralateral or to the ipsilateral compression of the paw, sham L-DOPA 25 % vs 6-OHDA L-DOPA 36 % and sham L-DOPA 0 % vs 6-OHDA L-DOPA 14 % respectively (**Figure 4.4B**) (Contralateral: sham vs sham L-DOPA $p < 0.001$; 6-OHDA vs 6-OHDA L-DOPA $p < 0.01$) (Ipsilateral: sham vs sham L-DOPA $p < 0.001$; 6-OHDA vs 6-OHDA L-DOPA $p < 0.05$) (Fisher's exact test).

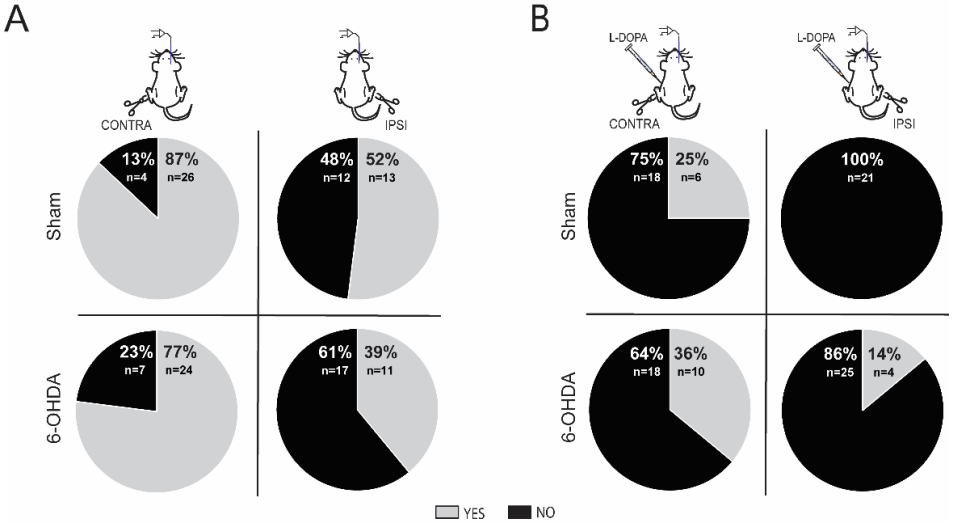

Figure 4.4. Incidence of sensory-evoked locus coeruleus phasic response four weeks after the surgery in sham and 6-OHDA animals, in absence or presence of L-DOPA. Graphs represent the percentage of neurons that responded (gray) or not (black) to paw compression. (A) No significant difference was observed between groups during basal situation. (B) No significant difference was observed between groups under L-DOPA (24 mg/kg plus benserazide 12 mg/kg, i.p.) effect. However, this parameter was dramatically decreased in both groups when compared to the respective basal incidence. Data are expressed as *n* cells from a total of 8-10 sham and 8-11 6-OHDA animals. Fisher's exact test.

Next, parameters of the phasic response triggered by the compression of the contralateral paw were analysed. As described in **Figure 4.5A**, 6-OHDA lesioned animals showed higher post-stimulus frequency and longer duration of the suppression period compared to the sham group ($p < 0.05$ and $p < 0.01$, respectively, Bonferroni's post hoc test). As happened for the tonic activity, L-DOPA acute administration restored basal phasic values (post-stimulus frequency and suppression period) in the 6-OHDA lesioned group, without affecting those in the sham group. The percentage of change according to the basal firing rate did not differ among all experimental groups ($p > 0.05$, 2-way ANOVA test). Interestingly, the greater post-stimulus frequency along with the lower tonic activity resulted in a significantly higher phasic:tonic ratio in the 6-OHDA lesioned animals compared to sham rats ($p < 0.01$, Bonferroni's post hoc test). Also here, L-DOPA administration restored this parameter ($p < 0.05$, Bonferroni's post hoc test). In the same line, when analysing the parameters of the phasic response evoked by the compression of the ipsilateral paw (**Figure 4.5B**), we found that the suppression period was significantly longer in the 6-OHDA lesioned group ($p < 0.05$, unpaired Student's t-test) without modifying the rest of the parameters. Analysis of the parameters related to the compression of the ipsilateral paw could not be performed when L-DOPA was present due to the low or non-existent positive response (**Figure 4.4B**).

Finally, we tested if the application of 5 successive compressions in the contralateral (**Figure 4.6A**) or ipsilateral (**Figure 4.6B**) paw influences the sensory-evoked responses. In all cases, the factor linked to the reiteration of paw compression was not significant ($p > 0.05$, 2-way ANOVA test). In support of the results obtained with one paw compression, significant differences were seen between groups for the post-stimulus frequency ($p < 0.01$, 2-way ANOVA test; **Figure 4.6A**) and the suppression period ($p < 0.05$, Bonferroni's post hoc test; **Figure 4.6A and B**).

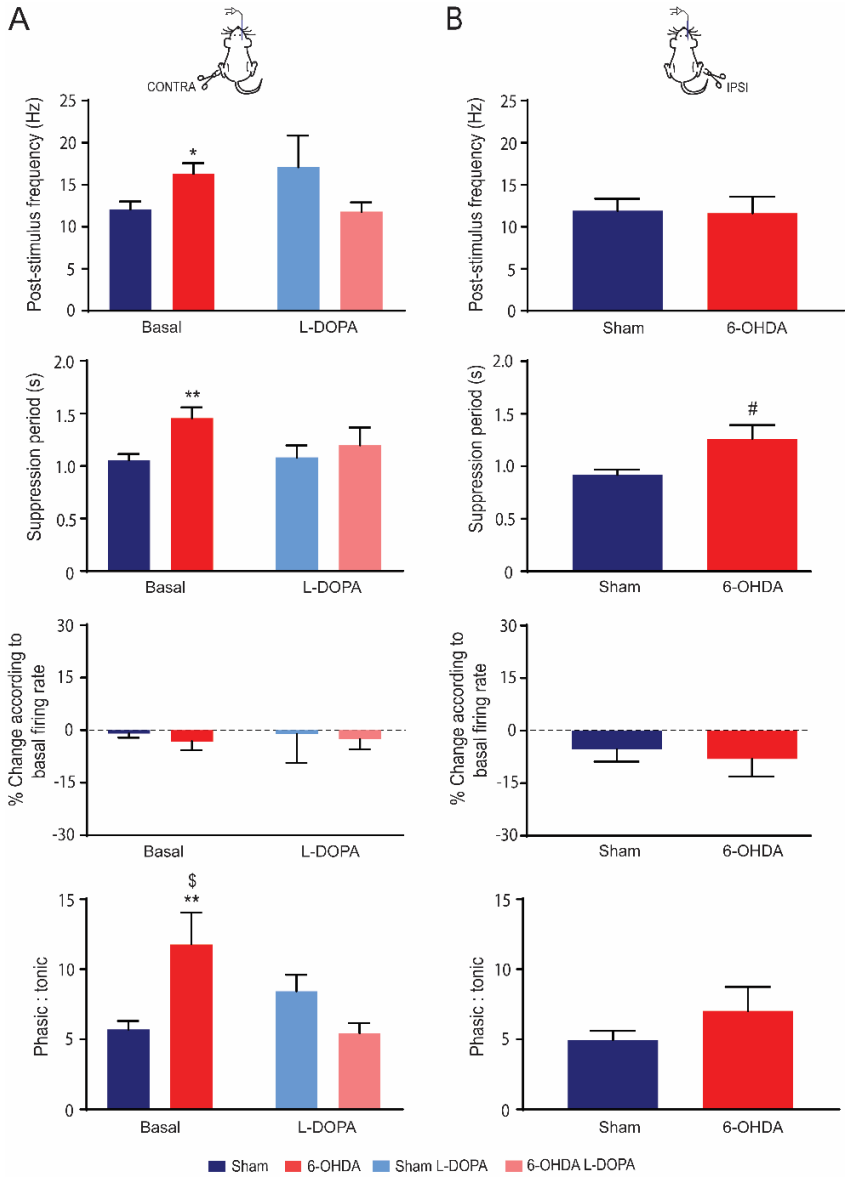

Figure 4.5. Sensory-evoked locus coeruleus phasic response to single paw compressions four weeks after the surgery in sham and 6-OHDA animals, in absence or presence of L-DOPA. (A) Graphs representing the effect of a single contralateral paw compression on the phasic response of LC cells (n=26 and n=6 cells from sham animals basal or with L-DOPA (24 mg/kg plus benserazide 12 mg/kg, i.p.), respectively; n=24 and n=10 cells from 6-OHDA animals basal or with L-DOPA, respectively). (B) Graphs representing the effect of a single ipsilateral paw compression on the phasic response (n=13 cells from sham animals; n=11 cells from 6-OHDA animals). Data are shown as the mean ± S.E.M. of *n* cells from a total of 3-8 sham and 4-10 6-OHDA animals. $^{*}p < 0.05$ and $^{**}p < 0.01$ vs respective sham, $^{*}p < 0.05$ vs 6-OHDA L-DOPA Bonferroni's post hoc test; $\#p < 0.05$ vs sham, unpaired Student's t-test.

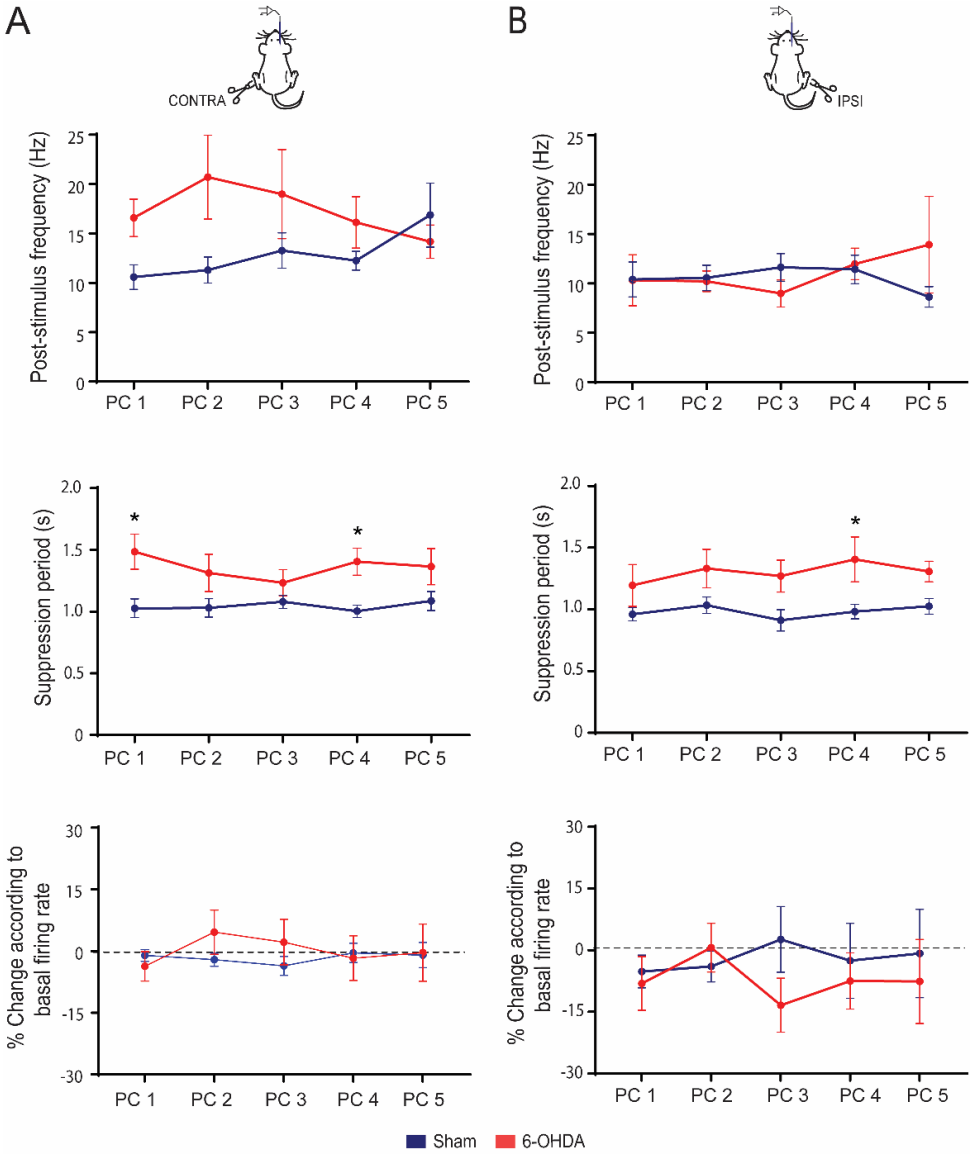

Figure 4.6. Sensory-evoked locus coeruleus phasic response to sequential contralateral paw compressions four weeks after the surgery in sham and 6-OHDA animals. (A) Graphs representing the effect of 5 sequential contralateral paw compressions on the phasic LC response (n=14 cells from sham animals; n=15 cells from 6-OHDA animals). (B) Graphs representing the effect of 5 sequential ipsilateral paw compressions on the phasic LC response (n=9 cells from sham animals; n=7 cells from 6-OHDA animals). Data are shown as the mean ± S.E.M. of *n* cells from a total of 7-8 sham and 7 6-OHDA animals. $^{*}p < 0.05$ vs sham, Bonferroni's post hoc test.

4.1.3. Correlation between tonic locus coeruleus activity and sensory-evoked response does not change after dopaminergic denervation

Due to the prolonged suppression period observed after the compression of the contralateral or ipsilateral paws in 6-OHDA lesion animals, we hypothesized that this parameter could be related to the decreased tonic basal firing rate or to the increased post-stimulus frequency previously observed (**Table 4.2** and **Figure 4.5A**, respectively). The correlation analysis between the suppression period and the basal firing rate was significant in sham and 6-OHDA lesioned animals ($p < 0.05$, Pearson correlation; **Figure 4.7A and B**, upper panel), stressing that low firing rate was associated to a large suppression period. On the contrary, no relationship was observed between the suppression period and the post-stimulus frequency in the tested groups ($p > 0.05$, Pearson correlation; **Figure 4.7A and B**, bottom panels).

This relationship was also present, regardless the experimental group, two weeks after the surgery. The correlation analysis between the suppression period and the basal firing rate was significant in sham and 6-OHDA group ($p < 0.01$, Pearson correlation; **Figure 4.8A and B**, upper panel). In addition, two weeks after the lesion, we observed that the relationship the suppression period was not related to the post-stimulus frequency ($p > 0.05$, Pearson correlation; **Figure 4.8A and B**, bottom panels).

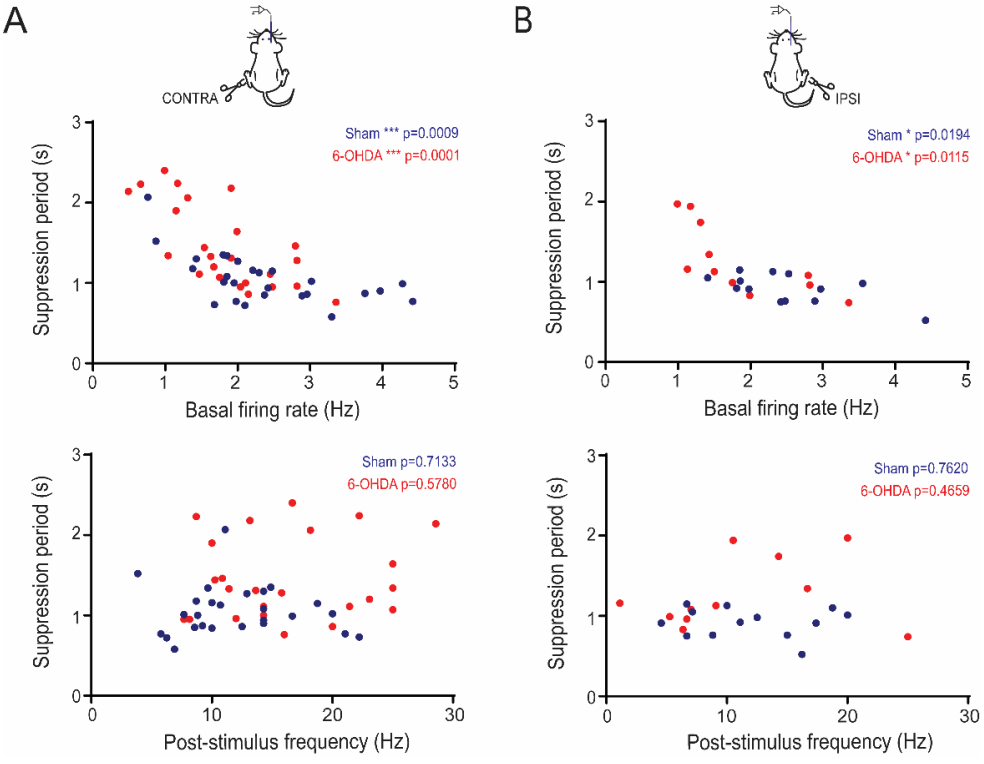

Figure 4.7. Relationship between tonic and phasic locus coeruleus neuron parameters four weeks after the surgery in sham and 6-OHDA animals. (A) Correlation analysis after a single contralateral paw compression (n=26 from sham animals, respectively; n=24 cells from 6-OHDA animals). In both groups, the suppression period in the sensory-evoked phasic response was significantly correlated with the tonic basal firing rate (upper panel) but not with the post-stimulus frequency (bottom panel). (B) Correlation analysis after a single ipsilateral paw compression (n=13 cells from sham animals; n=11 cells from 6-OHDA animals). As happened with the compression of the contralateral paw, the suppression period in the sensory-evoked phasic response was significantly correlated with the tonic basal firing rate (upper panel) but not with the post-stimulus frequency (bottom panel). Each dot represents the value from one neuron from a total of 7-8 sham and 7-10 6-OHDA animals. $^{*}p < 0.05$ and $^{***}p < 0.001$, Pearson correlation.

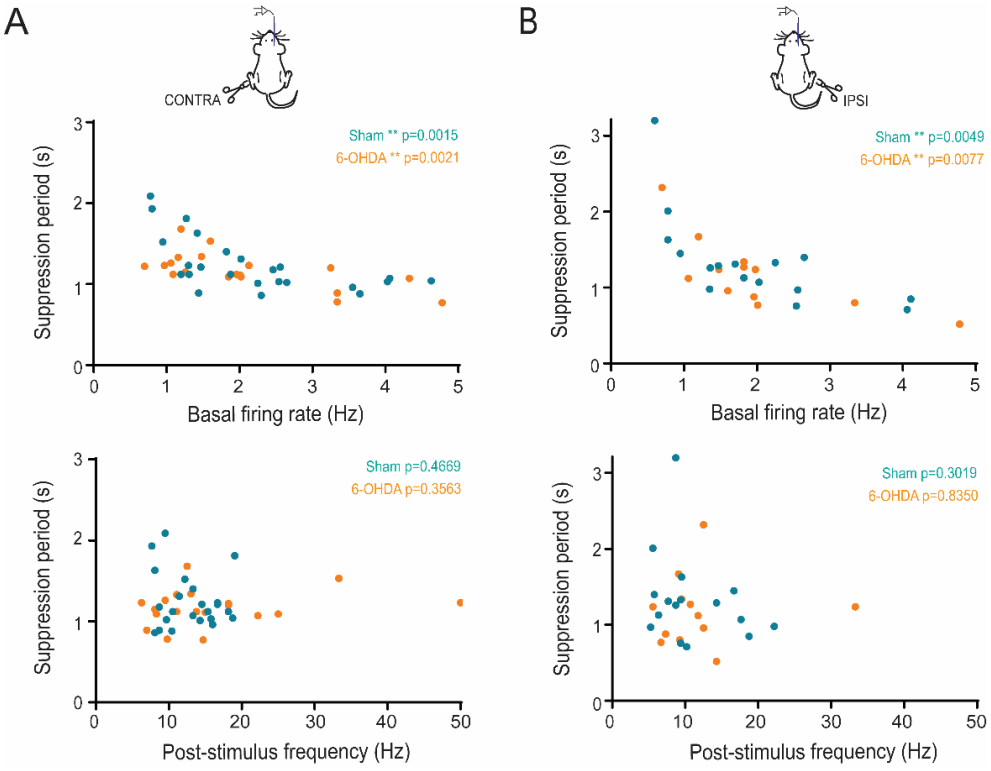

Figure 4.8. Relationship between tonic and phasic locus coeruleus neuron parameters two weeks after the surgery in sham and 6-OHDA animals. (A) Correlation analysis after a single contralateral paw compression (n=24 from sham animals, respectively; n=19 cells from 6-OHDA animals). In sham and 6-OHDA animals, the suppression period in the sensory-evoked phasic response was significantly correlated with the tonic basal firing rate (upper panel) but not with the post-stimulus frequency (bottom panel). (B) Correlation analysis after a single ipsilateral paw compression (n=16 cells from sham animals; n=12 cells from 6-OHDA animals). Again, the suppression period in the sensory-evoked phasic response was significantly correlated with the tonic basal firing rate (upper panel) but not with the post-stimulus frequency (bottom panel). Each dot represents the value from one neuron from a total of 8 sham and 9 6-OHDA animals $^{**}p < 0.01$, Pearson correlation.

4.1.4. Dopamine depletion does not modify α_2-adrenoceptor response in the locus coeruleus

Another set of animals (8 sham and 9 6-OHDA animals) was employed to evaluate if the observed alterations in the tonic and phasic activity of LC neurons were due to an altered sensitivity of α_2-adrenoceptors in the LC. To that end, increasing doses of the α_2-adrenoceptor agonist UK 14,304 (2.5-40 μg/kg, i.v.) were tested in tonic and phasic conditions. As it is shown in **Figure 4.9A**, UK 14,304 completely inhibited the firing rate, which was recovered by the administration of the α_2-adrenoceptor antagonist RX 821002 (100 μg/kg, i.v.) in both groups. As shown in **Figure 4.9B**, dose–effect curves in both groups did not differ ($p > 0.05$, RM 2-way ANOVA test) and the ED_{50} values were also similar in the sham and 6-OHDA animals (sham 13.81 ± 2.14, n=8; 6-OHDA 10.27 ± 1.30, n=9) ($p > 0.05$, unpaired Student's t-test). The effect of the α_2-adrenoceptor agonist was also determined in the phasic activity when the contralateral paw was compressed, revealing no modifications in the percentage of change according to the basal post-stimulus frequency ($p > 0.05$, 2-way ANOVA test; **Figure 4.9C**). As expected for the complete inhibitory effect of the drug, significant changes in the percentage of change according to the basal suppression period were seen for the highest tested doses in both groups ($p < 0.05$ and $p < 0.001$, Bonferroni's post hoc test; **Figure 4.9D**).

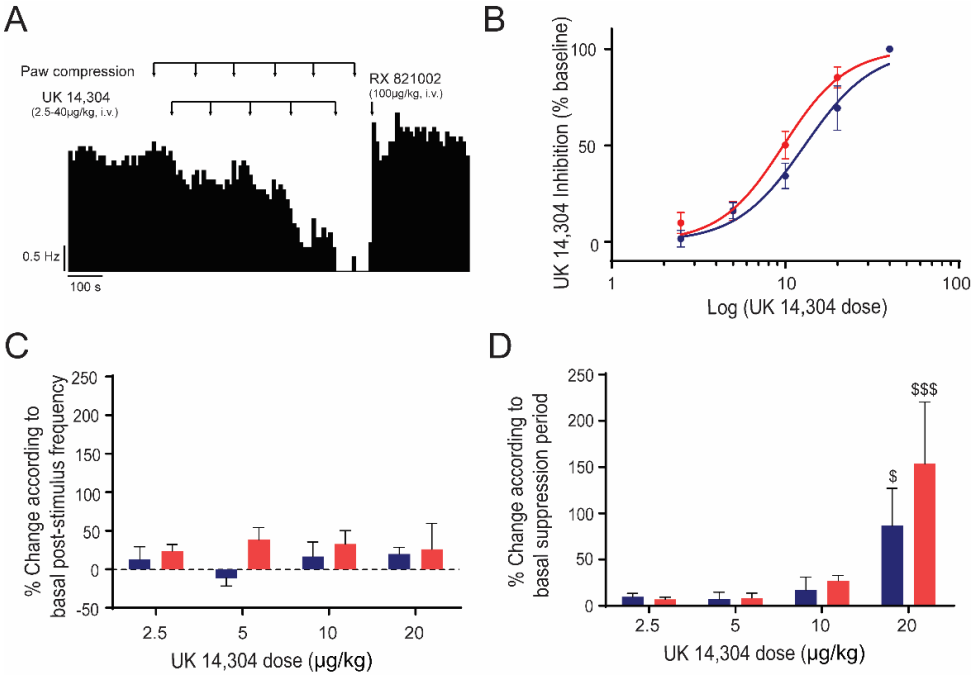

Figure 4.9. Effects of UK 14,304 on locus coeruleus neurons in sham and 6-OHDA lesioned animals. (A) Representative example showing the effect of cumulative doses of UK 14,304 (2.5-40µg/kg, i.v.) on the tonic firing frequency. Paw compressions followed each dose administration. (B) Dose–effect curves for UK 14,304 in sham and 6-OHDA lesioned rats. Percentage of reduction from the tonic basal firing rate was represented over drug doses. (C) Percentage of change according to the basal post-stimulus frequency when administering cumulative doses of UK 14,304. (D) Percentage of change according to the basal suppression period when administering cumulative doses of UK 14,304. Data are shown as the mean ± S.E.M. of one cell from a total of 8 sham and 9 6-OHDA animals. $\$p < 0.05$ vs respective 2,5 and 5 dose; and $\$\$\$p < 0.01$ vs all respective doses, Bonferroni's post hoc test.

Annex I. Statistical analysis of the experiments included in Study I

			Unpaired t test		
	P value	P value summary	t (df)	n Sham	n 6-OHDA
Tonic LC neurons (2 weeks)					
Basal firing rate	0.9137	ns	$t_{95} = 0.1087$	55	42
Coefficient of variation	0.2497	ns	$t_{95} = 1.158$	55	42
Spikes in burst (%)	0.5938	ns	$t_{39} = 0.5378$	22	19
Spikes/burst	0.4759	ns	$t_{39} = 0.7199$	22	19
Mean burst interspike (ms)	0.6041	ns	$t_{39} = 0.5227$	22	19
Mean burst length	0.5891	ns	$t_{39} = 0.5496$	22	19
Phasic LC activity (CL single PC) (2 weeks)					
Evoked firing frequency	0.1855	ns	$t_{41} = 1.347$	24	19
Suppression period	0.4543	ns	$t_{41} = 0.7554$	24	19
% of change according to the basal firing rate	0.3235	ns	$t_{41} = 0.9994$	24	19
Phasic LC activity (IL single PC) (2 weeks)					
Evoked firing frequency	0.7150	ns	$t_{26} = 0.7150$	16	12
Suppression period	0.4613	ns	$t_{26} = 0.7478$	16	12
% of change according to the basal firing rate	0.1330	ns	$t_{25} = 1.553$	15	12
Phasic LC activity (IL single PC) (4 weeks)					
Evoked firing frequency	0.9032	ns	$t_{22} = 0.1231$	13	11
Suppression period	0.0164	*	$t_{22} = 2.598$	13	11
% of change according to the basal firing rate	0.6460	ns	$t_{21} = 0.466$	13	10
Phasic:tonic ratio	0.2425	ns	$t_{22} = 1.201$	13	11
UK 14,304 ED_{50}	0.1678	ns	$t_{15} = 1.449$	8	9

	2-way ANOVA F (DFn, DFd)		
	Interaction	L-DOPA	Lesion
Tonic LC neurons (4 weeks)			
Basal firing rate	F (1, 188) = 0.9132	F (1, 188) = 0.103	F (1, 188) = 4.534 *
Coefficient of variation	F (1, 188) = 0.0005	F (1, 188) = 2.204	F (1, 188) = 0.606
Spikes in burst (%)	F (1, 80) = 0.2455	F (1, 80) = 0.0552	F (1, 80) = 0.3545
Spikes/burst	F (1, 80) = 1.117	F (1, 80) = 1.117	F (1, 80) = 2.715
Burst interspike (ms)	F (1, 80) = 0.0095	F (1, 80) = 1.774	F (1, 80) = 0.021
Burst length	F (1, 80) = 0.0000	F (1, 80) = 3.645	F (1, 80) = 2.276
Phasic LC activity (CL single PC) (4 weeks)			
Evoked firing frequency	F (1, 62) = 8.175 **	F (1, 62) = 0.025	F (1, 62) = 0.0962
Suppression period	F (1, 62) = 1.301	F (1, 62) = 0.3681	F (1, 62) = 4.173 *
% of change according to the basal firing rate	F (1, 57) = 0.0159	F (1, 57) = 0.0039	F (1, 57) = 0.3382
Phasci:tonic ratio	F (1, 62) = 4.545 *	F (1, 62) = 0.714	F (1, 62) = 0.523

	2-way ANOVA F (DFn, DFd)		
	Interaction	PC	Lesion
Phasic LC activity (CL 5 PC) (2 weeks)			
Evoked firing frequency	F (4, 123) = 0.8049	F (4, 123) = 0.4213	F (1, 123) = 1.567
Suppression period	F (4, 123) = 0.3092	F (4, 123) = 0.4672	F (1, 123) = 0.0176
% of change according to the basal firing rate	F (4, 123) = 0.4464	F (4, 123) = 0.9091	F (1, 123) = 0.0046
Phasic LC activity (IL 5 PC) (2 weeks)			
Evoked firing frequency	F (4, 83) = 0.0168	F (4, 83) = 0.7705	F (1, 83) = 4.085 *
Suppression period	F (4, 83) = 0.1892	F (4, 83) = 0.0663	F (1, 83) = 0.0425
% of change according to the basal firing rate	F (4, 83) = 0.3801	F (4, 83) = 0.715	F (1, 83) = 5.957 *
Phasic LC activity (CL 5 PC) (4 weeks)			
Evoked firing frequency	F (4, 119) = 1.363	F (4, 119) = 0.3761	F (1, 119) = 7.158 **
Suppression period	F (4, 119) = 0.6785	F (4, 119) = 0.304	F (1, 119) = 23.77 ***
% of change according to the basal firing rate	F (4, 119) = 1.363	F (4, 119)= 0.3761	F (1, 119) = 7.158
Phasic LC activity (IL 5 PC) (4 weeks)			
Evoked firing frequency	F (4, 61) = 1.106	F (4, 61) = 0.2456	F (1, 61) = 0.2167
Suppression period	F (4, 61) = 0.2428	F (4, 61) = 0.5132	F (1, 61) = 21.78 ***
% of change according to the basal firing rate	F (4, 61) = 0.4608	F (4, 61) = 0.1191	F (1, 61) = 1.152

	Fisher's exact test			
	P value	P value summary	n Sham	n 6-OHDA
Incidence of burst firing				
Incidence of burst firing (%) (2 weeks)	0.6801	ns	55	42
Incidence of burst firing (%) (4 weeks)	>0.9999	ns	75	51
Incidence of burst firing L-DOPA (%)	0.3319	ns	31	35
Incidence of sensory-evoked response				
Incidence of CL sensory-evoked response (2 weeks)	0.2047	ns	28	27
Incidence of IL sensory-evoked response (2 weeks)	0.3651	ns	23	22
Incidence of CL sensory-evoked response (4 weeks)	0.5077	ns	30	31
Incidence of IL sensory-evoked response (4 weeks)	0.4145	ns	25	28
Incidence of CL sensory-evoked response L-DOPA	0.5487	ns	24	28
Incidence of IL sensory-evoked response L-DOPA	0.1291	ns	21	29
Incidence of CL sensory-evoked response L-DOPA (Sham)	<0.001	***	30 (Sham)	24 (Sham L-DOPA)
Incidence of IL sensory-evoked response L-DOPA (Sham)	<0.001	***	25 (Sham)	21 (Sham L-DOPA
Incidence of CL sensory-evoked response L-DOPA (6-OHDA)	<0.01	**	31 (6-OHDA)	28 (6-OHDA L-DOPA)
Incidence of IL sensory-evoked response L-DOPA (6-OHDA)	0.0379	*	28 (6-OHDA)	29 (6-OHDA L-DOPA)

	Pearson correlation			
	P value	P value summary	r	n
Suppression period – Evoked firing rate (Sham)	0.0009	***	-0.6118	26
Suppression period – Evoked firing rate (6-OHDA)	0.0001	***	-0.7034	24
Suppression period – Basal firing rate (Sham)	0.7133	ns	-0.07569	26
Suppression period – Basal firing rate (6-OHDA)	0.5780	ns	0.1195	24

	2-way ANOVA F (DFn, DFd)		
	Interaction	Dose	Lesion
UK 14,304 inhibition (% baseline)	F (4, 60) = 1.577	F (4, 60) = 155.9 ***	F (1, 15) = 1.825
% of change according to the basal evoked firing rate	F (3, 51) = 0.7363	F (3, 51) = 0.1951	F (1, 51) = 3.014
% of change according to the basal suppression period	F (3, 51) = 1.336	F (3, 51) = 14.53 ***	F (1, 51) = 2.373

4.2. STUDY II: Dopaminergic depletion reduces low frequency oscillations in the locus coeruleus and projecting cortical areas

Since LC and mPFC receive dense reciprocal innervation and both regions are important for some PD non-motor symptoms as impaired cognitive processing, nociception or depression, we evaluated the impact of dopaminergic loss on the oscillatory activity and synchronization in the LC and between the LC and the mPFC. Finally, we studied the impact of the paw compression in the oscillatory activity, in absence or presence of L-DOPA. Detailed statistical results belonging to this study are shown in **Annex II**.

4.2.1. Dopaminergic loss decreased low frequency oscillatory activity and synchronization between the locus coeruleus and medial prefrontal cortex

To evaluate the impact of the 6-OHDA lesion in the oscillatory activity and synchronization in the LC and between the LC and the prefrontal cortex, we recorded simultaneously LC spikes, LFP from the LC and ECoG from the mPFC activity. A total of 9 sham (59 neurons for LFP and 41 neurons for ECoG and coherence analysis) and 11 6-OHDA lesioned animals (31 neurons for LFP and 29 neurons for ECoG and coherence analysis) were used.

The proportion of neurons that showed an oscillatory pattern was similar in sham (36%) and 6-OHDA lesioned (34%) animals ($p > 0.05$, Fisher´s exact test), as the autocorrelograms revealed (**Figure 4.10**).

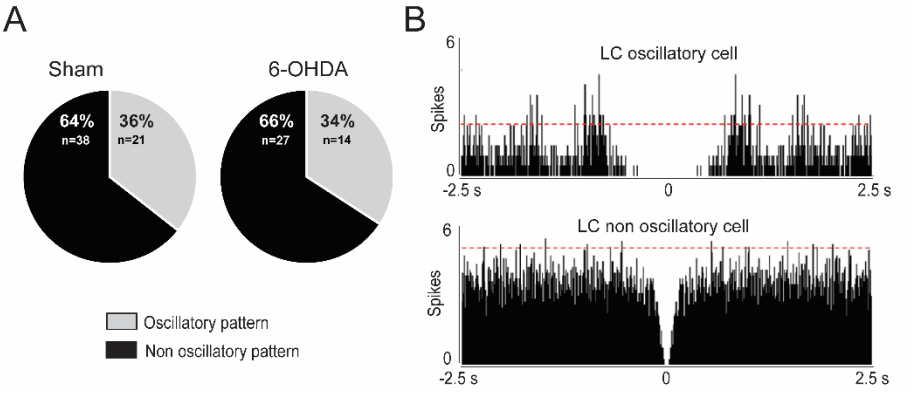

Figure 4.10. Oscillatory activity of locus coeruleus neurons. (A) Oscillatory pattern of LC neurons expressed as the percentage of neurons. The oscillatory activity of LC neurons was similar in sham and 6-OHDA lesioned group. Data are expressed as percentage of n cells from a total of 9 sham and 11 6-OHDA animals. (B) Autocorrelograms showing the pattern of oscillatory and non-oscillatory LC neurons. Red dashed line represents twice the magnitude of the random fluctuation.

Although the LFP and the ECoG power spectra were represented in the 0-30 Hz frequency range, a maximum peak was revealed at delta band with a minor peak in theta band, being practically absent in both groups from alpha band on (**Figure 4.11**).

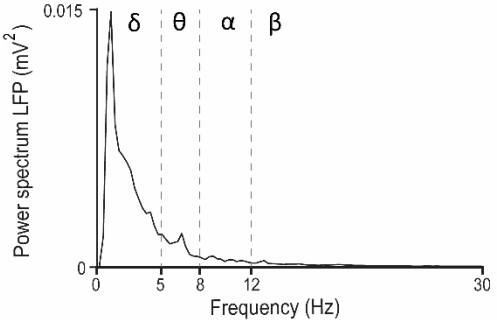

Figure 4.11. Representative oscillatory activity in the locus coeruleus LFP. Representative power spectrum of the LC LFP in a control animal in the 0-30 Hz frequency range, where 0-5 Hz corresponds to delta, 5-8 Hz to theta, 8-12 Hz to alpha and 12-30 Hz to beta. Note that the highest activity corresponds to the low-frequency (delta) oscillations.

Analysis of the power spectrum in the delta-range (0-5 Hz) for the LFP or ECoG showed a peak between 0.3-0.9 Hz in both experimental groups, and AUC values for the low frequency range oscillations were significantly lower after the dopaminergic lesion ($p < 0.001$ and $p < 0.01$, respectively, unpaired Student's t-test; **Figure 4.12A and B**). The analysis of the theta, alpha and beta bands did not reveal any difference between the groups (see **Annex II**). As the maximum range of activity was mostly circumscribe to the delta-band, the analysis was later restricted to this last frequency band, from 0 to 5 Hz. Coherence analysis between simultaneously recorded LFP and ECoG showed similar results to the power spectrum analysis. Regardless the experimental group, coherence analysis was significant only in the delta frequency range where AUC values were lower in the 6-OHDA group ($p < 0.05$, unpaired Student's t-test; **Figure 4.12C**).

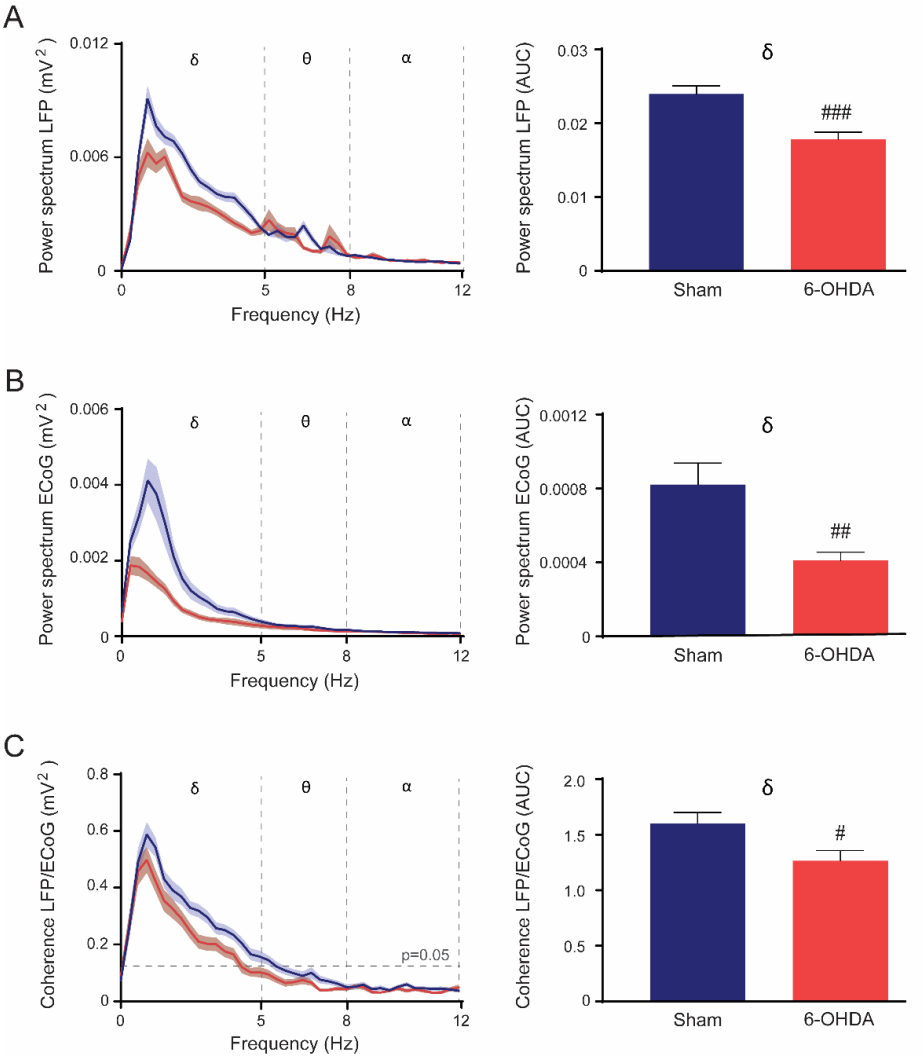

Figure 4.12. Effect of the 6-OHDA lesion on the power spectrum analysis of LFP and ECoG and LFP/ECoG coherence analysis. Power spectrum and coherence curves (left) were used to analyse AUC values (delta frequency range, δ) (right). (A) Power spectrum of the LFP showed maximum activity at delta-range in both groups and its oscillatory activity analysed as the AUC decreased after the lesion with 6-OHDA. (B) Power spectrum for the ECoG showed maximum activity at delta-range in both groups and its power spectrum analysis showed lower AUC values after DA depletion. (C) Coherence analysis between the LFP and the ECoG was significant in the delta range for both, sham and 6-OHDA animals (the horizontal dashed line indicates p = 0.05); note that coherence AUC decreased in the 6-OHDA group compared to sham. Data are expressed as mean ± S.E.M. and represented by a solid line and an upper and lower area defined by the S.E.M. #p < 0.05, ##p < 0.01 and ###p < 0.001 vs sham, unpaired Student's t-test. A total of 9 sham (59 recordings for LFP and 41 recordings for ECoG and coherence analysis) and 11 6-OHDA lesioned animals (31 recordings for LFP and 29 recordings for ECoG and coherence analysis) were used.

4.2.2. Dopamine acute replacement restored locus coeruleus oscillatory activity after 6-OHDA lesion

After performing recordings in basal conditions, a group of these animals (6 sham and 8 6-OHDA animals) received an acute dose of L-DOPA (24 mg/kg plus 12 mg/kg of benserazide, i.p.). A total of 47 noradrenergic neurons were recorded in the LC under the effect of the L-DOPA administration: 20 neurons from the sham group and 27 neurons from the 6-OHDA group. The percentage of neurons showing oscillatory patterns was similar when L-DOPA was administered in sham and 6-OHDA lesioned animals, 32% vs 41% respectively ($p > 0.05$, Fisher´s exact test).

After the acute administration of L-DOPA, the maximum oscillatory peak of the LFP, ECoG and coherence LFP/ECoG remained in the delta band, between 0.6 and 1.2 Hz; non remarkable oscillatory activity was found in other oscillatory frequency bands (**Figure 4.13**, left column). The posterior analysis of the power spectrum of the LFP under L-DOPA condition did not show the difference between groups observed in basal conditions, revealing that DA replacement reverted the modifications induced by the lesion with 6-OHDA ($p > 0.05$, 2-way ANOVA test) (**Figure 4.13A**). L-DOPA administration did not change the ECoG power spectrum, which was significantly lower in 6-OHDA lesioned rats ($p < 0.01$, Bonferroni's post hoc test). Similarly, L-DOPA did not alter the LFP or the ECoG in the sham group ($p > 0.05$, 2-way ANOVA test; **Figure 4.13B**). Finally, the coherence analysis between the LFP and the ECoG showed that L-DOPA administration significantly increased the AUC value in the 6-OHDA group ($p < 0.001$, Bonferroni's post hoc test) suggesting again a functional recovery of the synchrony induced by 6-OHDA lesion. L-DOPA did not modify coherence values in the sham group ($p > 0.05$, 2-way ANOVA test; **Figure 4.13C**).

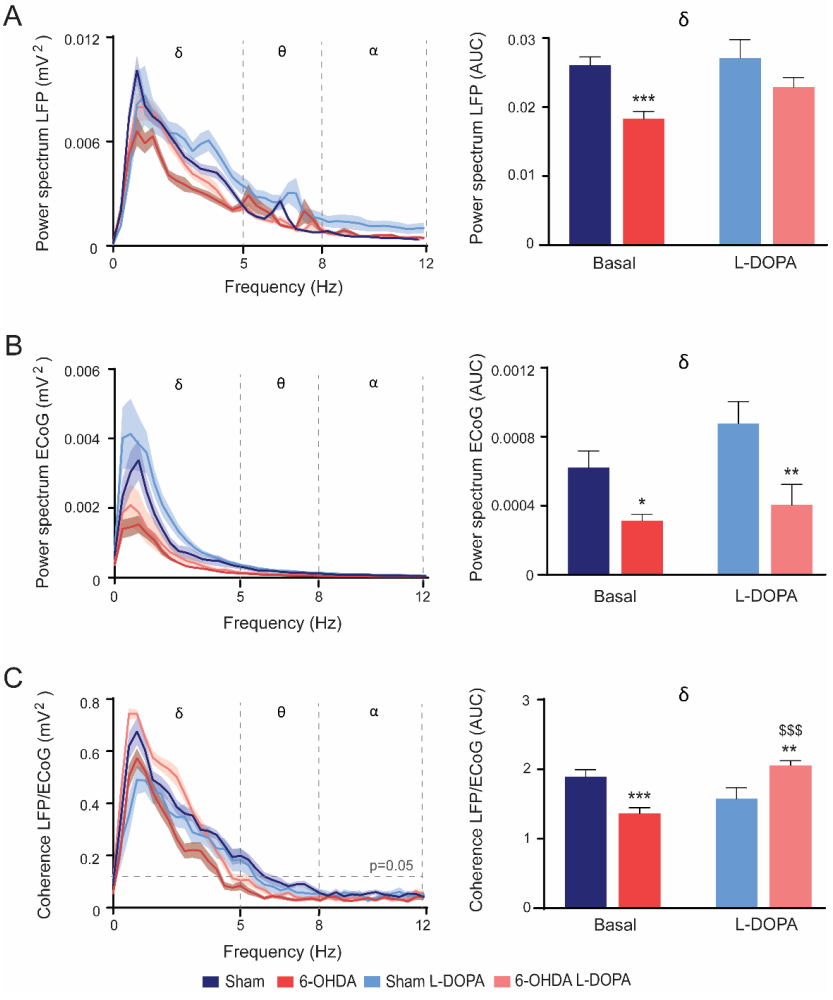

Figure 4.13. Effect of L-DOPA administration on the LFP, ECoG and LFP/ECoG coherence from sham and 6-OHDA animals. Power spectrum and coherence curves (left) were used to analyse AUC values (delta frequency range, δ) (right). (A) Power spectrum for the LFP showed a maximum activity at delta-range in all experimental groups that was significantly lower only in the 6-OHDA group. Acute L-DOPA (24 mg/kg plus 12 mg/kg of benserazide, i.p.) administration restored this value. (B) Power spectrum for the ECoG showed a maximum activity at delta-range in all groups which again was reduced in the 6-OHDA group. In this case L-DOPA failed to recover the basal value. (C) Coherence analysis between the LFP and ECoG was increased in the 6-OHDA lesioned group compared to sham after L-DOPA administration (the horizontal dashed line indicates p = 0.05). The data are shown as mean ± SEM. * $p < 0.05$, ** $p < 0.01$ and *** $p < 0.001$ vs respective sham; $$$ $p < 0.001$ vs 6-OHDA basal (Bonferroni's post hoc test). From a total of 6 sham animals n = 43 basal and n= 20 L-DOPA recordings were analysed for LFP analysis and n = 18 basal and n= 11 L-DOPA recordings were analysed for ECoG and coherence analysis. From a total of 8 6-OHDA animals n = 36 basal and n= 27 L-DOPA recordings were analysed for LFP analysis and n = 18 basal and n= 15 L-DOPA recordings were analysed for ECoG and coherence analysis).

4.2.3. Paw compression induces an event related potential in the locus coeruleus and cortex that may depend on the dopaminergic lesion

To determine how a noxious stimulus may modify LFP and cortical activity, one compression/neuron in the contralateral hind paw of the animal was applied before and after L-DOPA administration and the event related potential was analysed. For studying the sensory stimulus effect 6 sham (n = 15 basal and n= 12 L-DOPA recordings for LFP analysis and n = 15 basal and n= 8 L-DOPA recordings for ECoG and coherence analysis) and 8 6-OHDA animals (n = 21 basal and n= 15 L-DOPA recordings for LFP analysis and n = 21 basal and n= 12 L-DOPA recordings for ECoG and coherence analysis) were used.

In all groups, the compression of the paw produced an evoked potential both, in the LFP and the ECoG, that matched in time the LC phasic response described in **Study I**. In the LFP, the evoked potential consisted in a negative peak immediately after the paw compression followed by a second positive peak at ~ 0.4 s after the compression, being less pronounced in the sham animals (**Figure 4.14A, left**). The magnitude between the negative and the positive peak was higher in the 6-OHDA lesioned group ($p < 0.05$, Bonferroni's post hoc test). Interestingly, this difference disappeared after acute administration of L-DOPA (**Figure 4.14A, right**). In the ECoG, the evoked potential showed a first positive peak just after the paw compression followed by a second negative peak at ~ 0.7 s (**Figure 4.14B, left**).. In this case, L-DOPA decreased the evoked potential trigger by the paw compression in the 6-OHDA lesioned animals in comparison with its respective sham values ($p < 0.05$, Bonferroni's post hoc test; **Figure 4.14B, right**).

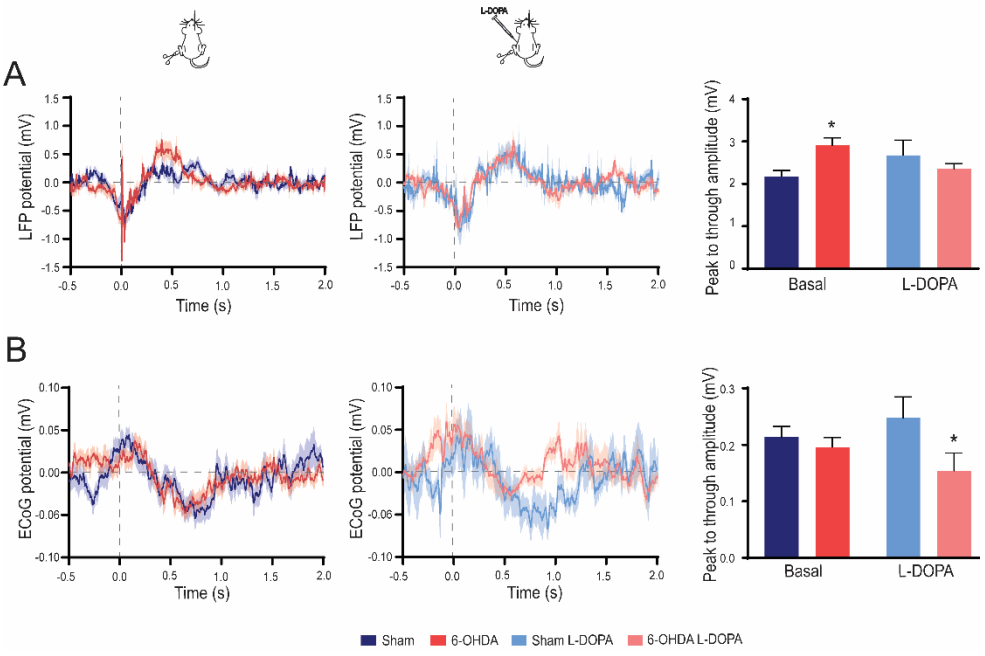

Figure 4.14. Phasic sensory-evoked response in the LFP and the ECoG from sham and 6-OHDA animals, in presence or absence of L-DOPA. (A) Average LFP evoked potential from the LC during 0.5 s before and 2 s after the paw compression in basal (left panel) and under L-DOPA (24 mg/kg plus 12 mg/kg of benserazide, i.p.) effect (middle panel). Quantitative analysis of the peak to through amplitude (right panel) was significantly higher in the 6-OHDA basal group compared to its respective sham. L-DOPA reversed this effect. (B) Average ECoG evoked potential during 0.5 s before and 2 s after the paw compression in basal (left panel) and under L-DOPA (24 mg/kg plus 12 mg/kg of benserazide, i.p.) effect (middle panel). Quantitative analysis of the peak to through amplitude (right panel) was significantly decreased only in the 6-OHDA L-DOPA group compared to its respective sham. The data are shown as mean ± SEM. * $p < 0.05$ vs respective sham, Bonferroni's post hoc test. (From a total of 6 sham animals n = 15 basal and n= 12 L-DOPA recordings were analysed for LFP analysis and n = 15 basal and n= 8 L-DOPA recordings were analysed for ECoG and coherence analysis) (From a total of 8 6-OHDA animals n = 21 basal and n= 15 L-DOPA recordings were analysed for LFP analysis and n = 21 basal and n= 12 L-DOPA recordings were analysed for ECoG and coherence analysis).

Annex II. Statistical analysis of the experiments included in Study II

	Unpaired t test				
	P value	P value summary	t (df)	n Sham	n 6-OHDA
Power spectrum LFP delta-band (AUC)	0.0002	***	t_{98}=3.93	59	41
Power spectrum ECoG delta-band (AUC)	0.0024	**	t_{58}=3.18	31	29
Coherence LFP/ECoG delta-band (AUC)	0.0162	*	t_{58}=2.48	31	29
Power spectrum LFP theta-band (AUC)	0.9781	ns	t_{98}=0.02	59	41
Power spectrum ECoG theta-band (AUC)	0.3762	ns	t_{58}=0.89	31	29
Power spectrum LFP alpha-band (AUC)	0.7773	ns	t_{98}=0.28	59	41
Power spectrum ECoG alpha-band (AUC)	0.6264	ns	t_{58}=0.48	31	29
Power spectrum LFP beta-band (AUC)	0.6693	ns	t_{98}=0.43	59	41
Power spectrum ECoG beta-band (AUC)	0.9564	ns	t_{58}=0.05	31	29

	2-way ANOVA F (DFn, DFd)		
	Interaction	L-DOPA	Lesion
Power spectrum LFP (AUC)	F (1, 122) = 1.35	F (1, 122) = 3.479	F (1, 122) = 15.8 ***
Power spectrum ECoG (AUC)	F (1, 58) = 0.7322	F (1, 58) = 3.212	F (1, 58) = 16.14 ***
Coherence LFP/ECoG (AUC)	F (1, 58) = 24.79 ***	F (1, 58) = 3.334	F (1, 58) = 0.0429
Peak to through amplitude (LFP)	F (1, 54) = 6.54 *	F (1, 54) = 0.018	F (1, 54) = 0.994
Peak to through amplitude (ECoG)	F (1, 52) = 2.309	F (1, 52) = 0.024	F (1, 52) = 5.041 *

	Fisher's exact test			
	P value	P value summary	n Sham	n 6-OHDA
Oscillatory pattern (%)	>0.9999	ns	59	41
Oscillatory pattern L-DOPA (%)	0.5546	ns	19	27

4.3. STUDY III: Dopaminergic depletion alters the excitability and spontaneous glutamatergic transmission in the locus coeruleus

To evaluate ex vivo the impact of DA depletion on LC neuron activity, we investigated the basal electrophysiological properties as well as the glutamatergic and GABAergic synaptic activity in brain slices from sham and 6-OHDA lesioned rats. Detailed statistical results belonging to this study are shown in **Annex III**.

4.3.1. Basal electrophysiological properties of the locus coeruleus neurons are compromised after the 6-OHDA lesion

Four weeks after the vehicle or 6-OHDA injection, 73 noradrenergic neurons were recorded in the LC: 28 neurons from the sham group (n = 13 animals) and 45 neurons from the 6-OHDA group (n = 14 animals). All experiments where performed in whole-cell mode.

One minute after the cell was opened, we inspected the intrinsic membrane properties of LC neurons using voltage-clamp configuration. As shown in **Table 4.3**, after DA depletion membrane capacitance and time constant were significantly lower than in sham animals ($p < 0.05$ and $p < 0.01$, respectively; unpaired Student's t-test). The rest of the parameters, membrane resistance and series resistance, were not modified ($p > 0.05$, unpaired Student's t-test). Next, IRK currents were recorded when negative voltage pulses were injected. Current-voltage curves showed the typical presence of inward rectification in both experimental groups (**Figure 4.15A**); however, this current was decreased after the 6-OHDA lesion ($p < 0.001$, Bonferroni's post hoc test; **Figure 4.15B**).

Table 4.3. Intrinsic membrane properties of locus coeruleus neurons from sham and 6-OHDA animals.

	Sham (n=28)	6-OHDA (n=45)
Membrane capacitance (pF)	110.70 ± 7.61	86.61 ± 6.41 #
Membrane resistance (MΩ)	509.70 ± 78.72	677.70 ± 115.70
Series resistance (MΩ)	14.68 ± 0.10	15.73 ± 1.12
Time constant (ms)	1.547 ± 0.13	1.17 ± 0.07 ##

Data are expressed as the mean ± S.E.M of n cells from a total of 13 sham and 14 6-OHDA animals. #p < 0.05 and ##p < 0.01 vs sham, unpaired Student's t-test.

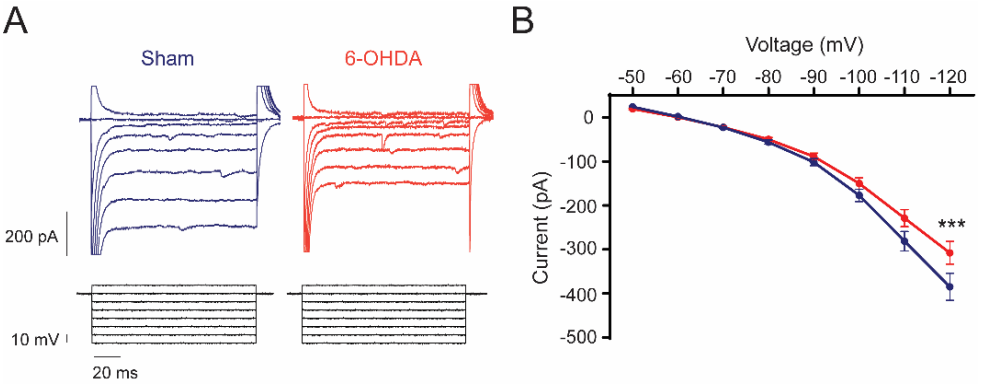

4.15. Inwardly-rectifying potassium currents in locus coeruleus neurons from sham and 6-OHDA animals. (A) Representative traces of IRK currents responses to graded series of voltage pulses (-10 mV increments from -50 mV to -120 mV, 100ms/step). (B) Graph represents IRK current response. Note that negative voltage injection produce significantly smaller IRK currents in the 6-OHDA lesioned group. Data are shown as the mean ± S.E.M. of 28 and 45 cells from a total of 13 sham and 14 6-OHDA animals, respectively. ***p < 0.001 vs respective sham, Bonferroni's post hoc test.

After studying the intrinsic properties, spontaneous action potentials were analysed (I=0). As previously reported for in vivo experiments (see **Study I**), neurons from 6-OHDA lesioned animals showed lower basal firing frequency ($p < 0.01$, unpaired Student's t-test). However, parameters related to the action potential were similar in both experimental groups ($p > 0.05$, unpaired Student's t-test; **Table 4.4**).

Table 4.4. Action potential properties of locus coeruleus neurons from sham and 6-OHDA animals.

	Sham	6-OHDA
Basal firing rate (Hz)	1.731 ± 0.4226 (28)	0.5923 ± 0.1616 (42) ##
Resting potential (mV)	-50.58 ± 3.03 (15)	-52.51 ± 1.802 (39)
Threshold (mV)	-32.32 ± 3.544 (10)	-33.09 ± 1.406 (19)
Peak amplitude (mV)	72.07 ± 4.012 (10)	75.74 ± 4.314 (19)
AP duration (ms)	1.02 ± 0.12 (10)	0.965 ± 0.09848 (19)
AHP amplitude (mV)	25.14 ± 1.029 (10)	24.39 ± 0.836 (19)

Data are expressed as mean ± S.E.M. of *n* cells. ##$p < 0.01$ (unpaired Student's t-test). A total of 13 sham and 14 6-OHDA lesioned animals were used.

Next, in current clamp configuration, we analysed LC neuron excitability by evaluating evoked spike frequency triggered by depolarizing currents steps (**Figure 4.16A**). LC neurons from 6-OHDA lesioned animals were significantly more excitable than those from sham rats were ($p < 0.05$, 2-way ANOVA test). Next, we applied hyperpolarizing current injections and assessed the change in the evoked potential (**Figure 4.16B**). Hyperpolarizing steps induced more negative potentials in neurons from 6-OHDA lesioned rats than in sham animals ($p < 0.01$, 2-way ANOVA test). Interestingly, the time to recover spontaneous firing activity after depolarization was significantly longer in 6-OHDA lesioned animals ($p < 0.001$, 2-way ANOVA test), which was independent from the amount of injected current ($p > 0.05$, 2-way ANOVA test; **Figure 4.16C**).

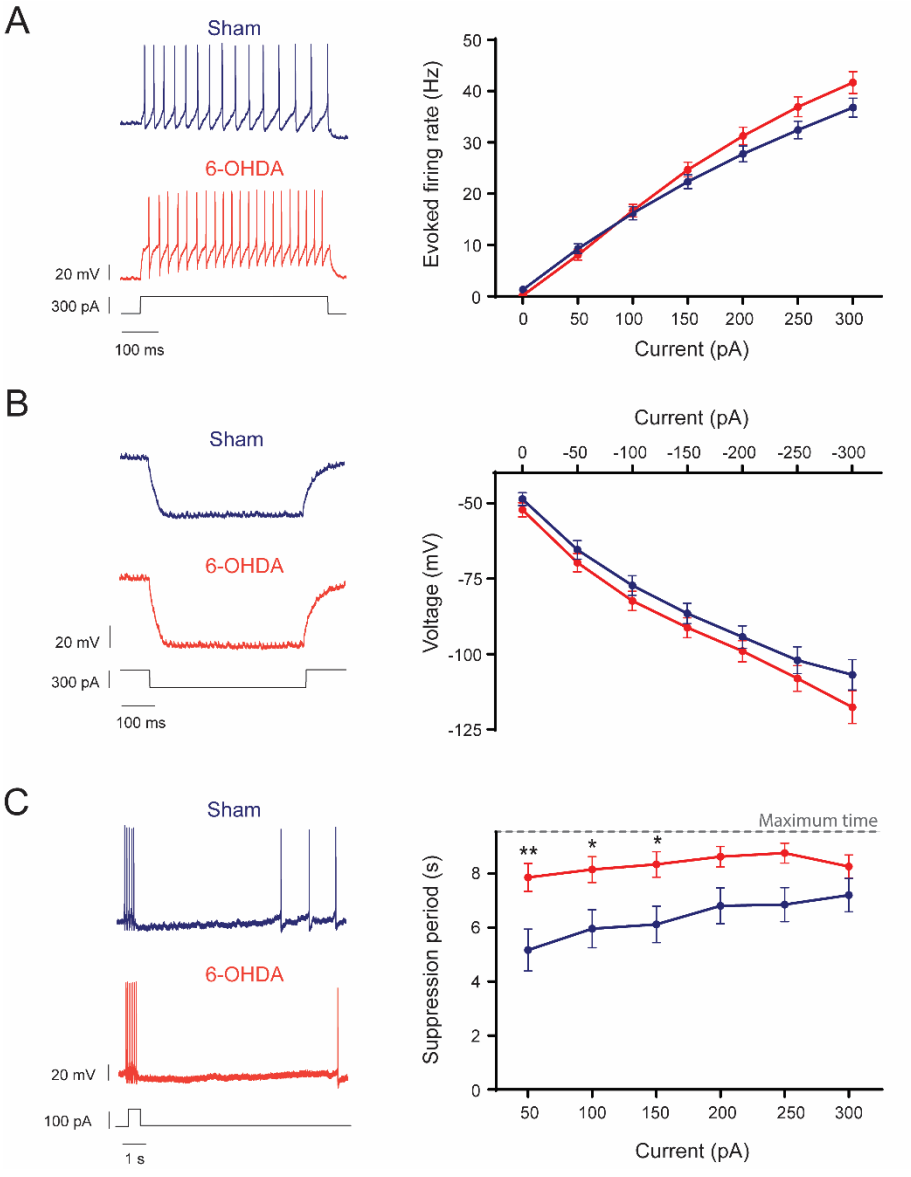

Figure 4.16. Basal properties of locus coeruleus neurons from sham and 6-OHDA animals. (A) Depolarizing current steps evoked significantly higher firing frequencies in 6-OHDA lesioned animals when compared to sham rats. (B) Hyperpolarising current steps produced more negative potentials in the 6-OHDA lesioned group. (C) Relationship between the duration of the suppression period and the injected current (the horizontal dashed line indicates the maximum recorded time at 9.5 s); Data are shown as the mean ± S.E.M. of 23-27 and 27-32 cells from a total of 12 sham and 13 6-OHDA animals, respectively. $^{*}p < 0.05$ and $^{**}p < 0.01$ vs respective sham, Bonferroni's post hoc test.

4.3.2. Dopaminergic loss does not affect the GABAergic transmission in the locus coeruleus

To study the inhibitory GABAergic transmission in the LC, we first isolated $GABA_A$ receptor mediated currents by adding NMDA, AMPA/kainate, $GABA_B$ and glycine receptor antagonists to the external solution. Recordings were obtained from 16 and 25 cells from a total of 6 sham and 9 6-OHDA animals, respectively. To confirm that the recorded currents were mediated by $GABA_A$ receptors, the $GABA_A$ antagonist gabazine (10 μM) was perfused at the end of the recordings and, as expected, all sIPSC and eIPSC were abolished (see Experimental procedures).

Mean event frequency and amplitude of sIPSC was similar in sham and 6-OHDA lesioned animals ($p > 0.05$, unpaired Student's t-test; **Figure 4.17B**). In relation to the kinetic parameters, no differences were observed in the half-width, rise time or decay time of the sIPSC ($p > 0.05$, unpaired Student's t-test; **Figure 4.17C**).

Evoked GABAergic transmission was analysed showing that for all tested frequencies (5, 10 and 20 Hz), eIPSC amplitudes were similar in the neurons from sham and 6-OHDA lesioned rats ($p > 0.05$, 2-way ANOVA test; **Figure 4.18** middle panels). Trains of stimulation at 5 and 10 Hz, revealed no synaptic plasticity ($p > 0.05$, 2-way ANOVA test) as all electric pulses produced IPSC of similar magnitude in sham and 6-OHDA lesioned animals (**Figure 4.18A and B** right panels). Trains of stimulation at 20 Hz revealed that neurons presented a moderate short-term facilitation ($p > 0.05$, 2-way ANOVA test), being significant in the sham animals when comparing the first and last stimulus ($p < 0.05$, Bonferroni's post hoc test; **Figure 4.18C**).

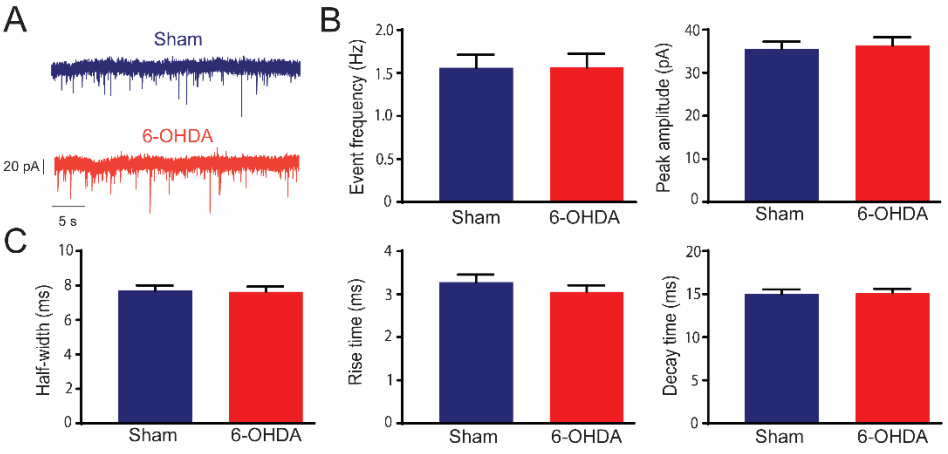

Figure 4.17. Spontaneous GABAergic postsynaptic currents in locus coeruleus neurons from sham and 6-OHDA animals. (A) Representative current traces of $GABA_A$-mediated sIPSC in sham and 6-OHDA animals. (B) Mean frequency and amplitude of sIPSC in LC neurons. (C) sIPSC kinetics parameters in LC neurons were similar in both experimental groups. Data are shown as the mean ± S.E.M. of 16 and 25 cells from a total of 6 sham and 9 6-OHDA animals, respectively.

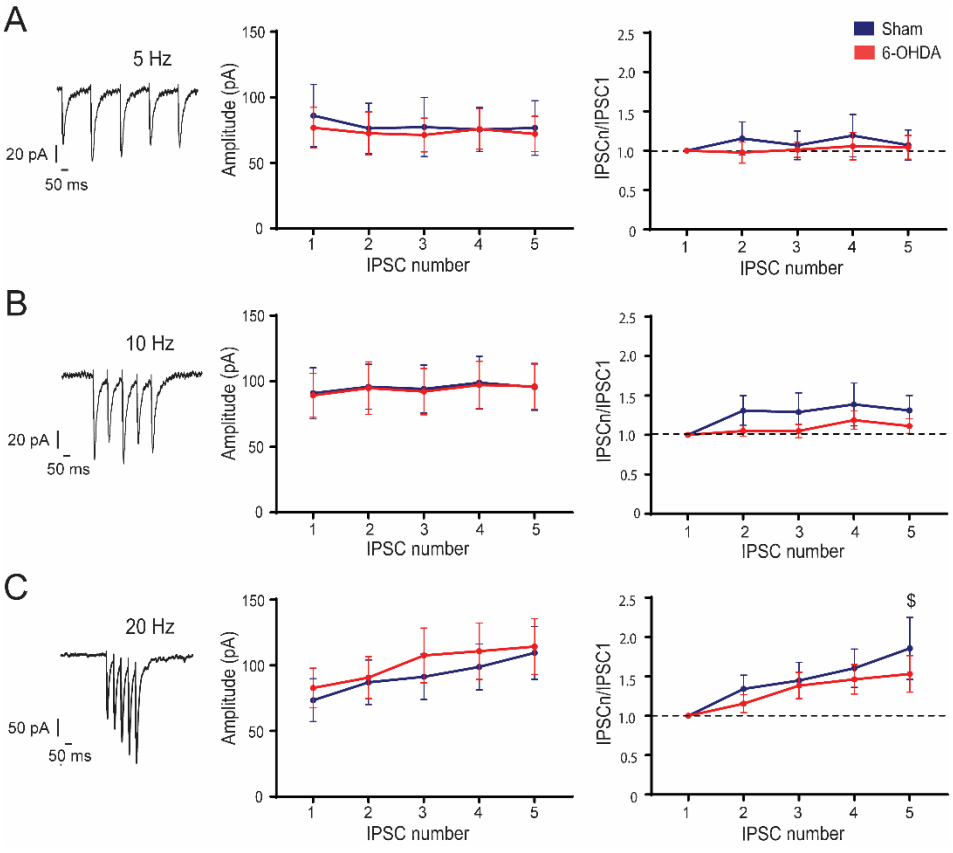

Figure 4.18. Evoked GABAergic postsynaptic currents in LC neurons from sham and 6-OHDA animals. (A) Representative train of electrically evoked IPSCs at 5 Hz (left panel), population graph showing IPSC amplitude (middle panel) and graph of normalized IPSCs (right panel). IPSC short-term plasticity was similar in both groups. (B) Same as (A) for 10 Hz stimulation trains. (C) Representative train of electrically evoked IPSCs at 20 Hz (left panel), amplitude analysis (middle) did not show modifications after dopaminergic loss; however, normalized IPSCs (right panel) were different among the stimuli denoting short term facilitation that was significant in the sham group. Data are shown as the mean ± S.E.M. of 11-17 and 14-18 cells from a total of 5-7 sham and 6-OHDA animals per group, respectively. $ $p < 0.05$ vs IPSC1 in sham, Bonferroni's post hoc test.

4.3.3. Dopaminergic loss increases spontaneous glutamatergic transmission in the locus coeruleus

Next, we evaluated whether excitatory transmission in the LC was different after DA depletion. In our preparation at the recorded potential, AMPA receptors govern the glutamatergic transmission since NMDA component is absent and the receptor antagonist, picrotoxin, blocked $GABA_A$ transmission. Recordings were obtained from 27 and 29 cells from a total of 7 sham and 10 6-OHDA animals, respectively. To further confirm that AMPA receptor-transmission was recorded at the end of the experiment, the AMPA receptor antagonist DNQX (20 μM) was perfused and completely abolished the recorded sEPSC and eEPSC (see Experimental procedures).

Mean sEPSC frequency was significantly increased after the 6-OHDA lesion ($p < 0.05$, unpaired Student's t-test), but the amplitude was similar in both experimental groups ($p > 0.05$, unpaired Student's t-test; **Figure 4.19B**). Regarding the kinetic parameters, no differences were found in peak amplitude, half-width, rise time or decay time of sEPSC ($p > 0.05$, unpaired Student's t-test; **Figure 4.19C**).

Afterwards, we analyzed the influence of the DA depletion in the evoked glutamatergic transmission. The stimulation was performed at a frequency of 10 Hz and no changes were detected in the mean amplitudes of the eEPSC ($p > 0.05$, 2-way ANOVA test). Analysis of the normalized eEPSC revealed a moderate facilitating response in both experimental groups ($p < 0.01$, 2-way ANOVA test; **Figure 4.20**).

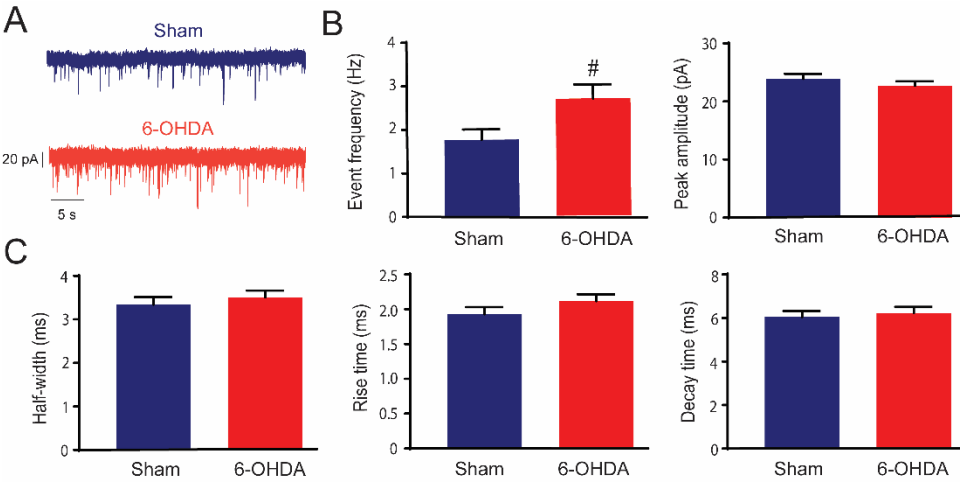

Figure 4.19. Spontaneous glutamatergic postsynaptic currents in locus coeruleus neurons from sham and 6-OHDA animals. (A) Representative current traces showing sEPSC in sham and 6-OHDA animals. (B) Mean frequency and amplitude of sEPSC in LC neurons, showing increased event frequency after the dopaminergic loss. (C) sEPSC kinetics parameters in LC neurons were similar in both experimental groups. Data are shown as the mean ± S.E.M. of 27 and 29 cells from a total of 7 sham and 10 6-OHDA animals, respectively. #$p < 0.05$ vs sham, unpaired Student's t-test.

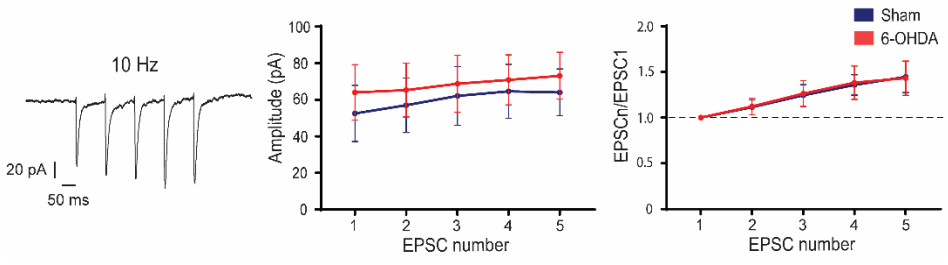

Figure 4.20. Evoked glutamatergic postsynaptic currents in LC neurons from sham and 6-OHDA animals. Representative trace of electrically EPSCs at 10 Hz (left panel). Population graph showing EPSC amplitude (middle panel) was similar in both groups. Normalized EPSCs (right panel) denoting short-term facilitation in sham and 6-OHDA lesioned rats. Data are shown as the mean ± S.E.M of 10 and 11 cells from a total of 6 sham and 7 6-OHDA animals, respectively.

Annex III. Statistical analysis of the experiments included in Study III

			Unpaired t test		
	P value	P value summary	t (df)	n Sham	n 6-OHDA
Membrane properties					
Membrane capacitance (pF)	0.0195	*	t_{70}=2.39	28	44
Membrane resistance (MΩ)	0.2921	ns	t_{70}=1.06	28	44
Series resistance (MΩ)	0.5207	ns	t_{70}=0.65	28	44
Time constant (ms)	0.0084	**	t_{70}=2.71	28	44
Action potential properties					
Basal firing rate (Hz)	0.0053	**	t_{68}=2.88	28	42
Resting potential (mV)	0.5368	ns	t_{52}=0.62	15	39
Threshold (mV)	0.8518	ns	t_{27}=0.19	10	19
Peak amplitude (mV)	0.3778	ns	t_{27}=0.89	10	19
AP duration (ms)	0.7137	ns	t_{27}=0.37	10	19
AHP amplitude (mV)	0.8735	ns	t_{27}=0.16	10	19
sIPSC					
Event frequency	0.9892	ns	t_{39}=0.01	16	25
Peak amplitude	0.7792	ns	t_{39}=0.28	16	25
Half-width	0.8835	ns	t_{39}=0.14	16	25
Rise time	0.3408	ns	t_{39}=0.96	16	25
Decay time	0.8690	ns	t_{39}=0.16	16	25
sEPSC					
Event frequency	0.0259	*	t_{54}=2.29	27	29
Peak amplitude	0.3059	ns	t_{54}=1.03	27	29
Half-width	0.4775	ns	t_{54}=0.71	27	29
Rise time	0.1836	ns	t_{54}=1.34	27	29
Decay time	0.0641	ns	t_{54}=0.47	27	29

	2-way ANOVA F (DFn, DFd)		
	Interaction	Factor	Lesion
IRK current response	F (7, 560) = 2.1890 *	F (7, 560) = 175.5000 ***	F (1, 560) = 9.2560 **
Depolarizing currents	F (6, 399) = 1.531	F (6, 399) = 183.6000 ***	F (1, 399) = 6.0190 *
Hyperpolarizing currents	F (6, 328) = 0.2059	F (6, 328) = 67.7400 ***	F (1, 328) = 7.8810 **
Suppression period	F (5, 342) = 0.4798	F (5, 342) = 1.6550	F (1, 342) = 37.8800 ***

	2-way ANOVA F (DFn, DFd)		
	Interaction	IPSC or EPSC number	Lesion
eIPSC amplitude (5 Hz)	F (4, 92) = 0.2365	F (4, 92) = 0.7475	F (1, 23) = 0.0373
eIPSC amplitude (10 Hz)	F (4, 132) = 0.0241	F (4, 132) = 0.7505	F (1, 33) = 0.0020
eIPSC amplitude (20 Hz)	F (4, 116) = 0.3926	F (4, 116) = 10.19 ***	F (1, 29) = 0.1345
$IPSC_n/IPSC_1$ (5 Hz)	F (4, 92) = 0.2538	F (4, 92) = 0.3773	F (1, 23) = 0.1934
$IPSC_n/IPSC_1$ (10 Hz)	F (4, 132) = 0.6113	F (4, 132) = 2.551 *	F (1, 33) = 1.001
$IPSC_n/IPSC_1$ (20 Hz)	F (4, 116) = 0.4531	F (4, 116) = 8.485 ***	F (1, 29) = 0.3642
eEPSC amplitude (10 Hz)	F (4, 76) = 0.2494	F (4, 76) = 4.38 **	F (1, 19) = 0.1689
$EPSC_n/EPSC_1$ (10 Hz)	F (4, 76) = 0.0149	F (4, 76) = 8.305 ***	F (1, 19) = 0.0026

4.4. STUDY IV: Dopaminergic depletion produces a discrete impact in nociceptive and anxiety behaviour and decreased locus coeruleus metabolic activity

In this study, it was investigated the effect of DA depletion on the COX activity, and expression of TH and ERK 1 and 2 in the LC. Lastly, we assessed whether the nociceptive and anxiety-like behaviour, which are linked to the LC and altered in patients with PD, were affected by the DA loss. Detailed statistical results belonging to this study are shown in **Annex IV**.

4.4.1. Dopaminergic loss does not produce major molecular changes in the locus coeruleus

First, we performed COX staining; this maker provides information about metabolic and mitochondrial activity. We performed COX staining in the slices containing the LC from sham (6 animals) and 6-OHDA rats (6 animals) (**Figure 4.21A**). In line with the electrophysiological parameters, COX metabolic activity was significantly lower in the ipsilateral site to the lesion in 6-OHDA but not in sham animals ($p < 0.001$, paired Student's t-test; **Figure 4.21B**).

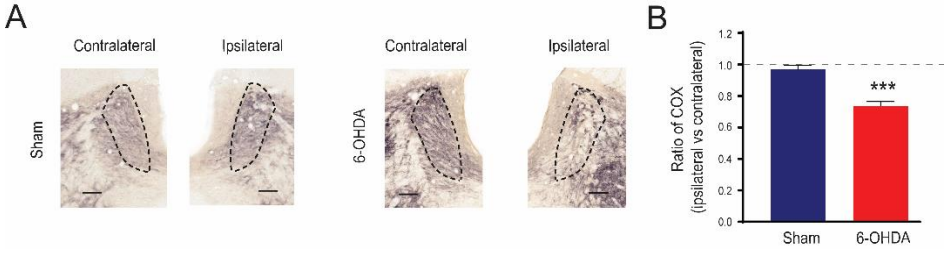

Figure 4.21. Cytochrome-c-oxidase expression in the locus coeruleus from sham and 6-OHDA lesioned animals. (A) Representative COX staining of sham and 6-OHDA animals (scale bar 100 μm). (B) Quantification shows a decreased COX staining in the 6-OHDA lesioned group. Data are expressed as mean ± S.E.M of 6 sham and 6 6-OHDA animals. *$p < 0.05$, unpaired Student's t-test.

As an additional molecular measurement in the LC, we assessed the amount of TH, the rate-limiting enzyme of NA biosynthesis. The results obtained did not show any difference between groups or between the ipsilateral and contralateral LC of the brain ($p > 0.05$, 2-way ANOVA test; **Figure 4.22**). Later, pERK1 and 2 were assessed, again, no differences were revealed after DA depletion or between the ipsilateral and contralateral LC ($p > 0.05$, 2-way ANOVA test; **Figure 4.23**).

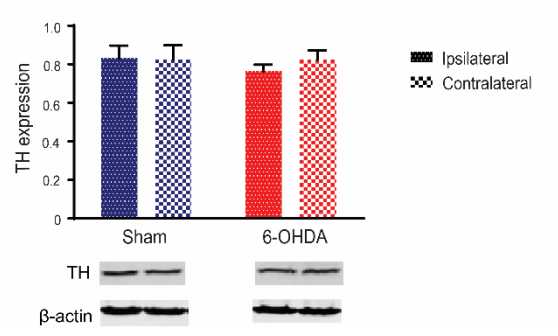

Figure 4.22. Tyrosine hydroxylase in the locus coeruleus from sham and 6-OHDA animals. Representative regions of the immunoblots and statistical data are represented. TH expression was measured in the LC in sham and 6-OHDA animals without any change. Data are shown as the mean ± S.E.M. of 6 sham and 6 6-OHDA animals per group.

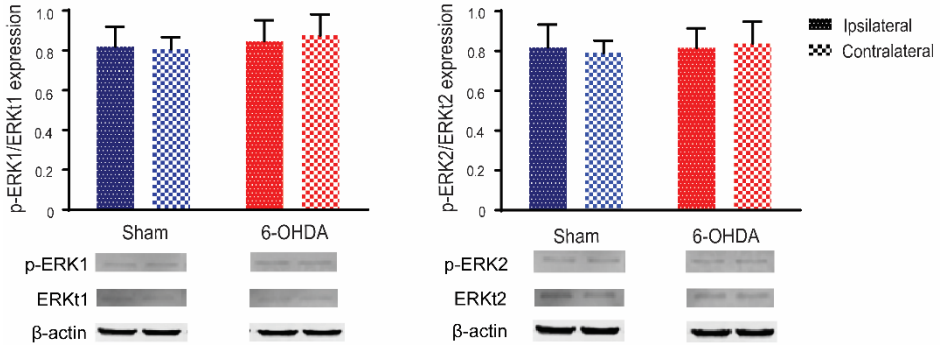

Figure 4.23. Phosphorylated extracellular signal-regulated kinase 1 and 2 levels in the LC from sham and 6-OHDA animals.
Representative regions of the immunoblots and statistical data are represented. No differences between groups were obtained after analysing the pERK1 (left) and pERK2 (right) expression. Data are shown as the mean ± S.E.M. of 6 sham and 6 6-OHDA animals per group.

4.4.2. Dopaminergic loss has minor impact in the nociceptive and anxious behavioural tests performed

Motor impairment

The body weight of both groups, sham and 6-OHDA, increased over time ($p < 0.001$, RM 2-way ANOVA test), being lower in the parkinsonian rats the last two weeks of evaluation ($p < 0.01$ and $p < 0.001$, Bonferroni's post hoc test). Weight loss in 6-OHDA animals has been previously described (Guimarães et al., 2013) (**Figure 4.24A**). Before the lesion and during four weeks after, motor impairment was evaluated with the cylinder test (once per week). As expected, DA depletion produced forelimb asymmetry during free exploration in the 6-OHDA group in all testing session after the surgery ($p < 0.001$, Bonferroni's post hoc test; **Figure 4.24B**). Overall the use of the ipsilateral paw was >80% in all the 6-OHDA lesioned rats.

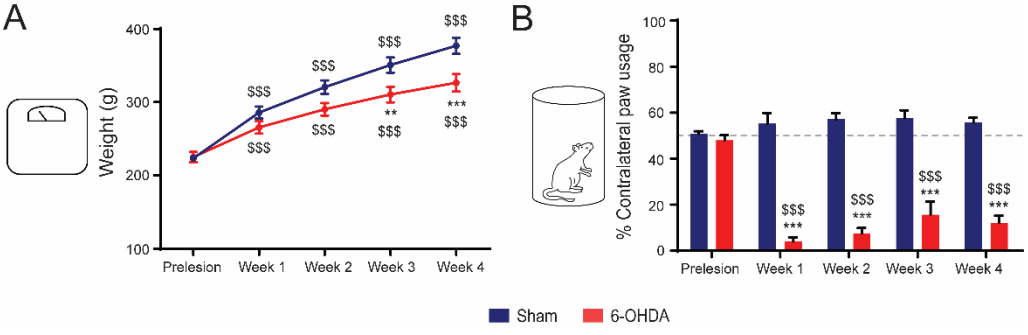

Figure 4.24. Evolution of rats' body weight and asymmetric locomotive behaviour during the study. (A) Body weight increased over time in both groups, being lower in the 6-OHDA lesioned animals. (B) Cylinder test performed before and 4 weeks after the 6-OHDA lesion confirmed the motor impairment induced by the severe dopaminergic lesion. Data are shown as the mean ± S.E.M. of 8 sham and 11 6-OHDA animals. **p < 0.01 and ***p < 0.001 vs respective sham, Bonferroni's post hoc test; $$$p < 0.001 vs respective prelesion, Bonferroni's post hoc test.

Nociceptive behaviour

The temporal evolution of the nociceptive behaviour was performed at 5 different time points: one week before the surgery and during four after (once per week). To do so, spontaneous, mechanical and thermal nociception were evaluated.

First, we evaluated spontaneous nociceptive behaviour using the dynamic weight bearing test (**Figure 4.25**). The percentage of weight distributed on each paw was represented in order to avoid errors from the body weight loss previously shown. Decreased weight distributed on the hind limb contralateral was observed in 6-OHDA animals ($p < 0.05$, RM 2-way ANOVA test). The weight distribution in the ipsilateral hind limb was similar in both groups ($p > 0.05$, RM 2-way ANOVA test). These results were accompanied by increased weight supported on the ipsilateral forelimb in 6-OHDA lesioned rats ($p < 0.01$, Bonferroni's post hoc test), since they used preferentially the ipsilateral site to the lesioned hemisphere while free exploration.

After, mechanical nociceptive behaviour was assessed using von Frey test (**Figure 4.26**). During two weeks after the lesion, the 6-OHDA group showed significantly reduced withdrawal threshold in the contralateral hind paw ($p < 0.05$ and $p < 0.01$, Bonferroni's post hoc test), denoting increased nociceptive responses. This difference was not seen in the last testing sessions. Results from the ipsilateral hind paw were not different between groups ($p > 0.05$, RM 2-way ANOVA).

Finally, we evaluated thermal nociceptive behaviour using cold (acetone test) or hot (plantar test and hot plate) stimuli. There was a discrete increased in the acetone response of the ipsilateral hindpaw in the 6-OHDA animals ($p < 0.05$, RM 2-way ANOVA) after the lesion. In the contralateral hindpaw, response to acetone was similar among the groups ($p > 0.05$, RM 2-way ANOVA; **Figure 4.27A**). In the

plantar test, heat application produced similar nociceptive responses in both hind paws among the groups ($p > 0.05$, RM 2-way ANOVA; **Figure 4.27B**). Analysis of the hot plate test neither revealed differences between groups ($p > 0.05$, RM 2-way ANOVA; **Figure 4.27C**). This response was stable over time.

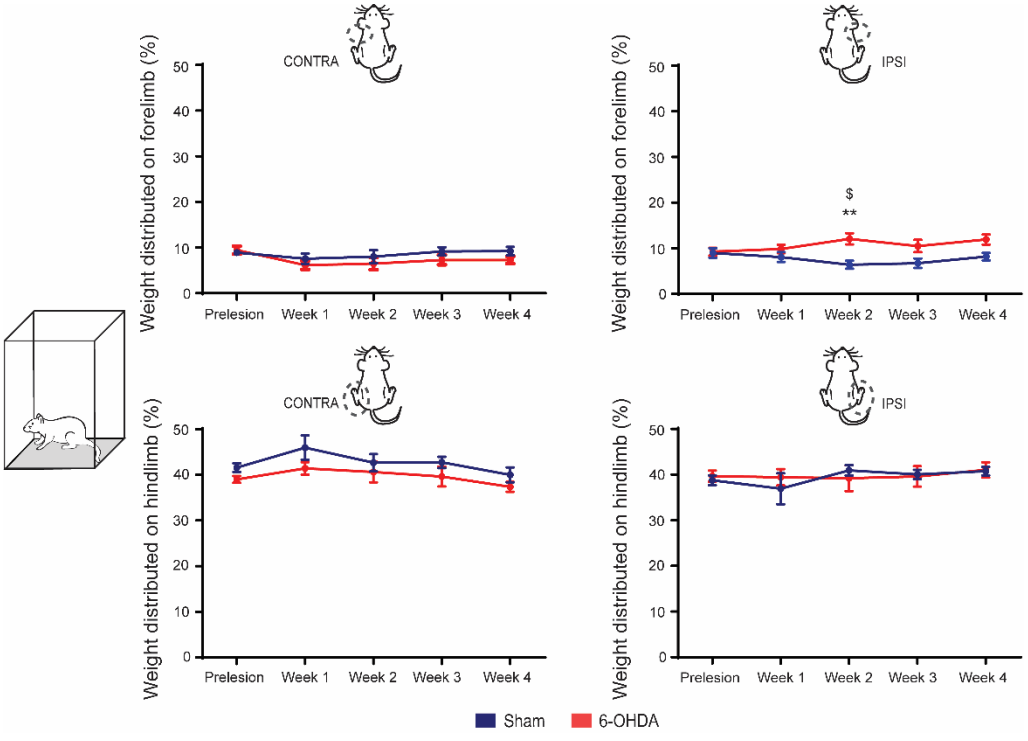

Figure 4.25. Evolution of spontaneous nociceptive behaviour during the study. Weight distributed on the contra- and ipsilateral fore (top) or hind (bottom) paws in percentage of the total weight, in the dynamic weight bearing test. Data are shown as the mean ± S.E.M. of 8 sham and 11 6-OHDA animals. $^{**}p < 0.01$ vs respective sham and $\$p < 0.05$ vs respective prelesion, Bonferroni's post hoc test.

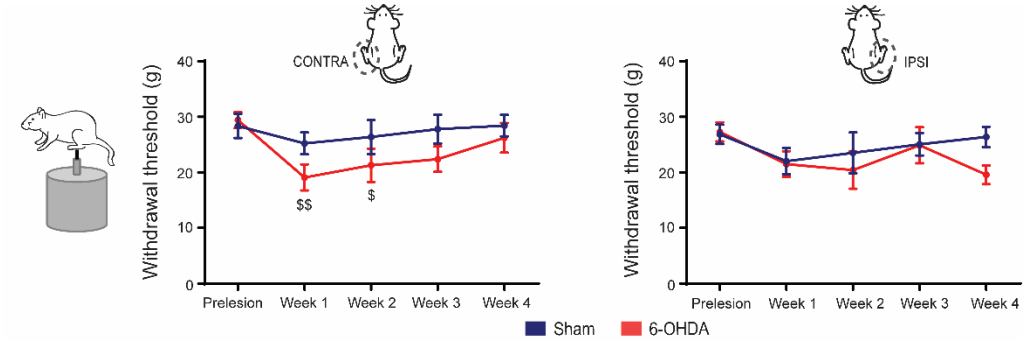

Figure 4.26. Evolution of mechanical nociceptive behaviour during the study. Mechanical hypersensitivity was evaluated with the von Frey test, a discrete progression over time was revealed after dopaminergic loss. Data are shown as the mean ± S.E.M. of 8 sham and 11 6-OHDA animals. $\$p < 0.05$ and $\$\$p < 0.01$ vs respective prelesion, Bonferroni's post hoc test.

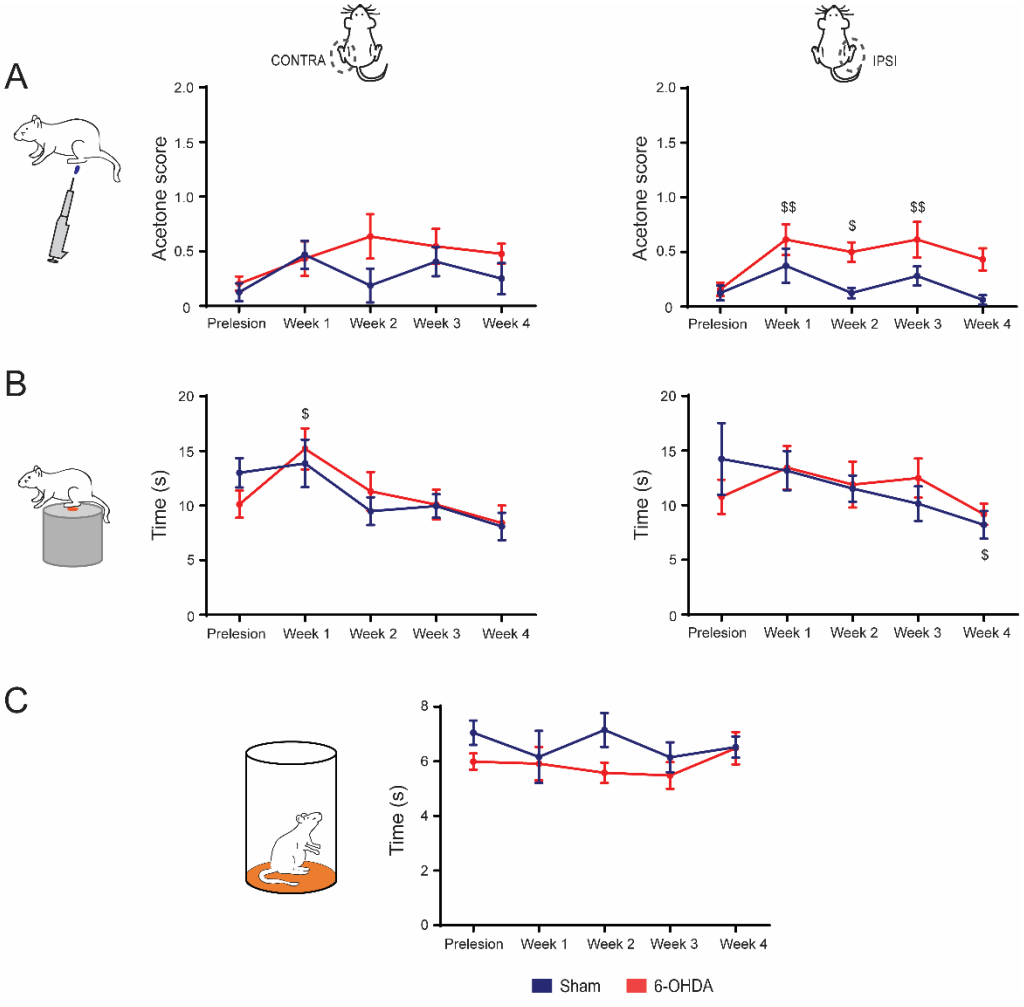

Figure 4.27. Evolution of thermal nociceptive behaviour during the study. (A) Response of contra- and ipsilateral hindpaws to acetone application showed an increased acetone score in the ipsilateral hindpaw of the 6-OHDA group over time. (B) Thermal hypersensitivity evaluated with the plantar test did not revealed differences between groups. (C) Hot plate test did not show any difference during the four weeks evaluated after the 6-OHDA lesion. Data are shown as the mean ± S.E.M. of 8 sham and 11 6-OHDA animals. $\$p < 0.05$ and $\$\$p < 0.01$ vs respective prelesion, Bonferroni's post hoc test.

Anxious behaviour

Six weeks after the dopaminergic denervation, anxiety-like behaviour was evaluated using two different paradigms, the marble burying test and the social interaction test. In the marble burying test, sham and 6-OHDA lesioned rats showed similar anxious behaviour, since both groups buried same amount of marbles ($p > 0.05$, unpaired Student's t-test; **Figure 4.28A**). The social interaction test neither showed anxious-like behaviour. The percentage of time that the studied rat spent interacting with an unfamiliar rat was similar in both experimental groups ($p > 0.05$, unpaired Student's t-test; **Figure 4.28B**).

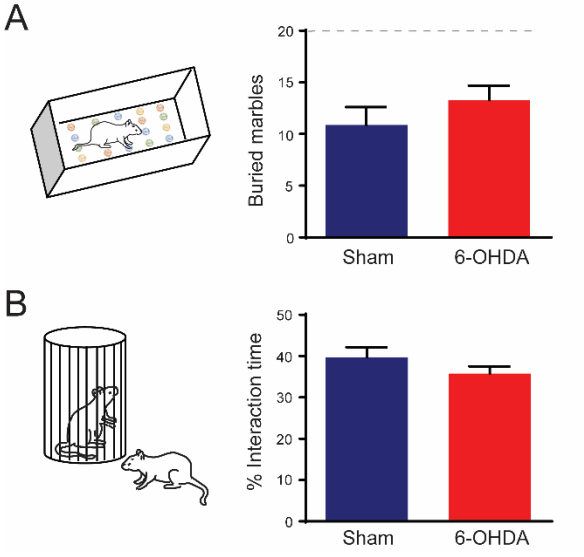

Figure 4.28. Evolution of anxiety-like behaviour during the study. (A) No differences were observed in the number of buried marbles in the arena after spending 10 minutes. (B) Percentage of interaction time between the studied rats with the unfamiliar ones was similar for both groups. Data are shown as the mean ± S.E.M. of 8 sham and 11 6-OHDA animals.

Annex IV. Statistical analysis of the experiments included in Study IV

	Unpaired t test				
	P value	P value summary	t (df)	n Sham	n 6-OHDA
COX staining	<0.001	***	t_{10}=6.4240	6	6
Buried marbles	0.3956	ns	t_{17}=0.8715	8	11
% Interaction time	0.1965	ns	t_{17}=1.344	8	11

	2-way ANOVA F (DFn, DFd)		
	Interaction	Lesion	Side
TH expression	F (1, 20) = 0.3374	F (1, 20) = 0.3757	F (1, 20) = 0.2154
pERK1/ERKt1	F (1, 20) = 0.8231	F (1, 20) = 0.6081	F (1, 20) = 0.9341
pERK2/ERKt2	F (1, 20) = 0.7991	F (1, 20) = 0.8186	F (1, 20) = 0.9725

	RM 2-way ANOVA F (DFn, DFd)		
	Interaction	Time	Lesion
Weight	F (4, 68) = 10.4 ***	F (4, 68) = 258.5 ***	F (1, 17) = 5.176 *
Cylinder test	F (4, 68) = 22.81 ***	F (4, 68) = 13.64 ***	F (1, 17) = 174.3 ***
Dynamic weight test (CL forelimb)	F (4, 68) = 0.69	F (4, 68) = 2.20	F (1, 17) = 1.50
Dynamic weight test (IL forelimb)	F (4, 68) = 3.07 *	F (4, 68) = 0.80	F (1, 17) = 7.24 *
Dynamic weight test (CL hindlimb)	F (4, 68) = 0.16	F (4, 68) = 2.44	F (1, 17) = 5.76 *
Dynamic weight test (IL hindlimb)	F (4, 68) = 0.56	F (4, 68) = 0.94	F (1, 17) = 0.02
Von Frey test (CL)	F (4, 68) = 0.8835	F (4, 68) = 2.887 *	F (1, 17) = 3.093
Von Frey test (IL)	F (4, 68) = 0.7976	F (4, 68) = 1.823	F (1, 17) = 0.9142
Acetone test (CL)	F (4, 68) = 1.171	F (4, 68) = 2.166	F (1, 17) = 1.569
Acetone test (IL)	F (4, 68) = 1.043	F (4, 68) = 4.227 **	F (1, 17) = 7.882 *
Plantar test (CL)	F (4, 68) = 0.8491	F (4, 68) = 5.505 ***	F (1, 17) = 0.01
Plantar test (IL)	F (4, 68) = 1.157	F (4, 68) = 3.028 *	F (1, 17) = 0.002
Hot plate test	F (4, 68) = 0.7129	F (4, 68) = 0.7159	F (1, 17) = 1.703

5. DISCUSSION

5. DISCUSSION

Study I

Study I indicates that DA loss influences LC tonic and phasic activity, but four weeks after the lesion are necessary to observe these changes. At this time point, 6-OHDA lesioned animals showed decreased firing rate. Furthermore, when the effect of a sensory stimulus (paw compression) in the phasic activity was assessed, lesioned animals showed increased post-stimulus frequency and prolonged suppression period. DA replacement with L-DOPA exogenous administration restored the alterations produced in the tonic and phasic parameters.

Dopamine depletion reduces tonic firing frequency in locus coeruleus neurons

Few studies carried out in 6-OHDA lesioned animals have reported electrophysiological changes in the basal activity of LC neurons as a consequence of the nigrostriatal degeneration. The present data are in agreement with previous work from our lab (Miguelez et al., 2011b, 2011a) showing decreased firing frequency in the LC from 6-OHDA lesioned animals. However, these data differ from other publications reporting that dopaminergic loss increases LC neuronal activity (Guiard et al., 2008; Wang et al., 2009). The basis for the discrepancy may rely on methodological variations, since the animal model used in each study was different. In the work from Wang et al (2009), the toxin was injected unilaterally in the SNc and Guiard and collaborators (2008) injected the toxin bilaterally in the ventral tegmental area. However, in our study the location of the toxin injection was the MFB, as it was done in the previous studies from our laboratory. Guiard et al. (2008) reported that the mean number of LC neurons recorded per track was

significantly lower in lesioned animals, suggesting that the observed effect in the firing frequency might be a compensatory mechanism due to the noradrenergic damage. Indeed, noradrenergic cell loss in the LC leads to hyperactivity of the remaining neurons (Szot et al., 2016), probably because the loss of NA and subsequent decreased of the tonic inhibitory control of the nucleus (Szot et al., 2012, 2016). In the model used in the present project, it is likely that the number of LC cells was unaffected as described by a previous study from our research group in which not only the mean number of LC neurons recorded per track was unaltered, but also the number of TH-positive cells, quantified by stereological method (Miguelez et al., 2011b). In our model the decreased basal firing rate may be a direct effect of the absence of DA and not a consequence of the NA cell loss, in fact when we administered L-DOPA tonic activity was recovered to sham values. Other studies measuring NA content in LC-projecting areas indirectly indicate that the LC activity is reduced. Indeed, rats lesioned with 6-OHDA in the MFB show lower levels of NA in the spinal cord, striatum, SNc, hippocampus and prefrontal cortex from the lesioned hemisphere (Bhide et al., 2015; Cao et al., 2016; Kamińska et al., 2017). In addition, LC hypoactivity is also shown in **Studies III and IV** where significant reduction in ex vivo spontaneous firing rate and COX activity was reported.

As described in the introduction, it is well known that LC tonic electrical activity is mainly regulated by α_2-adrenoceptors, which provide local feed-back inhibition leading to a progressive reduction in the firing activity (Cedarbaum and Aghajanian, 1976; Egan et al., 1983). However, in our study, neurons from lesioned and sham groups responded in a similar way to the systemic administration of an α_2-adrenoceptors agonist (UK 14,304), confirming that changes in these receptors are not responsible for the decreased tonic firing rate. In this line, a previous publication shows similar results with the administration of the α_2-adrenoceptors agonist,

clonidine (Miguelez et al., 2011b). Other aspects that could origin decreased LC spontaneous activity could be a reduction of TH expression or alteration of pacemaking currents (Williams et al., 1984, 1988, 1991; Osmanović et al., 1990; Forsythe et al., 1992; Alreja and Aghajanian, 1993; Osmanović and Shefner, 1993; de Oliveira et al., 2010; Sanchez-Padilla et al., 2014; Matschke et al., 2015, 2018), along with increased $GABA_A$-mediated GABAergic transmission (Corteen et al., 2011; Breton-Provencher and Sur, 2019). However, these options were further discussed and discarded in **Studies III and IV**.

Despite the high presence of α_2-adrenoceptors, the LC also contains α_1-adrenoceptors (Young and Kuhar, 1980; Chamba et al., 1991; Pudovkina et al., 2001; Osborne et al., 2002; Pudovkina and Westerink, 2005). There is compelling indirect pharmacological evidence about DA acting at α_1-adrenoreceptors in different tissues (see review Lei, 2014), and in particular in the LC, causing an activation of this nucleus (Pudovkina and Westerink, 2005; Lin et al., 2008). Apart from DA acting onto α_1-adrenoceptors, D_1-dopaminergic receptors may also exert tonic activation of LC neurons. These latter receptors are present on the somas of the LC noradrenergic neurons (Shelkar et al., 2017) and, although signal transduction driven by D_1-dopaminergic receptors has not yet been examined in the LC, studies in other brain regions and cell types have established that D_1 receptor activation produces a stimulatory effect via adenylyl cyclase activity regulated by Gs-type G proteins (see review (Undieh, 2010)). Thus, it is possible that dopaminergic loss compromises the equilibrium in the LC, preventing the activation of α_1-adrenoceptors or D_1-dopaminergic receptors by DA and the subsequent LC stimulation. Under control conditions, substantial amounts of DA are present in the LC (Versteeg et al., 1976; Kaehler et al., 1999b) and the nigrostriatal lesion induced by 6-OHDA may decrease the dopaminergic levels directly in the LC, through its direct innervation from the

SNc (Breton-Provencher and Sur, 2019). Another mechanism that could also influence LC tonic activity is the $GABA_B$ mediated GABAergic tonic inhibition. This possibility is further discussed in **Study III**.

Dopamine depletion enhances phasic activity in locus coeruleus neurons

The phasic activity in the LC is driven by both, noxious and non-noxious stimuli (Cedarbaum and Aghajanian, 1978; Aston-Jones and Bloom, 1981b) and it is important for arousal (Carter et al., 2010), attention (Vazey et al., 2018), adaptation to changing environmental circumstances (Snyder et al., 2012; Cope et al., 2019), stress vulnerability (Curtis et al., 2012) and nociception (Alba-Delgado et al., 2012b; Borges et al., 2017a).

The transmission of the sensory information triggered by a noxious stimulus is driven by the primary afferents, which reaches the dorsal horn of the spinal cord and synapses with second-order neurons. Mostly, the signal is contralaterally transmitted to different supra-spinal structures, such as the PGi, which strongly innervates the LC (Andrezik et al., 1981; Aston-Jones et al., 1986; Ennis et al., 1992; Llorca-Torralba et al., 2016; Neves et al., 2018; Vazey et al., 2018; Breton-Provencher and Sur, 2019). Once the noxious stimulus arrives at the LC, phasic activity is triggered, which is composed by two phases: an excitation (post-stimulus frequency) and a subsequent inhibition (suppression period). In our study when the contralateral paw was compressed, LC neurons from 6-OHDA animals showed increased excitation followed by enlarged inhibition. Interestingly, changes in both modes of activity, tonic and phasic, were reverted by acute L-DOPA administration, suggesting the involvement of DA in the control of these functional parameters.

The mechanism involved in the generation of the excitatory component of the phasic response is linked to glutamate released from the PGi, which is strongly activated by noxious inputs (Azami et al., 1981; Tung et al., 1989; Ennis et al., 1992; Chiang and Aston-Jones, 1993). However, the generation of the suppression period is not completely understood although an implication of α_2-adrenoceptors has been proposed (Cedarbaum and Aghajanian, 1978), as we discuss below.

Excitatory component

Various studies in anesthetized rats have demonstrated that noxious stimulation (footshock or paw compression) evokes the excitatory component of the phasic response in the LC. This excitation is triggered by glutamate released from the PGi, acting onto non-NMDA receptors in the LC, since the phasic response is abolished by non-NMDA receptor blockage or PGi inhibition (Tung et al., 1989; Ennis et al., 1992; Chiang and Aston-Jones, 1993). Therefore, in future experiments it would be interesting to assess the functionality of the PGi after dopaminergic loss in basal conditions and during noxious stimulation.

Some publications have also suggested the participation of α_2-mediated mechanism in this excitatory component of the phasic response. Simson et al. initially proposed that systemic blockade of α_2-adrenoceptors augments the responsiveness to the paw compression (Simson and Weiss, 1988). However, more recent publications do not support this observation. Administration of atomoxetine, a potent NA uptake inhibitor that indirectly activates α_2-adrenoceptors, does not modify the excitatory component induced by footshock in anesthetized rats (Bari and Aston-Jones, 2013). In our study administration of the α_2-adrenoceptor agonist, UK 14,304, neither modified the post-stimulus frequency in any experimental group, indicating that the changes observed in the 6-OHDA lesioned group do not depend

on α_2-adrenoceptor activation. In addition, α_2-adrenoceptor antagonists do not modify glutamate-induced excitation in the LC ex vivo (Zamalloa et al., 2009).

Some authors also suggest the implication of other neurotransmitter in the excitatory component of the response, as the serotonin system. Modulation of serotonin content but not direct antagonism of 5-HT receptors seems to alter this parameter (Simson and Weiss, 1988); specifically, serotonin depletion (PCPA treated) increases the excitation while serotonin precursor administration attenuates it (Shiekhattar and Aston-Jones, 1993). In 6-OHDA lesioned animals, some publications have reported lower serotonin levels in different brain areas (Karstaedt et al., 1994; Kamińska et al., 2017) and less sensitivity to serotonergic drugs in the LC (Miguelez et al., 2011b). However, previous publications from our group using the same animal model used in our study, did not find modifications in the electrophysiological properties of the dorsal raphe nucleus (Miguelez et al., 2011b, 2016a) neither in the serotonin content in projecting areas in the lesioned hemisphere (Miguelez et al., 2016b).

Inhibitory component

The α_2-adrenoceptors seem to be responsible, at least in part, for the inhibitory component of the phasic response. Administration of α_2-adrenoceptors antagonists attenuates the suppression period (Cedarbaum and Aghajanian, 1978) while NA uptake inhibitor administration increases it (Bari and Aston-Jones, 2013). In our work, an α_2-adrenoceptor agonist increased the suppression period triggered by the paw compression. However, the effect of the α_2-adrenoceptor agonist was similar in sham and 6-OHDA lesioned animals, indicating again no changes in the sensitivity of these receptors.

We also observed that the duration of the suppression period was not correlated with the magnitude of the post-stimulus frequency, but with the tonic activity of the nucleus, in both experimental groups. Since the suppression period is probably regulated by the tonic activity rather than by α_2-adrenoceptors, any change in this activity induced by other mechanisms will modify it. Indeed, those drugs that reduce the suppression period, α_2-adrenoceptors antagonists, also augment the basal firing frequency (Ugedo et al., 1998; Miguelez et al., 2009), while drugs enlarging the suppression period have the opposite effect on the firing rate (Bari and Aston-Jones, 2013).

Correlation between the spontaneous activity and the suppression period explains the similar enlarged effect on this last parameter in the 6-OHDA lesioned rats, regardless the stimulated hindpaw (contralateral or ipsilateral to the recording electrode). Indeed, ipsilateral paw compression also evoked a phasic response in the LC that was similar in sham and 6-OHDA lesioned rats. Although spinal ascending projections to the LC are mainly contralateral, bilateral pathway has been suggested since unilateral noxious stimulation results in bilateral activation of the LC in both hemispheres (Proudfit, 2002; Hayashida et al., 2008; Alba-Delgado et al., 2012b; Neves et al., 2018). It is not clear, however, how ipsilateral stimulation triggers this response. One possibility could be that the LC from the intact hemisphere is responsible for it. In this sense, reciprocal innervation between both LC has been described (Li et al., 2016), and direct LC stimulation triggers a phasic response in the contralateral LC similar to that analysed in the present study (Marzo et al., 2014). Thus, the lack of alteration that we observed in the response to the compression of the ipsilateral paw is probably due to the control exerted by the contralateral intact LC.

Our results show that dopaminergic depletion alters the phasic-tonic balance of LC neurons, producing decreased tonic but enhanced phasic activity in 6-OHDA lesioned rats. The behavioural meaning of this increased phasic:tonic ratio is however not well understood. Some authors suggest that in stressful conditions, elevated tonic activity constrains LC phasic activity ('hyperarausal') in order to scan diverse stimuli providing adaptation to the challenging environment (Valentino and Foote, 1987, 1988; Curtis et al., 2012). By contrast, when stress or painful situations are persistent, the electrophysiological changes are the opposite ones, inducing reduced tonic and exacerbated phasic responses (Bravo et al., 2013; George et al., 2013; Borges et al., 2017a). Other authors have also related increased phasic:tonic ratio to improved task performance but also to attention-deficit/hyperactivity disorder (Aston-Jones and Cohen, 2005; Gilzenrat et al., 2010; Howells et al., 2012). In this line, neonatal disruption of the nigrostriatal dopaminergic pathway with 6-OHDA induces attention-deficit/hyperactivity like disorder in mice (Bouchatta et al., 2018). Patients with a history of attention-deficit/hyperactivity disorder show also higher risk of developing diseases of the basal ganglia and cerebellum, including PD (Curtin et al., 2018).

Dopamine replacement restores tonic and phasic activity in locus coeruleus neurons

L-DOPA is the metabolic precursor of NA through its decarboxylation into DA by the aromatic amino acid decarboxylase and the β-hydroxylation of DA by the DA beta-hydroxylase. The observed changes in this study can be attributed to a direct action of L-DOPA on adrenergic receptors (Alachkar et al., 2010) or to the ability of DA to act on α_1-adrenoreceptors or D_1-dopaminergic receptors probably promoting LC neuron activation. A previous study from our group reported that

chronic treatment with L-DOPA is also able to recover the reduced firing frequency in 6-OHDA rats (Miguelez et al., 2011a).

The effect of L-DOPA on the phasic response may be related to the improvement on the spontaneous activity (for the inhibitory component) or to the modulation of glutamatergic transmission (for the excitatory component), which is increased in many brain nuclei during parkinsonian conditions (Aristieta et al., 2012; Schintu et al., 2016; Chang et al., 2019). Indeed, it has been proven that L-DOPA inhibits excitatory synaptic transmission in the nucleus tractus solitarius in control rats (Ohi et al., 2017) and reduces glutamate efflux in the primary motor cortex of 6-OHDA lesioned rats (Lindenbach et al., 2016). Apart from restoring the excitatory and inhibitory components, L-DOPA dramatically suppressed the probability to trigger the phasic response in the LC. This effect occurred in sham and 6-OHDA lesioned animals, suggesting a mechanism not dependant on the integrity of the nigrostriatal pathway that probably involves structures at the spinal level, rather than supraspinal nuclei. L-DOPA derived DA acting on D2 receptors may affect the primary sensory afferent system, as D2 receptors are present in the spinal dorsal horn (Yokoyama et al., 1994), where primary afferents terminate.

Persistent dopamine loss is necessary to observe changes in the locus coeruleus neurons

Finally, although we have shown changes in tonic and phasic electrophysiological properties of LC neurons four weeks after the induction of the dopaminergic loss, minor changes occurred two weeks after the 6-OHDA lesion. This finding suggests the need of a persistent DA deficit in order to observe consistent changes in the noradrenergic system. This is a methodological issue, as mentioned above, that should be taken into account when using the 6-OHDA

model. In agreement with our results, a recent study performed in mice lesioned in the medial forebrain bundle with 6-OHDA, found that although striatal dopaminergic terminals degenerate already one week after the lesion, dopaminergic cells are progressively affected over three week-time. The lesion was considered stable only three weeks after the 6-OHDA injection (Rentsch et al., 2019). Likewise, other studies performed in rats observed stable changes four weeks after the 6-OHDA lesion in the MFB (Sun et al., 2011) or in the SNpc (Schwarting and Huston, 1996).

Conclusion

In this study, we conclude that dopaminergic persistent loss has an impact in the electrophysiological activity of LC neurons favouring an increased phasic:tonic ratio. These changes are likely to contribute to the expression of behavioural modifications and may depend on different mechanisms including PGi hyperactivity and α_1, D_1, $GABA_B$, but not α_2, receptors changes. Interestingly, dopamine replacement was able to restore LC functionality indicating that direct DA loss was responsible for the observed changes.

Study II

In Study II several findings were obtained. Dopaminergic loss induced decreased low frequency oscillatory activity and synchronization between the LC and mPFC and DA acute replacement reversed these changes. Finally, DA loss induced changes in the noxious stimulation related potential in the LC suggesting an increased or decreased probability of response depending on DA availability.

Dopaminergic depletion decreases low frequency oscillatory activity in the locus coeruleus

A large number of studies have been performed in anesthetized parkinsonian animals showing low frequency oscillations increment in the basal ganglia (substantia nigra reticulata, subthalamic nucleus and entopeduncular nucleus) and a strong synchronization between them and the cerebral cortex (Magill et al., 2001; Belluscio et al., 2003; Parr-Brownlie et al., 2007; Walters et al., 2007; Galati et al., 2009; Aristieta et al., 2016, 2019). However, so far no study has analyzed whether the pattern of oscillatory activity changes in non-basal ganglia nuclei that are also involved in PD, in particular the LC under DA loss circumstances. Although different publications have reported the oscillatory activity of the LC in basal conditions and in models of other pathologies, the methodology of data analysis is very heterogeneous (Christie et al., 1989; Ishimatsu and Williams, 1996; Lestienne et al., 1997; Eschenko et al., 2012; Bari and Aston-Jones, 2013; Manohar et al., 2017; Torres-Sanchez et al., 2018; Totah et al., 2018; Vazey et al., 2018). In this study, we followed the methodology previously used in our laboratory and in other publications carried out in the basal ganglia studies (Magill et al., 2001; Galati et al., 2009, 2010; Aristieta et al., 2016, 2019).

First, we analyzed the spike wave autocorrelogram of LC neurons in order to evaluate the presence of rhythmic fluctuations in their spike rate. Previous studies from our laboratory, using the same model of 6-OHDA lesion, saw increased proportion of oscillatory neurons in the output basal ganglia, along with an evident hyperactive neuronal discharge pattern (Aristieta et al., 2016, 2019). In our study, the majority of the LC neurons showed non-oscillatory activity (around 60-70 %), and the lesion with 6-OHDA did not modify this percentage. Thus, lack of modification may be due to the absence of change in the neuronal discharge pattern in spontaneous active LC neurons, shown in the **Study I**.

Power spectrum analysis found that nigrostriatal degeneration causes changes in the LFP of the LC in 6-OHDA lesioned rats. LFP recordings reflect the activity of the neural population surrounding the electrode, providing a measure of mostly the synaptic activity (reviewed in (König, 1994; Buzsáki et al., 2012)). Here, we expressed the data with a frequency-domain analysis, which segregates the signal in its different components according to its frequency domain. In the LC, we saw mainly the presence of low-frequency oscillations with a peak of oscillatory activity in the delta-frequency band (0-5 Hz), as previously shown in awake and anaesthetized rats in the LFP of this nucleus during spontaneous activity (Manohar et al., 2017; Torres-Sanchez et al., 2018). The delta activity in the LC was attenuated after DA loss and reverted after acute administration of L-DOPA. It seems, therefore, that low frequency oscillatory activity is under the control of DA; conversely, its decrement is a direct consequence of the lack of DA in our model.

Dopaminergic depletion decreases the synchronization between the locus coeruleus and prefrontal cortex

The analysis of the oscillatory activity in the LC and its relation with the projection targets in a model of PD will help us to better understand brain connectivity impairments beyond the basal ganglia. The LC extensively innervates the mPFC and modulates its activity (Chandler et al., 2014; Hirschberg et al., 2017), mainly through an ipsilateral pathway (Chandler and Waterhouse, 2012). LC cells that innervate the mPFC contain enriched mRNA transcripts coding for markers of excitability and transmitter release and they present increased excitatory synaptic transmission, spontaneous firing rate and excitability compared to other LC neuron subtypes in control animals (Chandler et al., 2014). In addition, release of NA is higher in the mPFC than in other cortical areas (Agster et al., 2013). At the same time, the LC is strongly innervated by the mPFC (Lu et al., 2012; Torres-Sanchez et al., 2018; Breton-Provencher and Sur, 2019). Overall, these publications support the importance of the relation between both areas.

As seen in the ECoG of awake, non-anesthetized naturally sleeping and anaesthetized control rats (Fujisawa and Buzsáki, 2011; Eschenko et al., 2012; Li et al., 2016; Manohar et al., 2017; Torres-Sanchez et al., 2018), the power spectrum from the PFC showed low-frequency oscillations, with major activity in the delta-frequency band. Although we observed delta oscillations in the mPFC of the 6-OHDA lesioned animals, the average of the AUC of the power spectra was decreased when compared to that obtained in sham animals, and acute L-DOPA administration did not reverse the impaired activity. Likewise, patients with PD have attenuated delta activity in the mPFC, which is associated with cognitive dysfunctions, even after taking the prescribed dopaminergic medication (Parker et al., 2015). One possible mechanism for this pattern may be that DA release in the

mPFC facilitates delta-band oscillations, as mPFC activity is synchronized at low-frequency bands with dopaminergic neurons (Fujisawa and Buzsáki, 2011). Thus, DA loss might lead to adaptive changes underlying the alterations in oscillatory activity.

In order to understand how DA loss affects rhythmic brain activity between the LC and the mPFC, we studied their synchronization/coherence to measure whether oscillations in the two places show a consistent phase relationship. Studying the synchrony between brain nuclei may be crucial because this parameter encodes information about connexion between different areas and its relevance in the processing of sensory signals (reviewed in (Engel et al., 2001, 2012)). The connectivity between both areas is of interest, since the mPFC (Hirschberg et al., 2017; Hiser and Koenigs, 2018; Cope et al., 2019) and its coherence with the LC (Eschenko et al., 2012; Zitnik et al., 2016; Torres-Sanchez et al., 2018) play an essential role in emotions and cognition, which are alterations that appear in patients with PD (Svenningsson et al., 2012; Aarsland et al., 2017; Schrag and Taddei, 2017; Ryan et al., 2019). In the present study coherence analysis identified coordination between the LC and the mPFC in the delta frequency range, similar to that observed in other studies with other animal models (Torres-Sanchez et al., 2018; Totah et al., 2018). This coherence was decreased in 6-OHDA lesioned animals, which suggests an impairment in the neuronal communication between both areas. In fact, it has been previously seen that when the power spectrum of the LC and mPFC decrease at the delta frequency band, the coherence between them is also impaired (Manohar et al., 2017). In addition, L-DOPA acute administration re-established the coherence pattern, probably as a consequence of the restored activity in the LC, since an increased in the AUC of the power spectrum of the LC, without affecting the cortical

activity, is capable of increasing in the coordination between both nuclei (Torres-Sanchez et al., 2018).

Dopaminergic depletion increases noxious stimulus-induced potentials in the locus coeruleus

As mentioned in the discussion from **Study I**, LC neurons are characterized by its activation following a peripheral noxious stimulus. Previous studies with simultaneous and multi-unit extracellular recordings in awake and anesthetized rats demonstrate that paw compression produces a similar phasic response in the entire population of LC neurons, suggesting high synchrony all over the nucleus during the evoked discharge (Aston-Jones and Bloom, 1981b; Chen and Sara, 2007). However, a recent paper reports that the LC response to a sensory stimulus under anaesthesia is not necessarily homogeneous and units tend to respond independently to each other (Totah et al., 2018).

In the previous sections, the analysis of the power spectrum represented the signal in a frequency domain, through identification of the bands with higher dominance. However, this type of analysis hides temporal information and it is difficult to determine when different frequency components are present. Moreover, delta oscillations observed before need around 1 to 3 seconds to be completed. For these reasons, we evaluated the effects of paw compression with a time-domain analysis as previously made in other studies (Bari and Aston-Jones, 2013; Vazey et al., 2018).

The peak to through amplitude of the average evoked potential in the LC was significantly higher in the 6-OHDA lesioned animals compared to that in sham animals, and this effect was reversed by acute L-DOPA administration. Since LFP represents integrated synaptic activity, it seems that DA depletion increases the

average synaptic input and the spiking output in the LC when a sensory-evoked response is triggered, or alternatively it increases the LC sensitivity to stimulus probability, as suggested when the event-related potentials are reduced and sensitivity to stimulus probability is lowered (Ehlers and Somes, 2002). In any case, L-DOPA administration restores these inputs. When the paw compression evoked potential in the mPFC was represented, it was clear the apparition of a transient potential in both groups. A recent study also described a transient gamma power increase in the mPFC after LC phasic discharge, that was abolished after LC firing inhibition (Neves et al., 2018). These findings, together with those that show a decrement in LC-mPFC synchronization, indicate that DA loss impairs the influence that the LC elicits over cortical sensory processing areas (Waterhouse and Woodward, 1980; Armstrong-James and Fox, 1983) suggesting that DA is a significant contributor to sensory processing by LC and mPFC networks. Altogether, these results may contribute to understand the mechanisms involved in non-motor symptoms of PD such as impairment in pain sensitivity and cognitive function.

Conclusion

To the best of our knowledge, this is the first time that oscillatory activity of the LC, its synchronization with the mPFC and phasic activity (event-related potential) have been analysed in the 6-OHDA animal model, both, in absence and presence of L-DOPA. In summary, our results highlight that rodents show low-frequency activity in the mPFC and LC activity and synchronization between both areas, and that this activity is attenuated when DA signaling is dysfunctional. In addition, our results show that changes in phasic activity induced by DA loss in the LC do not occur in the mPFC. Our data provide insight into how mPFC and LC networks are impaired in PD or other diseases involving DA.

Study III

Although extensive work has been performed in brain slices from parkinsonian animals, limited work has focused in other nuclei beyond the basal ganglia. Here, after charactering the electrophysiological modifications produced in LC cells by the 6-OHDA lesion in vivo (**Study I**), we further studied the impact of the DA depletion on the synaptic transmission ex vivo. We carried out patch clamp recordings in brain slices from 6-OHDA rats four weeks after the lesion. DA loss induced modifications in some LC cell intrinsic properties, as lower values of membrane capacitance and time constant, decreased conductance through IRK channels and hyperexcitability. In 6-OHDA rats, spontaneous glutamatergic, but not GABAergic, transmission was enhanced. Glutamatergic or GABAergic short-term plasticity was neither modified in parkinsonian rats.

Basal electrophysiological properties of locus coeruleus neurons are compromised after the 6-OHDA lesion

First of all, we verified that in control animals, passive membrane properties, potassium conductance, action potential parameters, excitability and potentials after hyperpolarizing steps of LC neurons in our study were comparable to those in previous reports from rat slices (Williams et al., 1988; Murai and Akaike, 2005; Howorth et al., 2009a; Chandler et al., 2014; Bruzos-Cidón et al., 2015; Rohampour et al., 2017).

Dopamine loss results in membrane changes in locus coeruleus neurons

In 6-OHDA lesioned rats, two passive membrane properties of LC neurons, time constant and cell capacitance, showed lower values after the DA loss. Although the exact physiological meaning of these parameters is unclear, some authors have

related them to the neuronal surface area in different brain regions (Isokawa, 1997; Iwasaki et al., 2008; Pineda et al., 2008) including the LC (Zhang et al., 2010). Although the size of LC neurons after the 6-OHDA lesion have not been reported in our study or the existing literature, different publications using animal models (6-OHDA or MPTP) or patients with PD show smaller cell volume in the SNpc, ventral tegmental area or retrorubral field (Rudow et al., 2008; Ahmad et al., 2009; Healy-Stoffel et al., 2014).

Dopamine loss increases excitability of locus coeruleus neurons

LC neurons from 6-OHDA animals showed enhanced excitability when depolarizing currents were injected, as previously shown in the dorsal raphe nucleus from the same animal model (Prinz et al., 2013). In addition, the duration of the suppression period after depolarization was enlarged in the 6-OHDA group, as observed in **Study I** in vivo. The hyperexcitability observed in LC neurons from brain slices may be responsible, at least in part, for the higher post-stimulus frequency observed in 6-OHDA lesioned rats after applying an external stimulus (paw compression), extensively described in **Study I**.

Given that K^+ conductance through IRK channels activated by G proteins seems to have a significant role preventing the excessive excitability of the cell (Llamosas et al., 2017; Torrecilla et al., 2013), we characterized the impact of dopaminergic loss on IRK conductances. In control conditions, the activation of these channels leads to K^+ inward rectification in a voltage-dependant manner which is enhanced when α_2-adrenoceptor, galanin or μ and δ opioid receptors are additionally activated (Williams et al., 1982, 1988; Sadeghi et al., 2015; Bai et al., 2018). In agreement with previous reports, in our study neurons from both groups showed IRK currents (Williams et al., 1988; Bruzos-Cidón et al., 2015), although they were significantly decreased after the dopaminergic loss. This modification may

be a result of the decreased expression or impaired functionality of IRK channels and it may underlie hyperexcitability of LC cells in parkinsonian rats.

LC neurons from 6-OHDA lesioned rats also showed more negative potentials than sham animals for the same hyperpolarizing steps. One reason for this difference could be a dysfunction of the hyperpolarization-activated cyclic nucleotide-gated cation channels, as previously seen in external globus pallidus and subthalamic nucleus from parkinsonian rats (Chan et al., 2011; Yang et al., 2015). This possibility is, however, unlikely as the presence the mentioned channels in the LC from rodents is not well defined (Santin et al., 2013).

Pacemaking intrinsic properties of locus coeruleus neurons may not be responsible for the decreased spontaneous firing rate

LC neurons from 6-OHDA lesioned animals exhibited slower firing frequency *ex vivo*, in accordance with the **Study I** performed in vivo. Given that LC spontaneous activity requires a complex combination of persistent pacemaking currents, it is possible that changes in those channels could account for the modifications observed in the basal firing rate. The speed of the spontaneous depolarization of LC neurons is determined by a combination of Na^+ and K^+ currents, which are activated at potentials close to the threshold for action potential generation (around -68 to -42 mV) (Williams et al., 1991; Alreja and Aghajanian, 1993; de Oliveira et al., 2010). At the same time, afterhyperpolarization amplitude is regulated by Ca^{2+} (L- and T-type Ca^{2+} channels) (Williams et al., 1988; Sanchez-Padilla et al., 2014; Matschke et al., 2015) and K^+ (voltage-dependant and SK channels) currents (Williams et al., 1984, 1988; Osmanović et al., 1990; Forsythe et al., 1992; Osmanović and Shefner, 1993; Matschke et al., 2018). In our study, the analysis of different parameters of the action potential waveform, as afterhyperpolarization amplitude and depolarization duration, did not reveal

changes between the two experimental groups, depicting that the channels involved in the pacemaking may not be modified by the DA loss. However, impairment of Ca^{2+} channels cannot be ruled out, as combined, but not isolated, blockade of L- and T-type Ca^{2+} channels is necessary to alter afterhyperpolarization of the action potential or firing rate in the LC (Sanchez-Padilla et al., 2014; Matschke et al., 2015). As mentioned in **Study I**, involvement of other receptors, as α_1-adrenoceptor, D_1 dopaminergic or GABAergic receptors, could be responsible for the decreased firing tone in the 6-OHDA group.

Dopamine loss increases spontaneous glutamatergic input to locus coeruleus neurons, without effect on GABAergic transmission

In the present study, DA depletion increased spontaneous glutamatergic synaptic transmission within the LC whereas GABAergic transmission remained unaltered.

Dopamine depletion does not affect GABAergic transmission in locus coeruleus neurons from 6-OHDA lesioned rats

The LC receives extensive GABA inhibitory input from the prepositus hypoglossi (Aston-Jones et al., 1986; Breton-Provencher and Sur, 2019) or GABAergic interneurons, whose distribution is still unclear as they have been observed in the peri-LC dendritic area, below the 4th ventricle dorsomedial to the LC and dorsal to Barrington's nucleus or wide-spread within the LC (Aston-Jones et al., 2004; Jin et al., 2016; Breton-Provencher and Sur, 2019). As a consequence of the release of GABA, acting onto $GABA_A$ receptors, noradrenergic neurons from the LC are inhibited (Corteen et al., 2011; Breton-Provencher and Sur, 2019). Contrary to our expectations, GABAergic spontaneous synaptic transmission and short-term plasticity were not modified in 6-OHDA lesioned rats indicating that the inhibitory

transmission through $GABA_A$ receptors was intact, and therefore it was not responsible for the lower firing tone observed in those animals.

Although GABAergic synaptic transmission mediated by $GABA_A$ receptors, also called phasic transmission, was not modified in our animal model, it is still possible that GABAergic tonic transmission could account for the observed changes. In parkinsonian rats, it has been described that this type of transmission is enhanced in the globus pallidus, contributing to the lower firing activity observed in pallidal cells recorded from brain slices (Miguelez et al., 2012; Chazalon et al., 2018). In the LC, tonic GABAergic inhibition is mediated by $GABA_B$ receptors, which regulates the spontaneous firing rate in developing rats (Wang et al., 2015). Therefore, enhanced GABAergic tonic transmission through $GABA_B$ receptors might lead to increased inhibitory control of the cell activity.

Dopamine depletion enhanced spontaneous glutamatergic transmission in LC neurons from 6-OHDA lesioned rats

Patients with PD show increased expression of metabotropic glutamate receptors in the putamen, hippocampus and amygdala (Kang et al., 2019) and those patients experiencing L-DOPA-induced motor complications present upregulation of AMPA glutamate receptors in the putamen (Calon et al., 2003). Moreover, studies in parkinsonian animals show enhanced release of glutamate and AMPA receptor-mediated excitatory transmission in the dorsal striatum and rostromedial tegmental nucleus, respectively (Schintu et al., 2016; Chang et al., 2019).

In our model, DA depletion influenced the spontaneous glutamatergic synaptic transmission within the LC, corresponding to an increased presynaptic release of glutamate. This higher glutamatergic input could arise from the PGi (Ennis and Aston-Jones, 1987) or the prefrontal cortex (Lu et al., 2012; Torres-Sanchez et al., 2018; Breton-Provencher and Sur, 2019), as they represent the main

glutamatergic afferences to the LC. So far, PGi function after DA loss has not been assessed, but as we suggest in **Study I**, it may be enhanced, especially in terms of phasic stimulation. It is also possible that the increased glutamatergic input could be provided from nuclei different from the PGi. Indeed, different publications using parkinsonian rats lesioned with 6-OHDA in the SNc or the MFB show increased discharge frequency of mPFC pyramidal neurons due to the loss of DA or DA/NA cortical release (Wang et al., 2010; Fan et al., 2019).

Although spontaneous glutamatergic transmission was increased in our model, short-term plasticity was similar in both experimental groups, and showed facilitation profile. We applied electrical stimulation as previously described (Bruzos-Cidón et al., 2015; Arami et al., 2016), but optogenetic techniques or the use of oblique slices (Kaeidi et al., 2015) for better preserving glutamatergic projections could be applied in future experiments in order to manipulate specific inputs to the LC noradrenergic neurons.

Conclusion

Altogether, our data indicate that LC neurons are affected by 6-OHDA lesion, since membrane and intrinsic excitability properties and glutamatergic transmission are altered. Although our results support that there is a hypoactivity of the LC neurons after dopaminergic loss as observed in vivo, no changes were obtained in the action potential parameters or the inhibitory GABAergic transmission through $GABA_A$ receptors. However, the increased excitability observed ex vivo in the LC neurons may contribute to the increased response triggered by the noxious stimulus in **Study I**.

Study IV

In this study, we found that dopaminergic cell loss decreased COX activity, without altering TH or ERK expression in the LC. We also used a battery of behavioural tests for assessing nociception and anxiety in our animal model. In general, 6-OHDA lesioned rats showed moderate decreased in the nociceptive threshold and no changes in the anxious behaviour.

Reduced COX activity is observed in 6-OHDA lesioned animals

In order to gain new information about LC activity in our model, we quantified COX (complex IV) activity, which is an enzyme of the mitochondrial electron transport chain and a metabolic marker of electrical activity (Wong-Riley, 1989). Neurons tonically active need to maintain greater COX activity to produce enough energy to satisfy the neuronal demand (Karmy et al., 1991). Previous studies have revealed parallel changes in the electrical and metabolic activity of the dorsal raphe nucleus, substantia nigra reticulata and globus pallidus internus from parkinsonian animals (Blandini et al., 2007; Kaya et al., 2008). Here, dopamine depletion reduced COX activity in the LC four weeks after the lesion. Thus, the observed decreased metabolic activity is in line with the decreased spontaneous firing activity (**Study I**), confirming a reduction in LC activity in the 6-OHDA lesioned model of PD. Moreover, deficiencies in various complexes of the respiratory chain have been reported in PD patients (Yoshino et al., 1992; Haas et al., 1995; Müftüoglu et al., 2004; Valente et al., 2004; Holper et al., 2019). In particular, COX activity is reduced in the frontal cortex (Holper et al., 2019) and leukocytes (Müftüoglu et al., 2004) of the patients with the disease.

The impairment of the LC observed in the previous studies might be accompanied by loss of LC cells or decreased TH expression. However, dopaminergic

lesion does not reduce the number of LC noradrenergic neurons in animal models of PD induced by 6-OHDA injection in the MFB (Miguelez et al., 2011b) or the caudado putamen (Oliveira et al., 2017). To rule out the second possibility, TH expression in the LC was measured with the WB technique and no changes were observed in the 6-OHDA lesioned rats. Altogether, previous and present results suggest the decrease LC activity is not due to TH loss.

ERK1/2 are members of the mitogen-activated protein kinase implicated in the activation of transcriptional factors in the nucleus of the cell. Its activated form through phosphorylation, pERK1/2, is related to the modulation of pain, and its affective/emotional components (Ji et al., 2009; Borges et al., 2015). Many publications reveal ERK activation in painful conditions at the spinal cord level, presumably because of its implication in the sensory component of the pain (Ji et al., 1999, 2002; Dai et al., 2002). However, results regarding ERK activation at supraspinal levels are more complex to interpret. Specifically, there are conflicting results in the LC, since ERK1/2 is activated in painful conditions, after acute (Seo et al., 2008; Imbe et al., 2009) or prolonged states (Borges et al., 2014, 2017b), but also after the administration of analgesic drugs (Seo et al., 2008). Moreover, lower levels of pERK1/2 occur in the LC from a model of neuropathic pain in comparison with the control group (Borges et al., 2013). These paradoxical results may be explained by the involvement of the LC in different dimensions of pain, as the sensory and emotional ones. Therefore, in the LC, ERK seems to be regulated in different ways depending on the pathophysiological disorder and the stress induced in the model, as chronic stress was related to decrease ERK1/2 activation while acute stress evoked its activation (Imbe et al., 2004; Kwon et al., 2006). In our study, we did not detect changes in the activation of ERK1/2 in the LC of 6-OHDA lesioned animals in basal

conditions suggesting that more strong changes in neuronal activity are necessary for increasing ERK expression in the LC.

Nociceptive responses are slightly altered in the 6-OHDA lesioned model

Pain and anxiety are common non-motor disturbances in patients with PD, whose prevalence goes from 30 to even 80% (Djaldetti et al., 2004; Wasner and Deuschl, 2012; Priebe et al., 2016; Schapira et al., 2017; Schrag and Taddei, 2017; Titova et al., 2017). Because of its significant presence, it is necessary for researchers to have a better understanding of these symptoms in PD, which may require an impairment of the noradrenergic system and the LC (**Introduction 1.2.1**). The LC is critical for pain and negative emotions modulation, given its implications in the descending and ascending pathways through inputs to the spinal cord, frontal cortices and limbic system (Hentall et al., 2003; Curtis et al., 2012; Alba-Delgado et al., 2013; Hickey et al., 2014; McCall et al., 2015, 2017; Szot et al., 2016; Hirschberg et al., 2017; Li et al., 2018a; Llorca-Torralba et al., 2019). For this reason, we analysed the nociceptive responses and anxiety-like behaviours in a PD rat model with altered activity of the LC.

Although recent publications have revealed modifications in nociception in 6-OHDA lesioned rats, the results are very controversial. This disagreement is specially notorious in unilateral models (as the one used in this study), showing reduced thresholds and increase response to nociceptive inputs in the ipsilateral hind paw (Tassorelli et al., 2007; Takeda et al., 2014; Campos et al., 2019), contralateral hind paw (Charles et al., 2018) or bilaterally in both hind paws (Takeda et al., 2005; Gee et al., 2015; Gómez-Paz et al., 2018; Domenici et al., 2019; Romero-Sánchez et al., 2019). In most of the mentioned studies mechanic nociceptive

transmission was analysed using the von Frey test (Takeda et al., 2005, 2014; Charles et al., 2018; Gómez-Paz et al., 2018; Domenici et al., 2019; Romero-Sánchez et al., 2019) while thermal nociception has been less frequently explored. So far only one study has reported lower thresholds in the acetone test (Gómez-Paz et al., 2018) while contradictory results reporting decreased threshold (Charles et al., 2018) or no change (Domenici et al., 2019) have been obtained with the plantar test. In our experimental conditions, unilateral 6-OHDA injection induced spontaneous and mechanical nociceptive behaviour score increment in the contralateral paw to the lesion, and increased responses to a cold stimulus in the ipsilateral paw. However, the results in the spontaneous and cold-thermal nociceptive behaviour should be interpreted cautiously. On the one hand, the difference observed in the dynamic weight bearing test may be influenced by the motor impairment induced after the lesion, as lesioned rats with 6-OHDA present gait deficits (Chang et al., 1999; Metz et al., 2005; Zhou et al., 2015). On the other hand, the results of the nociceptive behaviour tested with the acetone test in the 6-OHDA lesioned rats were similar in both paws. Although statistical analysis revealed significant differences in the ipsilateral hind paw, the relevance of this effect may not be very important as the mean score in lesioned animals was very discrete (0.6 out of 12 points).

In order to understand the discrepant behavioural results, it should be stressed that integrity of the LC may have differed among the cited publications. In our study, the LC integrity was assured by the administration of desipramine before the stereotaxic injection of 6-OHDA, as previously corroborated (Miguelez et al., 2011b). This is a general practice, and absence of this pretreatment will lead to noradrenergic damage and lower NA levels in projecting areas (Kamińska et al., 2017). In this line, most of the mentioned publications have revealed decreased number of LC neurons (Campos et al., 2019) or no use of desipramine during the

stereotaxic injection, implying direct noradrenergic damage (Takeda et al., 2005, 2014; Tassorelli et al., 2007; Gómez-Paz et al., 2018; Domenici et al., 2019; Romero-Sánchez et al., 2019). In fact, lesions in noradrenergic neurons or the induction of very low firing frequencies in the LC (median 0.2 Hz) were accompanied by thermal hyperalgesia but not by increased response during mechanical tests (Martin et al., 1999; Howorth et al., 2009b). In our hands, we observed that specific dopaminergic damage is not enough for observing substantial changes in the nociceptive behaviour, especially in thermal and spontaneous behaviour. Altogether, differences in the methodology during the lesion and the type of nociceptive tests can differently affect the pattern of nociceptive responses.

In our work, although DA degeneration increased the responsiveness of LC neurons to nociceptive inputs (**Study I**), behavioural consequences were more modest than those reported in previous publications. The information provided by the electrophysiological experiments and the behavioural assays was different and changes in one did not imply modifications in the other. This is however not surprising, as both ascending and descending pathways are differentially involved in both experimental conditions. The phasic response recorded after the paw compression is related with the ascending noradrenergic pathway through the PGi to supraspinal levels and this via is more related with the motivational-affective dimensions (Llorca-Torralba et al., 2016, 2019). Conversely, the descending noradrenergic pathway to the spinal cord is involved in the paw withdrawal evaluated in the tests that we performed, which is mainly ipsilateral (Hirschberg et al., 2017).

Anxiety-like behaviour was not present in the 6-OHDA lesioned model

In the literature, various studies have investigated the effect of unilateral 6-OHDA lesion in rats on anxiety-like behaviour, and conflicting results can be found. The majority of the studies in which 6-OHDA animals presented anxiety-like behaviours are based on the elevated plus maze or the open field test (Eskow Jaunarajs et al., 2010; O'Connor et al., 2016; Guo et al., 2018; Sun et al., 2018; Mishra et al., 2019), whose results may be overestimated when animal suffer hypolocomotion. Here, we performed the marble burying and social interaction tests and no differences were observed between the groups. The result obtained in the marble burying test is in line with a paper published in the 6-OHDA model (O'Connor et al., 2016). Decreased social interaction is reported in other publications (Eskow Jaunarajs et al., 2010; Mishra et al., 2019), although we did not observed any difference. This disparity might be explained by the difference in the time of evaluation, which was shorter in our study, 5 vs 13 (Eskow Jaunarajs et al., 2010) weeks after the lesion. Another reason that can potentially influence the results is the size of the cage used. Indeed, in Mishra et al., 2019 the test was performed in an automated three-chambered apparatus, which is considerably bigger than the one used in our study (45 vs 112 cm). Considering that it has been proven that 6-OHDA rats travel less distance than sham animals (Eskow Jaunarajs et al., 2010; Guo et al., 2018), performing the social interaction test in larger cages may influence the results.

As both studied behavioural responses are the result of the integration between the right and left hemispheres, the affection of both of them may be essential to observe changes in the non-motor behaviour. In this line several publications using bilateral models of the disease show more consistent changes in

anxious behaviour (Branchi et al., 2008; Chen et al., 2011; Campos et al., 2013; Loiodice et al., 2019; Vieira et al., 2019).

Conclusion

The understanding of the pathophysiology of the non-motor symptoms present in PD have gained interest in the scientific community during the past decades. This study aimed to evaluate the contribution of the impairment in the noradrenergic system in non-motor symptomatology in a model of PD. The impaired COX activity in the nucleus confirmed the decreased basal function of LC neurons after dopaminergic depletion. Unlike our expectations, the results obtained showed discrete increment of the nociceptive responses and no anxiety-like behaviour.

6. CONCLUSIONS

6. CONCLUSIONS

The results obtained in this work lead us to the following conclusions:

1. The dopaminergic degeneration induced by the 6-OHDA injection produces electrophysiological changes in the LC, which are evident in the fourth, but not in the second week after the lesion.
2. DA loss produces a reduction in the LC basal firing activity recorded in vivo. By contrast, phasic discharge evoked by noxious mechanical stimulation is enhanced, leading to a major phasic:tonic ratio.
3. L-DOPA acute administration highly abolishes LC phasic response to peripheral noxious stimuli. At the same time, DA replacement in the 6-OHDA lesioned group restores the alterations produced in the tonic and phasic parameters.
4. The efficacy of the α_2-adrenoceptor agonist, UK 14,304, in the LC is not modified by the DA loss. Therefore, α_2-adrenoceptors may not be responsible for the hypoactivity and hyperresponsiveness observed in parkinsonian animals.
5. Dopaminergic depletion reduces low frequency oscillations in the mPFC and LC and the mPFC-LC synchronization, which is restored after DA replacement. This result demonstrates the impairment of the neural communication between both areas in a situation of DA deficit.

6. Noxious stimulation is associated with a shift in the potential of the LC and mPFC, supporting their implication in the sensory processing. After dopaminergic loss, the evoked potential increases in the LC, suggesting enhanced sensitivity to the stimulus, which is restored after L-DOPA administration.

7. Ex vivo, basal electrophysiological properties of LC neurons are compromised after the 6-OHDA lesion. DA loss induces membrane changes, dysfunctional K^+ conductance through IRK channels, low firing frequency and hyperexcitability of LC neurons while pacemaking intrinsic properties remain unaffected.

8. DA loss increases glutamatergic spontaneous transmission in the LC. However, GABAergic spontaneous transmission and excitatory or inhibitory short-term plasticity are not modified in the 6-OHDA lesioned animals.

9. 6-OHDA injection decreases LC metabolic activity without producing molecular changes in TH and pERK1/2 expression. The results confirm the hypoactive state of the LC after the DA depletion.

10. The lesion with 6-OHDA induces discrete increment in the nociceptive responses and no anxiety-like behaviour, demonstrating that the LC affection observed in the parkinsonian animals has a minor impact at behavioural level.

In summary, the present study demonstrates that dopaminergic deficit strongly influences the LC-noradrenergic system. Persistent DA loss leads to hypoactivity and hyperresponsiveness in the LC, along with a dysfunctional mPFC-LC network, which were demonstrated by electrophysiological and histochemical approaches in vivo and ex vivo. DA replacement restores LC neuron oscillatory pattern and tonic and phasic activity. This finding confirms that the changes observed in the parkinsonian rats were directly due to the dopaminergic loss and stresses the implication of the DA in the modulation of the noradrenergic system. However, all these LC affections have discrete impact in nociceptive and anxious behaviour.

7. BIBLIOGRAPHY

7. BIBLIOGRAPHY

Aarsland, D., Creese, B., Politis, M., Chaudhuri, K. R., Ffytche, D. H., Weintraub, D., et al. (2017). Cognitive decline in Parkinson disease. *Nat. Rev. Neurol.* 13, 217–231. doi:10.1038/nrneurol.2017.27.

Af Bjerkén, S., Stenmark Persson, R., Barkander, A., Karalija, N., Pelegrina-Hidalgo, N., Gerhardt, G. A., et al. (2019). Noradrenaline is crucial for the substantia nigra dopaminergic cell maintenance. *Neurochem. Int.* 131, 104551. doi:10.1016/j.neuint.2019.104551.

Agster, K. L., Mejias-Aponte, C. A., Clark, B. D., and Waterhouse, B. D. (2013). Evidence for a regional specificity in the density and distribution of noradrenergic varicosities in rat cortex. *J. Comp. Neurol.* 521, 2195–2207. doi:10.1002/cne.23270.

Ahlskog, J. E., Uitti, R. J., Tyce, G. M., O'Brien, J. F., Petersen, R. C., and Kokmen, E. (1996). Plasma catechols and monoamine oxidase metabolites in untreated Parkinson's and Alzheimer's diseases. *J. Neurol. Sci.* 136, 162–168. doi:10.1016/0022-510x(95)00318-v.

Ahmad, S. O., Park, J.-H., Stenho-Bittel, L., and Lau, Y.-S. (2009). Effects of endurance exercise on ventral tegmental area neurons in the chronic 1-methyl-4-phenyl-1,2,3,6-tetrahydropyridine and probenecid-treated mice. *Neurosci. Lett.* 450, 102–105. doi:10.1016/j.neulet.2008.11.065.

Alachkar, A., Brotchie, J. M., and Jones, O. T. (2010). Locomotor response to L-DOPA in reserpine-treated rats following central inhibition of aromatic L-amino acid decarboxylase: further evidence for non-dopaminergic actions of L-DOPA and its metabolites. *Neurosci. Res.* 68, 44–50. doi:10.1016/j.neures.2010.06.003.

Alba-Delgado, C., Borges, G., Sánchez-Blázquez, P., Ortega, J. E., Horrillo, I., Mico, J. A., et al. (2012a). The function of alpha-2-adrenoceptors in the rat locus coeruleus is preserved in the chronic constriction injury model of neuropathic pain. *Psychopharmacology (Berl.)* 221, 53–65. doi:10.1007/s00213-011-2542-7.

Alba-Delgado, C., Llorca-Torralba, M., Horrillo, I., Ortega, J. E., Mico, J. A., Sánchez-Blázquez, P., et al. (2013). Chronic pain leads to concomitant

noradrenergic impairment and mood disorders. *Biol. Psychiatry* 73, 54–62. doi:10.1016/j.biopsych.2012.06.033.

Alba-Delgado, C., Mico, J. A., Sánchez-Blázquez, P., and Berrocoso, E. (2012b). Analgesic antidepressants promote the responsiveness of locus coeruleus neurons to noxious stimulation: implications for neuropathic pain. *Pain* 153, 1438–1449. doi:10.1016/j.pain.2012.03.034.

Albers, J. A., Chand, P., and Anch, A. M. (2017). Multifactorial sleep disturbance in Parkinson's disease. *Sleep Med.* 35, 41–48. doi:10.1016/j.sleep.2017.03.026.

Alexander, G. E., DeLong, M. R., and Strick, P. L. (1986). Parallel organization of functionally segregated circuits linking basal ganglia and cortex. *Annu. Rev. Neurosci.* 9, 357–381. doi:10.1146/annurev.ne.09.030186.002041.

Alreja, M., and Aghajanian, G. K. (1993). Opiates suppress a resting sodium-dependent inward current and activate an outward potassium current in locus coeruleus neurons. *J. Neurosci. Off. J. Soc. Neurosci.* 13, 3525–3532.

Amaral, D. G., and Sinnamon, H. M. (1977). The locus coeruleus: neurobiology of a central noradrenergic nucleus. *Prog. Neurobiol.* 9, 147–196.

Ando, R., Choudhury, M. E., Yamanishi, Y., Kyaw, W. T., Kubo, M., Kannou, M., et al. (2018). Modafinil alleviates levodopa-induced excessive nighttime sleepiness and restores monoaminergic systems in a nocturnal animal model of Parkinson's disease. *J. Pharmacol. Sci.* 136, 266–271. doi:10.1016/j.jphs.2018.03.005.

Andrezik, J. A., Chan-Palay, V., and Palay, S. L. (1981). The nucleus paragigantocellularis lateralis in the rat. Demonstration of afferents by the retrograde transport of horseradish peroxidase. *Anat. Embryol. (Berl.)* 161, 373–390. doi:10.1007/bf00316049.

Arami, M. K., Hajizadeh, S., and Semnanian, S. (2016). Postnatal development changes in excitatory synaptic activity in the rat locus coeruleus neurons. *Brain Res.* 1648, 365–371. doi:10.1016/j.brainres.2016.07.036.

Archer, T. (2016). Noradrenergic-Dopaminergic Interactions Due to DSP-4-MPTP Neurotoxin Treatments: Iron Connection. *Curr. Top. Behav. Neurosci.* 29, 73–86. doi:10.1007/7854_2015_411.

Aristieta, A., Azkona, G., Sagarduy, A., Miguelez, C., Ruiz-Ortega, J. Á., Sanchez-Pernaute, R., et al. (2012). The role of the subthalamic nucleus in L-DOPA induced dyskinesia in 6-hydroxydopamine lesioned rats. *PloS One* 7, e42652. doi:10.1371/journal.pone.0042652.

Aristieta, A., Ruiz-Ortega, J. A., Miguelez, C., Morera-Herreras, T., and Ugedo, L. (2016). Chronic L-DOPA administration increases the firing rate but does not reverse enhanced slow frequency oscillatory activity and synchronization in substantia nigra pars reticulata neurons from 6-hydroxydopamine-lesioned rats. *Neurobiol. Dis.* 89, 88–100. doi:10.1016/j.nbd.2016.02.003.

Aristieta, A., Ruiz-Ortega, J. A., Morera-Herreras, T., Miguelez, C., and Ugedo, L. (2019). Acute L-DOPA administration reverses changes in firing pattern and low frequency oscillatory activity in the entopeduncular nucleus from long term L-DOPA treated 6-OHDA-lesioned rats. *Exp. Neurol.* 322, 113036. doi:10.1016/j.expneurol.2019.113036.

Armentero, M.-T., Fancellu, R., Nappi, G., Bramanti, P., and Blandini, F. (2006). Prolonged blockade of NMDA or mGluR5 glutamate receptors reduces nigrostriatal degeneration while inducing selective metabolic changes in the basal ganglia circuitry in a rodent model of Parkinson's disease. *Neurobiol. Dis.* 22, 1–9. doi:10.1016/j.nbd.2005.09.010.

Armstrong-James, M., and Fox, K. (1983). Effects of ionophoresed noradrenaline on the spontaneous activity of neurones in rat primary somatosensory cortex. *J. Physiol.* 335, 427–447. doi:10.1113/jphysiol.1983.sp014542.

Aston-Jones, G., and Bloom, F. E. (1981a). Activity of norepinephrine-containing locus coeruleus neurons in behaving rats anticipates fluctuations in the sleep-waking cycle. *J. Neurosci. Off. J. Soc. Neurosci.* 1, 876–886.

Aston-Jones, G., and Bloom, F. E. (1981b). Norepinephrine-containing locus coeruleus neurons in behaving rats exhibit pronounced responses to non-noxious environmental stimuli. *J. Neurosci. Off. J. Soc. Neurosci.* 1, 887–900.

Aston-Jones, G., and Cohen, J. D. (2005). An integrative theory of locus coeruleus-norepinephrine function: adaptive gain and optimal performance. *Annu. Rev. Neurosci.* 28, 403–450. doi:10.1146/annurev.neuro.28.061604.135709.

Aston-Jones, G., Ennis, M., Pieribone, V. A., Nickell, W. T., and Shipley, M. T. (1986). The brain nucleus locus coeruleus: restricted afferent control of a broad efferent network. *Science* 234, 734–737. doi:10.1126/science.3775363.

Aston-Jones, G., Zhu, Y., and Card, J. P. (2004). Numerous GABAergic afferents to locus ceruleus in the pericerulear dendritic zone: possible interneuronal pool. *J. Neurosci. Off. J. Soc. Neurosci.* 24, 2313–2321. doi:10.1523/JNEUROSCI.5339-03.2004.

Azami, J., Wright, D. M., and Roberts, M. H. (1981). Effects of morphine and naloxone on the responses to noxious stimulation of neurones in the nucleus reticularis paragigantocellularis. *Neuropharmacology* 20, 869–876. doi:10.1016/0028-3908(81)90080-0.

Bai, Y.-F., Ma, H.-T., Liu, L.-N., Li, H., Li, X.-X., Yang, Y.-T., et al. (2018). Activation of galanin receptor 1 inhibits locus coeruleus neurons via GIRK channels. *Biochem. Biophys. Res. Commun.* 503, 79–85. doi:10.1016/j.bbrc.2018.05.181.

Baldo, B. A., Daniel, R. A., Berridge, C. W., and Kelley, A. E. (2003). Overlapping distributions of orexin/hypocretin- and dopamine-beta-hydroxylase immunoreactive fibers in rat brain regions mediating arousal, motivation, and stress. *J. Comp. Neurol.* 464, 220–237. doi:10.1002/cne.10783.

Bari, A., and Aston-Jones, G. (2013). Atomoxetine modulates spontaneous and sensory-evoked discharge of locus coeruleus noradrenergic neurons. *Neuropharmacology* 64, 53–64. doi:10.1016/j.neuropharm.2012.07.020.

Beas, B. S., Wright, B. J., Skirzewski, M., Leng, Y., Hyun, J. H., Koita, O., et al. (2018). The locus coeruleus drives disinhibition in the midline thalamus via a dopaminergic mechanism. *Nat. Neurosci.* 21, 963–973. doi:10.1038/s41593-018-0167-4.

Belluscio, M. A., Kasanetz, F., Riquelme, L. A., and Murer, M. G. (2003). Spreading of slow cortical rhythms to the basal ganglia output nuclei in rats with nigrostriatal lesions. *Eur. J. Neurosci.* 17, 1046–1052.

Berghauzen-Maciejewska, K., Kuter, K., Kolasiewicz, W., Głowacka, U., Dziubina, A., Ossowska, K., et al. (2014). Pramipexole but not imipramine or fluoxetine reverses the “depressive-like” behaviour in a rat model of preclinical stages

of Parkinson's disease. *Behav. Brain Res.* 271, 343–353. doi:10.1016/j.bbr.2014.06.029.

Berridge, C. W., Stratford, T. L., Foote, S. L., and Kelley, A. E. (1997). Distribution of dopamine beta-hydroxylase-like immunoreactive fibers within the shell subregion of the nucleus accumbens. *Synap. N. Y. N* 27, 230–241. doi:10.1002/(SICI)1098-2396(199711)27:3<230::AID-SYN8>3.0.CO;2-E.

Berrocoso, E., Mico, J.-A., Vitton, O., Ladure, P., Newman-Tancredi, A., Depoortère, R., et al. (2011). Evaluation of milnacipran, in comparison with amitriptyline, on cold and mechanical allodynia in a rat model of neuropathic pain. *Eur. J. Pharmacol.* 655, 46–51. doi:10.1016/j.ejphar.2011.01.022.

Bertrand, E., Lechowicz, W., Szpak, G. M., and Dymecki, J. (1997). Qualitative and quantitative analysis of locus coeruleus neurons in Parkinson's disease. *Folia Neuropathol.* 35, 80–86.

Betarbet, R., Sherer, T. B., MacKenzie, G., Garcia-Osuna, M., Panov, A. V., and Greenamyre, J. T. (2000). Chronic systemic pesticide exposure reproduces features of Parkinson's disease. *Nat. Neurosci.* 3, 1301–1306. doi:10.1038/81834.

Betts, M. J., Kirilina, E., Otaduy, M. C. G., Ivanov, D., Acosta-Cabronero, J., Callaghan, M. F., et al. (2019). Locus coeruleus imaging as a biomarker for noradrenergic dysfunction in neurodegenerative diseases. *Brain* 142, 2558–2571. doi:10.1093/brain/awz193.

Bhide, N., Lindenbach, D., Barnum, C. J., George, J. A., Surrena, M. A., and Bishop, C. (2015). Effects of the beta-adrenergic receptor antagonist Propranolol on dyskinesia and L-DOPA-induced striatal DA efflux in the hemi-parkinsonian rat. *J. Neurochem.* 134, 222–232. doi:10.1111/jnc.13125.

Bing, G., Zhang, Y., Watanabe, Y., McEwen, B. S., and Stone, E. A. (1994). Locus coeruleus lesions potentiate neurotoxic effects of MPTP in dopaminergic neurons of the substantia nigra. *Brain Res.* 668, 261–265. doi:10.1016/0006-8993(94)90534-7.

Blandini, F., Levandis, G., Bazzini, E., Nappi, G., and Armentero, M.-T. (2007). Time-course of nigrostriatal damage, basal ganglia metabolic changes and behavioural alterations following intrastriatal injection of 6-

hydroxydopamine in the rat: new clues from an old model. *Eur. J. Neurosci.* 25, 397–405. doi:10.1111/j.1460-9568.2006.05285.x.

Blesa, J., Trigo-Damas, I., Quiroga-Varela, A., and Jackson-Lewis, V. R. (2015). Oxidative stress and Parkinson's disease. *Front. Neuroanat.* 9, 91. doi:10.3389/fnana.2015.00091.

Bohnen, N. I., Studenski, S. A., Constantine, G. M., and Moore, R. Y. (2008). Diagnostic performance of clinical motor and non-motor tests of Parkinson disease: a matched case-control study. *Eur. J. Neurol.* 15, 685–691. doi:10.1111/j.1468-1331.2008.02148.x.

Bonito-Oliva, A., Masini, D., and Fisone, G. (2014). A mouse model of non-motor symptoms in Parkinson's disease: focus on pharmacological interventions targeting affective dysfunctions. *Front. Behav. Neurosci.* 8, 290. doi:10.3389/fnbeh.2014.00290.

Borges, G., Berrocoso, E., Mico, J. A., and Neto, F. (2015). ERK1/2: Function, signaling and implication in pain and pain-related anxio-depressive disorders. *Prog. Neuropsychopharmacol. Biol. Psychiatry* 60, 77–92. doi:10.1016/j.pnpbp.2015.02.010.

Borges, G., Miguelez, C., Neto, F., Mico, J. A., Ugedo, L., and Berrocoso, E. (2017a). Activation of Extracellular Signal-Regulated Kinases (ERK 1/2) in the Locus Coeruleus Contributes to Pain-Related Anxiety in Arthritic Male Rats. *Int. J. Neuropsychopharmacol.* 20, 463. doi:10.1093/ijnp/pyx005.

Borges, G., Miguelez, C., Neto, F., Mico, J. A., Ugedo, L., and Berrocoso, E. (2017b). Activation of Extracellular Signal-Regulated Kinases (ERK 1/2) in the Locus Coeruleus Contributes to Pain-Related Anxiety in Arthritic Male Rats. *Int. J. Neuropsychopharmacol.* 20, 463. doi:10.1093/ijnp/pyx005.

Borges, G., Neto, F., Mico, J. A., and Berrocoso, E. (2014). Reversal of monoarthritis-induced affective disorders by diclofenac in rats. *Anesthesiology* 120, 1476–1490. doi:10.1097/ALN.0000000000000177.

Borges, G. S., Berrocoso, E., Ortega-Alvaro, A., Mico, J. A., and Neto, F. L. (2013). Extracellular signal-regulated kinase activation in the chronic constriction injury model of neuropathic pain in anaesthetized rats. *Eur. J. Pain Lond. Engl.* 17, 35–45. doi:10.1002/j.1532-2149.2012.00181.x.

Bouchatta, O., Manouze, H., Bouali-Benazzouz, R., Kerekes, N., Ba-M'hamed, S., Fossat, P., et al. (2018). Neonatal 6-OHDA lesion model in mouse induces Attention-Deficit/ Hyperactivity Disorder (ADHD)-like behaviour. *Sci. Rep.* 8, 15349. doi:10.1038/s41598-018-33778-0.

Braak, H., and Del Tredici, K. (2016). Potential Pathways of Abnormal Tau and α-Synuclein Dissemination in Sporadic Alzheimer's and Parkinson's Diseases. *Cold Spring Harb. Perspect. Biol.* 8. doi:10.1101/cshperspect.a023630.

Braak, H., Del Tredici, K., Rüb, U., de Vos, R. A. I., Jansen Steur, E. N. H., and Braak, E. (2003). Staging of brain pathology related to sporadic Parkinson's disease. *Neurobiol. Aging* 24, 197–211.

Braak, H., Ghebremedhin, E., Rüb, U., Bratzke, H., and Del Tredici, K. (2004). Stages in the development of Parkinson's disease-related pathology. *Cell Tissue Res.* 318, 121–134. doi:10.1007/s00441-004-0956-9.

Branchi, I., D'Andrea, I., Armida, M., Cassano, T., Pèzzola, A., Potenza, R. L., et al. (2008). Nonmotor symptoms in Parkinson's disease: investigating early-phase onset of behavioral dysfunction in the 6-hydroxydopamine-lesioned rat model. *J. Neurosci. Res.* 86, 2050–2061. doi:10.1002/jnr.21642.

Bravo, L., Alba-Delgado, C., Torres-Sanchez, S., Mico, J. A., Neto, F. L., and Berrocoso, E. (2013). Social stress exacerbates the aversion to painful experiences in rats exposed to chronic pain: the role of the locus coeruleus. *Pain* 154, 2014–2023. doi:10.1016/j.pain.2013.06.021.

Breton-Provencher, V., and Sur, M. (2019). Active control of arousal by a locus coeruleus GABAergic circuit. *Nat. Neurosci.* 22, 218–228. doi:10.1038/s41593-018-0305-z.

Brown, P., Oliviero, A., Mazzone, P., Insola, A., Tonali, P., and Di Lazzaro, V. (2001). Dopamine dependency of oscillations between subthalamic nucleus and pallidum in Parkinson's disease. *J. Neurosci. Off. J. Soc. Neurosci.* 21, 1033–1038.

Bruno, V. A., Fox, S. H., Mancini, D., and Miyasaki, J. M. (2016). Botulinum Toxin Use in Refractory Pain and Other Symptoms in Parkinsonism. *Can. J. Neurol. Sci. J. Can. Sci. Neurol.* 43, 697–702. doi:10.1017/cjn.2016.279.

Bruno, V., Freitas, M. E., Mancini, D., Lui, J. P., Miyasaki, J., and Fox, S. H. (2018). Botulinum Toxin Type A for Pain in Advanced Parkinson's Disease. *Can. J. Neurol. Sci. J. Can. Sci. Neurol.* 45, 23–29. doi:10.1017/cjn.2017.245.

Bruzos-Cidón, C., Llamosas, N., Ugedo, L., and Torrecilla, M. (2015). Dysfunctional inhibitory mechanisms in locus coeruleus neurons of the wistar kyoto rat. *Int. J. Neuropsychopharmacol.* 18, pyu122. doi:10.1093/ijnp/pyu122.

Buzsáki, G., Anastassiou, C. A., and Koch, C. (2012). The origin of extracellular fields and currents--EEG, ECoG, LFP and spikes. *Nat. Rev. Neurosci.* 13, 407–420. doi:10.1038/nrn3241.

Calon, F., Rajput, A. H., Hornykiewicz, O., Bédard, P. J., and Di Paolo, T. (2003). Levodopa-induced motor complications are associated with alterations of glutamate receptors in Parkinson's disease. *Neurobiol. Dis.* 14, 404–416. doi:10.1016/j.nbd.2003.07.003.

Campos, A. C. P., Berzuino, M. B., Hernandes, M. S., Fonoff, E. T., and Pagano, R. L. (2019). Monoaminergic regulation of nociceptive circuitry in a Parkinson's disease rat model. *Exp. Neurol.* 318, 12–21. doi:10.1016/j.expneurol.2019.04.015.

Campos, F. L., Carvalho, M. M., Cristovão, A. C., Je, G., Baltazar, G., Salgado, A. J., et al. (2013). Rodent models of Parkinson's disease: beyond the motor symptomatology. *Front. Behav. Neurosci.* 7, 175. doi:10.3389/fnbeh.2013.00175.

Cao, L.-F., Peng, X.-Y., Huang, Y., Wang, B., Zhou, F.-M., Cheng, R.-X., et al. (2016). Restoring Spinal Noradrenergic Inhibitory Tone Attenuates Pain Hypersensitivity in a Rat Model of Parkinson's Disease. *Neural Plast.* 2016, 6383240. doi:10.1155/2016/6383240.

Carter, M. E., Yizhar, O., Chikahisa, S., Nguyen, H., Adamantidis, A., Nishino, S., et al. (2010). Tuning arousal with optogenetic modulation of locus coeruleus neurons. *Nat. Neurosci.* 13, 1526–1533. doi:10.1038/nn.2682.

Cash, R., Dennis, T., L'Heureux, R., Raisman, R., Javoy-Agid, F., and Scatton, B. (1987). Parkinson's disease and dementia: norepinephrine and dopamine in locus ceruleus. *Neurology* 37, 42–46. doi:10.1212/wnl.37.1.42.

Cash, R., Ruberg, M., Raisman, R., and Agid, Y. (1984). Adrenergic receptors in Parkinson's disease. *Brain Res.* 322, 269–275. doi:10.1016/0006-8993(84)90117-3.

Castellanos, G., Fernández-Seara, M. A., Lorenzo-Betancor, O., Ortega-Cubero, S., Puigvert, M., Uranga, J., et al. (2015). Automated neuromelanin imaging as a diagnostic biomarker for Parkinson's disease. *Mov. Disord. Off. J. Mov. Disord. Soc.* 30, 945–952. doi:10.1002/mds.26201.

Cedarbaum, J. M., and Aghajanian, G. K. (1976). Noradrenergic neurons of the locus coeruleus: inhibition by epinephrine and activation by the alpha-antagonist piperoxane. *Brain Res.* 112, 413–419. doi:10.1016/0006-8993(76)90297-3.

Cedarbaum, J. M., and Aghajanian, G. K. (1978). Activation of locus coeruleus neurons by peripheral stimuli: modulation by a collateral inhibitory mechanism. *Life Sci.* 23, 1383–1392. doi:10.1016/0024-3205(78)90398-3.

Chamba, G., Weissmann, D., Rousset, C., Renaud, B., and Pujol, J. F. (1991). Distribution of alpha-1 and alpha-2 binding sites in the rat locus coeruleus. *Brain Res. Bull.* 26, 185–193. doi:10.1016/0361-9230(91)90225-9.

Chan, C. S., Glajch, K. E., Gertler, T. S., Guzman, J. N., Mercer, J. N., Lewis, A. S., et al. (2011). HCN channelopathy in external globus pallidus neurons in models of Parkinson's disease. *Nat. Neurosci.* 14, 85–92. doi:10.1038/nn.2692.

Chandler, D. J., Gao, W.-J., and Waterhouse, B. D. (2014). Heterogeneous organization of the locus coeruleus projections to prefrontal and motor cortices. *Proc. Natl. Acad. Sci. U. S. A.* 111, 6816–6821. doi:10.1073/pnas.1320827111.

Chandler, D. J., Jensen, P., McCall, J. G., Pickering, A. E., Schwarz, L. A., and Totah, N. K. (2019). Redefining Noradrenergic Neuromodulation of Behavior: Impacts of a Modular Locus Coeruleus Architecture. *J. Neurosci. Off. J. Soc. Neurosci.* 39, 8239–8249. doi:10.1523/JNEUROSCI.1164-19.2019.

Chandler, D., and Waterhouse, B. D. (2012). Evidence for broad versus segregated projections from cholinergic and noradrenergic nuclei to functionally and anatomically discrete subregions of prefrontal cortex. *Front. Behav. Neurosci.* 6, 20. doi:10.3389/fnbeh.2012.00020.

Chang, J. W., Wachtel, S. R., Young, D., and Kang, U. J. (1999). Biochemical and anatomical characterization of forepaw adjusting steps in rat models of Parkinson's disease: studies on medial forebrain bundle and striatal lesions. *Neuroscience* 88, 617–628. doi:10.1016/s0306-4522(98)00217-6.

Chang, Y., Du, C., Han, L., Lv, S., Zhang, J., Bian, G., et al. (2019). Enhanced AMPA receptor-mediated excitatory transmission in the rodent rostromedial tegmental nucleus following lesion of the nigrostriatal pathway. *Neurochem. Int.* 122, 85–93. doi:10.1016/j.neuint.2018.11.007.

Chan-Palay, V., and Asan, E. (1989). Alterations in catecholamine neurons of the locus coeruleus in senile dementia of the Alzheimer type and in Parkinson's disease with and without dementia and depression. *J. Comp. Neurol.* 287, 373–392. doi:10.1002/cne.902870308.

Charles, K.-A., Naudet, F., Bouali-Benazzouz, R., Landry, M., De Deurwaerdère, P., Fossat, P., et al. (2018). Alteration of nociceptive integration in the spinal cord of a rat model of Parkinson's disease. *Mov. Disord. Off. J. Mov. Disord. Soc.* 33, 1010–1015. doi:10.1002/mds.27377.

Chaudhuri, K. R., and Schapira, A. H. V. (2009). Non-motor symptoms of Parkinson's disease: dopaminergic pathophysiology and treatment. *Lancet Neurol.* 8, 464–474. doi:10.1016/S1474-4422(09)70068-7.

Chazalon, M., Paredes-Rodriguez, E., Morin, S., Martinez, A., Cristóvão-Ferreira, S., Vaz, S., et al. (2018). GAT-3 Dysfunction Generates Tonic Inhibition in External Globus Pallidus Neurons in Parkinsonian Rodents. *Cell Rep.* 23, 1678–1690. doi:10.1016/j.celrep.2018.04.014.

Chen, F.-J., and Sara, S. J. (2007). Locus coeruleus activation by foot shock or electrical stimulation inhibits amygdala neurons. *Neuroscience* 144, 472–481. doi:10.1016/j.neuroscience.2006.09.037.

Chen, L., Liu, J., Zhang, Q. J., Feng, J. J., Gui, Z. H., Ali, U., et al. (2011). Alterations of emotion, cognition and firing activity of the basolateral nucleus of the amygdala after partial bilateral lesions of the nigrostriatal pathway in rats. *Brain Res. Bull.* 85, 329–338. doi:10.1016/j.brainresbull.2011.05.009.

Chiang, C., and Aston-Jones, G. (1993). Response of locus coeruleus neurons to footshock stimulation is mediated by neurons in the rostral ventral medulla. *Neuroscience* 53, 705–715. doi:10.1016/0306-4522(93)90618-p.

Choi, Y., Yoon, Y. W., Na, H. S., Kim, S. H., and Chung, J. M. (1994). Behavioral signs of ongoing pain and cold allodynia in a rat model of neuropathic pain. *Pain* 59, 369–376. doi:10.1016/0304-3959(94)90023-x.

Chotibut, T., Apple, D. M., Jefferis, R., and Salvatore, M. F. (2012). Dopamine Transporter Loss in 6-OHDA Parkinson's Model Is Unmet by Parallel Reduction in Dopamine Uptake. *PLoS ONE* 7. doi:10.1371/journal.pone.0052322.

Christie, M. J., Williams, J. T., and North, R. A. (1989). Electrical coupling synchronizes subthreshold activity in locus coeruleus neurons in vitro from neonatal rats. *J. Neurosci. Off. J. Soc. Neurosci.* 9, 3584–3589.

Connolly, B. S., and Lang, A. E. (2014). Pharmacological treatment of Parkinson disease: a review. *JAMA* 311, 1670–1683. doi:10.1001/jama.2014.3654.

Cope, Z. A., Vazey, E. M., Floresco, S. B., and Aston Jones, G. S. (2019). DREADD-mediated modulation of locus coeruleus inputs to mPFC improves strategy set-shifting. *Neurobiol. Learn. Mem.* 161, 1–11. doi:10.1016/j.nlm.2019.02.009.

Corteen, N. L., Cole, T. M., Sarna, A., Sieghart, W., and Swinny, J. D. (2011). Localization of GABA-A receptor alpha subunits on neurochemically distinct cell types in the rat locus coeruleus. *Eur. J. Neurosci.* 34, 250–262. doi:10.1111/j.1460-9568.2011.07740.x.

Cotzias, G. C., Van Woert, M. H., and Schiffer, L. M. (1967). Aromatic amino acids and modification of parkinsonism. *N. Engl. J. Med.* 276, 374–379. doi:10.1056/NEJM196702162760703.

Couto, M. I., Monteiro, A., Oliveira, A., Lunet, N., and Massano, J. (2014). Depression and anxiety following deep brain stimulation in Parkinson's disease: systematic review and meta-analysis. *Acta Med. Port.* 27, 372–382. doi:10.20344/amp.4928.

Cullen, K. P., Grant, L. M., Kelm-Nelson, C. A., Brauer, A. F. L., Bickelhaupt, L. B., Russell, J. A., et al. (2018). Pink1 –/– Rats Show Early-Onset Swallowing Deficits and Correlative Brainstem Pathology. *Dysphagia* 33, 749–758. doi:10.1007/s00455-018-9896-5.

Curtin, K., Fleckenstein, A. E., Keeshin, B. R., Yurgelun-Todd, D. A., Renshaw, P. F., Smith, K. R., et al. (2018). Increased risk of diseases of the basal ganglia and cerebellum in patients with a history of attention-deficit/hyperactivity disorder. *Neuropsychopharmacol. Off. Publ. Am. Coll. Neuropsychopharmacol.* 43, 2548–2555. doi:10.1038/s41386-018-0207-5.

Curtis, A. L., Leiser, S. C., Snyder, K., and Valentino, R. J. (2012). Predator stress engages corticotropin-releasing factor and opioid systems to alter the operating mode of locus coeruleus norepinephrine neurons. *Neuropharmacology* 62, 1737–1745. doi:10.1016/j.neuropharm.2011.11.020.

Czernecki, V., Schüpbach, M., Yaici, S., Lévy, R., Bardinet, E., Yelnik, J., et al. (2008). Apathy following subthalamic stimulation in Parkinson disease: a dopamine responsive symptom. *Mov. Disord. Off. J. Mov. Disord. Soc.* 23, 964–969. doi:10.1002/mds.21949.

Dahlstroem, A., and Fuxe, K. (1964). EVIDENCE FOR THE EXISTENCE OF MONOAMINE-CONTAINING NEURONS IN THE CENTRAL NERVOUS SYSTEM. I. DEMONSTRATION OF MONOAMINES IN THE CELL BODIES OF BRAIN STEM NEURONS. *Acta Physiol. Scand. Suppl.*, SUPPL 232:1-55.

Dai, Y., Iwata, K., Fukuoka, T., Kondo, E., Tokunaga, A., Yamanaka, H., et al. (2002). Phosphorylation of extracellular signal-regulated kinase in primary afferent neurons by noxious stimuli and its involvement in peripheral sensitization. *J. Neurosci. Off. J. Soc. Neurosci.* 22, 7737–7745.

de Freitas, R. L., Medeiros, P., da Silva, J. A., de Oliveira, R. C., de Oliveira, R., Ullah, F., et al. (2016). The μ1-opioid receptor and 5-HT2A- and 5HT2C-serotonergic receptors of the locus coeruleus are critical in elaborating hypoalgesia induced by tonic and tonic-clonic seizures. *Neuroscience* 336, 133–145. doi:10.1016/j.neuroscience.2016.08.040.

de Lau, L. M. L., and Breteler, M. M. B. (2006). Epidemiology of Parkinson's disease. *Lancet Neurol.* 5, 525–535. doi:10.1016/S1474-4422(06)70471-9.

de Oliveira, R. B., Howlett, M. C. H., Gravina, F. S., Imtiaz, M. S., Callister, R. J., Brichta, A. M., et al. (2010). Pacemaker currents in mouse locus coeruleus neurons. *Neuroscience* 170, 166–177. doi:10.1016/j.neuroscience.2010.06.028.

Del Tredici, K., Rüb, U., De Vos, R. A. I., Bohl, J. R. E., and Braak, H. (2002). Where does parkinson disease pathology begin in the brain? *J. Neuropathol. Exp. Neurol.* 61, 413–426.

Delaville, C., Chetrit, J., Abdallah, K., Morin, S., Cardoit, L., De Deurwaerdère, P., et al. (2012a). Emerging dysfunctions consequent to combined monoaminergic depletions in Parkinsonism. *Neurobiol. Dis.* 45, 763–773. doi:10.1016/j.nbd.2011.10.023.

Delaville, C., Navailles, S., and Benazzouz, A. (2012b). Effects of noradrenaline and serotonin depletions on the neuronal activity of globus pallidus and substantia nigra pars reticulata in experimental parkinsonism. *Neuroscience* 202, 424–433. doi:10.1016/j.neuroscience.2011.11.024.

Delfs, J. M., Zhu, Y., Druhan, J. P., and Aston-Jones, G. S. (1998). Origin of noradrenergic afferents to the shell subregion of the nucleus accumbens: anterograde and retrograde tract-tracing studies in the rat. *Brain Res.* 806, 127–140. doi:10.1016/s0006-8993(98)00672-6.

DeLong, M. R. (1990). Primate models of movement disorders of basal ganglia origin. *Trends Neurosci.* 13, 281–285. doi:10.1016/0166-2236(90)90110-v.

Deutch, A. Y., Goldstein, M., and Roth, R. H. (1986). Activation of the locus coeruleus induced by selective stimulation of the ventral tegmental area. *Brain Res.* 363, 307–314. doi:10.1016/0006-8993(86)91016-4.

Devos, D., Moreau, C., Maltête, D., Lefaucheur, R., Kreisler, A., Eusebio, A., et al. (2014). Rivastigmine in apathetic but dementia and depression-free patients with Parkinson's disease: a double-blind, placebo-controlled, randomised clinical trial. *J. Neurol. Neurosurg. Psychiatry* 85, 668–674. doi:10.1136/jnnp-2013-306439.

Devoto, P., Flore, G., Longu, G., Pira, L., and Gessa, G. L. (2003). Origin of extracellular dopamine from dopamine and noradrenaline neurons in the medial prefrontal and occipital cortex. *Synap. N. Y. N* 50, 200–205. doi:10.1002/syn.10264.

Devoto, P., Flore, G., Pani, L., and Gessa, G. L. (2001). Evidence for co-release of noradrenaline and dopamine from noradrenergic neurons in the cerebral cortex. *Mol. Psychiatry* 6, 657–664. doi:10.1038/sj.mp.4000904.

Devoto, P., Flore, G., Pira, L., Longu, G., and Gessa, G. L. (2004). Alpha2-adrenoceptor mediated co-release of dopamine and noradrenaline from noradrenergic neurons in the cerebral cortex. *J. Neurochem.* 88, 1003–1009. doi:10.1046/j.1471-4159.2003.02239.x.

Devoto, P., Flore, G., Saba, P., Fà, M., and Gessa, G. L. (2005a). Co-release of noradrenaline and dopamine in the cerebral cortex elicited by single train and repeated train stimulation of the locus coeruleus. *BMC Neurosci.* 6, 31. doi:10.1186/1471-2202-6-31.

Devoto, P., Flore, G., Saba, P., Fà, M., and Gessa, G. L. (2005b). Stimulation of the locus coeruleus elicits noradrenaline and dopamine release in the medial prefrontal and parietal cortex. *J. Neurochem.* 92, 368–374. doi:10.1111/j.1471-4159.2004.02866.x.

Dietrichs, E., and Odin, P. (2017). Algorithms for the treatment of motor problems in Parkinson's disease. *Acta Neurol. Scand.* 136, 378–385. doi:10.1111/ane.12733.

Djaldetti, R., Shifrin, A., Rogowski, Z., Sprecher, E., Melamed, E., and Yarnitsky, D. (2004). Quantitative measurement of pain sensation in patients with Parkinson disease. *Neurology* 62, 2171–2175. doi:10.1212/01.wnl.0000130455.38550.9d.

Djaldetti, R., Yust-Katz, S., Kolianov, V., Melamed, E., and Dabby, R. (2007). The effect of duloxetine on primary pain symptoms in Parkinson disease. *Clin. Neuropharmacol.* 30, 201–205. doi:10.1097/wnf.0b013e3180340319.

Dluzen, D. E. (1992). 1-Methyl-4-phenyl-1,2,3,6-tetrahydropyridine (MPTP) reduces norepinephrine concentrations in the olfactory bulbs of male mice. *Brain Res.* 586, 144–147. doi:10.1016/0006-8993(92)91385-r.

Domenici, R. A., Campos, A. C. P., Maciel, S. T., Berzuino, M. B., Hernandes, M. S., Fonoff, E. T., et al. (2019). Parkinson's disease and pain: Modulation of nociceptive circuitry in a rat model of nigrostriatal lesion. *Exp. Neurol.* 315, 72–81. doi:10.1016/j.expneurol.2019.02.007.

Drug Approval Package: Gocovri (amantadine extended-release) Available at: https://www.accessdata.fda.gov/drugsatfda_docs/nda/2017/208944Orig1s000TOC.cfm [Accessed December 9, 2019].

Dubé, G. R., and Marshall, K. C. (1997). Modulation of excitatory synaptic transmission in locus coeruleus by multiple presynaptic metabotropic glutamate receptors. *Neuroscience* 80, 511–521. doi:10.1016/s0306-4522(97)00004-3.

Egan, T. M., Henderson, G., North, R. A., and Williams, J. T. (1983). Noradrenaline-mediated synaptic inhibition in rat locus coeruleus neurones. *J. Physiol.* 345, 477–488. doi:10.1113/jphysiol.1983.sp014990.

Egan, T. M., and North, R. A. (1986). Actions of acetylcholine and nicotine on rat locus coeruleus neurons in vitro. *Neuroscience* 19, 565–571. doi:10.1016/0306-4522(86)90281-2.

Ehlers, C. L., and Somes, C. (2002). Long latency event-related potentials in mice: effects of stimulus characteristics and strain. *Brain Res.* 957, 117–128. doi:10.1016/s0006-8993(02)03612-0.

Elam, M., Clark, D., and Svensson, T. H. (1986). Electrophysiological effects of the enantiomers of 3-PPP on neurons in the locus coeruleus of the rat. *Neuropharmacology* 25, 1003–1008. doi:10.1016/0028-3908(86)90194-2.

Engel, A. K., Fries, P., and Singer, W. (2001). Dynamic predictions: oscillations and synchrony in top-down processing. *Nat. Rev. Neurosci.* 2, 704–716. doi:10.1038/35094565.

Engel, A. K., Senkowski, D., and Schneider, T. R. (2012). "Multisensory Integration through Neural Coherence," in *The Neural Bases of Multisensory Processes* Frontiers in Neuroscience., eds. M. M. Murray and M. T. Wallace (Boca Raton (FL): CRC Press/Taylor & Francis). Available at: http://www.ncbi.nlm.nih.gov/books/NBK92855/ [Accessed January 21, 2020].

Engels, G., Douw, L., Kerst, Y., Weinstein, H., Scherder, E., and Vlaar, A. (2019). Non-motor symptoms in Parkinson's disease: An explorative network study. *Parkinsonism Relat. Disord.* 66, 237–240. doi:10.1016/j.parkreldis.2019.08.002.

Ennis, M., and Aston-Jones, G. (1987). Two physiologically distinct populations of neurons in the ventrolateral medulla innervate the locus coeruleus. *Brain Res.* 425, 275–282. doi:10.1016/0006-8993(87)90510-5.

Ennis, M., Aston-Jones, G., and Shiekhattar, R. (1992). Activation of locus coeruleus neurons by nucleus paragigantocellularis or noxious sensory stimulation is mediated by intracoerulear excitatory amino acid neurotransmission. *Brain Res.* 598, 185–195. doi:10.1016/0006-8993(92)90182-9.

Eschenko, O., Magri, C., Panzeri, S., and Sara, S. J. (2012). Noradrenergic neurons of the locus coeruleus are phase locked to cortical up-down states during sleep. *Cereb. Cortex N. Y. N 1991* 22, 426–435. doi:10.1093/cercor/bhr121.

Eskow Jaunarajs, K. L., Dupre, K. B., Ostock, C. Y., Button, T., Deak, T., and Bishop, C. (2010). Behavioral and neurochemical effects of chronic L-DOPA treatment on nonmotor sequelae in the hemiparkinsonian rat. *Behav. Pharmacol.* 21, 627–637. doi:10.1097/FBP.0b013e32833e7e80.

Fahn, S. (2008). The history of dopamine and levodopa in the treatment of Parkinson's disease. *Mov. Disord. Off. J. Mov. Disord. Soc.* 23 Suppl 3, S497-508. doi:10.1002/mds.22028.

Fan, L.-L., Deng, B., Yan, J.-B., Hu, Z.-H., Ren, A.-H., and Yang, D.-W. (2019). Lesions of mediodorsal thalamic nucleus reverse abnormal firing of the medial prefrontal cortex neurons in parkinsonian rats. *Neural Regen. Res.* 14, 1635–1642. doi:10.4103/1673-5374.255982.

Fearnley, J. M., and Lees, A. J. (1991). Ageing and Parkinson's disease: substantia nigra regional selectivity. *Brain J. Neurol.* 114 (Pt 5), 2283–2301. doi:10.1093/brain/114.5.2283.

Ferro, M. M., Bellissimo, M. I., Anselmo-Franci, J. A., Angellucci, M. E. M., Canteras, N. S., and Da Cunha, C. (2005). Comparison of bilaterally 6-OHDA- and MPTP-lesioned rats as models of the early phase of Parkinson's disease: histological, neurochemical, motor and memory alterations. *J. Neurosci. Methods* 148, 78–87. doi:10.1016/j.jneumeth.2005.04.005.

File, S. E., and Hyde, J. R. (1978). Can social interaction be used to measure anxiety? *Br. J. Pharmacol.* 62, 19–24. doi:10.1111/j.1476-5381.1978.tb07001.x.

Fitoussi, A., Dellu-Hagedorn, F., and De Deurwaerdère, P. (2013). Monoamines tissue content analysis reveals restricted and site-specific correlations in brain regions involved in cognition. *Neuroscience* 255, 233–245. doi:10.1016/j.neuroscience.2013.09.059.

Flatters, S. J. L., and Bennett, G. J. (2004). Ethosuximide reverses paclitaxel- and vincristine-induced painful peripheral neuropathy. *Pain* 109, 150–161. doi:10.1016/j.pain.2004.01.029.

Florin-Lechner, S. M., Druhan, J. P., Aston-Jones, G., and Valentino, R. J. (1996). Enhanced norepinephrine release in prefrontal cortex with burst stimulation of the locus coeruleus. *Brain Res.* 742, 89–97. doi:10.1016/s0006-8993(96)00967-5.

Fornai, F., Alessandrì, M. G., Torracca, M. T., Bassi, L., and Corsini, G. U. (1997). Effects of noradrenergic lesions on MPTP/MPP+ kinetics and MPTP-induced nigrostriatal dopamine depletions. *J. Pharmacol. Exp. Ther.* 283, 100–107.

Fornai, F., Bassi, L., Torracca, M. T., Scalori, V., and Corsini, G. U. (1995). Norepinephrine loss exacerbates methamphetamine-induced striatal dopamine depletion in mice. *Eur. J. Pharmacol.* 283, 99–102.

Forsythe, I. D., Linsdell, P., and Stanfield, P. R. (1992). Unitary A-currents of rat locus coeruleus neurones grown in cell culture: rectification caused by internal Mg2+ and Na+. *J. Physiol.* 451, 553–583. doi:10.1113/jphysiol.1992.sp019179.

Freedman, J. E., and Aghajanian, G. K. (1984). Idazoxan (RX 781094) selectively antagonizes alpha 2-adrenoceptors on rat central neurons. *Eur. J. Pharmacol.* 105, 265–272. doi:10.1016/0014-2999(84)90618-6.

Frisina, P. G., Haroutunian, V., and Libow, L. S. (2009). The neuropathological basis for depression in Parkinson's disease. *Parkinsonism Relat. Disord.* 15, 144–148. doi:10.1016/j.parkreldis.2008.04.038.

Fujisawa, S., and Buzsáki, G. (2011). A 4 Hz oscillation adaptively synchronizes prefrontal, VTA, and hippocampal activities. *Neuron* 72, 153–165. doi:10.1016/j.neuron.2011.08.018.

Galati, S., D'Angelo, V., Olivola, E., Marzetti, F., Di Giovanni, G., Stanzione, P., et al. (2010). Acute inactivation of the medial forebrain bundle imposes oscillations in the SNr: a challenge for the 6-OHDA model? *Exp. Neurol.* 225, 294–301. doi:10.1016/j.expneurol.2010.06.020.

Galati, S., Stanzione, P., D'Angelo, V., Fedele, E., Marzetti, F., Sancesario, G., et al. (2009). The pharmacological blockade of medial forebrain bundle induces an acute pathological synchronization of the cortico-subthalamic nucleus-globus pallidus pathway. *J. Physiol.* 587, 4405–4423. doi:10.1113/jphysiol.2009.172759.

Gaspar, P., and Gray, F. (1984). Dementia in idiopathic Parkinson's disease. A neuropathological study of 32 cases. *Acta Neuropathol. (Berl.)* 64, 43–52. doi:10.1007/bf00695605.

Gee, L. E., Chen, N., Ramirez-Zamora, A., Shin, D. S., and Pilitsis, J. G. (2015). The effects of subthalamic deep brain stimulation on mechanical and thermal thresholds in 6OHDA-lesioned rats. *Eur. J. Neurosci.* 42, 2061–2069. doi:10.1111/ejn.12992.

George, S. A., Knox, D., Curtis, A. L., Aldridge, J. W., Valentino, R. J., and Liberzon, I. (2013). Altered locus coeruleus-norepinephrine function following single prolonged stress. *Eur. J. Neurosci.* 37, 901–909. doi:10.1111/ejn.12095.

German, D. C., Manaye, K. F., White, C. L., Woodward, D. J., McIntire, D. D., Smith, W. K., et al. (1992). Disease-specific patterns of locus coeruleus cell loss. *Ann. Neurol.* 32, 667–676. doi:10.1002/ana.410320510.

Giaime, E., Tong, Y., Wagner, L. K., Yuan, Y., Huang, G., and Shen, J. (2017). Age-Dependent Dopaminergic Neurodegeneration and Impairment of the Autophagy-Lysosomal Pathway in LRRK-Deficient Mice. *Neuron* 96, 796-807.e6. doi:10.1016/j.neuron.2017.09.036.

Giasson, B. I., Duda, J. E., Quinn, S. M., Zhang, B., Trojanowski, J. Q., and Lee, V. M.-Y. (2002). Neuronal α-Synucleinopathy with Severe Movement Disorder in Mice Expressing A53T Human α-Synuclein. *Neuron* 34, 521–533. doi:10.1016/S0896-6273(02)00682-7.

Gilzenrat, M. S., Nieuwenhuis, S., Jepma, M., and Cohen, J. D. (2010). Pupil diameter tracks changes in control state predicted by the adaptive gain theory of locus coeruleus function. *Cogn. Affect. Behav. Neurosci.* 10, 252–269. doi:10.3758/CABN.10.2.252.

Gjerstad, M. D., Alves, G., Wentzel-Larsen, T., Aarsland, D., and Larsen, J. P. (2006). Excessive daytime sleepiness in Parkinson disease: is it the drugs or the disease? *Neurology* 67, 853–858. doi:10.1212/01.wnl.0000233980.25978.9d.

Goedert, M., and Compston, A. (2018). Parkinson's disease - the story of an eponym. *Nat. Rev. Neurol.* 14, 57–62. doi:10.1038/nrneurol.2017.165.

Goldstein, D. S., Holmes, C., and Sharabi, Y. (2012). Cerebrospinal fluid biomarkers of central catecholamine deficiency in Parkinson's disease and other synucleinopathies. *Brain J. Neurol.* 135, 1900–1913. doi:10.1093/brain/aws055.

Gómez-Paz, A., Drucker-Colín, R., Milán-Aldaco, D., Palomero-Rivero, M., and Ambriz-Tututi, M. (2018). Intrastriatal Chromospheres' Transplant Reduces Nociception in Hemiparkinsonian Rats. *Neuroscience* 387, 123–134. doi:10.1016/j.neuroscience.2017.08.052.

Grant, L. M., Kelm-Nelson, C. A., Hilby, B. L., Blue, K. V., Paul Rajamanickam, E. S., Pultorak, J. D., et al. (2015). Evidence for early and progressive ultrasonic vocalization and oromotor deficits in a PINK1 gene knockout rat model of Parkinson's disease. *J. Neurosci. Res.* 93, 1713–1727. doi:10.1002/jnr.23625.

Grant, M. M., and Weiss, J. M. (2001). Effects of chronic antidepressant drug administration and electroconvulsive shock on locus coeruleus electrophysiologic activity. *Biol. Psychiatry* 49, 117–129. doi:10.1016/s0006-3223(00)00936-7.

Graybiel, A. M. (2005). The basal ganglia: learning new tricks and loving it. *Curr. Opin. Neurobiol.* 15, 638–644. doi:10.1016/j.conb.2005.10.006.

Guajardo, H. M., Snyder, K., Ho, A., and Valentino, R. J. (2017). Sex Differences in mu-Opioid Receptor Regulation of the Rat Locus Coeruleus and Their Cognitive Consequences. *Neuropsychopharmacol. Off. Publ. Am. Coll. Neuropsychopharmacol.* 42, 1295–1304. doi:10.1038/npp.2016.252.

Guiard, B. P., El Mansari, M., Merali, Z., and Blier, P. (2008). Functional interactions between dopamine, serotonin and norepinephrine neurons: an in-vivo electrophysiological study in rats with monoaminergic lesions. *Int. J. Neuropsychopharmacol.* 11, 625–639. doi:10.1017/S1461145707008383.

Guimarães, J., Moura, E., Silva, E., Aguiar, P., Garrett, C., and Vieira-Coelho, M. A. (2013). Locus Coeruleus Is Involved in Weight Loss in a Rat Model of Parkinson's Disease: An Effect Reversed by Deep Brain Stimulation. *Brain Stimulat.* 6, 845–855. doi:10.1016/j.brs.2013.06.002.

Guo, X.-Z., Shan, C., Hou, Y.-F., Zhu, G., Tao, B., Sun, L.-H., et al. (2018). Osteocalcin Ameliorates Motor Dysfunction in a 6-Hydroxydopamine-Induced Parkinson's Disease Rat Model Through AKT/GSK3β Signaling. *Front. Mol. Neurosci.* 11, 343. doi:10.3389/fnmol.2018.00343.

Haas, R. H., Nasirian, F., Nakano, K., Ward, D., Pay, M., Hill, R., et al. (1995). Low platelet mitochondrial complex I and complex II/III activity in early untreated Parkinson's disease. *Ann. Neurol.* 37, 714–722. doi:10.1002/ana.410370604.

Hakusui, S., Yasuda, T., Yanagi, T., Tohyama, J., Hasegawa, Y., Koike, Y., et al. (1994). A radiological analysis of heart sympathetic functions with meta-[123I]iodobenzylguanidine in neurological patients with autonomic failure. *J. Auton. Nerv. Syst.* 49, 81–84. doi:10.1016/0165-1838(94)90023-x.

Halliday, G., Lees, A., and Stern, M. (2011). Milestones in Parkinson's disease--clinical and pathologic features. *Mov. Disord. Off. J. Mov. Disord. Soc.* 26, 1015–1021. doi:10.1002/mds.23669.

Hargreaves, K., Dubner, R., Brown, F., Flores, C., and Joris, J. (1988). A new and sensitive method for measuring thermal nociception in cutaneous hyperalgesia. *Pain* 32, 77–88. doi:10.1016/0304-3959(88)90026-7.

Hayashida, K.-I., Obata, H., Nakajima, K., and Eisenach, J. C. (2008). Gabapentin acts within the locus coeruleus to alleviate neuropathic pain. *Anesthesiology* 109, 1077–1084. doi:10.1097/ALN.0b013e31818dac9c.

Healy-Stoffel, M., Omar Ahmad, S., Stanford, J. A., and Levant, B. (2014). Differential effects of intrastriatal 6-hydroxydopamine on cell number and morphology in midbrain dopaminergic subregions of the rat. *Brain Res.* 1574, 113–119. doi:10.1016/j.brainres.2014.05.045.

Hentall, I. D., Mesigil, R., Pinzon, A., and Noga, B. R. (2003). Temporal and spatial profiles of pontine-evoked monoamine release in the rat's spinal cord. *J. Neurophysiol.* 89, 2943–2951. doi:10.1152/jn.00608.2002.

Hickey, L., Li, Y., Fyson, S. J., Watson, T. C., Perrins, R., Hewinson, J., et al. (2014). Optoactivation of locus ceruleus neurons evokes bidirectional changes in thermal nociception in rats. *J. Neurosci. Off. J. Soc. Neurosci.* 34, 4148–4160. doi:10.1523/JNEUROSCI.4835-13.2014.

Hirao, K., Pontone, G. M., and Smith, G. S. (2015). Molecular imaging of neuropsychiatric symptoms in Alzheimer's and Parkinson's disease. *Neurosci. Biobehav. Rev.* 49, 157–170. doi:10.1016/j.neubiorev.2014.11.010.

Hirschberg, S., Li, Y., Randall, A., Kremer, E. J., and Pickering, A. E. (2017). Functional dichotomy in spinal- vs prefrontal-projecting locus coeruleus modules splits descending noradrenergic analgesia from ascending aversion and anxiety in rats. *eLife* 6. doi:10.7554/eLife.29808.

Hiser, J., and Koenigs, M. (2018). The Multifaceted Role of the Ventromedial Prefrontal Cortex in Emotion, Decision Making, Social Cognition, and Psychopathology. *Biol. Psychiatry* 83, 638–647. doi:10.1016/j.biopsych.2017.10.030.

Holets, V. R., Hökfelt, T., Rökaeus, A., Terenius, L., and Goldstein, M. (1988). Locus coeruleus neurons in the rat containing neuropeptide Y, tyrosine hydroxylase or galanin and their efferent projections to the spinal cord, cerebral cortex and hypothalamus. *Neuroscience* 24, 893–906. doi:10.1016/0306-4522(88)90076-0.

Holper, L., Ben-Shachar, D., and Mann, J. J. (2019). Multivariate meta-analyses of mitochondrial complex I and IV in major depressive disorder, bipolar disorder, schizophrenia, Alzheimer disease, and Parkinson disease. *Neuropsychopharmacol. Off. Publ. Am. Coll. Neuropsychopharmacol.* 44, 837–849. doi:10.1038/s41386-018-0090-0.

Howells, F. M., Stein, D. J., and Russell, V. A. (2012). Synergistic tonic and phasic activity of the locus coeruleus norepinephrine (LC-NE) arousal system is required for optimal attentional performance. *Metab. Brain Dis.* 27, 267–274. doi:10.1007/s11011-012-9287-9.

Howorth, P. W., Teschemacher, A. G., and Pickering, A. E. (2009a). Retrograde adenoviral vector targeting of nociresponsive pontospinal noradrenergic neurons in the rat in vivo. *J. Comp. Neurol.* 512, 141–157. doi:10.1002/cne.21879.

Howorth, P. W., Thornton, S. R., O'Brien, V., Smith, W. D., Nikiforova, N., Teschemacher, A. G., et al. (2009b). Retrograde viral vector-mediated inhibition of pontospinal noradrenergic neurons causes hyperalgesia in rats. *J. Neurosci. Off. J. Soc. Neurosci.* 29, 12855–12864. doi:10.1523/JNEUROSCI.1699-09.2009.

Hurst, J. H., LeWitt, P. A., Burns, R. S., Foster, N. L., and Lovenberg, W. (1985). CSF dopamine-beta-hydroxylase activity in Parkinson's disease. *Neurology* 35, 565–568. doi:10.1212/wnl.35.4.565.

Imbe, H., Murakami, S., Okamoto, K., Iwai-Liao, Y., and Senba, E. (2004). The effects of acute and chronic restraint stress on activation of ERK in the rostral ventromedial medulla and locus coeruleus. *Pain* 112, 361–371. doi:10.1016/j.pain.2004.09.015.

Imbe, H., Okamoto, K., Donishi, T., Kawai, S., Enoki, K., Senba, E., et al. (2009). Activation of ERK in the locus coeruleus following acute noxious stimulation. *Brain Res.* 1263, 50–57. doi:10.1016/j.brainres.2009.01.052.

Ishimatsu, M., and Williams, J. T. (1996). Synchronous activity in locus coeruleus results from dendritic interactions in pericoerulear regions. *J. Neurosci. Off. J. Soc. Neurosci.* 16, 5196–5204.

Isokawa, M. (1997). Membrane time constant as a tool to assess cell degeneration. *Brain Res. Brain Res. Protoc.* 1, 114–116. doi:10.1016/s1385-299x(96)00016-5.

Iwasaki, S., Chihara, Y., Komuta, Y., Ito, K., and Sahara, Y. (2008). Low-voltage-activated potassium channels underlie the regulation of intrinsic firing properties of rat vestibular ganglion cells. *J. Neurophysiol.* 100, 2192–2204. doi:10.1152/jn.01240.2007.

Jain, S., and Goldstein, D. S. (2012). Cardiovascular dysautonomia in Parkinson Disease: From pathophysiology to pathogenesis. *Neurobiol. Dis.* 46, 572–580. doi:10.1016/j.nbd.2011.10.025.

Ji, R. R., Baba, H., Brenner, G. J., and Woolf, C. J. (1999). Nociceptive-specific activation of ERK in spinal neurons contributes to pain hypersensitivity. *Nat. Neurosci.* 2, 1114–1119. doi:10.1038/16040.

Ji, R.-R., Befort, K., Brenner, G. J., and Woolf, C. J. (2002). ERK MAP kinase activation in superficial spinal cord neurons induces prodynorphin and NK-1 upregulation and contributes to persistent inflammatory pain hypersensitivity. *J. Neurosci. Off. J. Soc. Neurosci.* 22, 478–485.

Ji, R.-R., Gereau, R. W., Malcangio, M., and Strichartz, G. R. (2009). MAP kinase and pain. *Brain Res. Rev.* 60, 135–148. doi:10.1016/j.brainresrev.2008.12.011.

Jin, X., Li, S., Bondy, B., Zhong, W., Oginsky, M. F., Wu, Y., et al. (2016). Identification of a Group of GABAergic Neurons in the Dorsomedial Area of the Locus Coeruleus. *PloS One* 11, e0146470. doi:10.1371/journal.pone.0146470.

Kaehler, S. T., Singewald, N., and Philippu, A. (1999a). Dependence of serotonin release in the locus coeruleus on dorsal raphe neuronal activity. *Naunyn. Schmiedebergs Arch. Pharmacol.* 359, 386–393. doi:10.1007/pl00005365.

Kaehler, S. T., Sinner, C., Chatterjee, S. S., and Philippu, A. (1999b). Hyperforin enhances the extracellular concentrations of catecholamines, serotonin and glutamate in the rat locus coeruleus. *Neurosci. Lett.* 262, 199–202. doi:10.1016/s0304-3940(99)00087-7.

Kaeidi, A., Azizi, H., Javan, M., Ahmadi Soleimani, S. M., Fathollahi, Y., and Semnanian, S. (2015). Direct Facilitatory Role of Paragigantocellularis Neurons in Opiate Withdrawal-Induced Hyperactivity of Rat Locus Coeruleus Neurons: An In Vitro Study. *PloS One* 10, e0134873. doi:10.1371/journal.pone.0134873.

Kalia, L. V., and Lang, A. E. (2015). Parkinson's disease. *Lancet Lond. Engl.* 386, 896–912. doi:10.1016/S0140-6736(14)61393-3.

Kamińska, K., Lenda, T., Konieczny, J., Czarnecka, A., and Lorenc-Koci, E. (2017). Depressive-like neurochemical and behavioral markers of Parkinson's disease after 6-OHDA administered unilaterally to the rat medial forebrain bundle. *Pharmacol. Rep. PR* 69, 985–994. doi:10.1016/j.pharep.2017.05.016.

Kang, Y., Henchcliffe, C., Verma, A., Vallabhajosula, S., He, B., Kothari, P. J., et al. (2019). 18F-FPEB PET/CT Shows mGluR5 Upregulation in Parkinson's Disease. *J. Neuroimaging Off. J. Am. Soc. Neuroimaging* 29, 97–103. doi:10.1111/jon.12563.

Karmy, G., Carr, P. A., Yamamoto, T., Chan, S. H., and Nagy, J. I. (1991). Cytochrome oxidase immunohistochemistry in rat brain and dorsal root ganglia: visualization of enzyme in neuronal perikarya and in parvalbumin-

positive neurons. *Neuroscience* 40, 825–839. doi:10.1016/0306-4522(91)90015-g.

Karstaedt, P. J., Kerasidis, H., Pincus, J. H., Meloni, R., Graham, J., and Gale, K. (1994). Unilateral destruction of dopamine pathways increases ipsilateral striatal serotonin turnover in rats. *Exp. Neurol.* 126, 25–30. doi:10.1006/exnr.1994.1039.

Kaya, A. H., Vlamings, R., Tan, S., Lim, L. W., Magill, P. J., Steinbusch, H. W. M., et al. (2008). Increased electrical and metabolic activity in the dorsal raphe nucleus of Parkinsonian rats. *Brain Res.* 1221, 93–97. doi:10.1016/j.brainres.2008.05.019.

Kempadoo, K. A., Mosharov, E. V., Choi, S. J., Sulzer, D., and Kandel, E. R. (2016). Dopamine release from the locus coeruleus to the dorsal hippocampus promotes spatial learning and memory. *Proc. Natl. Acad. Sci. U. S. A.* 113, 14835–14840. doi:10.1073/pnas.1616515114.

Kilbourn, M. R., Sherman, P., and Abbott, L. C. (1998). Reduced MPTP neurotoxicity in striatum of the mutant mouse tottering. *Synap. N. Y. N* 30, 205–210. doi:10.1002/(SICI)1098-2396(199810)30:2<205::AID-SYN10>3.0.CO;2-0.

Kim, M.-A., Lee, H. S., Lee, B. Y., and Waterhouse, B. D. (2004). Reciprocal connections between subdivisions of the dorsal raphe and the nuclear core of the locus coeruleus in the rat. *Brain Res.* 1026, 56–67. doi:10.1016/j.brainres.2004.08.022.

Kim, S., Kwon, S.-H., Kam, T.-I., Panicker, N., Karuppagounder, S. S., Lee, S., et al. (2019). Transneuronal Propagation of Pathologic α-Synuclein from the Gut to the Brain Models Parkinson's Disease. *Neuron* 103, 627-641.e7. doi:10.1016/j.neuron.2019.05.035.

Kimura, M., Suto, T., Morado-Urbina, C. E., Peters, C. M., Eisenach, J. C., and Hayashida, K.-I. (2015). Impaired Pain-evoked Analgesia after Nerve Injury in Rats Reflects Altered Glutamate Regulation in the Locus Coeruleus. *Anesthesiology* 123, 899–908. doi:10.1097/ALN.0000000000000796.

Kish, S. J., Shannak, K., and Hornykiewicz, O. (1988). Uneven pattern of dopamine loss in the striatum of patients with idiopathic Parkinson's disease.

Pathophysiologic and clinical implications. *N. Engl. J. Med.* 318, 876–880. doi:10.1056/NEJM198804073181402.

Kish, S. J., Shannak, K. S., Rajput, A. H., Gilbert, J. J., and Hornykiewicz, O. (1984). Cerebellar norepinephrine in patients with Parkinson's disease and control subjects. *Arch. Neurol.* 41, 612–614. doi:10.1001/archneur.1984.04210080020007.

König, P. (1994). A method for the quantification of synchrony and oscillatory properties of neuronal activity. *J. Neurosci. Methods* 54, 31–37. doi:10.1016/0165-0270(94)90157-0.

Kravitz, A. V., Freeze, B. S., Parker, P. R. L., Kay, K., Thwin, M. T., Deisseroth, K., et al. (2010). Regulation of parkinsonian motor behaviours by optogenetic control of basal ganglia circuitry. *Nature* 466, 622–626. doi:10.1038/nature09159.

Kreiner, G., Rafa-Zabłocka, K., Barut, J., Chmielarz, P., Kot, M., Bagińska, M., et al. (2019). Stimulation of noradrenergic transmission by reboxetine is beneficial for a mouse model of progressive parkinsonism. *Sci. Rep.* 9, 5262. doi:10.1038/s41598-019-41756-3.

Kühn, A. A., Kempf, F., Brücke, C., Gaynor Doyle, L., Martinez-Torres, I., Pogosyan, A., et al. (2008). High-frequency stimulation of the subthalamic nucleus suppresses oscillatory beta activity in patients with Parkinson's disease in parallel with improvement in motor performance. *J. Neurosci. Off. J. Soc. Neurosci.* 28, 6165–6173. doi:10.1523/JNEUROSCI.0282-08.2008.

Kühn, A. A., Kupsch, A., Schneider, G.-H., and Brown, P. (2006). Reduction in subthalamic 8-35 Hz oscillatory activity correlates with clinical improvement in Parkinson's disease. *Eur. J. Neurosci.* 23, 1956–1960. doi:10.1111/j.1460-9568.2006.04717.x.

Kwon, M.-S., Seo, Y.-J., Shim, E.-J., Choi, S.-S., Lee, J.-Y., and Suh, H.-W. (2006). The effect of single or repeated restraint stress on several signal molecules in paraventricular nucleus, arcuate nucleus and locus coeruleus. *Neuroscience* 142, 1281–1292. doi:10.1016/j.neuroscience.2006.07.027.

Langston, J. W., Ballard, P., Tetrud, J. W., and Irwin, I. (1983). Chronic Parkinsonism in humans due to a product of meperidine-analog synthesis. *Science* 219, 979–980. doi:10.1126/science.6823561.

Leclair-Visonneau, L., Magy, L., Volteau, C., Clairembault, T., Le Dily, S., Préterre, C., et al. (2018). Heterogeneous pattern of autonomic dysfunction in Parkinson's disease. *J. Neurol.* 265, 933–941. doi:10.1007/s00415-018-8789-8.

Lei, S. (2014). Cross interaction of dopaminergic and adrenergic systems in neural modulation. *Int. J. Physiol. Pathophysiol. Pharmacol.* 6, 137–142.

Léna, C., de Kerchove D'Exaerde, A., Cordero-Erausquin, M., Le Novère, N., del Mar Arroyo-Jimenez, M., and Changeux, J. P. (1999). Diversity and distribution of nicotinic acetylcholine receptors in the locus ceruleus neurons. *Proc. Natl. Acad. Sci. U. S. A.* 96, 12126–12131. doi:10.1073/pnas.96.21.12126.

Lestienne, R., Hervé-Minvielle, A., Robinson, D., Briois, L., and Sara, S. J. (1997). Slow oscillations as a probe of the dynamics of the locus coeruleus-frontal cortex interaction in anesthetized rats. *J. Physiol. Paris* 91, 273–284. doi:10.1016/s0928-4257(97)82407-2.

Li, L., Feng, X., Zhou, Z., Zhang, H., Shi, Q., Lei, Z., et al. (2018a). Stress Accelerates Defensive Responses to Looming in Mice and Involves a Locus Coeruleus-Superior Colliculus Projection. *Curr. Biol. CB* 28, 859-871.e5. doi:10.1016/j.cub.2018.02.005.

Li, Y., Hickey, L., Perrins, R., Werlen, E., Patel, A. A., Hirschberg, S., et al. (2016). Retrograde optogenetic characterization of the pontospinal module of the locus coeruleus with a canine adenoviral vector. *Brain Res.* 1641, 274–290. doi:10.1016/j.brainres.2016.02.023.

Li, Y., Jiao, Q., Du, X., Bi, M., Han, S., Jiao, L., et al. (2018b). Investigation of Behavioral Dysfunctions Induced by Monoamine Depletions in a Mouse Model of Parkinson's Disease. *Front. Cell. Neurosci.* 12, 241. doi:10.3389/fncel.2018.00241.

Li, Y., Wang, C., Wang, J., Zhou, Y., Ye, F., Zhang, Y., et al. (2019). Mild cognitive impairment in de novo Parkinson's disease: A neuromelanin MRI study in locus coeruleus. *Mov. Disord. Off. J. Mov. Disord. Soc.* 34, 884–892. doi:10.1002/mds.27682.

Lin, Y., Quartermain, D., Dunn, A. J., Weinshenker, D., and Stone, E. A. (2008). Possible dopaminergic stimulation of locus coeruleus alpha1-adrenoceptors

involved in behavioral activation. *Synap. N. Y. N* 62, 516–523. doi:10.1002/syn.20517.

Lindenbach, D., Conti, M. M., Ostock, C. Y., George, J. A., Goldenberg, A. A., Melikhov-Sosin, M., et al. (2016). The Role of Primary Motor Cortex (M1) Glutamate and GABA Signaling in l-DOPA-Induced Dyskinesia in Parkinsonian Rats. *J. Neurosci. Off. J. Soc. Neurosci.* 36, 9873–9887. doi:10.1523/JNEUROSCI.1318-16.2016.

Lisman, J. E., and Grace, A. A. (2005). The hippocampal-VTA loop: controlling the entry of information into long-term memory. *Neuron* 46, 703–713. doi:10.1016/j.neuron.2005.05.002.

Llamosas, N., Ugedo, L., and Torrecilla, M. (2017). Inactivation of GIRK channels weakens the pre- and postsynaptic inhibitory activity in dorsal raphe neurons. *Physiol. Rep.* 5. doi:10.14814/phy2.13141.

Llorca-Torralba, M., Borges, G., Neto, F., Mico, J. A., and Berrocoso, E. (2016). Noradrenergic Locus Coeruleus pathways in pain modulation. *Neuroscience* 338, 93–113. doi:10.1016/j.neuroscience.2016.05.057.

Llorca-Torralba, M., Mico, J. A., and Berrocoso, E. (2018). Behavioral effects of combined morphine and MK-801 administration to the locus coeruleus of a rat neuropathic pain model. *Prog. Neuropsychopharmacol. Biol. Psychiatry* 84, 257–266. doi:10.1016/j.pnpbp.2018.03.007.

Llorca-Torralba, M., Suarez-Pereira, I., Bravo, L., Camarena-Delgado, C., Garcia-Partida, J. A., Mico, J. A., et al. (2019). Chemogenetic Silencing of the Locus Coeruleus-Basolateral Amygdala Pathway Abolishes Pain-Induced Anxiety and Enhanced Aversive Learning in Rats. *Biol. Psychiatry* 85, 1021–1035. doi:10.1016/j.biopsych.2019.02.018.

Loiodice, S., Wing Young, H., Rion, B., Méot, B., Montagne, P., Denibaud, A.-S., et al. (2019). Implication of nigral dopaminergic lesion and repeated L-dopa exposure in neuropsychiatric symptoms of Parkinson's disease. *Behav. Brain Res.* 360, 120–127. doi:10.1016/j.bbr.2018.12.007.

Lu, Y., Simpson, K. L., Weaver, K. J., and Lin, R. C. S. (2012). Differential distribution patterns from medial prefrontal cortex and dorsal raphe to the locus coeruleus in rats. *Anat. Rec. Hoboken NJ 2007* 295, 1192–1201. doi:10.1002/ar.22505.

Luchtman, D. W., Shao, D., and Song, C. (2009). Behavior, neurotransmitters and inflammation in three regimens of the MPTP mouse model of Parkinson's disease. *Physiol. Behav.* 98, 130–138. doi:10.1016/j.physbeh.2009.04.021.

Lundblad, M., Usiello, A., Carta, M., Håkansson, K., Fisone, G., and Cenci, M. A. (2005). Pharmacological validation of a mouse model of l-DOPA-induced dyskinesia. *Exp. Neurol.* 194, 66–75. doi:10.1016/j.expneurol.2005.02.002.

Magill, P. J., Bolam, J. P., and Bevan, M. D. (2001). Dopamine regulates the impact of the cerebral cortex on the subthalamic nucleus-globus pallidus network. *Neuroscience* 106, 313–330.

Manohar, A., Curtis, A. L., Zderic, S. A., and Valentino, R. J. (2017). Brainstem network dynamics underlying the encoding of bladder information. *eLife* 6. doi:10.7554/eLife.29917.

Mansour, A., Fox, C. A., Burke, S., Meng, F., Thompson, R. C., Akil, H., et al. (1994). Mu, delta, and kappa opioid receptor mRNA expression in the rat CNS: an in situ hybridization study. *J. Comp. Neurol.* 350, 412–438. doi:10.1002/cne.903500307.

Marcus, J. N., Aschkenasi, C. J., Lee, C. E., Chemelli, R. M., Saper, C. B., Yanagisawa, M., et al. (2001). Differential expression of orexin receptors 1 and 2 in the rat brain. *J. Comp. Neurol.* 435, 6–25.

Marien, M., Briley, M., and Colpaert, F. (1993). Noradrenaline depletion exacerbates MPTP-induced striatal dopamine loss in mice. *Eur. J. Pharmacol.* 236, 487–489.

Martin, W. J., Gupta, N. K., Loo, C. M., Rohde, D. S., and Basbaum, A. I. (1999). Differential effects of neurotoxic destruction of descending noradrenergic pathways on acute and persistent nociceptive processing. *Pain* 80, 57–65. doi:10.1016/s0304-3959(98)00194-8.

Martin-Bastida, A., Pietracupa, S., and Piccini, P. (2017). Neuromelanin in parkinsonian disorders: an update. *Int. J. Neurosci.* 127, 1116–1123. doi:10.1080/00207454.2017.1325883.

Martínez-Fernández, R., Rodríguez-Rojas, R., Del Álamo, M., Hernández-Fernández, F., Pineda-Pardo, J. A., Dileone, M., et al. (2018). Focused ultrasound subthalamotomy in patients with asymmetric Parkinson's

disease: a pilot study. *Lancet Neurol.* 17, 54–63. doi:10.1016/S1474-4422(17)30403-9.

Martinez-Martin, P., Chaudhuri, K. R., Rojo-Abuin, J. M., Rodriguez-Blazquez, C., Alvarez-Sanchez, M., Arakaki, T., et al. (2015). Assessing the non-motor symptoms of Parkinson's disease: MDS-UPDRS and NMS Scale. *Eur. J. Neurol.* 22, 37–43. doi:10.1111/ene.12165.

Martinez-Martin, P., Rodriguez-Blazquez, C., Kurtis, M. M., Chaudhuri, K. R., and NMSS Validation Group (2011). The impact of non-motor symptoms on health-related quality of life of patients with Parkinson's disease. *Mov. Disord. Off. J. Mov. Disord. Soc.* 26, 399–406. doi:10.1002/mds.23462.

Marzo, A., Totah, N. K., Neves, R. M., Logothetis, N. K., and Eschenko, O. (2014). Unilateral electrical stimulation of rat locus coeruleus elicits bilateral response of norepinephrine neurons and sustained activation of medial prefrontal cortex. *J. Neurophysiol.* 111, 2570–2588. doi:10.1152/jn.00920.2013.

Masilamoni, G. J., Groover, O., and Smith, Y. (2017). Reduced noradrenergic innervation of ventral midbrain dopaminergic cell groups and the subthalamic nucleus in MPTP-treated parkinsonian monkeys. *Neurobiol. Dis.* 100, 9–18. doi:10.1016/j.nbd.2016.12.025.

Mason, S. T., and Fibiger, H. C. (1979). Regional topography within noradrenergic locus coeruleus as revealed by retrograde transport of horseradish peroxidase. *J. Comp. Neurol.* 187, 703–724. doi:10.1002/cne.901870405.

Matschke, L. A., Bertoune, M., Roeper, J., Snutch, T. P., Oertel, W. H., Rinné, S., et al. (2015). A concerted action of L- and T-type Ca(2+) channels regulates locus coeruleus pacemaking. *Mol. Cell. Neurosci.* 68, 293–302. doi:10.1016/j.mcn.2015.08.012.

Matschke, L. A., Rinné, S., Snutch, T. P., Oertel, W. H., Dolga, A. M., and Decher, N. (2018). Calcium-activated SK potassium channels are key modulators of the pacemaker frequency in locus coeruleus neurons. *Mol. Cell. Neurosci.* 88, 330–341. doi:10.1016/j.mcn.2018.03.002.

Maurice, N., Deniau, J. M., Glowinski, J., and Thierry, A. M. (1999). Relationships between the prefrontal cortex and the basal ganglia in the rat: physiology of the cortico-nigral circuits. *J. Neurosci. Off. J. Soc. Neurosci.* 19, 4674–4681.

Mavridis, M., Degryse, A. D., Lategan, A. J., Marien, M. R., and Colpaert, F. C. (1991). Effects of locus coeruleus lesions on parkinsonian signs, striatal dopamine and substantia nigra cell loss after 1-methyl-4-phenyl-1,2,3,6-tetrahydropyridine in monkeys: a possible role for the locus coeruleus in the progression of Parkinson's disease. *Neuroscience* 41, 507–523. doi:10.1016/0306-4522(91)90345-o.

McCall, J. G., Al-Hasani, R., Siuda, E. R., Hong, D. Y., Norris, A. J., Ford, C. P., et al. (2015). CRH Engagement of the Locus Coeruleus Noradrenergic System Mediates Stress-Induced Anxiety. *Neuron* 87, 605–620. doi:10.1016/j.neuron.2015.07.002.

McCall, J. G., Siuda, E. R., Bhatti, D. L., Lawson, L. A., McElligott, Z. A., Stuber, G. D., et al. (2017). Locus coeruleus to basolateral amygdala noradrenergic projections promote anxiety-like behavior. *eLife* 6. doi:10.7554/eLife.18247.

McMillan, P. J., White, S. S., Franklin, A., Greenup, J. L., Leverenz, J. B., Raskind, M. A., et al. (2011). Differential response of the central noradrenergic nervous system to the loss of locus coeruleus neurons in Parkinson's disease and Alzheimer's disease. *Brain Res.* 1373, 240–252. doi:10.1016/j.brainres.2010.12.015.

Medrano, M. C., Santamarta, M. T., Pablos, P., Aira, Z., Buesa, I., Azkue, J. J., et al. (2017). Characterization of functional mu opioid receptor turnover in rat locus coeruleus: an electrophysiological and immunocytochemical study. *Br. J. Pharmacol.* 174, 2758–2772. doi:10.1111/bph.13901.

Mejías-Aponte, C. A., Drouin, C., and Aston-Jones, G. (2009). Adrenergic and Noradrenergic Innervation of the Midbrain Ventral Tegmental Area and Retrorubral Field: Prominent Inputs from Medullary Homeostatic Centers. *J. Neurosci.* 29, 3613–3626. doi:10.1523/JNEUROSCI.4632-08.2009.

Metz, G. A., Tse, A., Ballermann, M., Smith, L. K., and Fouad, K. (2005). The unilateral 6-OHDA rat model of Parkinson's disease revisited: an electromyographic and behavioural analysis. *Eur. J. Neurosci.* 22, 735–744. doi:10.1111/j.1460-9568.2005.04238.x.

Micieli, G., Tosi, P., Marcheselli, S., and Cavallini, A. (2003). Autonomic dysfunction in Parkinson's disease. *Neurol. Sci. Off. J. Ital. Neurol. Soc. Ital. Soc. Clin. Neurophysiol.* 24 Suppl 1, S32-34. doi:10.1007/s100720300035.

Miguelez, C., Aristieta, A., Cenci, M. A., and Ugedo, L. (2011a). The locus coeruleus is directly implicated in L-DOPA-induced dyskinesia in parkinsonian rats: an electrophysiological and behavioural study. *PloS One* 6, e24679. doi:10.1371/journal.pone.0024679.

Miguelez, C., Fernandez-Aedo, I., Torrecilla, M., Grandoso, L., and Ugedo, L. (2009). alpha(2)-Adrenoceptors mediate the acute inhibitory effect of fluoxetine on locus coeruleus noradrenergic neurons. *Neuropharmacology* 56, 1068–1073. doi:10.1016/j.neuropharm.2009.03.004.

Miguelez, C., Grandoso, L., and Ugedo, L. (2011b). Locus coeruleus and dorsal raphe neuron activity and response to acute antidepressant administration in a rat model of Parkinson's disease. *Int. J. Neuropsychopharmacol.* 14, 187–200. doi:10.1017/S146114571000043X.

Miguelez, C., Morin, S., Martinez, A., Goillandeau, M., Bezard, E., Bioulac, B., et al. (2012). Altered pallido-pallidal synaptic transmission leads to aberrant firing of globus pallidus neurons in a rat model of Parkinson's disease. *J. Physiol.* 590, 5861–5875. doi:10.1113/jphysiol.2012.241331.

Miguelez, C., Navailles, S., De Deurwaerdère, P., and Ugedo, L. (2016a). The acute and long-term L-DOPA effects are independent from changes in the activity of dorsal raphe serotonergic neurons in 6-OHDA lesioned rats. *Br. J. Pharmacol.* 173, 2135–2146. doi:10.1111/bph.13447.

Miguelez, C., Navailles, S., Delaville, C., Marquis, L., Lagière, M., Benazzouz, A., et al. (2016b). L-DOPA elicits non-vesicular releases of serotonin and dopamine in hemiparkinsonian rats in vivo. *Eur. Neuropsychopharmacol. J. Eur. Coll. Neuropsychopharmacol.* 26, 1297–1309. doi:10.1016/j.euroneuro.2016.05.004.

Mishra, A., Singh, S., Tiwari, V., Parul, null, and Shukla, S. (2019). Dopamine D1 receptor activation improves adult hippocampal neurogenesis and exerts anxiolytic and antidepressant-like effect via activation of Wnt/β-catenin pathways in rat model of Parkinson's disease. *Neurochem. Int.* 122, 170–186. doi:10.1016/j.neuint.2018.11.020.

Monaca, C., Laloux, C., Jacquesson, J.-M., Gelé, P., Maréchal, X., Bordet, R., et al. (2004). Vigilance states in a parkinsonian model, the MPTP mouse. *Eur. J. Neurosci.* 20, 2474–2478. doi:10.1111/j.1460-9568.2004.03694.x.

Müftüoglu, M., Elibol, B., Dalmizrak, O., Ercan, A., Kulaksiz, G., Ogüs, H., et al. (2004). Mitochondrial complex I and IV activities in leukocytes from patients with parkin mutations. *Mov. Disord. Off. J. Mov. Disord. Soc.* 19, 544–548. doi:10.1002/mds.10695.

Mulvey, B., Bhatti, D. L., Gyawali, S., Lake, A. M., Kriaucionis, S., Ford, C. P., et al. (2018). Molecular and Functional Sex Differences of Noradrenergic Neurons in the Mouse Locus Coeruleus. *Cell Rep.* 23, 2225–2235. doi:10.1016/j.celrep.2018.04.054.

Munhoz, R. P., Picillo, M., Fox, S. H., Bruno, V., Panisset, M., Honey, C. R., et al. (2016). Eligibility Criteria for Deep Brain Stimulation in Parkinson's Disease, Tremor, and Dystonia. *Can. J. Neurol. Sci. J. Can. Sci. Neurol.* 43, 462–471. doi:10.1017/cjn.2016.35.

Murai, Y., and Akaike, T. (2005). Orexins cause depolarization via nonselective cationic and K+ channels in isolated locus coeruleus neurons. *Neurosci. Res.* 51, 55–65. doi:10.1016/j.neures.2004.09.005.

Murphy, P. R., O'Connell, R. G., O'Sullivan, M., Robertson, I. H., and Balsters, J. H. (2014). Pupil diameter covaries with BOLD activity in human locus coeruleus. *Hum. Brain Mapp.* 35, 4140–4154. doi:10.1002/hbm.22466.

Murueta-Goyena, A., Del Pino, R., Reyero, P., Galdós, M., Arana, B., Lucas-Jiménez, O., et al. (2019). Parafoveal thinning of inner retina is associated with visual dysfunction in Lewy body diseases. *Mov. Disord. Off. J. Mov. Disord. Soc.* 34, 1315–1324. doi:10.1002/mds.27728.

Nambu, A., Tokuno, H., and Takada, M. (2002). Functional significance of the cortico-subthalamo-pallidal "hyperdirect" pathway. *Neurosci. Res.* 43, 111–117. doi:10.1016/s0168-0102(02)00027-5.

Nayyar, T., Bubser, M., Ferguson, M. C., Neely, M. D., Goodwin, J. S., Montine, T. J., et al. (2009). Cortical serotonin and norepinephrine denervation in parkinsonism: preferential loss of the beaded serotonin innervation. *Eur. J. Neurosci.* 30, 207–216. doi:10.1111/j.1460-9568.2009.06806.x.

Nebe, A., and Ebersbach, G. (2009). Pain intensity on and off levodopa in patients with Parkinson's disease. *Mov. Disord. Off. J. Mov. Disord. Soc.* 24, 1233–1237. doi:10.1002/mds.22546.

Neves, R. M., van Keulen, S., Yang, M., Logothetis, N. K., and Eschenko, O. (2018). Locus coeruleus phasic discharge is essential for stimulus-induced gamma oscillations in the prefrontal cortex. *J. Neurophysiol.* 119, 904–920. doi:10.1152/jn.00552.2017.

Newman, L. A., Darling, J., and McGaughy, J. (2008). Atomoxetine reverses attentional deficits produced by noradrenergic deafferentation of medial prefrontal cortex. *Psychopharmacology (Berl.)* 200, 39–50. doi:10.1007/s00213-008-1097-8.

Nitz, D., and Siegel, J. M. (1997). GABA release in the locus coeruleus as a function of sleep/wake state. *Neuroscience* 78, 795–801. doi:10.1016/s0306-4522(96)00549-0.

Njung'e, K., and Handley, S. L. (1991). Evaluation of marble-burying behavior as a model of anxiety. *Pharmacol. Biochem. Behav.* 38, 63–67. doi:10.1016/0091-3057(91)90590-x.

O'Connor, D. T., Cervenka, J. H., Stone, R. A., Levine, G. L., Parmer, R. J., Franco-Bourland, R. E., et al. (1994). Dopamine beta-hydroxylase immunoreactivity in human cerebrospinal fluid: properties, relationship to central noradrenergic neuronal activity and variation in Parkinson's disease and congenital dopamine beta-hydroxylase deficiency. *Clin. Sci. Lond. Engl. 1979* 86, 149–158. doi:10.1042/cs0860149.

O'Connor, K. A., Feustel, P. J., Ramirez-Zamora, A., Molho, E., Pilitsis, J. G., and Shin, D. S. (2016). Investigation of diazepam efficacy on anxiety-like behavior in hemiparkinsonian rats. *Behav. Brain Res.* 301, 226–237. doi:10.1016/j.bbr.2015.12.045.

Oertel, W. H., Henrich, M. T., Janzen, A., and Geibl, F. F. (2019). The locus coeruleus: Another vulnerability target in Parkinson's disease. *Mov. Disord. Off. J. Mov. Disord. Soc.* doi:10.1002/mds.27785.

Ohi, Y., Kodama, D., and Haji, A. (2017). L-DOPA inhibits excitatory synaptic transmission in the rat nucleus tractus solitarius through release of dopamine. *Neuroscience* 360, 18–27. doi:10.1016/j.neuroscience.2017.07.043.

Ohtsuka, C., Sasaki, M., Konno, K., Koide, M., Kato, K., Takahashi, J., et al. (2013). Changes in substantia nigra and locus coeruleus in patients with early-stage

Parkinson's disease using neuromelanin-sensitive MR imaging. *Neurosci. Lett.* 541, 93–98. doi:10.1016/j.neulet.2013.02.012.

Okada, A., Nakamura, T., Suzuki, J., Suzuki, M., Hirayama, M., Katsuno, M., et al. (2016). Impaired Pain Processing Correlates with Cognitive Impairment in Parkinson's Disease. *Intern. Med. Tokyo Jpn.* 55, 3113–3118. doi:10.2169/internalmedicine.55.7067.

Olanow, C. W., Kieburtz, K., Odin, P., Espay, A. J., Standaert, D. G., Fernandez, H. H., et al. (2014). Continuous intrajejunal infusion of levodopa-carbidopa intestinal gel for patients with advanced Parkinson's disease: a randomised, controlled, double-blind, double-dummy study. *Lancet Neurol.* 13, 141–149. doi:10.1016/S1474-4422(13)70293-X.

Olanow, C. W., Stern, M. B., and Sethi, K. (2009). The scientific and clinical basis for the treatment of Parkinson disease (2009). *Neurology* 72, S1-136. doi:10.1212/WNL.0b013e3181a1d44c.

Oliveira, L. M., Tuppy, M., Moreira, T. S., and Takakura, A. C. (2017). Role of the locus coeruleus catecholaminergic neurons in the chemosensory control of breathing in a Parkinson's disease model. *Exp. Neurol.* 293, 172–180. doi:10.1016/j.expneurol.2017.04.006.

Ortega, J. E., Mendiguren, A., Pineda, J., and Meana, J. J. (2012). Regulation of central noradrenergic activity by 5-HT(3) receptors located in the locus coeruleus of the rat. *Neuropharmacology* 62, 2472–2479. doi:10.1016/j.neuropharm.2012.02.018.

Osborne, P. B., Vidovic, M., Chieng, B., Hill, C. E., and Christie, M. J. (2002). Expression of mRNA and functional alpha(1)-adrenoceptors that suppress the GIRK conductance in adult rat locus coeruleus neurons. *Br. J. Pharmacol.* 135, 226–232. doi:10.1038/sj.bjp.0704453.

Osmanović, S. S., and Shefner, S. A. (1993). Calcium-activated hyperpolarizations in rat locus coeruleus neurons in vitro. *J. Physiol.* 469, 89–109. doi:10.1113/jphysiol.1993.sp019806.

Osmanović, S. S., Shefner, S. A., and Brodie, M. S. (1990). Functional significance of the apamin-sensitive conductance in rat locus coeruleus neurons. *Brain Res.* 530, 283–289. doi:10.1016/0006-8993(90)91296-s.

Ostock, C. Y., Bhide, N., Goldenberg, A. A., George, J. A., and Bishop, C. (2018). Striatal norepinephrine efflux in l-DOPA-induced dyskinesia. *Neurochem. Int.* 114, 85–98. doi:10.1016/j.neuint.2018.01.010.

Ostock, C. Y., Hallmark, J., Palumbo, N., Bhide, N., Conti, M., George, J. A., et al. (2015). Modulation of L-DOPA's antiparkinsonian and dyskinetic effects by α2-noradrenergic receptors within the locus coeruleus. *Neuropharmacology* 95, 215–225. doi:10.1016/j.neuropharm.2015.03.008.

Ostock, C. Y., Lindenbach, D., Goldenberg, A. A., Kampton, E., and Bishop, C. (2014). Effects of noradrenergic denervation by anti-DBH-saporin on behavioral responsivity to L-DOPA in the hemi-parkinsonian rat. *Behav. Brain Res.* 270, 75–85. doi:10.1016/j.bbr.2014.05.009.

Packard, M. G., and Knowlton, B. J. (2002). Learning and memory functions of the Basal Ganglia. *Annu. Rev. Neurosci.* 25, 563–593. doi:10.1146/annurev.neuro.25.112701.142937.

Palma, J.-A., and Kaufmann, H. (2018). Treatment of autonomic dysfunction in Parkinson disease and other synucleinopathies. *Mov. Disord. Off. J. Mov. Disord. Soc.* 33, 372–390. doi:10.1002/mds.27344.

Park, A., and Stacy, M. (2009). Non-motor symptoms in Parkinson's disease. *J. Neurol.* 256 Suppl 3, 293–298. doi:10.1007/s00415-009-5240-1.

Parker, K. L., Chen, K.-H., Kingyon, J. R., Cavanagh, J. F., and Narayanan, N. S. (2015). Medial frontal ~4-Hz activity in humans and rodents is attenuated in PD patients and in rodents with cortical dopamine depletion. *J. Neurophysiol.* 114, 1310–1320. doi:10.1152/jn.00412.2015.

Parker, R. M., Barnes, J. M., Ge, J., Barber, P. C., and Barnes, N. M. (1996). Autoradiographic distribution of [3H]-(S)-zacopride-labelled 5-HT3 receptors in human brain. *J. Neurol. Sci.* 144, 119–127. doi:10.1016/s0022-510x(96)00211-0.

Parker, W. D., Parks, J. K., and Swerdlow, R. H. (2008). Complex I deficiency in Parkinson's disease frontal cortex. *Brain Res.* 1189, 215–218. doi:10.1016/j.brainres.2007.10.061.

Parr-Brownlie, L. C., Poloskey, S. L., Flanagan, K. K., Eisenhofer, G., Bergstrom, D. A., and Walters, J. R. (2007). Dopamine lesion-induced changes in

subthalamic nucleus activity are not associated with alterations in firing rate or pattern in layer V neurons of the anterior cingulate cortex in anesthetized rats. *Eur. J. Neurosci.* 26, 1925–1939. doi:10.1111/j.1460-9568.2007.05814.x.

Patt, S., and Gerhard, L. (1993). A Golgi study of human locus coeruleus in normal brains and in Parkinson's disease. *Neuropathol. Appl. Neurobiol.* 19, 519–523.

Pavese, N., Rivero-Bosch, M., Lewis, S. J., Whone, A. L., and Brooks, D. J. (2011). Progression of monoaminergic dysfunction in Parkinson's disease: a longitudinal 18F-dopa PET study. *NeuroImage* 56, 1463–1468. doi:10.1016/j.neuroimage.2011.03.012.

Paxinos and Watson (1997). The rat brain in stereotaxic coordinates (6th Edition). Available at: https://scholar.google.com/scholar_lookup?title=The%20Rat%20Brain%20in%20Stereotaxic%20Coordinates&publication_year=2007&author=G.%20Paxinos&author=C.%20Watson [Accessed February 18, 2020].

Pérez, V., Marin, C., Rubio, A., Aguilar, E., Barbanoj, M., and Kulisevsky, J. (2009). Effect of the additional noradrenergic neurodegeneration to 6-OHDA-lesioned rats in levodopa-induced dyskinesias and in cognitive disturbances. *J. Neural Transm. Vienna Austria 1996* 116, 1257–1266. doi:10.1007/s00702-009-0291-0.

Pifl, C., Kish, S. J., and Hornykiewicz, O. (2012). Thalamic noradrenaline in Parkinson's disease: deficits suggest role in motor and non-motor symptoms. *Mov. Disord. Off. J. Mov. Disord. Soc.* 27, 1618–1624. doi:10.1002/mds.25109.

Pifl, Ch., Schingnitz, G., and Hornykiewicz, O. (1991). Effect of 1-methyl-4-phenyl-1,2,3,6-tetrahydropyridine on the regional distribution of brain monoamines in the rhesus monkey. *Neuroscience* 44, 591–605. doi:10.1016/0306-4522(91)90080-8.

Pineda, R. H., Knoeckel, C. S., Taylor, A. D., Estrada-Bernal, A., and Ribera, A. B. (2008). Kv1 potassium channel complexes in vivo require Kvbeta2 subunits in dorsal spinal neurons. *J. Neurophysiol.* 100, 2125–2136. doi:10.1152/jn.90667.2008.

Poewe, W., Seppi, K., Tanner, C. M., Halliday, G. M., Brundin, P., Volkmann, J., et al. (2017). Parkinson disease. *Nat. Rev. Dis. Primer* 3, 17013. doi:10.1038/nrdp.2017.13.

Postuma, R. B., Berg, D., Stern, M., Poewe, W., Olanow, C. W., Oertel, W., et al. (2015). MDS clinical diagnostic criteria for Parkinson's disease. *Mov. Disord. Off. J. Mov. Disord. Soc.* 30, 1591–1601. doi:10.1002/mds.26424.

Priebe, J. A., Kunz, M., Morcinek, C., Rieckmann, P., and Lautenbacher, S. (2016). Electrophysiological assessment of nociception in patients with Parkinson's disease: A multi-methods approach. *J. Neurol. Sci.* 368, 59–69. doi:10.1016/j.jns.2016.06.058.

Prinz, A., Selesnew, L.-M., Liss, B., Roeper, J., and Carlsson, T. (2013). Increased excitability in serotonin neurons in the dorsal raphe nucleus in the 6-OHDA mouse model of Parkinson's disease. *Exp. Neurol.* 248, 236–245. doi:10.1016/j.expneurol.2013.06.015.

Proudfit, H. K. (2002). The challenge of defining brainstem pain modulation circuits. *J. Pain Off. J. Am. Pain Soc.* 3, 350–354; discussion 358-359. doi:10.1054/jpai.2002.127777.

Pudovkina, O. L., Kawahara, Y., de Vries, J., and Westerink, B. H. (2001). The release of noradrenaline in the locus coeruleus and prefrontal cortex studied with dual-probe microdialysis. *Brain Res.* 906, 38–45. doi:10.1016/s0006-8993(01)02553-7.

Pudovkina, O. L., and Westerink, B. H. C. (2005). Functional role of alpha1-adrenoceptors in the locus coeruleus: a microdialysis study. *Brain Res.* 1061, 50–56. doi:10.1016/j.brainres.2005.08.049.

Pusswald, G., Wiesbauer, P., Pirker, W., Novak, K., Foki, T., and Lehrner, J. (2019). Depression, quality of life, activities of daily living, and subjective memory after deep brain stimulation in Parkinson disease-A reliable change index analysis. *Int. J. Geriatr. Psychiatry* 34, 1698–1705. doi:10.1002/gps.5184.

Rascol, O., Zesiewicz, T., Chaudhuri, K. R., Asgharnejad, M., Surmann, E., Dohin, E., et al. (2016). A Randomized Controlled Exploratory Pilot Study to Evaluate the Effect of Rotigotine Transdermal Patch on Parkinson's Disease-Associated Chronic Pain. *J. Clin. Pharmacol.* 56, 852–861. doi:10.1002/jcph.678.

Rektorova, I., Balaz, M., Svatova, J., Zarubova, K., Honig, I., Dostal, V., et al. (2008). Effects of ropinirole on nonmotor symptoms of Parkinson disease: a prospective multicenter study. *Clin. Neuropharmacol.* 31, 261–266. doi:10.1097/WNF.0b013e31815d25ce.

Remy, P., Doder, M., Lees, A., Turjanski, N., and Brooks, D. (2005). Depression in Parkinson's disease: loss of dopamine and noradrenaline innervation in the limbic system. *Brain J. Neurol.* 128, 1314–1322. doi:10.1093/brain/awh445.

Rentsch, P., Stayte, S., Morris, G. P., and Vissel, B. (2019). Time dependent degeneration of the nigrostriatal tract in mice with 6-OHDA lesioned medial forebrain bundle and the effect of activin A on L-Dopa induced dyskinesia. *BMC Neurosci.* 20, 5. doi:10.1186/s12868-019-0487-7.

Research, C. for D. E. and (2019). Drug Trials Snapshots: NOURIANZ. *FDA*. Available at: http://www.fda.gov/drugs/drug-trials-snapshots-nourianz [Accessed December 9, 2019].

Reyes, B. a. S., Chavkin, C., and van Bockstaele, E. J. (2009). Subcellular targeting of kappa-opioid receptors in the rat nucleus locus coeruleus. *J. Comp. Neurol.* 512, 419–431. doi:10.1002/cne.21880.

Reyes, B. A. S., Glaser, J. D., and Van Bockstaele, E. J. (2007). Ultrastructural evidence for co-localization of corticotropin-releasing factor receptor and mu-opioid receptor in the rat nucleus locus coeruleus. *Neurosci. Lett.* 413, 216–221. doi:10.1016/j.neulet.2006.11.069.

Rohampour, K., Azizi, H., Fathollahi, Y., and Semnanian, S. (2017). Peripheral nerve injury potentiates excitatory synaptic transmission in locus coeruleus neurons. *Brain Res. Bull.* 130, 112–117. doi:10.1016/j.brainresbull.2017.01.012.

Romero-Sánchez, H. A., Mendieta, L., Austrich-Olivares, A. M., Garza-Mouriño, G., Benitez-Diaz Mirón, M., Coen, A., et al. (2019). Unilateral lesion of the nigroestriatal pathway with 6-OHDA induced allodynia and hyperalgesia reverted by pramipexol in rats. *Eur. J. Pharmacol.*, 172814. doi:10.1016/j.ejphar.2019.172814.

Rommelfanger, K. S., and Weinshenker, D. (2007). Norepinephrine: The redheaded stepchild of Parkinson's disease. *Biochem. Pharmacol.* 74, 177–190. doi:10.1016/j.bcp.2007.01.036.

Rommelfanger, K. S., Weinshenker, D., and Miller, G. W. (2004). Reduced MPTP toxicity in noradrenaline transporter knockout mice. *J. Neurochem.* 91, 1116–1124. doi:10.1111/j.1471-4159.2004.02785.x.

Rudow, G., O'Brien, R., Savonenko, A. V., Resnick, S. M., Zonderman, A. B., Pletnikova, O., et al. (2008). Morphometry of the human substantia nigra in ageing and Parkinson's disease. *Acta Neuropathol. (Berl.)* 115, 461–470. doi:10.1007/s00401-008-0352-8.

Ruiz-Ortega, J. A., and Ugedo, L. (1997). The stimulatory effect of clonidine on locus coeruleus neurons of rats with inactivated alpha 2-adrenoceptors: involvement of imidazoline receptors located in the nucleus paragigantocellularis. *Naunyn. Schmiedebergs Arch. Pharmacol.* 355, 288–294. doi:10.1007/pl00004945.

Ryan, M., Eatmon, C. V., and Slevin, J. T. (2019). Drug treatment strategies for depression in Parkinson disease. *Expert Opin. Pharmacother.* 20, 1351–1363. doi:10.1080/14656566.2019.1612877.

Sadeghi, M., Tzschentke, T. M., and Christie, M. J. (2015). μ-Opioid receptor activation and noradrenaline transport inhibition by tapentadol in rat single locus coeruleus neurons. *Br. J. Pharmacol.* 172, 460–468. doi:10.1111/bph.12566.

Sanchez-Padilla, J., Guzman, J. N., Ilijic, E., Kondapalli, J., Galtieri, D. J., Yang, B., et al. (2014). Mitochondrial oxidant stress in locus coeruleus is regulated by activity and nitric oxide synthase. *Nat. Neurosci.* 17, 832–840. doi:10.1038/nn.3717.

Santiago, R. M., Barbieiro, J., Lima, M. M. S., Dombrowski, P. A., Andreatini, R., and Vital, M. A. B. F. (2010). Depressive-like behaviors alterations induced by intranigral MPTP, 6-OHDA, LPS and rotenone models of Parkinson's disease are predominantly associated with serotonin and dopamine. *Prog. Neuropsychopharmacol. Biol. Psychiatry* 34, 1104–1114. doi:10.1016/j.pnpbp.2010.06.004.

Santin, J. M., Watters, K. C., Putnam, R. W., and Hartzler, L. K. (2013). Temperature influences neuronal activity and CO2/pH sensitivity of locus coeruleus neurons in the bullfrog, Lithobates catesbeianus. *Am. J. Physiol. Regul. Integr. Comp. Physiol.* 305, R1451-1464. doi:10.1152/ajpregu.00348.2013.

Sasaki, M., Shibata, E., Tohyama, K., Takahashi, J., Otsuka, K., Tsuchiya, K., et al. (2006). Neuromelanin magnetic resonance imaging of locus ceruleus and substantia nigra in Parkinson's disease. *Neuroreport* 17, 1215–1218. doi:10.1097/01.wnr.0000227984.84927.a7.

Sauerbier, A., Cova, I., Rosa-Grilo, M., Taddei, R. N., Mischley, L. K., and Chaudhuri, K. R. (2017). Treatment of Nonmotor Symptoms in Parkinson's Disease. *Int. Rev. Neurobiol.* 132, 361–379. doi:10.1016/bs.irn.2017.03.002.

Scavone, J. L., Mackie, K., and Van Bockstaele, E. J. (2010). Characterization of cannabinoid-1 receptors in the locus coeruleus: relationship with mu-opioid receptors. *Brain Res.* 1312, 18–31. doi:10.1016/j.brainres.2009.11.023.

Schapira, A. H., Cooper, J. M., Dexter, D., Clark, J. B., Jenner, P., and Marsden, C. D. (1990). Mitochondrial complex I deficiency in Parkinson's disease. *J. Neurochem.* 54, 823–827. doi:10.1111/j.1471-4159.1990.tb02325.x.

Schapira, A. H. V. (2008). Mitochondria in the aetiology and pathogenesis of Parkinson's disease. *Lancet Neurol.* 7, 97–109. doi:10.1016/S1474-4422(07)70327-7.

Schapira, A. H. V., Chaudhuri, K. R., and Jenner, P. (2017). Non-motor features of Parkinson disease. *Nat. Rev. Neurosci.* 18, 435–450. doi:10.1038/nrn.2017.62.

Schestatsky, P., Kumru, H., Valls-Solé, J., Valldeoriola, F., Marti, M. J., Tolosa, E., et al. (2007). Neurophysiologic study of central pain in patients with Parkinson disease. *Neurology* 69, 2162–2169. doi:10.1212/01.wnl.0000295669.12443.d3.

Schintu, N., Zhang, X., Alvarsson, A., Marongiu, R., Kaplitt, M. G., Greengard, P., et al. (2016). p11 modulates L-DOPA therapeutic effects and dyskinesia via distinct cell types in experimental Parkinsonism. *Proc. Natl. Acad. Sci. U. S. A.* 113, 1429–1434. doi:10.1073/pnas.1524303113.

Schrag, A., and Taddei, R. N. (2017). Depression and Anxiety in Parkinson's Disease. *Int. Rev. Neurobiol.* 133, 623–655. doi:10.1016/bs.irn.2017.05.024.

Schwarting, R. K., and Huston, J. P. (1996). The unilateral 6-hydroxydopamine lesion model in behavioral brain research. Analysis of functional deficits,

recovery and treatments. *Prog. Neurobiol.* 50, 275–331. doi:10.1016/s0301-0082(96)00040-8.

Schwarz, L. A., Miyamichi, K., Gao, X. J., Beier, K. T., Weissbourd, B., DeLoach, K. E., et al. (2015). Viral-genetic tracing of the input-output organization of a central noradrenaline circuit. *Nature* 524, 88–92. doi:10.1038/nature14600.

Schwarz, S. T., Xing, Y., Tomar, P., Bajaj, N., and Auer, D. P. (2017). In Vivo Assessment of Brainstem Depigmentation in Parkinson Disease: Potential as a Severity Marker for Multicenter Studies. *Radiology* 283, 789–798. doi:10.1148/radiol.2016160662.

Senard, J. M., Valet, P., Durrieu, G., Berlan, M., Tran, M. A., Montastruc, J. L., et al. (1990). Adrenergic supersensitivity in parkinsonians with orthostatic hypotension. *Eur. J. Clin. Invest.* 20, 613–619. doi:10.1111/j.1365-2362.1990.tb01909.x.

Seo, Y.-J., Kwon, M.-S., Choi, H.-W., Jang, J.-E., Lee, J.-K., Jung, J.-S., et al. (2008). The differential effect of morphine and beta-endorphin administered intracerebroventricularly on pERK and pCaMK-II expression induced by various nociceptive stimuli in mice brains. *Neuropeptides* 42, 319–330. doi:10.1016/j.npep.2008.01.003.

Shannak, K., Rajput, A., Rozdilsky, B., Kish, S., Gilbert, J., and Hornykiewicz, O. (1994). Noradrenaline, dopamine and serotonin levels and metabolism in the human hypothalamus: observations in Parkinson's disease and normal subjects. *Brain Res.* 639, 33–41. doi:10.1016/0006-8993(94)91761-2.

Shelkar, G. P., Kumar, S., Singru, P. S., Subhedar, N. K., and Kokare, D. M. (2017). Noradrenergic inputs from locus coeruleus to posterior ventral tegmental area are essential to support ethanol reinforcement. *Addict. Biol.* 22, 291–302. doi:10.1111/adb.12321.

Shiekhattar, R., and Aston-Jones, G. (1993). Sensory responsiveness of brain noradrenergic neurons is modulated by endogenous brain serotonin. *Brain Res.* 623, 72–76. doi:10.1016/0006-8993(93)90011-b.

Shin, E., Rogers, J. T., Devoto, P., Björklund, A., and Carta, M. (2014). Noradrenaline neuron degeneration contributes to motor impairments and development of L-DOPA-induced dyskinesia in a rat model of Parkinson's disease. *Exp. Neurol.* 257, 25–38. doi:10.1016/j.expneurol.2014.04.011.

Shipley, M. T., Halloran, F. J., and de la Torre, J. (1985). Surprisingly rich projection from locus coeruleus to the olfactory bulb in the rat. *Brain Res.* 329, 294–299. doi:10.1016/0006-8993(85)90537-2.

Simson, P. E., and Weiss, J. M. (1988). Altered activity of the locus coeruleus in an animal model of depression. *Neuropsychopharmacol. Off. Publ. Am. Coll. Neuropsychopharmacol.* 1, 287–295.

Sinkkonen, S. T., Hanna, M. C., Kirkness, E. F., and Korpi, E. R. (2000). GABA(A) receptor epsilon and theta subunits display unusual structural variation between species and are enriched in the rat locus ceruleus. *J. Neurosci. Off. J. Soc. Neurosci.* 20, 3588–3595.

Slaets, S., Van Acker, F., Versijpt, J., Hauth, L., Goeman, J., Martin, J.-J., et al. (2015). Diagnostic value of MIBG cardiac scintigraphy for differential dementia diagnosis. *Int. J. Geriatr. Psychiatry* 30, 864–869. doi:10.1002/gps.4229.

Smith, C. C., and Greene, R. W. (2012). CNS dopamine transmission mediated by noradrenergic innervation. *J. Neurosci. Off. J. Soc. Neurosci.* 32, 6072–6080. doi:10.1523/JNEUROSCI.6486-11.2012.

Snyder, K., Wang, W.-W., Han, R., McFadden, K., and Valentino, R. J. (2012). Corticotropin-releasing factor in the norepinephrine nucleus, locus coeruleus, facilitates behavioral flexibility. *Neuropsychopharmacol. Off. Publ. Am. Coll. Neuropsychopharmacol.* 37, 520–530. doi:10.1038/npp.2011.218.

Sommerauer, M., Fedorova, T. D., Hansen, A. K., Knudsen, K., Otto, M., Jeppesen, J., et al. (2018a). Evaluation of the noradrenergic system in Parkinson's disease: an 11C-MeNER PET and neuromelanin MRI study. *Brain J. Neurol.* 141, 496–504. doi:10.1093/brain/awx348.

Sommerauer, M., Hansen, A. K., Parbo, P., Fedorova, T. D., Knudsen, K., Frederiksen, Y., et al. (2018b). Decreased noradrenaline transporter density in the motor cortex of Parkinson's disease patients. *Mov. Disord. Off. J. Mov. Disord. Soc.* 33, 1006–1010. doi:10.1002/mds.27411.

Somogyi, J., and Llewellyn-Smith, I. J. (2001). Patterns of colocalization of GABA, glutamate and glycine immunoreactivities in terminals that synapse on dendrites of noradrenergic neurons in rat locus coeruleus. *Eur. J. Neurosci.* 14, 219–228. doi:10.1046/j.0953-816x.2001.01638.x.

Sotiriou, E., Vassilatis, D. K., Vila, M., and Stefanis, L. (2010). Selective noradrenergic vulnerability in alpha-synuclein transgenic mice. *Neurobiol. Aging* 31, 2103–2114. doi:10.1016/j.neurobiolaging.2008.11.010.

Srinivasan, J., and Schmidt, W. J. (2003). Potentiation of parkinsonian symptoms by depletion of locus coeruleus noradrenaline in 6-hydroxydopamine-induced partial degeneration of substantia nigra in rats. *Eur. J. Neurosci.* 17, 2586–2592. doi:10.1046/j.1460-9568.2003.02684.x.

Srinivasan, J., and Schmidt, W. J. (2004). Behavioral and neurochemical effects of noradrenergic depletions with N-(2-chloroethyl)-N-ethyl-2-bromobenzylamine in 6-hydroxydopamine-induced rat model of Parkinson's disease. *Behav. Brain Res.* 151, 191–199. doi:10.1016/j.bbr.2003.08.016.

Stacy, M. (2002). Sleep disorders in Parkinson's disease: epidemiology and management. *Drugs Aging* 19, 733–739. doi:10.2165/00002512-200219100-00002.

Stark, A. J., Smith, C. T., Petersen, K. J., Trujillo, P., van Wouwe, N. C., Donahue, M. J., et al. (2018). [18F]fallypride characterization of striatal and extrastriatal D2/3 receptors in Parkinson's disease. *NeuroImage Clin.* 18, 433–442. doi:10.1016/j.nicl.2018.02.010.

Sun, W., Sugiyama, K., Asakawa, T., Yamaguchi, H., Akamine, S., Ouchi, Y., et al. (2011). Dynamic changes of striatal dopamine D2 receptor binding at later stages after unilateral lesions of the medial forebrain bundle in Parkinsonian rat models. *Neurosci. Lett.* 496, 157–162. doi:10.1016/j.neulet.2011.04.006.

Sun, Y.-N., Yao, L., Li, L.-B., Wang, Y., Du, C.-X., Guo, Y., et al. (2018). Activation and blockade of basolateral amygdala 5-HT6 receptor produce anxiolytic-like behaviors in an experimental model of Parkinson's disease. *Neuropharmacology* 137, 275–285. doi:10.1016/j.neuropharm.2018.05.016.

Svenningsson, P., Westman, E., Ballard, C., and Aarsland, D. (2012). Cognitive impairment in patients with Parkinson's disease: diagnosis, biomarkers, and treatment. *Lancet Neurol.* 11, 697–707. doi:10.1016/S1474-4422(12)70152-7.

Swanson, L. W. (1976). The locus coeruleus: a cytoarchitectonic, Golgi and immunohistochemical study in the albino rat. *Brain Res.* 110, 39–56. doi:10.1016/0006-8993(76)90207-9.

Szot, P., Franklin, A., Miguelez, C., Wang, Y., Vidaurrazaga, I., Ugedo, L., et al. (2016). Depressive-like behavior observed with a minimal loss of locus coeruleus (LC) neurons following administration of 6-hydroxydopamine is associated with electrophysiological changes and reversed with precursors of norepinephrine. *Neuropharmacology* 101, 76–86. doi:10.1016/j.neuropharm.2015.09.003.

Szot, P., Knight, L., Franklin, A., Sikkema, C., Foster, S., Wilkinson, C. W., et al. (2012). Lesioning noradrenergic neurons of the locus coeruleus in C57Bl/6 mice with unilateral 6-hydroxydopamine injection, to assess molecular, electrophysiological and biochemical changes in noradrenergic signaling. *Neuroscience* 216, 143–157. doi:10.1016/j.neuroscience.2012.04.046.

Tadaiesky, M. T., Dombrowski, P. A., Figueiredo, C. P., Cargnin-Ferreira, E., Da Cunha, C., and Takahashi, R. N. (2008). Emotional, cognitive and neurochemical alterations in a premotor stage model of Parkinson's disease. *Neuroscience* 156, 830–840. doi:10.1016/j.neuroscience.2008.08.035.

Takatsu, H., Nishida, H., Matsuo, H., Watanabe, S., Nagashima, K., Wada, H., et al. (2000). Cardiac sympathetic denervation from the early stage of Parkinson's disease: clinical and experimental studies with radiolabeled MIBG. *J. Nucl. Med. Off. Publ. Soc. Nucl. Med.* 41, 71–77.

Takeda, R., Ikeda, T., Tsuda, F., Abe, H., Hashiguchi, H., Ishida, Y., et al. (2005). Unilateral lesions of mesostriatal dopaminergic pathway alters the withdrawal response of the rat hindpaw to mechanical stimulation. *Neurosci. Res.* 52, 31–36. doi:10.1016/j.neures.2005.01.005.

Takeda, R., Ishida, Y., Ebihara, K., Abe, H., Matsuo, H., Ikeda, T., et al. (2014). Intrastriatal grafts of fetal ventral mesencephalon improve allodynia-like withdrawal response to mechanical stimulation in a rat model of Parkinson's disease. *Neurosci. Lett.* 573, 19–23. doi:10.1016/j.neulet.2014.05.007.

Takeuchi, T., Duszkiewicz, A. J., Sonneborn, A., Spooner, P. A., Yamasaki, M., Watanabe, M., et al. (2016). Locus coeruleus and dopaminergic consolidation of everyday memory. *Nature* 537, 357–362. doi:10.1038/nature19325.

Tassorelli, C., Armentero, M.-T., Greco, R., Fancellu, R., Sandrini, G., Nappi, G., et al. (2007). Behavioral responses and Fos activation following painful stimuli in a rodent model of Parkinson's disease. *Brain Res.* 1176, 53–61. doi:10.1016/j.brainres.2007.08.012.

Tétreault, P., Dansereau, M.-A., Doré-Savard, L., Beaudet, N., and Sarret, P. (2011). Weight bearing evaluation in inflammatory, neuropathic and cancer chronic pain in freely moving rats. *Physiol. Behav.* 104, 495–502. doi:10.1016/j.physbeh.2011.05.015.

Thiruchelvam, M., Brockel, B. J., Richfield, E. K., Baggs, R. B., and Cory-Slechta, D. A. (2000). Potentiated and preferential effects of combined paraquat and maneb on nigrostriatal dopamine systems: environmental risk factors for Parkinson's disease? *Brain Res.* 873, 225–234. doi:10.1016/s0006-8993(00)02496-3.

Timmerman, W., Cisci, G., Nap, A., de Vries, J. B., and Westerink, B. H. (1999). Effects of handling on extracellular levels of glutamate and other amino acids in various areas of the brain measured by microdialysis. *Brain Res.* 833, 150–160. doi:10.1016/s0006-8993(99)01538-3.

Timmermann, L., Oehlwein, C., Ransmayr, G., Fröhlich, H., Will, E., Schroeder, H., et al. (2017). Patients' perception of Parkinson's disease-associated pain following initiation of rotigotine: a multicenter non-interventional study. *Postgrad. Med.* 129, 46–54. doi:10.1080/00325481.2017.1258953.

Tinazzi, M., Del Vesco, C., Defazio, G., Fincati, E., Smania, N., Moretto, G., et al. (2008). Abnormal processing of the nociceptive input in Parkinson's disease: a study with CO2 laser evoked potentials. *Pain* 136, 117–124. doi:10.1016/j.pain.2007.06.022.

Titova, N., Schapira, A. H. V., Chaudhuri, K. R., Qamar, M. A., Katunina, E., and Jenner, P. (2017). "Chapter Three - Nonmotor Symptoms in Experimental Models of Parkinson's Disease," in *International Review of Neurobiology* Nonmotor Parkinson's: The Hidden Face., eds. K. R. Chaudhuri and N. Titova (Academic Press), 63–89. doi:10.1016/bs.irn.2017.05.018.

Torrecilla, M., Fernández-Aedo, I., Arrue, A., Zumarraga, M., and Ugedo, L. (2013). Role of GIRK channels on the noradrenergic transmission in vivo: an electrophysiological and neurochemical study on GIRK2 mutant mice. *Int. J. Neuropsychopharmacol.* 16, 1093–1104. doi:10.1017/S1461145712000971.

Torres-Sanchez, S., Perez-Caballero, L., Mico, J. A., Celada, P., and Berrocoso, E. (2018). Effect of Deep Brain Stimulation of the ventromedial prefrontal cortex on the noradrenergic system in rats. *Brain Stimulat.* 11, 222–230. doi:10.1016/j.brs.2017.10.003.

Totah, N. K., Neves, R. M., Panzeri, S., Logothetis, N. K., and Eschenko, O. (2018). The Locus Coeruleus Is a Complex and Differentiated Neuromodulatory System. *Neuron* 99, 1055-1068.e6. doi:10.1016/j.neuron.2018.07.037.

Trenkwalder, C., Chaudhuri, K. R., Martinez-Martin, P., Rascol, O., Ehret, R., Vališ, M., et al. (2015). Prolonged-release oxycodone-naloxone for treatment of severe pain in patients with Parkinson's disease (PANDA): a double-blind, randomised, placebo-controlled trial. *Lancet Neurol.* 14, 1161–1170. doi:10.1016/S1474-4422(15)00243-4.

Trenkwalder, C., Kies, B., Rudzinska, M., Fine, J., Nikl, J., Honczarenko, K., et al. (2011). Rotigotine effects on early morning motor function and sleep in Parkinson's disease: a double-blind, randomized, placebo-controlled study (RECOVER). *Mov. Disord. Off. J. Mov. Disord. Soc.* 26, 90–99. doi:10.1002/mds.23441.

Tung, C. S., Ugedo, L., Grenhoff, J., Engberg, G., and Svensson, T. H. (1989). Peripheral induction of burst firing in locus coeruleus neurons by nicotine mediated via excitatory amino acids. *Synap. N. Y. N* 4, 313–318. doi:10.1002/syn.890040407.

Uchiyama, M., Isse, K., Tanaka, K., Yokota, N., Hamamoto, M., Aida, S., et al. (1995). Incidental Lewy body disease in a patient with REM sleep behavior disorder. *Neurology* 45, 709–712. doi:10.1212/wnl.45.4.709.

Ugedo, L., Pineda, J., Ruiz-Ortega, J. A., and Martín-Ruiz, R. (1998). Stimulation of locus coeruleus neurons by non-I1/I2-type imidazoline receptors: an in vivo and in vitro electrophysiological study. *Br. J. Pharmacol.* 125, 1685–1694. doi:10.1038/sj.bjp.0702255.

Ulusoy, A., Rusconi, R., Pérez-Revuelta, B. I., Musgrove, R. E., Helwig, M., Winzen-Reichert, B., et al. (2013). Caudo-rostral brain spreading of α-synuclein through vagal connections. *EMBO Mol. Med.* 5, 1119–1127. doi:10.1002/emmm.201302475.

Undieh, A. S. (2010). Pharmacology of signaling induced by dopamine D(1)-like receptor activation. *Pharmacol. Ther.* 128, 37–60. doi:10.1016/j.pharmthera.2010.05.003.

Ungerstedt, U. (1968). 6-Hydroxy-dopamine induced degeneration of central monoamine neurons. *Eur. J. Pharmacol.* 5, 107–110. doi:10.1016/0014-2999(68)90164-7.

Valente, E. M., Abou-Sleiman, P. M., Caputo, V., Muqit, M. M. K., Harvey, K., Gispert, S., et al. (2004). Hereditary early-onset Parkinson's disease caused by mutations in PINK1. *Science* 304, 1158–1160. doi:10.1126/science.1096284.

Valentino, R. J., and Foote, S. L. (1987). Corticotropin-releasing factor disrupts sensory responses of brain noradrenergic neurons. *Neuroendocrinology* 45, 28–36. doi:10.1159/000124700.

Valentino, R. J., and Foote, S. L. (1988). Corticotropin-releasing hormone increases tonic but not sensory-evoked activity of noradrenergic locus coeruleus neurons in unanesthetized rats. *J. Neurosci. Off. J. Soc. Neurosci.* 8, 1016–1025.

Van Bockstaele, E. J., and Colago, E. E. (1996). Selective distribution of the NMDA-R1 glutamate receptor in astrocytes and presynaptic axon terminals in the nucleus locus coeruleus of the rat brain: an immunoelectron microscopic study. *J. Comp. Neurol.* 369, 483–496. doi:10.1002/(SICI)1096-9861(19960610)369:4<483::AID-CNE1>3.0.CO;2-0.

Van Bockstaele, E. J., Colago, E. E., Moriwaki, A., and Uhl, G. R. (1996). Mu-opioid receptor is located on the plasma membrane of dendrites that receive asymmetric synapses from axon terminals containing leucine-enkephalin in the rat nucleus locus coeruleus. *J. Comp. Neurol.* 376, 65–74. doi:10.1002/(SICI)1096-9861(19961202)376:1<65::AID-CNE4>3.0.CO;2-M.

Vazey, E. M., and Aston-Jones, G. (2012). The emerging role of norepinephrine in cognitive dysfunctions of Parkinson's disease. *Front. Behav. Neurosci.* 6, 48. doi:10.3389/fnbeh.2012.00048.

Vazey, E. M., and Aston-Jones, G. (2014). Designer receptor manipulations reveal a role of the locus coeruleus noradrenergic system in isoflurane general

anesthesia. *Proc. Natl. Acad. Sci. U. S. A.* 111, 3859–3864. doi:10.1073/pnas.1310025111.

Vazey, E. M., Moorman, D. E., and Aston-Jones, G. (2018). Phasic locus coeruleus activity regulates cortical encoding of salience information. *Proc. Natl. Acad. Sci. U. S. A.* 115, E9439–E9448. doi:10.1073/pnas.1803716115.

Versteeg, D. H., Van Der Gugten, J., De Jong, W., and Palkovits, M. (1976). Regional concentrations of noradrenaline and dopamine in rat brain. *Brain Res.* 113, 563–574. doi:10.1016/0006-8993(76)90057-3.

Videnovic, A. (2018). Disturbances of Sleep and Alertness in Parkinson's Disease. *Curr. Neurol. Neurosci. Rep.* 18, 29. doi:10.1007/s11910-018-0838-2.

Vieira, J. C. F., Bassani, T. B., Santiago, R. M., de O. Guaita, G., Zanoveli, J. M., da Cunha, C., et al. (2019). Anxiety-like behavior induced by 6-OHDA animal model of Parkinson's disease may be related to a dysregulation of neurotransmitter systems in brain areas related to anxiety. *Behav. Brain Res.* 371, 111981. doi:10.1016/j.bbr.2019.111981.

Vila, M. (2019). Neuromelanin, aging, and neuronal vulnerability in Parkinson's disease. *Mov. Disord.* 0. doi:10.1002/mds.27776.

Vo, Q., Gilmour, T. P., Venkiteswaran, K., Fang, J., and Subramanian, T. (2014). Polysomnographic Features of Sleep Disturbances and REM Sleep Behavior Disorder in the Unilateral 6-OHDA Lesioned Hemiparkinsonian Rat. *Park. Dis.* 2014, 852965. doi:10.1155/2014/852965.

Von Coelln, R., Thomas, B., Savitt, J. M., Lim, K. L., Sasaki, M., Hess, E. J., et al. (2004). Loss of locus coeruleus neurons and reduced startle in parkin null mice. *Proc. Natl. Acad. Sci. U. S. A.* 101, 10744–10749. doi:10.1073/pnas.0401297101.

Walters, J. R., Hu, D., Itoga, C. A., Parr-Brownlie, L. C., and Bergstrom, D. A. (2007). Phase relationships support a role for coordinated activity in the indirect pathway in organizing slow oscillations in basal ganglia output after loss of dopamine. *Neuroscience* 144, 762–776. doi:10.1016/j.neuroscience.2006.10.006.

Wang, H.-Y., Kuo, Z.-C., Fu, Y.-S., Chen, R.-F., Min, M.-Y., and Yang, H.-W. (2015). GABAB receptor-mediated tonic inhibition regulates the

spontaneous firing of locus coeruleus neurons in developing rats and in citalopram-treated rats. *J. Physiol.* 593, 161–180. doi:10.1113/jphysiol.2014.281378.

Wang, J., Li, Y., Huang, Z., Wan, W., Zhang, Y., Wang, C., et al. (2018). Neuromelanin-sensitive magnetic resonance imaging features of the substantia nigra and locus coeruleus in de novo Parkinson's disease and its phenotypes. *Eur. J. Neurol.* 25, 949-e73. doi:10.1111/ene.13628.

Wang, T., Zhang, Q.-J., Liu, J., Wu, Z.-H., and Wang, S. (2009). Firing activity of locus coeruleus noradrenergic neurons increases in a rodent model of Parkinsonism. *Neurosci. Bull.* 25, 15–20. doi:10.1007/s12264-009-1023-z.

Wang, Y., Zhang, Q. J., Liu, J., Ali, U., Gui, Z. H., Hui, Y. P., et al. (2010). Noradrenergic lesion of the locus coeruleus increases apomorphine-induced circling behavior and the firing activity of substantia nigra pars reticulata neurons in a rat model of Parkinson's disease. *Brain Res.* 1310, 189–199. doi:10.1016/j.brainres.2009.10.070.

Wasner, G., and Deuschl, G. (2012). Pains in Parkinson disease--many syndromes under one umbrella. *Nat. Rev. Neurol.* 8, 284–294. doi:10.1038/nrneurol.2012.54.

Watanabe, T., Wang, X., Tan, Z., and Frahm, J. (2019). Magnetic resonance imaging of brain cell water. *Sci. Rep.* 9, 5084. doi:10.1038/s41598-019-41587-2.

Waterhouse, B. D., and Woodward, D. J. (1980). Interaction of norepinephrine with cerebrocortical activity evoked by stimulation of somatosensory afferent pathways in the rat. *Exp. Neurol.* 67, 11–34. doi:10.1016/0014-4886(80)90159-4.

Weintraub, D., and Mamikonyan, E. (2019). The Neuropsychiatry of Parkinson Disease: A Perfect Storm. *Am. J. Geriatr. Psychiatry Off. J. Am. Assoc. Geriatr. Psychiatry* 27, 998–1018. doi:10.1016/j.jagp.2019.03.002.

West, C. H. K., Ritchie, J. C., Boss-Williams, K. A., and Weiss, J. M. (2009). Antidepressant drugs with differing pharmacological actions decrease activity of locus coeruleus neurons. *Int. J. Neuropsychopharmacol.* 12, 627–641. doi:10.1017/S1461145708009474.

West, C. H. K., Ritchie, J. C., and Weiss, J. M. (2010). Paroxetine-induced increase in activity of locus coeruleus neurons in adolescent rats: implication of a countertherapeutic effect of an antidepressant. *Neuropsychopharmacol. Off. Publ. Am. Coll. Neuropsychopharmacol.* 35, 1653–1663. doi:10.1038/npp.2010.34.

Westlund, K. N., Bowker, R. M., Ziegler, M. G., and Coulter, J. D. (1983). Noradrenergic projections to the spinal cord of the rat. *Brain Res.* 263, 15–31. doi:10.1016/0006-8993(83)91196-4.

Williams, J. T., Bobker, D. H., and Harris, G. C. (1991). Synaptic potentials in locus coeruleus neurons in brain slices. *Prog. Brain Res.* 88, 167–172. doi:10.1016/s0079-6123(08)63806-6.

Williams, J. T., Egan, T. M., and North, R. A. (1982). Enkephalin opens potassium channels on mammalian central neurones. *Nature* 299, 74–77. doi:10.1038/299074a0.

Williams, J. T., North, R. A., Shefner, S. A., Nishi, S., and Egan, T. M. (1984). Membrane properties of rat locus coeruleus neurones. *Neuroscience* 13, 137–156. doi:10.1016/0306-4522(84)90265-3.

Williams, J. T., North, R. A., and Tokimasa, T. (1988). Inward rectification of resting and opiate-activated potassium currents in rat locus coeruleus neurons. *J. Neurosci. Off. J. Soc. Neurosci.* 8, 4299–4306.

Willner, P. (1997). The mesolimbic dopamine system as a target for rapid antidepressant action. *Int. Clin. Psychopharmacol.* 12 Suppl 3, S7-14. doi:10.1097/00004850-199707003-00002.

Winklhofer, K. F., and Haass, C. (2010). Mitochondrial dysfunction in Parkinson's disease. *Biochim. Biophys. Acta* 1802, 29–44. doi:10.1016/j.bbadis.2009.08.013.

Wirdefeldt, K., Adami, H.-O., Cole, P., Trichopoulos, D., and Mandel, J. (2011). Epidemiology and etiology of Parkinson's disease: a review of the evidence. *Eur. J. Epidemiol.* 26 Suppl 1, S1-58. doi:10.1007/s10654-011-9581-6.

Wong-Riley, M. T. (1989). Cytochrome oxidase: an endogenous metabolic marker for neuronal activity. *Trends Neurosci.* 12, 94–101. doi:10.1016/0166-2236(89)90165-3.

Woolfe, G., and Macdonald, A. D. (1944). THE EVALUATION OF THE ANALGESIC ACTION OF PETHIDINE HYDROCHLORIDE (DEMEROL). *J. Pharmacol. Exp. Ther.* 80, 300.

Yamasaki, M., and Takeuchi, T. (2017). Locus Coeruleus and Dopamine-Dependent Memory Consolidation. *Neural Plast.* 2017, 8602690. doi:10.1155/2017/8602690.

Yang, C., Zhang, J.-R., Chen, L., Ge, S.-N., Wang, J.-L., Yan, Z.-Q., et al. (2015). Decreased HCN2 expression in STN contributes to abnormal high-voltage spindles in the cortex and globus pallidus of freely moving rats. *Brain Res.* 1618, 17–28. doi:10.1016/j.brainres.2015.05.009.

Yao, N., Wu, Y., Zhou, Y., Ju, L., Liu, Y., Ju, R., et al. (2015). Lesion of the locus coeruleus aggravates dopaminergic neuron degeneration by modulating microglial function in mouse models of Parkinson's disease. *Brain Res.* 1625, 255–274. doi:10.1016/j.brainres.2015.08.032.

Yokoyama, C., Okamura, H., Nakajima, T., Taguchi, J., and Ibata, Y. (1994). Autoradiographic distribution of [3H]YM-09151-2, a high-affinity and selective antagonist ligand for the dopamine D2 receptor group, in the rat brain and spinal cord. *J. Comp. Neurol.* 344, 121–136. doi:10.1002/cne.903440109.

Yoshino, H., Nakagawa-Hattori, Y., Kondo, T., and Mizuno, Y. (1992). Mitochondrial complex I and II activities of lymphocytes and platelets in Parkinson's disease. *J. Neural Transm. Park. Dis. Dement. Sect.* 4, 27–34. doi:10.1007/bf02257619.

Young, W. S., and Kuhar, M. J. (1980). Noradrenergic alpha 1 and alpha 2 receptors: light microscopic autoradiographic localization. *Proc. Natl. Acad. Sci. U. S. A.* 77, 1696–1700. doi:10.1073/pnas.77.3.1696.

Yssel, J. D., O'Neill, E., Nolan, Y. M., Connor, T. J., and Harkin, A. (2018). Treatment with the noradrenaline re-uptake inhibitor atomoxetine alone and in combination with the α2-adrenoceptor antagonist idazoxan attenuates loss of dopamine and associated motor deficits in the LPS inflammatory rat model of Parkinson's disease. *Brain. Behav. Immun.* 69, 456–469. doi:10.1016/j.bbi.2018.01.004.

Zamalloa, T., Bailey, C. P., and Pineda, J. (2009). Glutamate-induced post-activation inhibition of locus coeruleus neurons is mediated by AMPA/kainate receptors and sodium-dependent potassium currents. *Br. J. Pharmacol.* 156, 649–661. doi:10.1111/j.1476-5381.2008.00004.x.

Zarow, C., Lyness, S. A., Mortimer, J. A., and Chui, H. C. (2003). Neuronal loss is greater in the locus coeruleus than nucleus basalis and substantia nigra in Alzheimer and Parkinson diseases. *Arch. Neurol.* 60, 337–341. doi:10.1001/archneur.60.3.337.

Zerbi, V., Floriou-Servou, A., Markicevic, M., Vermeiren, Y., Sturman, O., Privitera, M., et al. (2019). Rapid Reconfiguration of the Functional Connectome after Chemogenetic Locus Coeruleus Activation. *Neuron* 103, 702-718.e5. doi:10.1016/j.neuron.2019.05.034.

Zhang, X., Cui, N., Wu, Z., Su, J., Tadepalli, J. S., Sekizar, S., et al. (2010). Intrinsic membrane properties of locus coeruleus neurons in Mecp2-null mice. *Am. J. Physiol. Cell Physiol.* 298, C635-646. doi:10.1152/ajpcell.00442.2009.

Zhou, M., Zhang, W., Chang, J., Wang, J., Zheng, W., Yang, Y., et al. (2015). Gait analysis in three different 6-hydroxydopamine rat models of Parkinson's disease. *Neurosci. Lett.* 584, 184–189. doi:10.1016/j.neulet.2014.10.032.

Zitnik, G. A., Curtis, A. L., Wood, S. K., Arner, J., and Valentino, R. J. (2016). Adolescent Social Stress Produces an Enduring Activation of the Rat Locus Coeruleus and Alters its Coherence with the Prefrontal Cortex. *Neuropsychopharmacol. Off. Publ. Am. Coll. Neuropsychopharmacol.* 41, 1376–1385. doi:10.1038/npp.2015.289.

Zweig, R. M., Cardillo, J. E., Cohen, M., Giere, S., and Hedreen, J. C. (1993). The locus ceruleus and dementia in Parkinson's disease. *Neurology* 43, 986–991. doi:10.1212/wnl.43.5.986.